The computer simulation of the hot metal forming processes

Prof. dr hab. inż. Andrzej Milenin
AGH University of Science and Technology, Kraków, Poland
E-mail: milenin@agh.edu.pl

The computer simulation of the hot metal forming processes
Milenin Andrzej, AGH University of Science and Technology, 2012

AKADEMIA GÓRNICZO-HUTNICZA IM. STANISŁAWA STASZICA W KRAKOWIE
AGH

Literature

1. O.C.Zienkiewicz, R.L.Taylor The Finite Element Method // Butterworth Heinemann, 3 vol, 5-th Edition, London, 2000
2. K.J. Bathe, Finite Element Procedures in Engineering Analysis, Prentice Hall Inc.
3. Segerlind L. J., Applied Finite Element Analysis // J. Wiley & Sons, New York, 1976, 1984, 1987, 427 pp. ISBN 0-471-80662-5.
4. Kobajashi S., Oh S.I., Altan T., Metal Forming and the Finie Element Metod, Oxford University Press, New York, Oxford, 1989.
5. Owen D.R.J., Histon E., Finite Elements In Plasticity: Theory and Practice, Pineridge Press, Swansea, 1980.
6. Wagoner R.H., Chenot J.L., Fundamentals of Metal Forming, John Wiley & Sons, Inc, New York, 1997.
7. Lenard J.G., Pietrzyk M., Cser L., Mathematical and Physical Simulation of the Properties of Hot Rolled Products, Elsevier, Amsterdam, 1999.
8. http://qform3d.ru
9. www.LCM.agh.edu.pl
10. Finite Element Procedures for Solids and Structures (MIT Open Recourse)
11. A. Milenin Podstawy MES. Zagadnienia termomechaniczne // AGH, Kraków, 2010
12. M. Pietrzyk Metody numeryczne w przeróbce plastycznej metali // AGH, Kraków, 1992

Annotation

In the proposed course questions of simulation with the aid of the finite elements method (FEM) of the processes of hot metal forming are examined. Course consists of three major parts.

In the first part the theoretical bases of the solution of the nonisothermic problems of hot metal forming are examined. The theory of plastic flow and the necessary aspects of the theory of thermal conductivity for this purpose is presented.

The second part of the course is dedicated to the solution of boundary-value problem with the aid of FEM. Algorithms and special features of the application of a FEM to the mechanical and thermal tasks, which correspond to the processes of hot metal forming, are given.

In the third part of the course numerous examples of the solution of the technological problems of hot metal forming with the aid of both the commercial programs and FEM programs developer by the author are present. Generalizations and recommendations regarding the selection of the method of the solution of the problems of metal forming, which appear in the procurement facility, are given.

The computer simulation of the hot metal forming processes

1. Bases of the theory of plastic flow of the incompressible materials.
2. Formulation of the boundary-value problem, which allows for simulation of hot deformation of metals. Bases of the finite elements method.
3. Finite elements method in the theory of plastic flow of the incompressible materials. Finite elements method in the tasks of calculations of the temperature distribution in the material during deformation.
4. Application of the finite elements method to the solution of the problems of hot metal forming. Calculation of the mechanical properties of the workable metal in the algorithm, based on FEM.
5. Special features of FEM simulation of the extrusion. Special features of FEM simulation of the forging and stamping. Special features of FEM simulation of the hot rolling.
6. Example of commercial FEM programs for the simulation of the processes of hot deformation of metals. Programs Qform and Forge3. Example of development of own FEM codes and solution of the unconventional problems in the theory of metal forming.

Introduction

History background

Richard Kurant

R. Kurant VARIATIONAL METHODS FOR THE SOLUTION OF PROBLEMS OF EQUILIBRIUM AND VIBRATIONS, 1942

History background

Walther Ritz

W. Ritz, Ueber eine neue Methode zur Loesung gewisser Variationsprobleme der mathematischen Physik, J. Reine Angew. Math. vol. 135 (1908);

The computer simulation of the hot metal forming processes
Milenin Andrzej, AGH University of Science and Technology, 2012
AKADEMIA GÓRNICZO-HUTNICZA IM. STANISŁAWA STASZICA W KRAKOWIE
AGH

History background. Hot metal forming

1980 O. Zienkiewicz, G.Gun, N.Biba. Flow formulation.

1990 Form2d (Qform), 2d rolling, drawing, couple thermo-mechanical models.

1995-2000 Qform3d, Forge3d, Deform3d – forging, 3d rolling.

2000-2010 Fracture, evolution of microstructure, prognoses of properties. Practical implementations of 3d solutions.

2010 Multi scale simulation.

FEM today. Optimization of metal forming processes (program QForm)

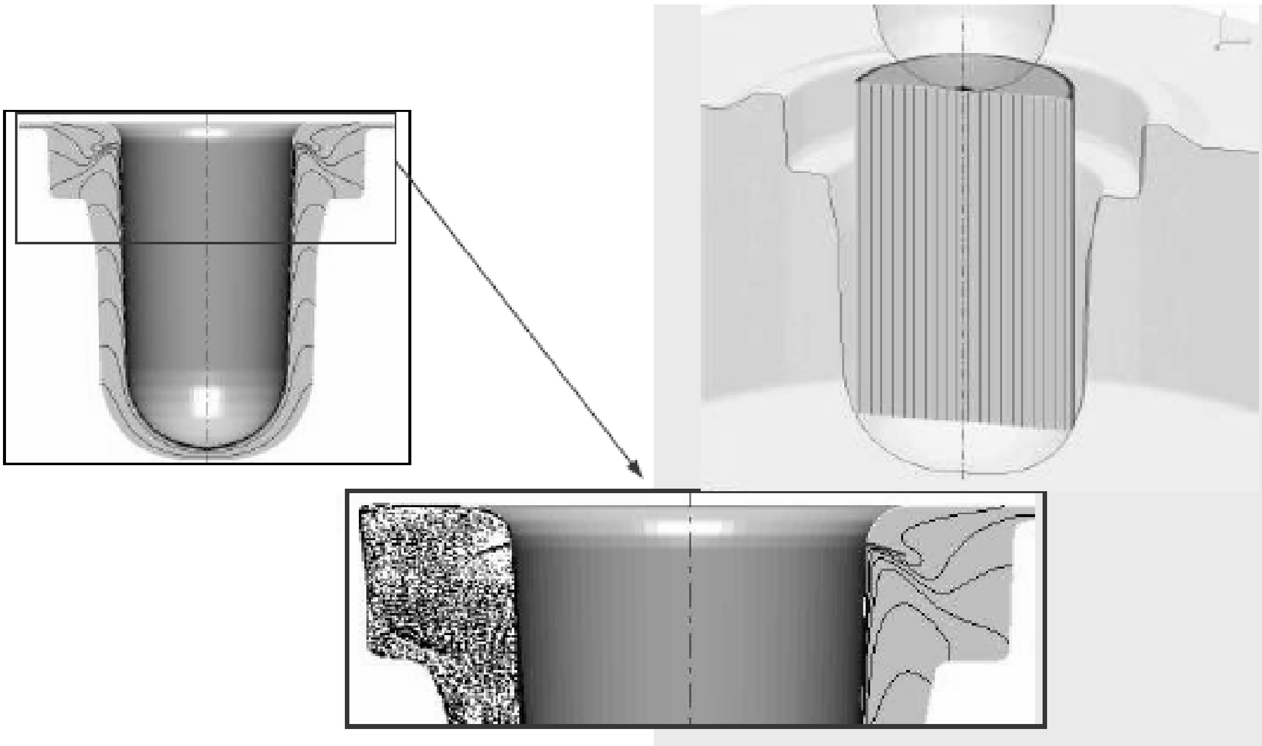

The computer simulation of the hot metal forming processes
Milenin Andrzej, AGH University of Science and Technology, 2012
AKADEMIA GÓRNICZO-HUTNICZA IM. STANISŁAWA STASZICA W KRAKOWIE
AGH

Predict of defects during metal forming processes (program QForm)

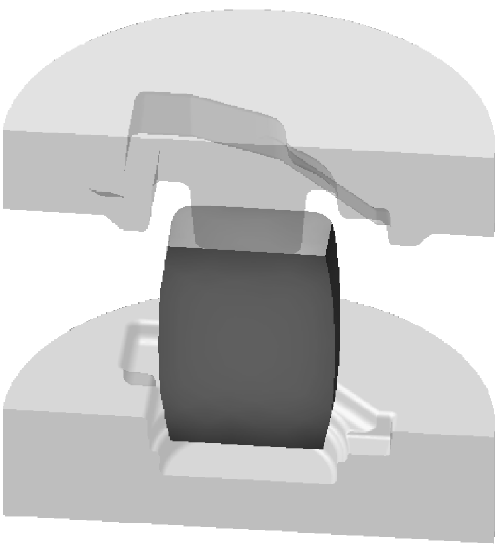

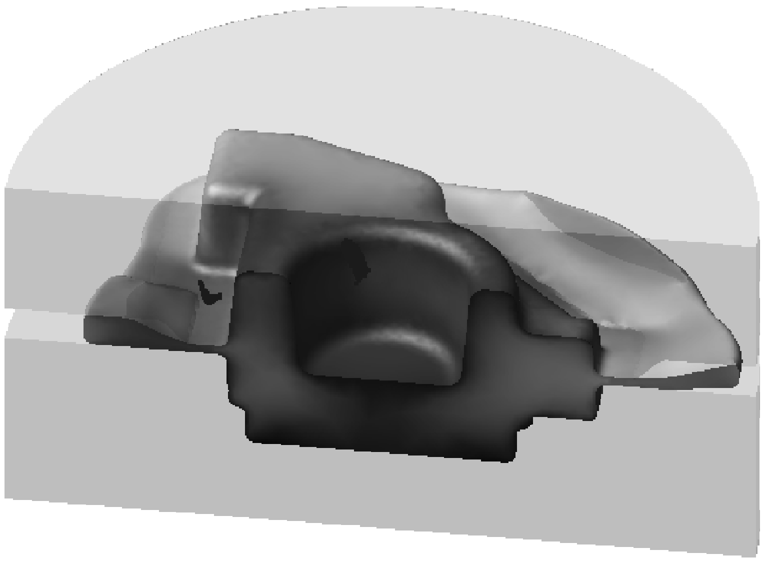

Simulation of very difficult processes

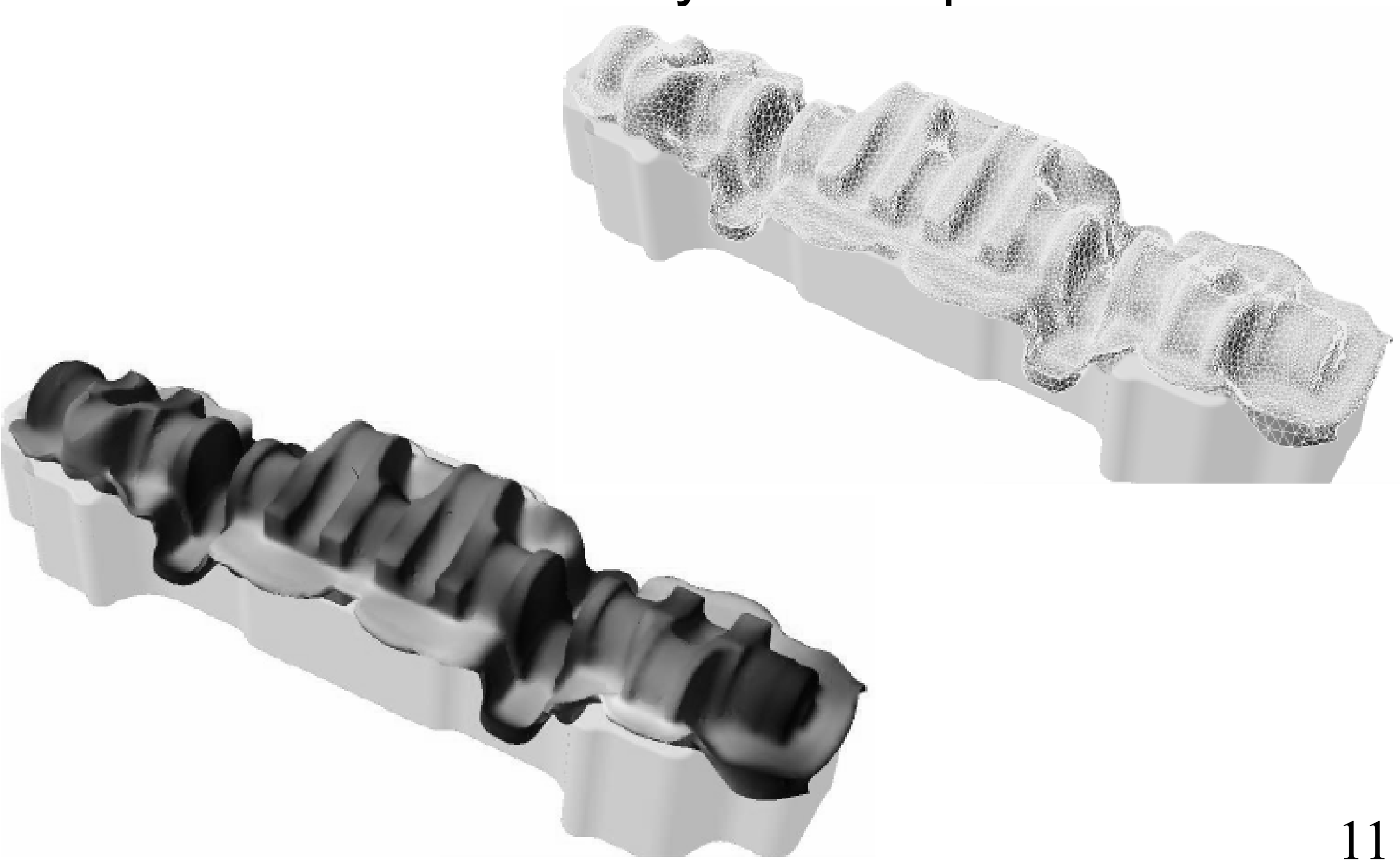

Precision of results (Qform)

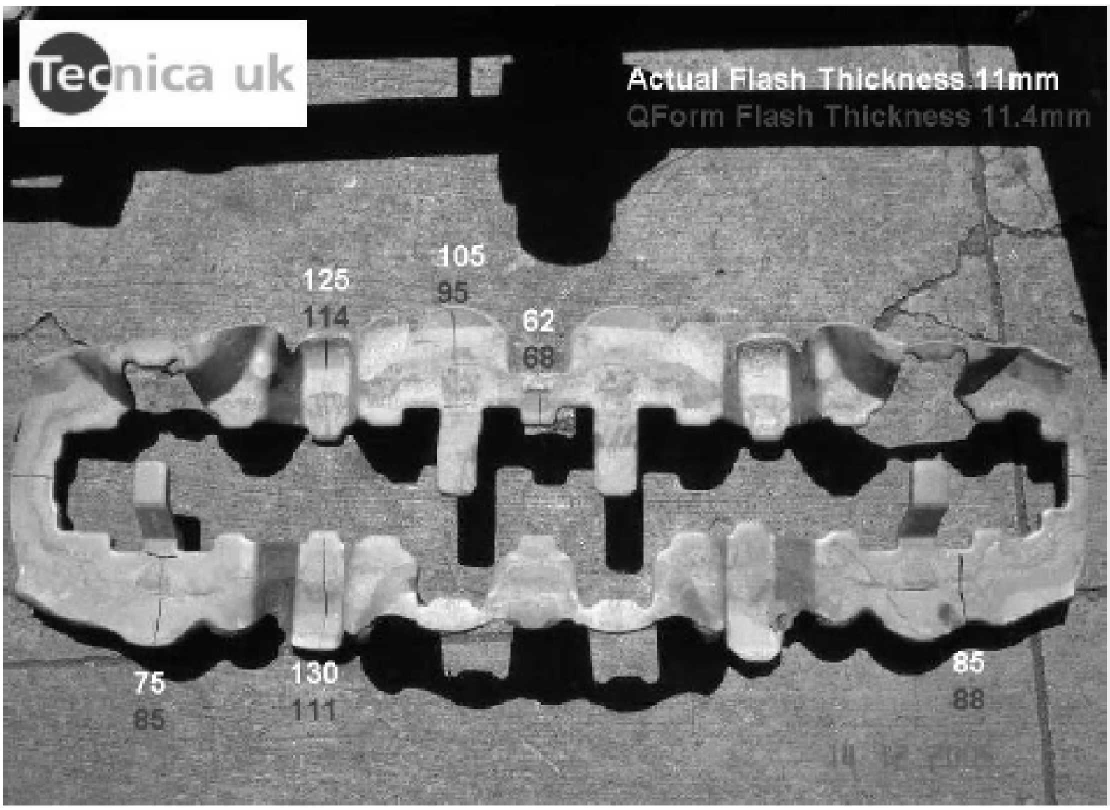

Saving of materials (QForm)

Material saving: billet weight reduced by 12%

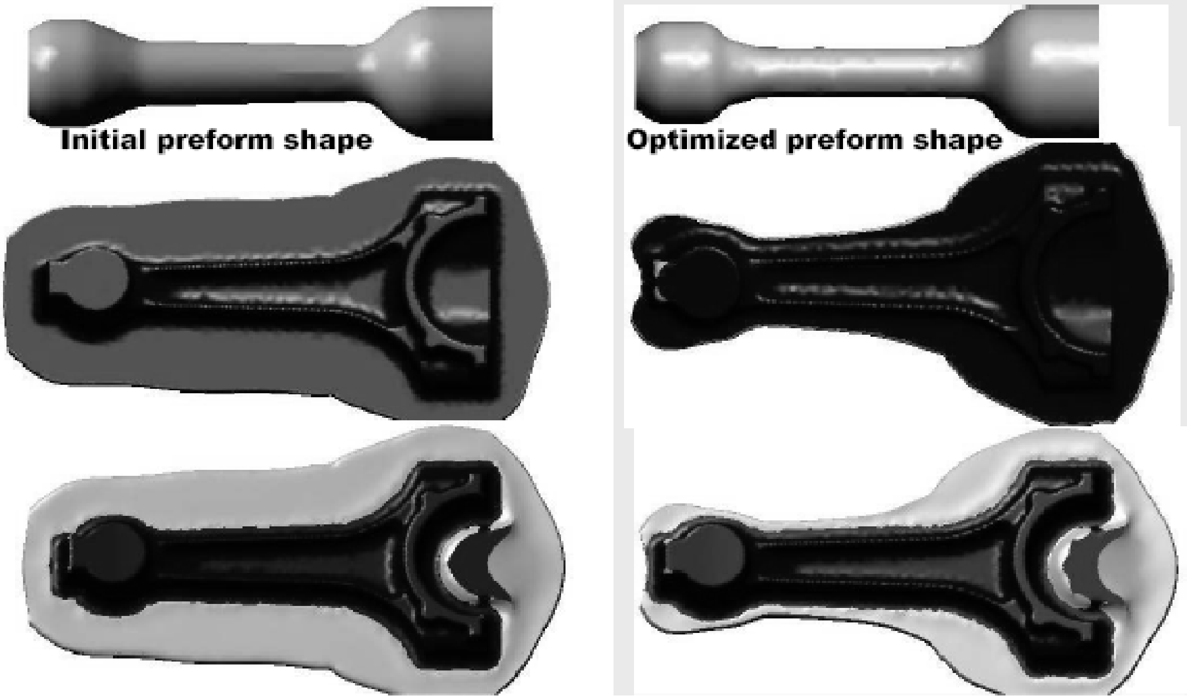

Optimization of different metal forming processes (program Rolling3)

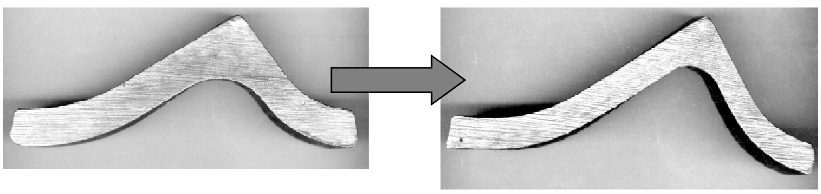

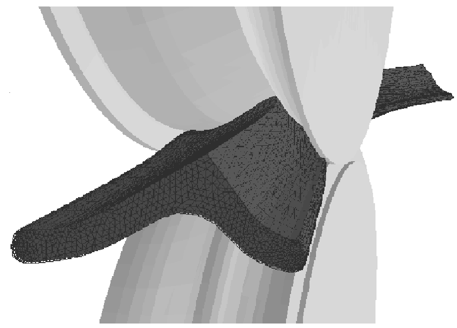

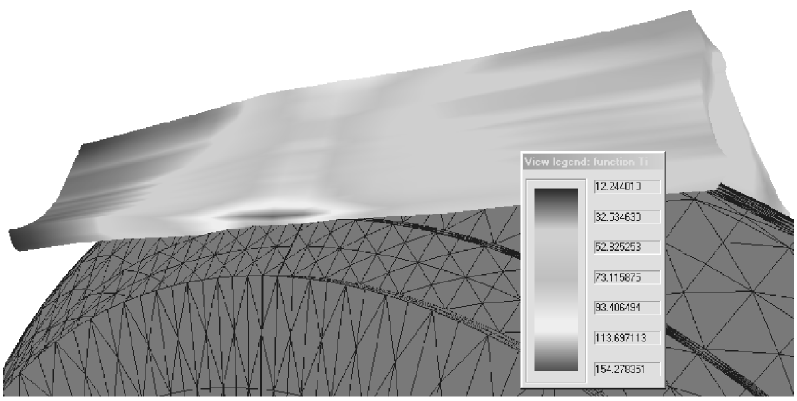

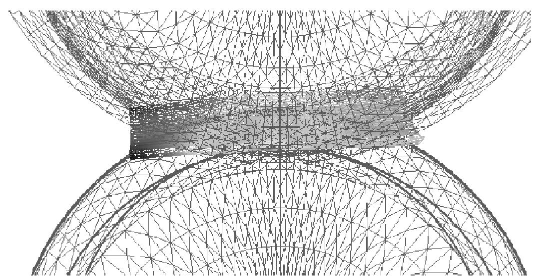

Structure and problems of FEM simulation of metal forming process

Formulation of boundary problem	**Use of FEM techniques**	**Analyze of results**
Mistakes in formulation of boundary problem	**Wrong choice of type of FE, solution methods, etc.**	**Mistakes in interpretation of results**

FEM - this is not the exact method !!!

The computer simulation of the hot metal forming processes
Milenin Andrzej, AGH University of Science and Technology, 2012
AKADEMIA GÓRNICZO-HUTNICZA IM. STANISŁAWA STASZICA W KRAKOWIE
AGH

Lection 1.

Bases of the theory of plastic flow of the incompressible materials.

Phisical bases of the theory of plastic flow

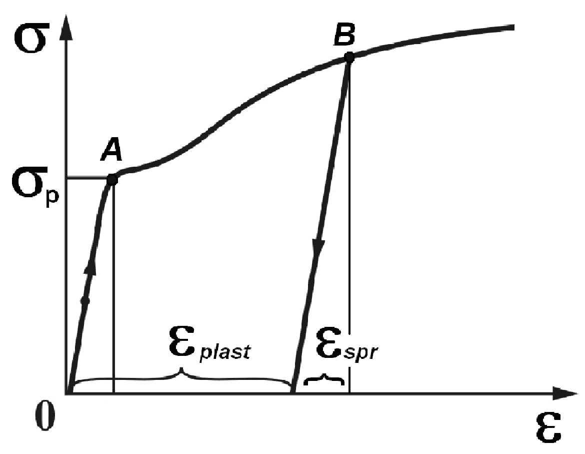

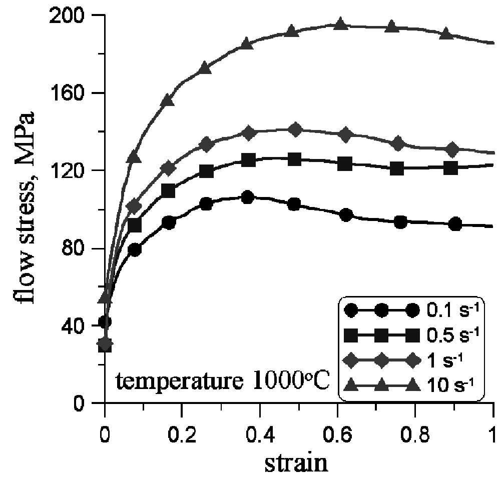

elastic	elastic-plastic	plastic

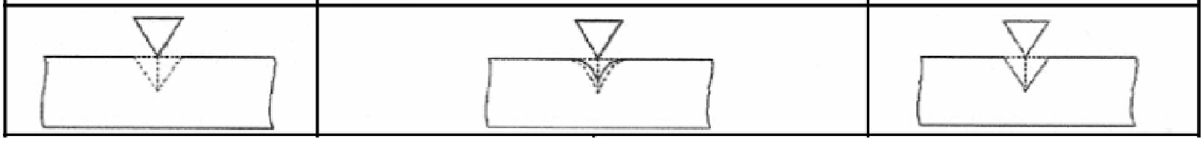

The computer simulation of the hot metal forming processes
Milenin Andrzej, AGH University of Science and Technology, 2012
AKADEMIA GÓRNICZO-HUTNICZA IM. STANISŁAWA STASZICA W KRAKOWIE
AGH

Mathematical bases of the theory of plastic flow (flow formulation)

a) Relationship between vector of velocity and tensor of strain rate: $\Longrightarrow$ $$\xi_{ij} = \frac{1}{2}\left(v_{i,j} + v_{j,i}\right)$$

b) Equilibrium equations: $\Longrightarrow$ $$\sigma_{ij,j} = 0$$

c) Physical equation (stress- strain rate relationship, constitutive equations) : $\Longrightarrow$ $$\sigma_{ij} = \delta_{ij}\sigma_0 + \frac{2\overline{\sigma}}{3\overline{\xi}}\xi_{ij}$$

d) Incompressibility equation: $\Longrightarrow$ $$\xi_0 = 0$$

$$\xi_0 = \frac{1}{3}div(\vec{v}) = 0 \qquad v_{i,j} = 0$$

Cauchy's strain tensor. Compatibility condition.

$$\vec{u} = \left(u_x, u_y, u_z\right)$$

$$\varepsilon_{ij} = \frac{1}{2}\left(u_{i,j} + u_{j,i}\right)$$

$$\vec{v} = \left(\frac{\partial u_x}{\partial \tau}, \frac{\partial u_y}{\partial \tau}, \frac{\partial u_z}{\partial \tau}\right)$$

$$\varepsilon_{xx} = \frac{\partial u_x}{\partial x} \qquad \varepsilon_{xy} = \frac{1}{2}\left(\frac{\partial u_x}{\partial y} + \frac{\partial u_y}{\partial x}\right)$$

$$\varepsilon_{yy} = \frac{\partial u_y}{\partial y} \qquad \varepsilon_{yz} = \frac{1}{2}\left(\frac{\partial u_y}{\partial z} + \frac{\partial u_z}{\partial y}\right)$$

$$\varepsilon_{zz} = \frac{\partial u_z}{\partial z} \qquad \varepsilon_{xz} = \frac{1}{2}\left(\frac{\partial u_x}{\partial z} + \frac{\partial u_z}{\partial x}\right)$$

$$\xi_{ij} = \frac{\partial \varepsilon_{ij}}{\partial \tau}$$

$$\xi_{ij} = \frac{1}{2}\left(v_{i,j} + v_{j,i}\right)$$

$$\xi_{xx} = \frac{\partial v_x}{\partial x} \qquad \xi_{xy} = \frac{1}{2}\left(\frac{\partial v_x}{\partial y} + \frac{\partial v_y}{\partial x}\right)$$

$$\xi_{yy} = \frac{\partial v_y}{\partial y} \qquad \xi_{yz} = \frac{1}{2}\left(\frac{\partial v_y}{\partial z} + \frac{\partial v_z}{\partial y}\right)$$

$$\xi_{zz} = \frac{\partial v_z}{\partial z} \qquad \xi_{xz} = \frac{1}{2}\left(\frac{\partial v_x}{\partial z} + \frac{\partial v_z}{\partial x}\right)$$

The computer simulation of the hot metal forming processes
Milenin Andrzej, AGH University of Science and Technology, 2012
AKADEMIA GÓRNICZO-HUTNICZA IM. STANISŁAWA STASZICA W KRAKOWIE
AGH

Equilibrium equations

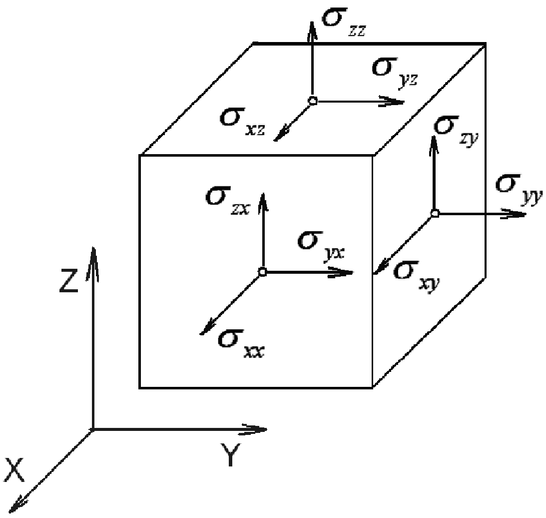

$$\left.\begin{aligned}
\frac{\partial \sigma_{xx}}{\partial x} + \frac{\partial \sigma_{xy}}{\partial y} + \frac{\partial \sigma_{xz}}{\partial z} + g_x = 0 \\
\frac{\partial \sigma_{yx}}{\partial x} + \frac{\partial \sigma_{yy}}{\partial y} + \frac{\partial \sigma_{yz}}{\partial z} + g_y = 0 \\
\frac{\partial \sigma_{zx}}{\partial x} + \frac{\partial \sigma_{zy}}{\partial y} + \frac{\partial \sigma_{zz}}{\partial z} + g_z = 0
\end{aligned}\right\}$$

$$\int_V \frac{\partial P_i}{\partial x_i} dV = \int_S P_i \nu_i dS$$

$$\int_V \frac{\partial \sigma_{ij}}{\partial x_j} dV = \int_S \sigma_{ij} \nu_i dS = 0 \qquad \frac{\partial \sigma_{ij}}{\partial x_j} = \sigma_{ij,j} = 0$$

Physical equations (constitutive equations)

Elastic-plastic formulation

$$\sigma_{ij}=\sigma_{ij}\left(\varepsilon_{ij}\right)=\delta_{ij}3k_V\varepsilon_0+\frac{\bar{\sigma}}{(1+\nu)\bar{\varepsilon}}\left(\varepsilon_{ij}-\delta_{ij}\varepsilon_0\right)$$

$$\varepsilon_0=\frac{\varepsilon_{xx}+\varepsilon_{yy}+\varepsilon_{zz}}{3}$$

$$\sigma_0=3k_V\varepsilon_0$$

$$k_V=\frac{E}{3(1-2\nu)}$$

Flow formulation

$$\sigma_{ij}=\delta_{ij}\sigma_0+\frac{2\bar{\sigma}}{3\bar{\xi}}\xi_{ij}$$

$$s_{ij}=\frac{2\bar{\sigma}}{3\bar{\xi}}\xi_{ij}$$

$$\bar{\sigma}=\bar{\sigma}\left(\bar{\varepsilon},\bar{\xi},t\right)$$

$$\bar{\varepsilon}=\frac{\sqrt{2}}{3}\sqrt{\left(\varepsilon_{xx}-\varepsilon_{yy}\right)^2+\left(\varepsilon_{yy}-\varepsilon_{zz}\right)^2+\left(\varepsilon_{zz}-\varepsilon_{xx}\right)^2+6\left(\varepsilon_{xy}^2+\varepsilon_{yz}^2+\varepsilon_{zx}^2\right)}$$

$$\bar{\xi}=\frac{\sqrt{2}}{3}\sqrt{\left(\xi_{xx}-\xi_{yy}\right)^2+\left(\xi_{yy}-\xi_{zz}\right)^2+\left(\xi_{zz}-\xi_{xx}\right)^2+6\left(\xi_{xy}^2+\xi_{yz}^2+\xi_{zx}^2\right)}$$

$$\bar{\sigma}=\frac{\sqrt{2}}{2}\sqrt{\left(\sigma_{xx}-\sigma_{yy}\right)^2+\left(\sigma_{yy}-\sigma_{zz}\right)^2+\left(\sigma_{zz}-\sigma_{xx}\right)^2+6\left(\sigma_{xy}^2+\sigma_{yz}^2+\sigma_{zx}^2\right)}$$

Variation formulations

Elastic-plastic formulation

$$J=\int_V\int_0^{\bar{\varepsilon}}\bar{\sigma}\left(\bar{\varepsilon}\right)d\bar{\varepsilon}dV+\frac{3}{2}\int_V k_V\varepsilon_0^2dV-\int_{S_\sigma}\sigma_i u_i\,dS$$

Flow formulation

$$J=\int_V\left(\int_0^{\bar{\xi}}\bar{\sigma}\left(\bar{\xi}\right)d\bar{\xi}\right)dV+\int_V\sigma_0\xi_0dV-\int_S\sigma_i v_i dS$$

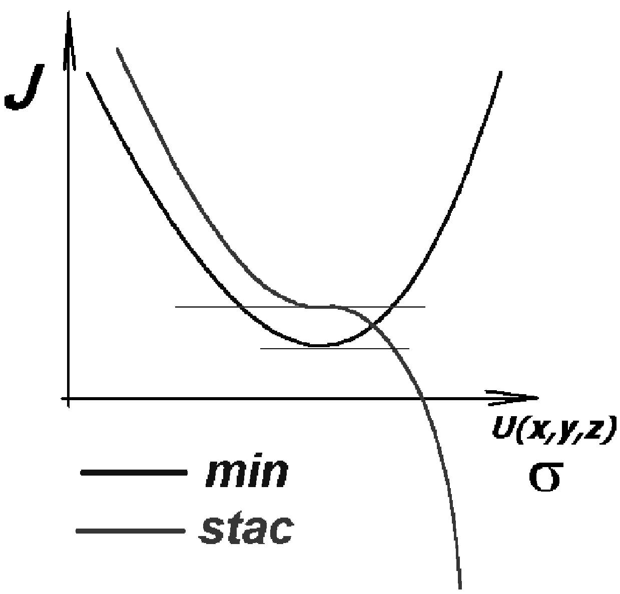

Penalty method

$$J = \int_V \left(\int_0^{\bar{\xi}} \bar{\sigma}\left(\bar{\xi}\right) d\bar{\xi} \right) dV + K_{pen} \int_V \xi_0^2 dV - \int_S \sigma_i v_i dS$$

$\boldsymbol{K_{pen}}$ – penalty multiplier

$$K_{pen} \rightarrow \infty$$

$$\xi_0 \rightarrow 0$$

$$\sigma_0 \approx K_{pen} \xi_0$$

Penalty method. Hagen–Poiseuille test.

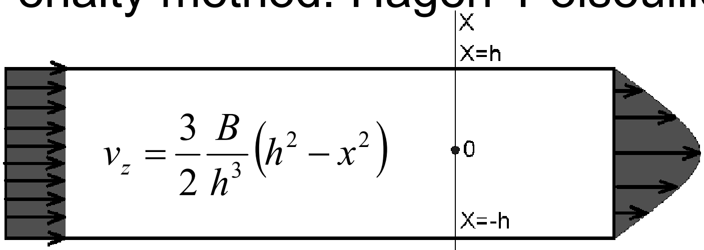

$$v_z = \frac{3}{2} \frac{B}{h^3} \left(h^2 - x^2 \right)$$

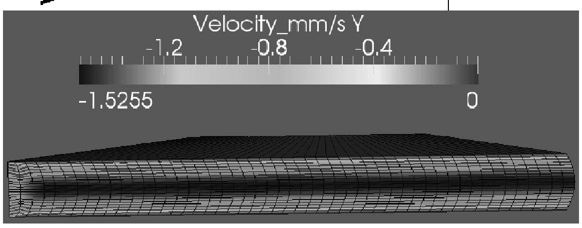

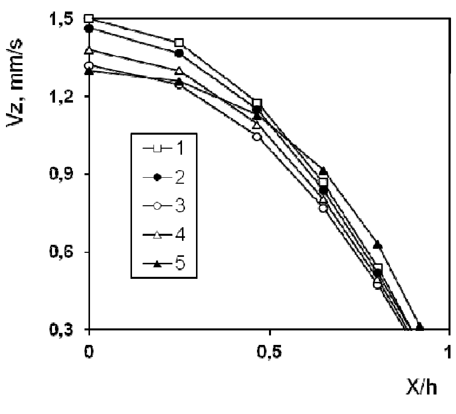

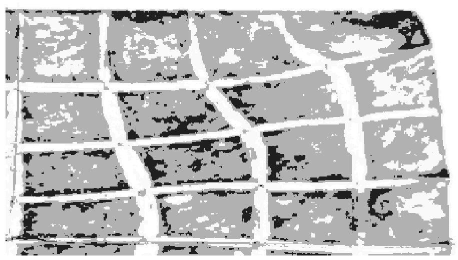

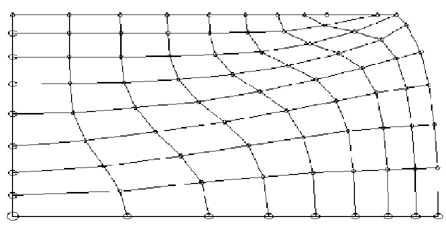

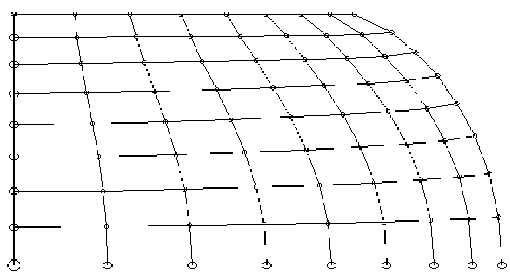

Nonlinear property of material

$$J = \int_V \left(\int_0^{\bar{\xi}} \bar{\sigma}\left(\bar{\xi}\right) d\bar{\xi} \right) dV + \int_V \sigma_0 \xi_0 dV - \int_S \sigma_i v_i dS$$

$$\bar{\sigma}\left(\bar{\xi}\right) = \mu \bar{\xi}$$

$$J = \int_V \frac{1}{2} \mu \bar{\xi}^2 dV + \int_V \sigma_0 \xi_0 dV - \int_S \sigma_i v_i dS \qquad \mu = \frac{\bar{\sigma}\left(\bar{\xi}\right)}{\bar{\xi}}$$

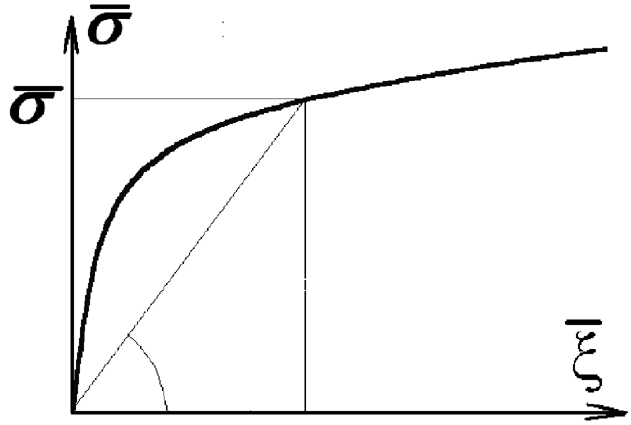

Boundary conditions

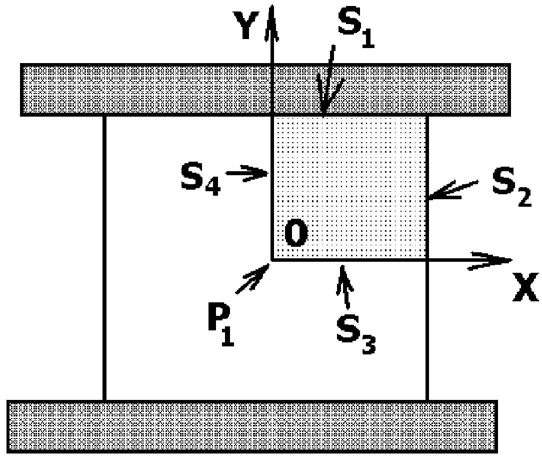

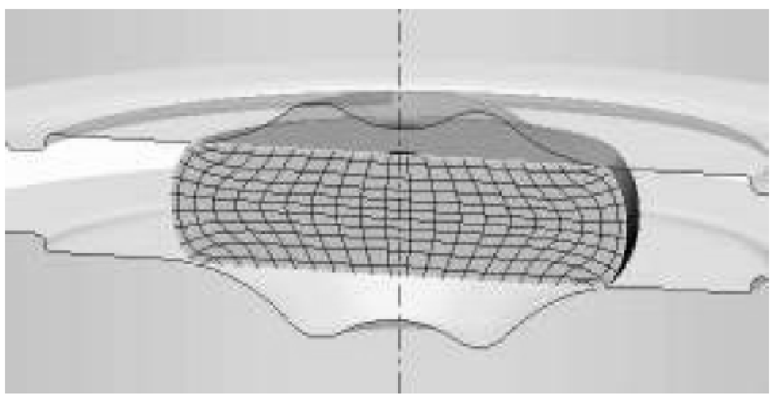

Boundary conditions

- S_1 $\quad v_y = -v_{tool}\,;\tau_{fric} = \sigma_{xy} = \sigma_{fric}\dfrac{v_x}{|v_x|} = \sigma_{fric}\,sign\,(v_x)$
- S_2 $\quad \sigma_x = \sigma_n = 0;\ \sigma_{xy} = 0;\ v_x = ?;\ v_y = ?$
- S_3 $\quad \sigma_{xy} = 0;\ v_y = 0;\ v_x = ?$
- S_4 $\quad \sigma_{xy} = 0; v_x = 0; v_y = ?$
- P_1 $\quad v_x = 0;\ v_y = 0;\ \sigma_{xy} = 0$
- P_2 $\quad v_x = 0;\quad v_y = -v_{tool}\,;\quad \sigma_{xy} = 0$

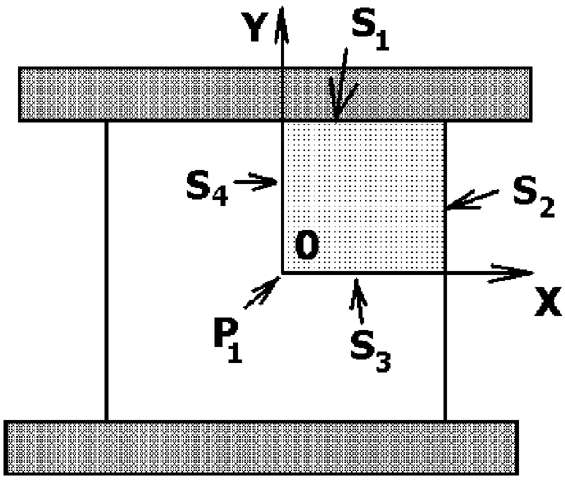

Boundary conditions

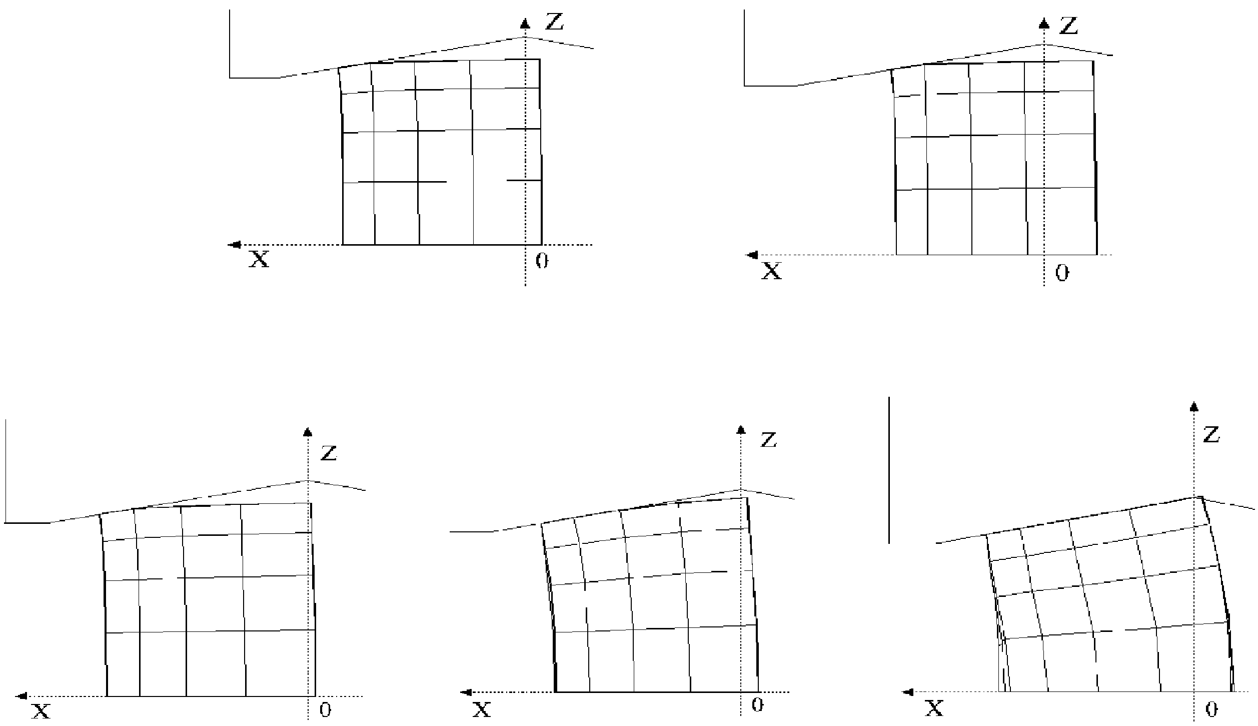

Boundary conditions

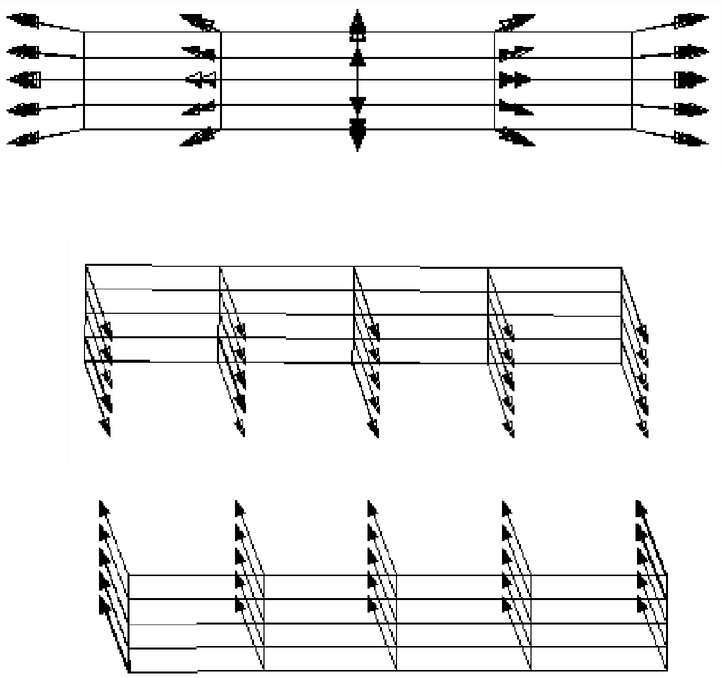

The computer simulation of the hot metal forming processes
Milenin Andrzej, AGH University of Science and Technology, 2012
AKADEMIA GÓRNICZO-HUTNICZA IM. STANISŁAWA STASZICA W KRAKOWIE
AGH

Boundary conditions

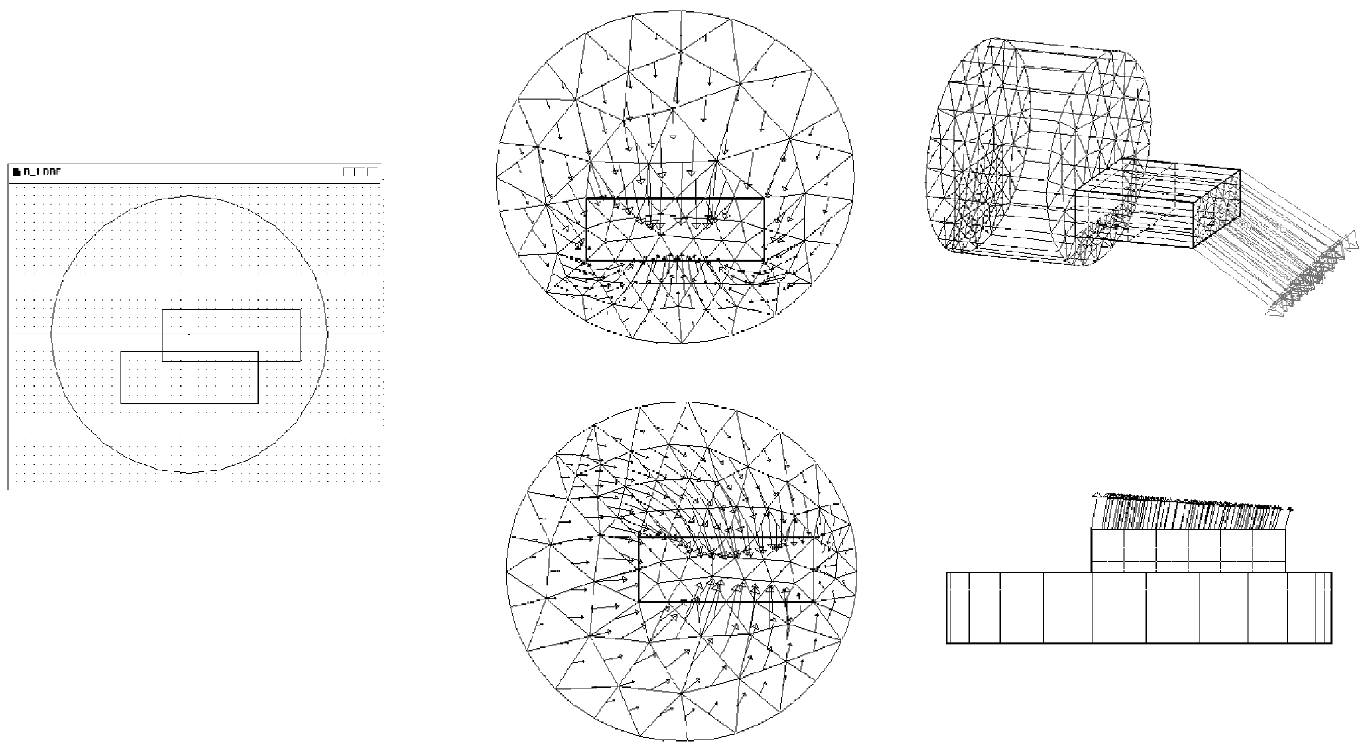

Boundary conditions

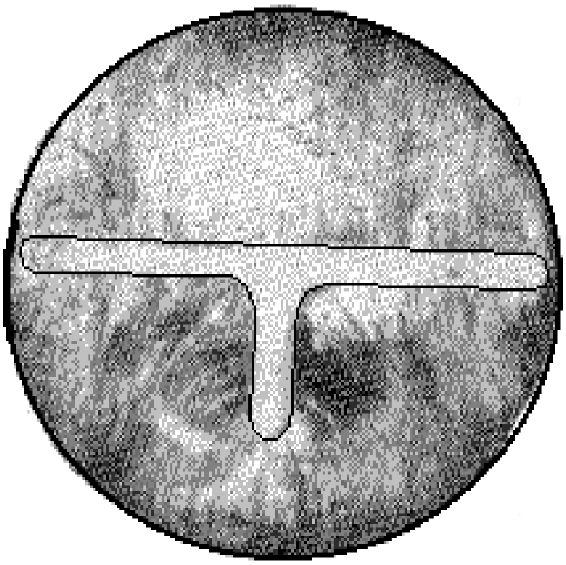

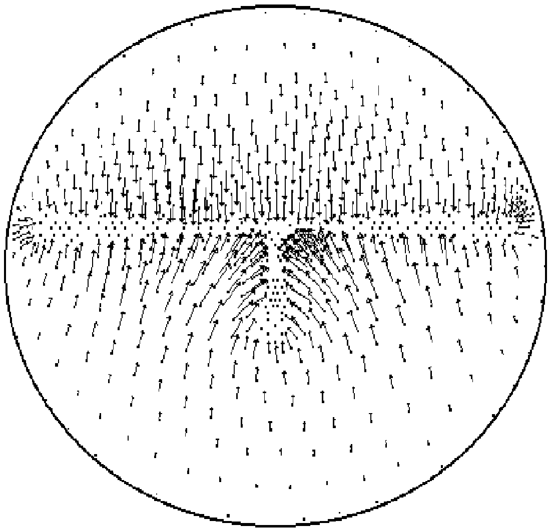

The computer simulation of the hot metal forming processes
Milenin Andrzej, AGH University of Science and Technology, 2012
AKADEMIA GÓRNICZO-HUTNICZA IM. STANISŁAWA STASZICA W KRAKOWIE
AGH

Lection 2

Formulation of the boundary-value problem, which allows of simulating hot deformation of metals.
Bases of the finite elements method.

Formulation of the boundary-value problem, which allows of simulating hot deformation of metals

- Equilibrium equations:

$$\sigma_{ij,i} = 0, \qquad (1)$$

- compatibility condition:

$$\xi_{ij} = \frac{1}{2}\left(v_{i,j} + v_{j,i}\right), \qquad (2)$$

- constitutive equations:

$$s_{ij} = \frac{2\overline{\sigma}}{3\overline{\xi}}\xi_{ij}, \qquad (3)$$

- incompressibility equation:

$$v_{i,j} = 0, \qquad (4)$$

- energy balance equation:

$$div\left(k\ grad\ (t)\right) + \beta\overline{\sigma}\overline{\xi} = c\rho\frac{dt}{d\tau} \qquad (5)$$

- and expression for flow stress:

$$\overline{\sigma} = \overline{\sigma}\left(\varepsilon, \overline{\xi}, t\right), \qquad (6)$$

σ_{ij} – stress tensor, ξ_{ij} – strain rate tensor and v_i – velocity component, $\sigma^{`}_{ij}$ – deviator of stress tensor, $\overline{\sigma}, \overline{\varepsilon}, \overline{\xi}$ – effective stress, effective strain and effective strain-rate, t – temperature, β – heat generation efficiency which is usually assumed as β=0.9-9.95, k – thermal conductivity.

Main conception of FEM

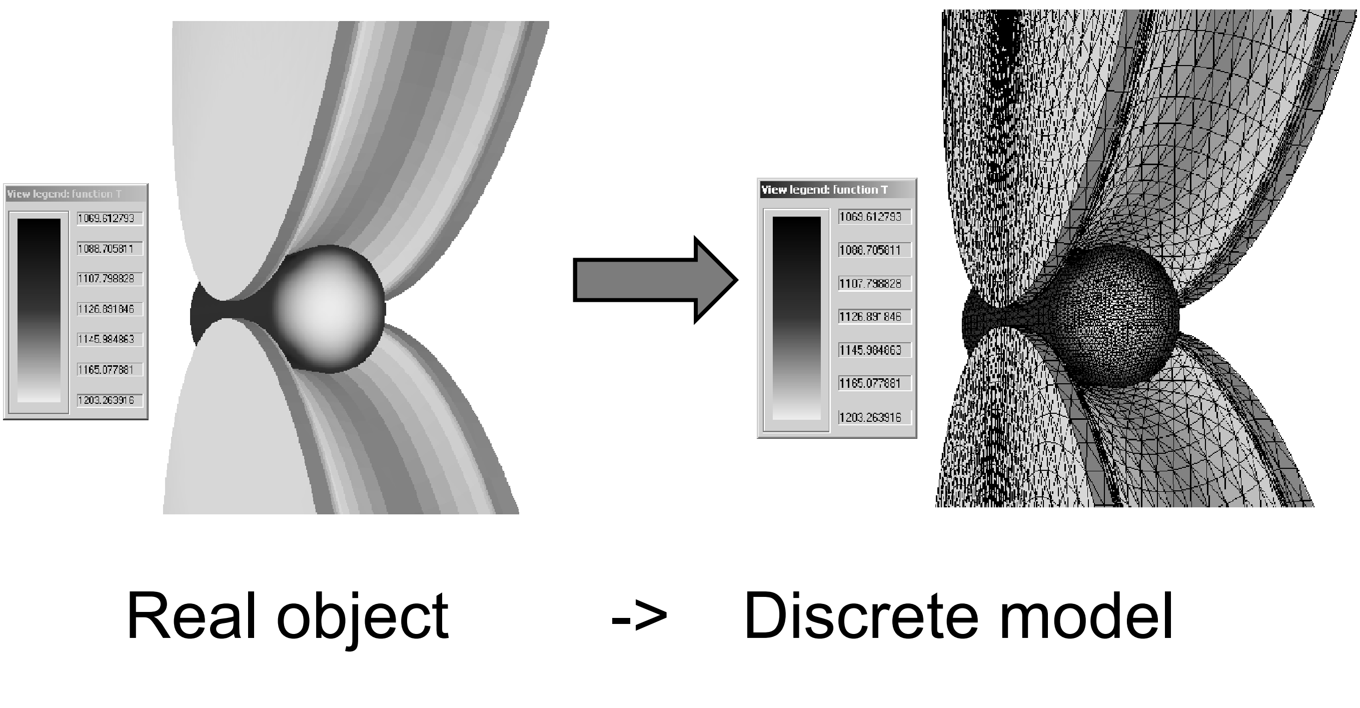

Real object -> Discrete model

Algorithm FEM

1. In the continuum, we are taking a limited number of points (nodes).
2. The values of temperature (or other features) on each node is defined as a parameters, which we designate.
3. Zone designation of temperature is composed of a limited number of zones, which are finite elements.
4. The temperature is approximated for each FE by using the polynomial, which is designated using nodal temperatures.
5. Value of temperature on nodes must be selected in such a way as to ensure the best approximation to the actual field temperatures. Such selection is performed by means of minimizing a functional, which corresponds to both the equation conduction of heat.

Discretization

One-dimensional example:

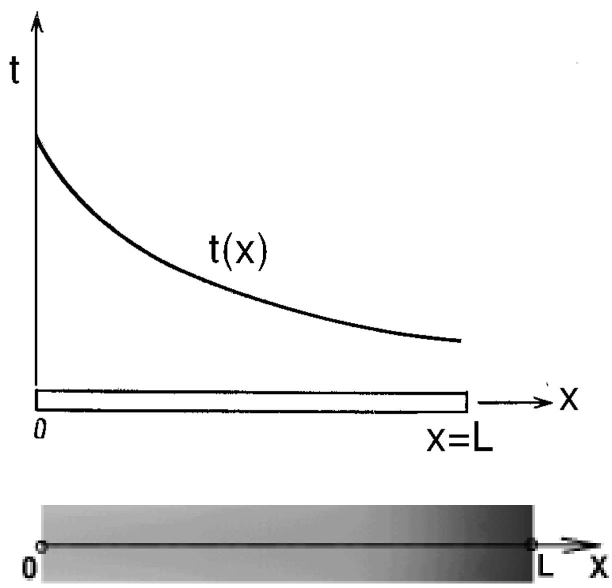

1d temperature distribution in bar

Discretization

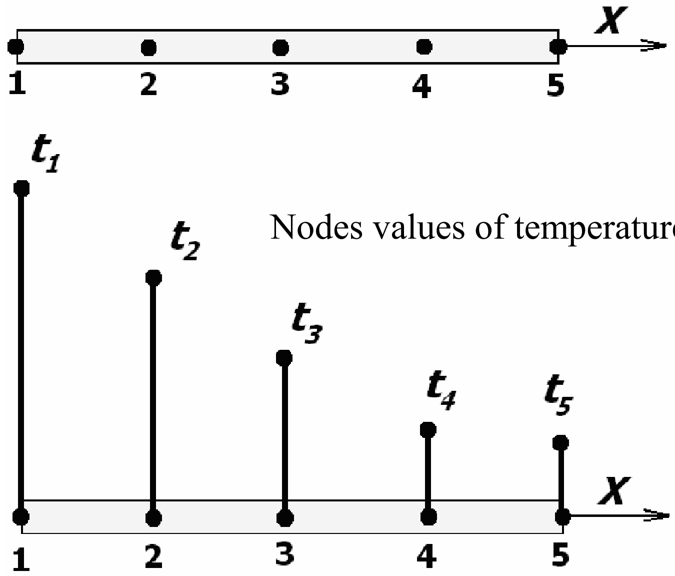

1. In the continuum, we are taking a limited number of points (nodes).

2. The values of temperature (or other features) on each node is defined as a parameters, which we designate.

The computer simulation of the hot metal forming processes
Milenin Andrzej, AGH University of Science and Technology, 2012
AKADEMIA GÓRNICZO-HUTNICZA IM. STANISŁAWA STASZICA W KRAKOWIE
AGH

Finite Elements

3. Zone designation of temperature is composed of a limited number of zones, which are finite elements.

4. The temperature is approximated for each FE by using the polynomial, which is designated using nodal temperatures.

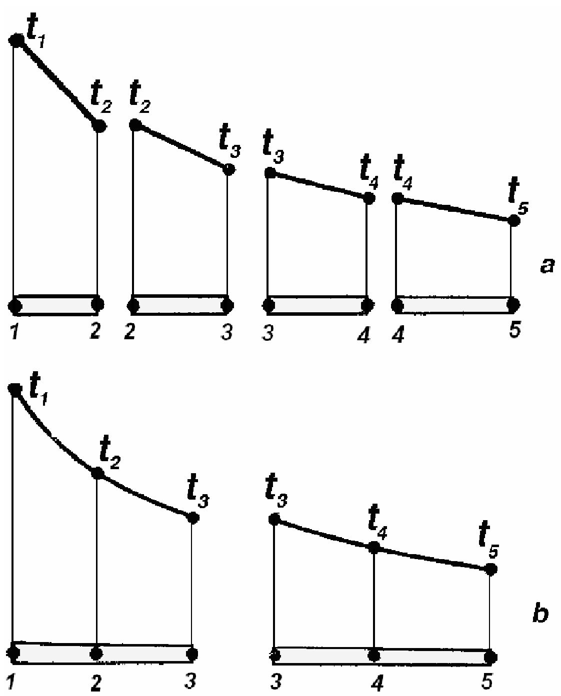

Approximation of temperature in two kinds of FE

Global interpolation of temperature

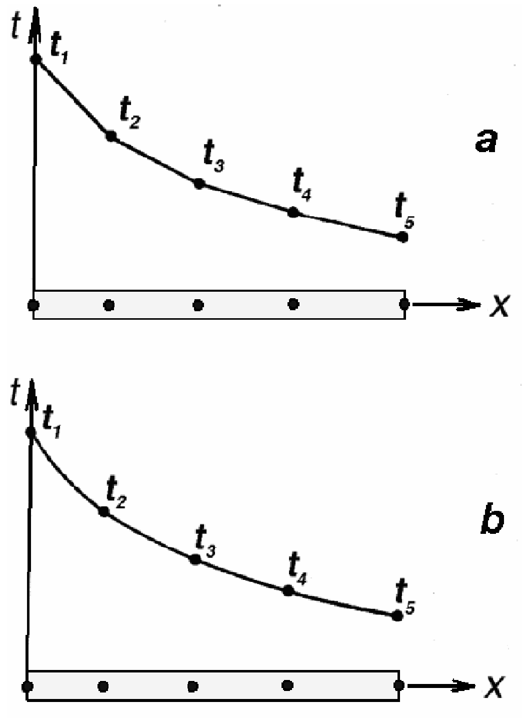

1-D finite element

$$t = a_1 + a_2 X$$

$$t = t_i \quad for \ X = X_i$$
$$t = t_j \quad for \ X = X_j$$

$$\left.\begin{array}{l} t_i = a_1 + a_2 X_i \\ t_j = a_1 + a_2 X_j \end{array}\right\}$$

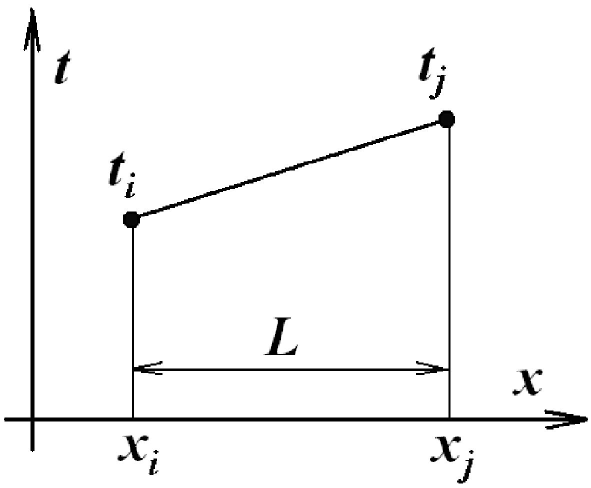

$$\boxed{a_1 = \frac{t_i X_j - t_j X_i}{L} \qquad a_2 = \frac{t_j - t_i}{L}}$$

Shape functions

$$t = \left(\frac{t_i X_j - t_j X_i}{L}\right) + \left(\frac{t_j - t_i}{L}\right) X$$

$$t = \left(\frac{X_j - X}{L}\right) t_i + \left(\frac{X - X_i}{L}\right) t_j$$

$$N_i = \frac{X_j - X}{L} \qquad N_j = \frac{X - X_i}{L}$$

$$t = N_i t_i + N_j t_j = [N]\{t\}$$

$$\{t\} = \begin{Bmatrix} t_i \\ t_j \end{Bmatrix} \qquad [N] = \lfloor N_i ; N_j \rfloor$$

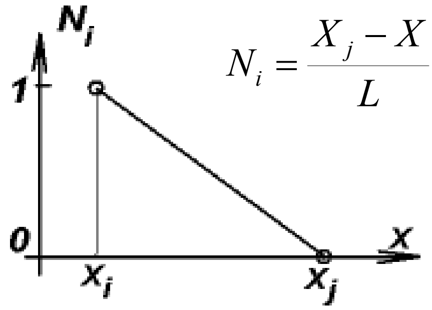

$$N_i = \frac{X_j - X}{L}$$

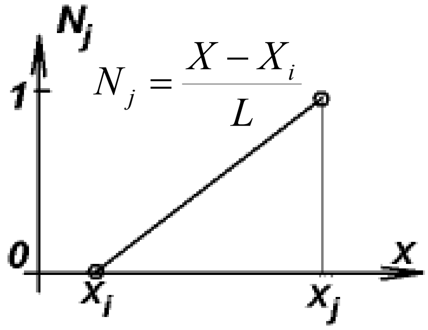

$$N_j = \frac{X - X_i}{L}$$

$$\boxed{\sum_{\beta=1}^{n} N_\beta = 1}$$

2D Finite Elements

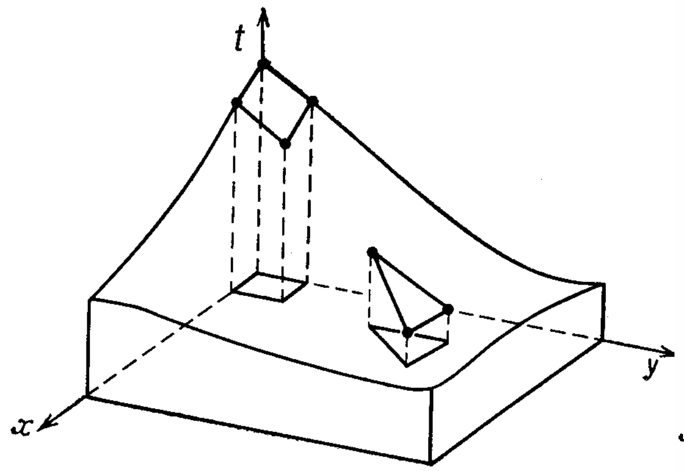

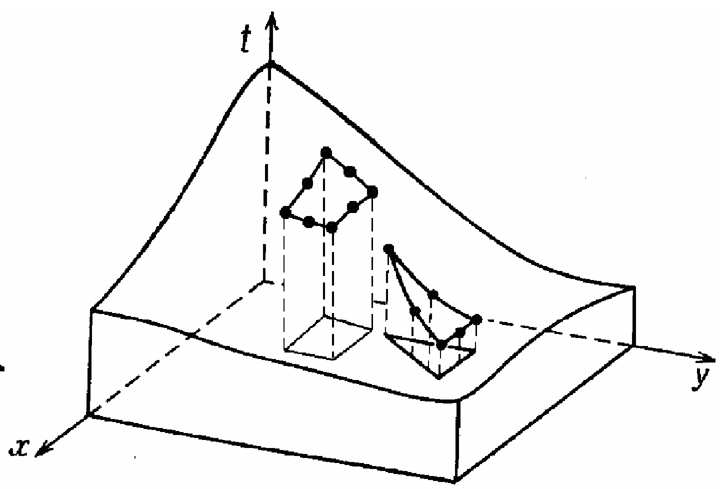

2D simplex finite element

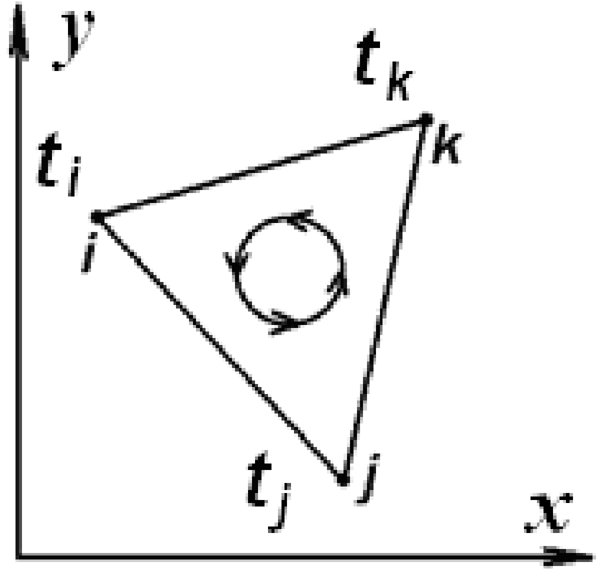

The computer simulation of the hot metal forming processes
Milenin Andrzej, AGH University of Science and Technology, 2012
AKADEMIA GÓRNICZO-HUTNICZA IM. STANISŁAWA STASZICA W KRAKOWIE
AGH

Shape functions of 2d simplex element

$$\left.\begin{aligned} &for\ X = X_i, Y = Y_i\ \ t = t_i, \Rightarrow t_i = a_1 + a_2 X_i + a_3 Y_i \\ &for\ X = X_j, Y = Y_j\ \ t = t_j, \Rightarrow t_j = a_1 + a_2 X_j + a_3 Y_j \\ &for\ X = X_k, Y = Y_k\ \ t = t_k, \Rightarrow t_k = a_1 + a_2 X_k + a_3 Y_k \end{aligned}\right\}$$

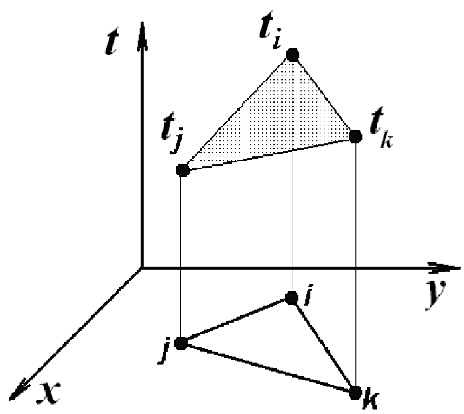

$$a_1 = \frac{1}{2A}\left[\left(X_j Y_k - X_k Y_j\right)t_i + \left(X_k Y_i - X_i Y_k\right)t_j + \left(X_i Y_j - X_j Y_i\right)t_k\right]$$

$$a_2 = \frac{1}{2A}\left[\left(Y_j - Y_k\right)t_i + \left(Y_k - Y_i\right)t_j + \left(Y_i - Y_j\right)t_k\right]$$

$$a_3 = \frac{1}{2A}\left[\left(X_k - X_j\right)t_i + \left(X_i - X_k\right)t_j + \left(X_j - X_i\right)t_k\right]$$

$$2A = \begin{vmatrix} 1 & X_i & Y_i \\ 1 & X_j & Y_j \\ 1 & X_k & Y_k \end{vmatrix} = X_j Y_k + X_i Y_j + X_k Y_i - X_j Y_i - X_k Y_j - X_i Y_k$$

A – area of FE

Shape functions of 2d simplex element

$$\boxed{\varphi = \varphi_i N_i + \varphi_j N_j + \varphi_k N_k = \{N\}^T \cdot \{\varphi\}}$$

$$t = t_i N_i + t_j N_j + t_k N_k = \{N\}^T \cdot \{t\}$$

$$\boxed{N_i = \frac{1}{2A}(a_i + b_i X + c_i Y)}$$

$$a_i = X_j Y_k - X_k Y_j$$
$$b_i = Y_j - Y_k$$
$$c_i = X_k - X_j$$

$$\boxed{N_j = \frac{1}{2A}(a_j + b_j X + c_j Y)}$$

$$a_j = X_k Y_i - X_i Y_k$$
$$b_j = Y_k - Y_i$$
$$c_j = X_i - X_k$$

$$\boxed{N_k = \frac{1}{2A}(a_k + b_k X + c_k Y)}$$

$$a_k = X_i Y_j - X_j Y_i$$
$$b_k = Y_i - Y_j$$
$$c_k = X_j - X_i$$

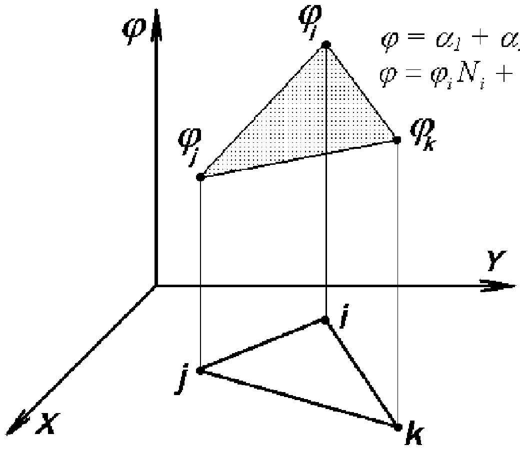

$$\varphi = \alpha_1 + \alpha_2 X + \alpha_3 Y$$
$$\varphi = \varphi_i N_i + \varphi_j N_j + \varphi_k N_k$$

The computer simulation of the hot metal forming processes
Milenin Andrzej, AGH University of Science and Technology, 2012
AKADEMIA GÓRNICZO-HUTNICZA IM. STANISŁAWA STASZICA W KRAKOWIE AGH

L – coordinates (natural coordinates)

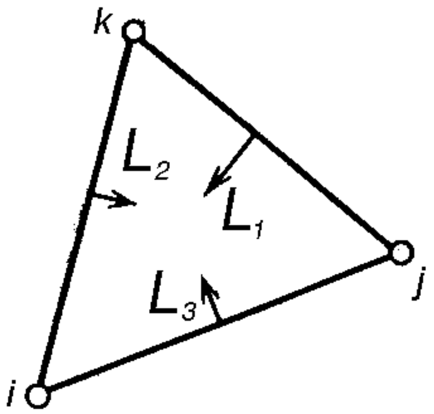

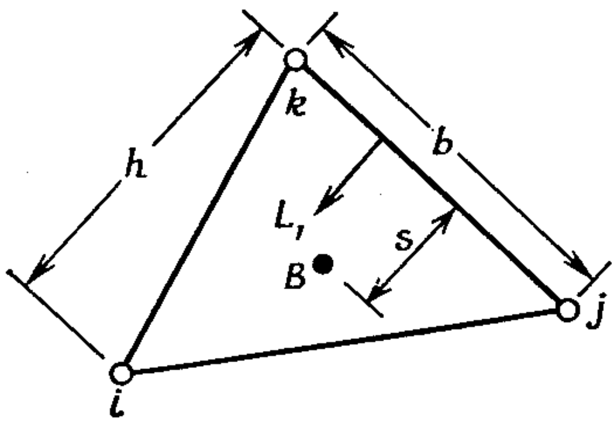

L – coordinates (natural coordinates)

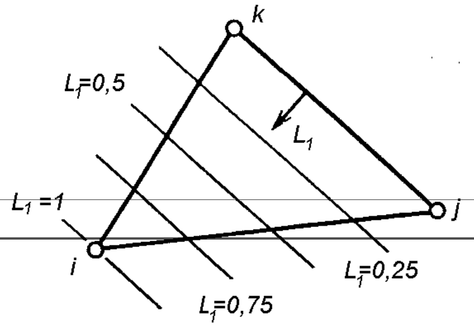

$$A = \frac{bh}{2} \qquad A_1 = \frac{bs}{2} \qquad \frac{A_1}{A} = \frac{s}{h} = L_1 \qquad L_1 = \frac{A_1}{A}$$

$$A_1 + A_2 + A_3 = A$$

$$L_1 + L_2 + L_3 = 1$$

$$N_i = L_1 \qquad L_1 = 1$$
$$N_j = L_2 \qquad L_1 = 0$$
$$N_k = L_3 \qquad L_1 = 0$$

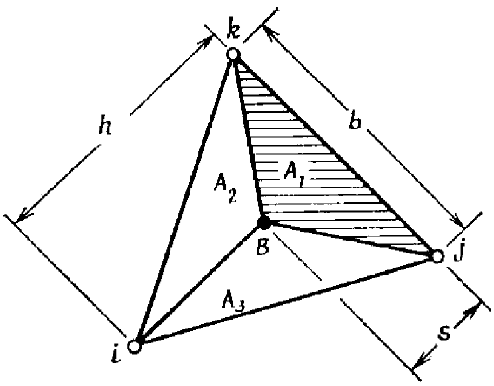

$$x = L_1 X_i + L_2 X_j + L_3 X_k$$
$$y = L_1 Y_i + L_2 Y_j + L_3 Y_k$$
$$1 = L_1 + L_2 + L_3$$

The computer simulation of the hot metal forming processes
Milenin Andrzej, AGH University of Science and Technology, 2012
AKADEMIA GÓRNICZO-HUTNICZA IM. STANISŁAWA STASZICA W KRAKOWIE
AGH

6 – nodes FE

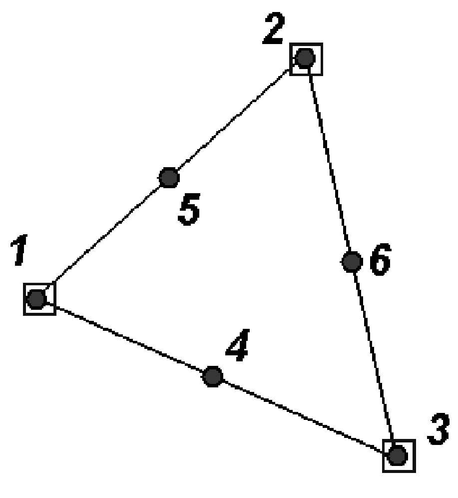

$$N_1 = L_1(2L_1 - 1)$$
$$N_2 = L_2(2L_2 - 1)$$
$$N_3 = L_3(2L_3 - 1)$$
$$N_4 = 4L_1L_3$$
$$N_5 = 4L_1L_2$$
$$N_6 = 4L_2L_3$$

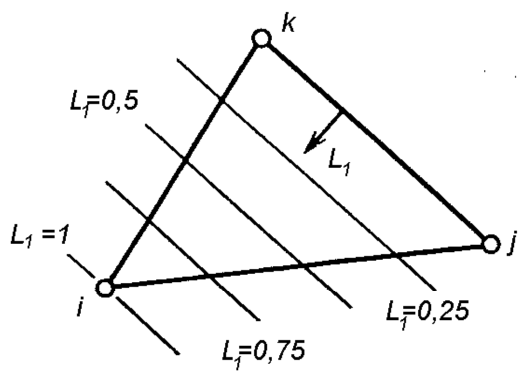

Types of FE

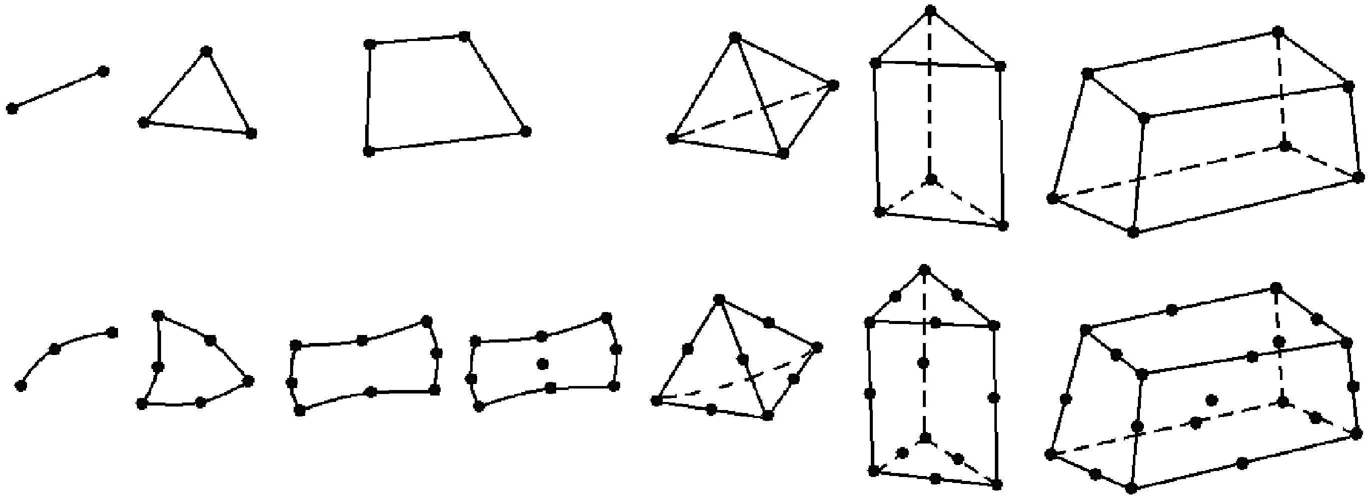

Motivation

1. Error in approximation

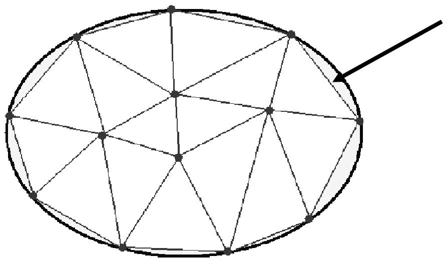

ΔS_j $\quad \Delta S = \sum_{N_j} \Delta S_j$

2. Error during differentiation

$$\sigma_x = \sigma_0 + \frac{2\overline{\sigma}}{3\overline{\xi}}\xi_x; \qquad \xi_x = \frac{\partial v_x}{\partial x}$$

3. Locking

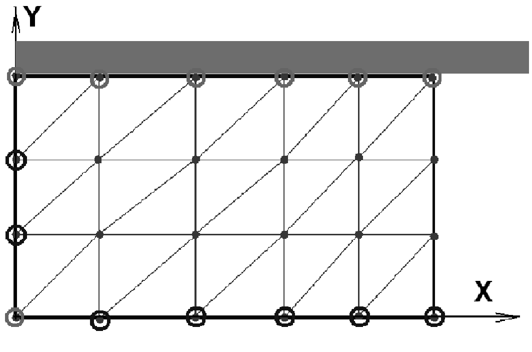

DOF = 2*10+7=27

Ncond = ne = 30

DOF<Ncond

4-nodes FE

$$\varphi = \alpha_1 + \alpha_2 x + \alpha_3 y + \alpha_4 xy$$

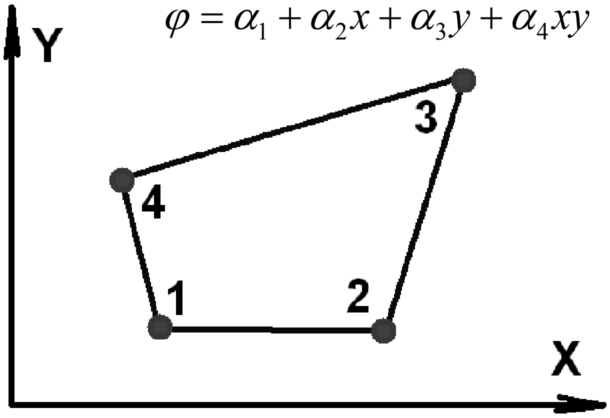

$$\varphi_1 = \alpha_1 + \alpha_2 x_1 + \alpha_3 y_1 + \alpha_4 x_1 y_1$$

$$\varphi_2 = \alpha_1 + \alpha_2 x_2 + \alpha_3 y_2 + \alpha_4 x_2 y_2$$

$$\varphi_3 = \alpha_1 + \alpha_2 x_3 + \alpha_3 y_3 + \alpha_4 x_3 y_3$$

$$\varphi_4 = \alpha_1 + \alpha_2 x_4 + \alpha_3 y_4 + \alpha_4 x_4 y_4$$

$$\boxed{\begin{array}{l} \dfrac{\partial \varphi}{\partial x} \neq const \\ \dfrac{\partial \varphi}{\partial y} \neq const \end{array}}$$

Shape functions ?

$$\varphi = N_1\varphi_1 + N_2\varphi_2 + N_3\varphi_3 + N_4\varphi_4$$

The computer simulation of the hot metal forming processes
Milenin Andrzej, AGH University of Science and Technology, 2012
AKADEMIA GÓRNICZO-HUTNICZA IM. STANISŁAWA STASZICA W KRAKOWIE AGH

Rectangular FE

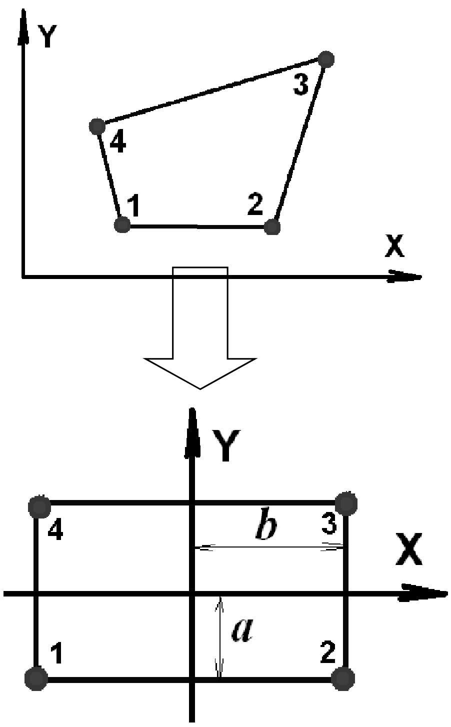

$$\varphi = \alpha_1 + \alpha_2 x + \alpha_3 y + \alpha_4 xy$$

$$\alpha_1 = \frac{\varphi_1 + \varphi_2 + \varphi_3 + \varphi_4}{4}$$

$$\alpha_2 = \frac{-\varphi_1 + \varphi_2 + \varphi_3 - \varphi_4}{4b}$$

$$\alpha_3 = \frac{-\varphi_1 - \varphi_2 + \varphi_3 + \varphi_4}{4a}$$

$$\alpha_4 = \frac{\varphi_1 - \varphi_2 + \varphi_3 - \varphi_4}{4ab}$$

Rectangular FE

Shape functions:

$$\varphi = \alpha_1 + \alpha_2 x + \alpha_3 y + \alpha_4 xy$$

$$\varphi = N_1\varphi_1 + N_2\varphi_2 + N_3\varphi_3 + N_4\varphi_4$$

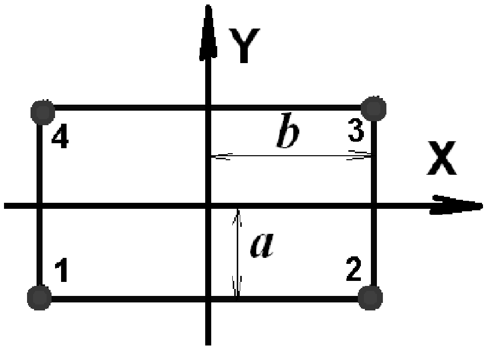

$$N_1 = \frac{1}{4ab}(b-x)(a-y)$$

$$N_2 = \frac{1}{4ab}(b+x)(a-y)$$

$$N_3 = \frac{1}{4ab}(b+x)(a+y)$$

$$N_4 = \frac{1}{4ab}(b-x)(a+y)$$

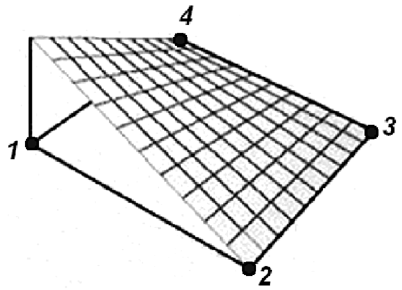

$$N_1 = \frac{1}{4ab}(b-x)(a-y)$$

Shape functions in local coordinate system

$$N_1 = \frac{1}{4ab}(b-x)(a-y) = \frac{1}{4}\left(1-\frac{x}{b}\right)\left(1-\frac{y}{a}\right) = \frac{1}{4}(1-\xi)(1-\eta)$$

$$N_2 = \frac{1}{4ab}(b+x)(a-y) = \frac{1}{4}\left(1+\frac{x}{b}\right)\left(1-\frac{y}{a}\right) = \frac{1}{4}(1+\xi)(1-\eta)$$

$$N_3 = \frac{1}{4ab}(b+x)(a+y) = \frac{1}{4}\left(1+\frac{x}{b}\right)\left(1+\frac{y}{a}\right) = \frac{1}{4}(1+\xi)(1+\eta)$$

$$N_4 = \frac{1}{4ab}(b-x)(a+y) = \frac{1}{4}\left(1-\frac{x}{b}\right)\left(1+\frac{y}{a}\right) = \frac{1}{4}(1-\xi)(1+\eta)$$

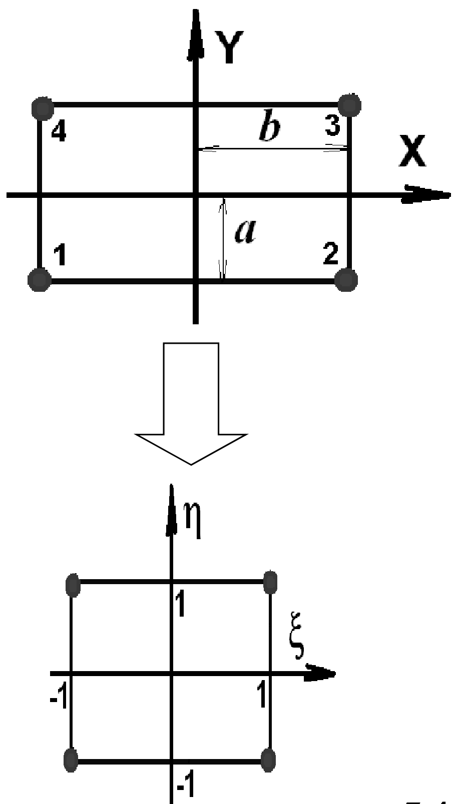

$$\xi = \frac{x}{b} \quad \eta = \frac{y}{a}$$

$$x = b\xi \quad y = a\eta$$

Types of FE

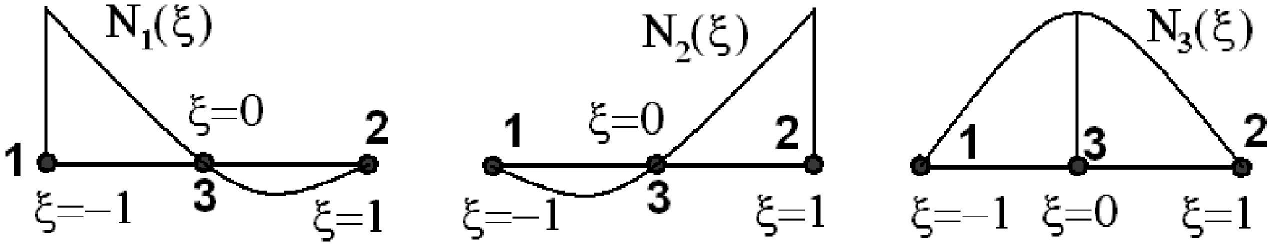

$$N_1(\xi) = -\frac{1}{2}\xi(1-\xi) \qquad N_3(\xi) = 1-\xi^2$$

$$N_2(\xi) = \frac{1}{2}\xi(1+\xi)$$

The computer simulation of the hot metal forming processes
Milenin Andrzej, AGH University of Science and Technology, 2012
AKADEMIA GÓRNICZO-HUTNICZA IM. STANISŁAWA STASZICA W KRAKOWIE

Types of FE

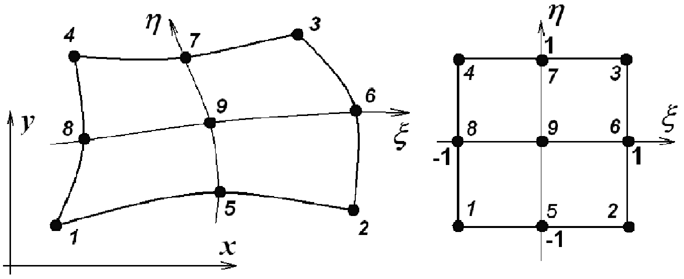

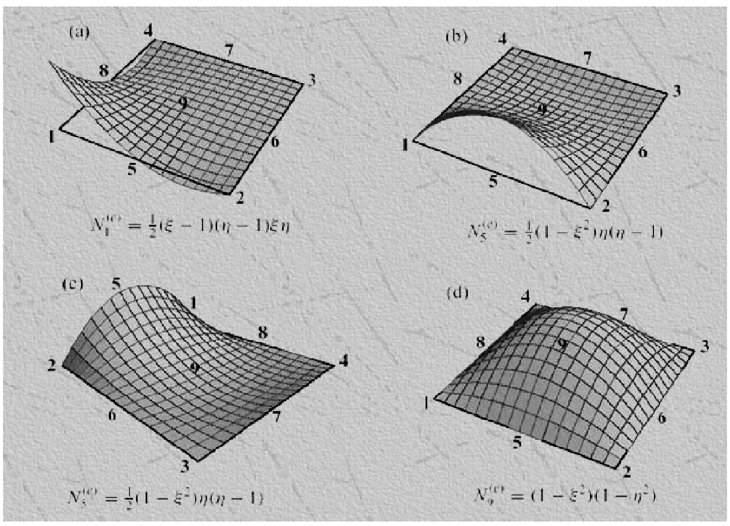

$$N_1 = \frac{1}{4}(1-\xi)(1-\eta)\xi\eta$$

$$N_2 = -\frac{1}{4}(1+\xi)(1-\eta)\xi\eta$$

$$N_3 = \frac{1}{4}(1+\xi)(1+\eta)\xi\eta$$

$$N_4 = -\frac{1}{4}(1-\xi)(1+\eta)\xi\eta$$

$$N_5 = -\frac{1}{2}(1-\xi^2)(1-\eta)\eta$$

$$N_6 = \frac{1}{2}(1+\xi)(1-\eta^2)\xi$$

$$N_7 = \frac{1}{2}(1-\xi^2)(1+\eta)\eta$$

$$N_8 = -\frac{1}{2}(1-\xi)(1-\eta^2)\xi$$

$$N_9 = (1-\xi^2)(1-\eta^2).$$

Types of FE

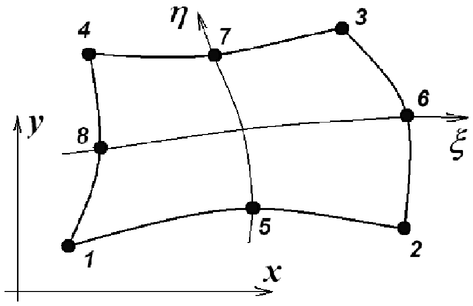

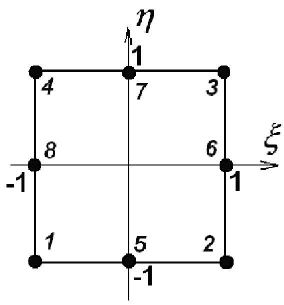

$$N_1 = -\frac{1}{4}(1-\xi)(1-\eta)(\xi+\eta+1)$$

$$N_2 = \frac{1}{4}(1+\xi)(1-\eta)(\xi-\eta-1)$$

$$N_3 = \frac{1}{4}(1+\xi)(1+\eta)(\xi+\eta-1)$$

$$N_4 = -\frac{1}{4}(1-\xi)(1+\eta)(\xi-\eta+1)$$

$$N_5 = \frac{1}{2}(1-\xi^2)(1-\eta)$$

$$N_6 = \frac{1}{2}(1-\eta^2)(1+\xi)$$

$$N_7 = \frac{1}{2}(1-\xi^2)(1+\eta)$$

$$N_8 = \frac{1}{2}(1-\eta^2)(1-\xi).$$

4-nodes 3d simplex FE

$$L_1 + L_2 + L_3 + L_4 = 1$$

$$N_1 = L_1$$

$$N_2 = L_2$$

$$N_3 = L_3$$

$$N_4 = L_4$$

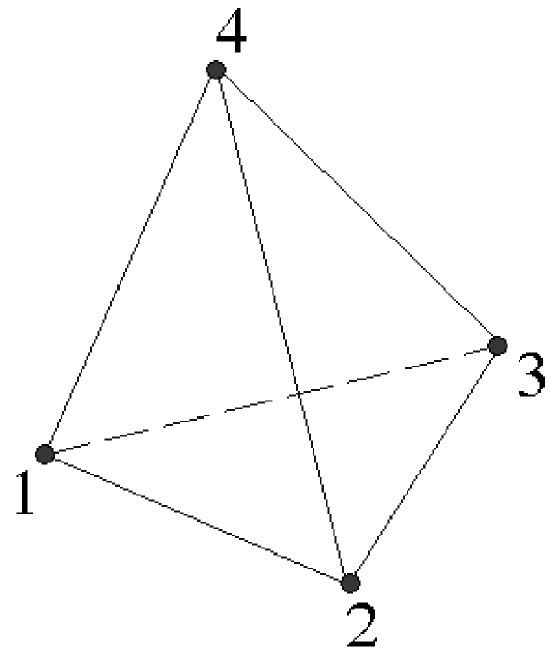

10-nodes 3d FE

$$N_1 = (2L_1 - 1)L_1$$
$$N_2 = (2L_2 - 1)L_2$$
$$N_3 = (2L_3 - 1)L_3$$
$$N_4 = (2L_4 - 1)L_4$$

$$N_5 = 4L_1L_2 \quad N_8 = 4L_1L_4$$
$$N_6 = 4L_2L_3 \quad N_9 = 4L_2L_4$$
$$N_7 = 4L_1L_3 \quad N_{10} = 4L_3L_4$$

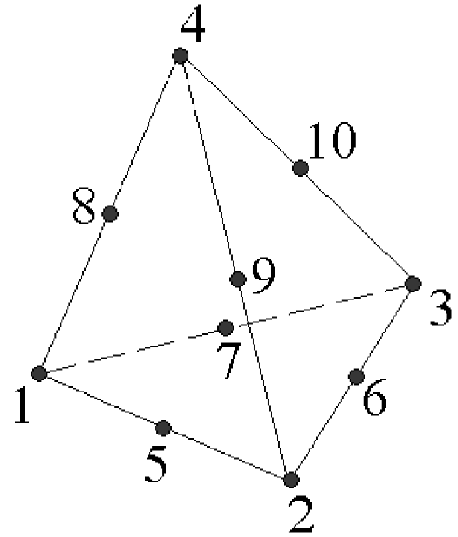

$$L_1 + L_2 + L_3 + L_4 = 1$$

8-nodes 3d FE

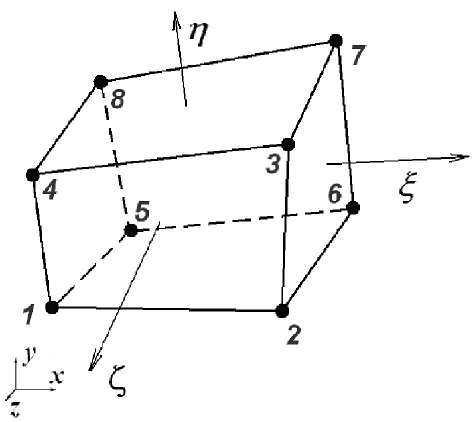

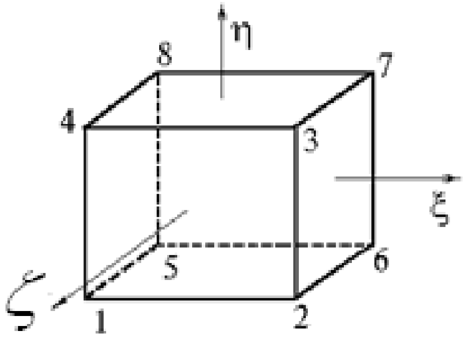

$$N_1 = \frac{1}{8}(1-\xi)(1-\eta)(1+\zeta)$$
$$N_2 = \frac{1}{8}(1+\xi)(1-\eta)(1+\zeta)$$
$$N_3 = \frac{1}{8}(1+\xi)(1+\eta)(1+\zeta)$$
$$N_4 = \frac{1}{8}(1-\xi)(1+\eta)(1+\zeta)$$
$$N_5 = \frac{1}{8}(1-\xi)(1-\eta)(1-\zeta)$$
$$N_6 = \frac{1}{8}(1+\xi)(1-\eta)(1-\zeta)$$
$$N_7 = \frac{1}{8}(1+\xi)(1+\eta)(1-\zeta)$$
$$N_8 = \frac{1}{8}(1-\xi)(1+\eta)(1-\zeta).$$

15 nodes prismatic 3d FE

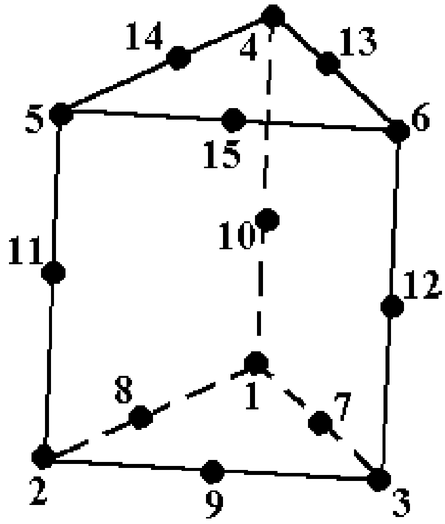

$$N_1 = \frac{1}{2}L_1(2L_1-1)(1-\xi) - \frac{1}{2}L_1(1-\xi^2)$$
$$N_2 = \frac{1}{2}L_2(2L_2-1)(1-\xi) - \frac{1}{2}L_2(1-\xi^2)$$
$$N_3 = \frac{1}{2}L_3(2L_3-1)(1-\xi) - \frac{1}{2}L_3(1-\xi^2)$$
$$N_4 = \frac{1}{2}L_1(2L_1-1)(1+\xi) - \frac{1}{2}L_1(1-\xi^2)$$
$$N_5 = \frac{1}{2}L_2(2L_2-1)(1+\xi) - \frac{1}{2}L_2(1-\xi^2)$$
$$N_6 = \frac{1}{2}L_3(2L_3-1)(1+\xi) - \frac{1}{2}L_3(1-\xi^2)$$
$$N_7 = 2L_3L_1(1-\xi)$$
$$N_8 = 2L_2L_1(1-\xi)$$
$$N_9 = 2L_3L_2(1-\xi)$$
$$N_{10} = L_1(1-\xi^2)$$
$$N_{11} = L_2(1-\xi^2)$$
$$N_{12} = L_3(1-\xi^2)$$
$$N_{13} = 2L_3L_1(1+\xi)$$
$$N_{14} = 2L_2L_1(1+\xi)$$
$$N_{15} = 2L_3L_2(1+\xi)$$

Transformation of coordinates

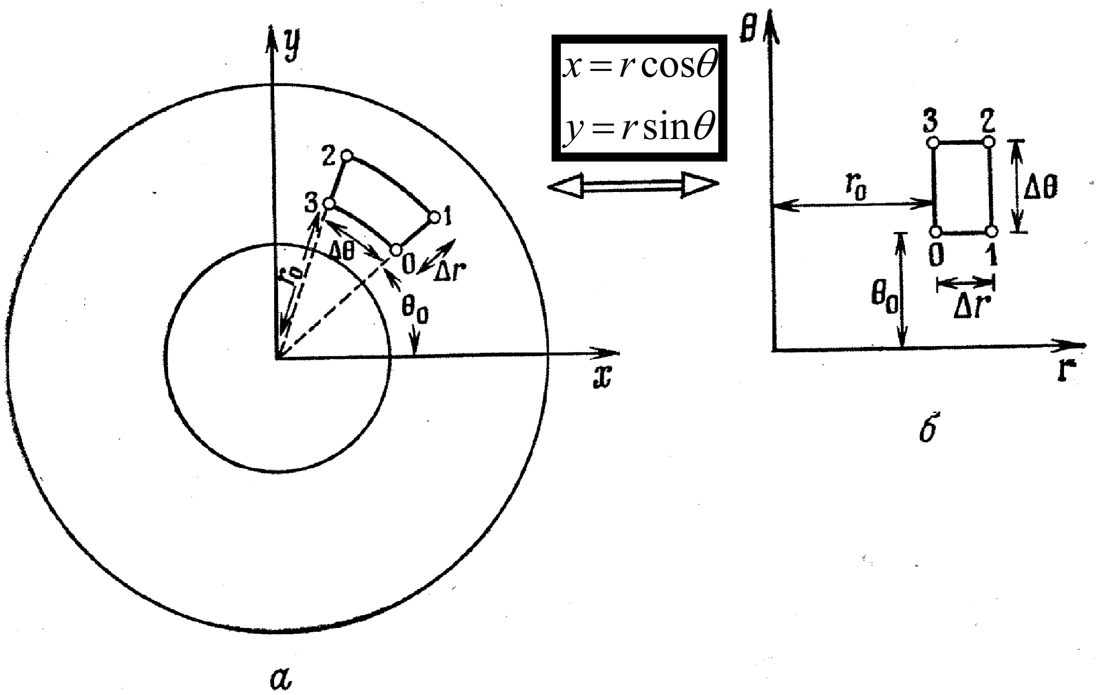

$$x = r\cos\theta$$
$$y = r\sin\theta$$

Jacobian matrix

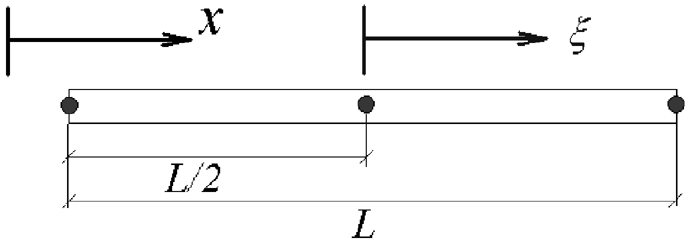

$$-1 \le \xi \le 1$$

$$X = X(\xi) \qquad \xi = \xi(x)$$

$$J = \left| \frac{dX(\xi)}{d\xi} \right| \qquad J = \begin{vmatrix} \dfrac{\partial X(\xi,\eta)}{\partial \xi} & \dfrac{\partial Y(\xi,\eta)}{\partial \xi} \\ \dfrac{\partial X(\xi,\eta)}{\partial \eta} & \dfrac{\partial Y(\xi,\eta)}{\partial \eta} \end{vmatrix} \qquad J = \begin{vmatrix} \dfrac{\partial X(\xi,\eta,\zeta)}{\partial \xi} & \dfrac{\partial Y(\xi,\eta,\zeta)}{\partial \xi} & \dfrac{\partial Z(\xi,\eta,\zeta)}{\partial \xi} \\ \dfrac{\partial X(\xi,\eta,\zeta)}{\partial \eta} & \dfrac{\partial Y(\xi,\eta,\zeta)}{\partial \eta} & \dfrac{\partial Z(\xi,\eta,\zeta)}{\partial \eta} \\ \dfrac{\partial X(\xi,\eta,\zeta)}{\partial \zeta} & \dfrac{\partial Y(\xi,\eta,\zeta)}{\partial \zeta} & \dfrac{\partial Z(\xi,\eta,\zeta)}{\partial \zeta} \end{vmatrix}$$

The computer simulation of the hot metal forming processes
Milenin Andrzej, AGH University of Science and Technology, 2012
AKADEMIA GÓRNICZO-HUTNICZA IM. STANISŁAWA STASZICA W KRAKOWIE
AGH

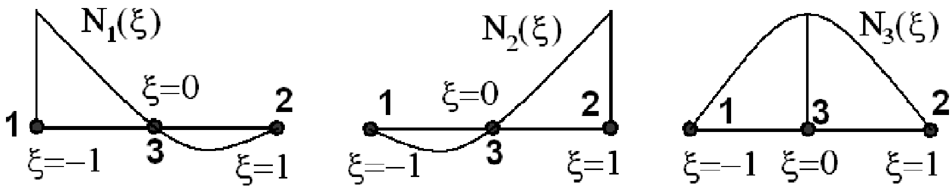

$$N_1(\xi) = -\frac{1}{2}\xi(1-\xi) \qquad N_2(\xi) = \frac{1}{2}\xi(1+\xi) \qquad N_3(\xi) = 1-\xi^2$$

$$x = x(\xi) = N_1 X_1 + N_2 X_2 + N_3 X_3 \qquad \frac{\partial N_i}{\partial x} = ?$$

$$\frac{dN_i}{d\xi} = \frac{dN_i}{dx}\frac{dx(\xi)}{d\xi}$$

$$\boxed{\frac{dN_i}{dx} = [J]^{-1}\frac{dN_i}{d\xi}}$$

$$\frac{dN_i}{dx} = \frac{1}{\dfrac{dx(\xi)}{d\xi}}\frac{dN_i(\xi)}{d\xi}$$

$$\frac{dx}{d\xi} = [J] = \frac{dN_1}{d\xi}X_1 + \frac{dN_2}{d\xi}X_2 + \frac{dN_3}{d\xi}X_3$$

Calculation of global derivatives

$$\begin{Bmatrix} \dfrac{\partial N_i}{\partial \xi} \\ \dfrac{\partial N_i}{\partial \eta} \end{Bmatrix} = J \begin{Bmatrix} \dfrac{\partial N_i}{\partial x} \\ \dfrac{\partial N_i}{\partial y} \end{Bmatrix}$$

$$\frac{\partial N_i}{\partial \xi} = \frac{\partial N_i}{\partial x}\frac{\partial x}{\partial \xi} + \frac{\partial N_i}{\partial y}\frac{\partial y}{\partial \xi}$$

$$\frac{\partial N_i}{\partial \eta} = \frac{\partial N_i}{\partial x}\frac{\partial x}{\partial \eta} + \frac{\partial N_i}{\partial y}\frac{\partial y}{\partial \eta}$$

$$\boxed{\begin{Bmatrix} \dfrac{\partial N_i}{\partial x} \\ \dfrac{\partial N_i}{\partial y} \end{Bmatrix} = J^{-1} \begin{Bmatrix} \dfrac{\partial N_i}{\partial \xi} \\ \dfrac{\partial N_i}{\partial \eta} \end{Bmatrix}}$$

$$S = \int_S \mathrm{dxdy} = \int_{-1}^{1}\int_{-1}^{1} \det J d\xi d\eta$$

$$J = \begin{bmatrix} \dfrac{\partial x}{\partial \xi} & \dfrac{\partial y}{\partial \xi} \\ \dfrac{\partial x}{\partial \eta} & \dfrac{\partial y}{\partial \eta} \end{bmatrix}$$

$$J^{-1} = \frac{1}{\det J} \begin{bmatrix} \dfrac{\partial y}{\partial \eta} & -\dfrac{\partial y}{\partial \xi} \\ -\dfrac{\partial x}{\partial \eta} & \dfrac{\partial x}{\partial \xi} \end{bmatrix}$$

$$V = \int_V dXdYdZ = \int_{-1}^{1}\int_{-1}^{1}\int_{-1}^{1} \det[J] d\xi d\eta d\zeta$$

Isoparametrical transformation

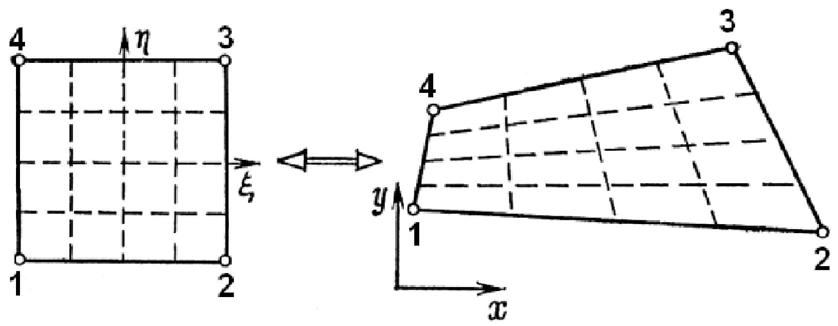

$$N_1 = \frac{1}{4}(1-\xi)(1-\eta)$$

$$N_2 = \frac{1}{4}(1+\xi)(1-\eta)$$

$$x = \sum_{i=1}^{N_{nodes}} N_i x_i = N_1 x_1 + N_2 x_2 + N_3 x_3 + N_4 x_4$$

$$N_3 = \frac{1}{4}(1+\xi)(1+\eta)$$

$$y = \sum_{i=1}^{N_{nodes}} N_i y_i = N_1 y_1 + N_2 y_2 + N_3 y_3 + N_4 y_4$$

$$N_4 = \frac{1}{4}(1-\xi)(1+\eta)$$

Subparametrical, isoparametrical and superparametrical elements

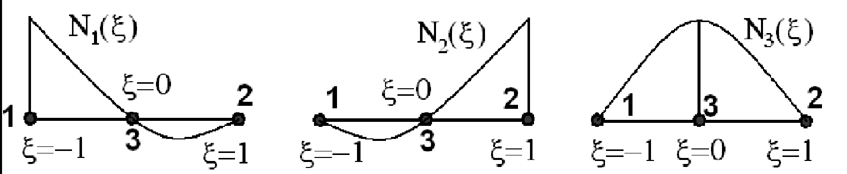

$N_1(\xi) = -\frac{1}{2}\xi(1-\xi)$ $\quad N_2(\xi) = \frac{1}{2}\xi(1+\xi)$ $\quad N_3(\xi) = 1-\xi^2$

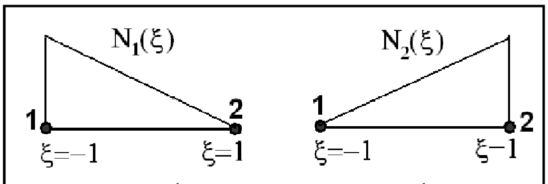

$N_1(\xi) = -\frac{1}{2}(1-\xi)$ $\quad N_2(\xi) = \frac{1}{2}(1+\xi).$

$$\varphi = N_1\varphi_1 + N_2\varphi_2 + N_3\varphi_3$$
$$x = f(\xi) = N_1X_1 + N_2X_2$$

Subparametrical

$$\varphi = N_1\varphi_1 + N_2\varphi_2 + N_3\varphi_3$$
$$x = f(\xi) = N_1X_1 + N_2X_2 + N_3X_3$$

Isoparametrical

$$\varphi = N_1\varphi_1 + N_2\varphi_2$$
$$x = f(\xi) = N_1X_1 + N_2X_2 + N_3X_3$$

Superparametrical

Isoparametrical transformation

$$N_1 = -\frac{1}{4}(1-\xi)(1-\eta)(\xi+\eta+1)$$
$$N_2 = \frac{1}{2}(1-\xi^2)(1-\eta)$$
$$N_3 = \frac{1}{4}(1+\xi)(1-\eta)(\xi-\eta-1)$$
$$N_4 = \frac{1}{2}(1-\eta^2)(1+\xi)$$
$$N_5 = \frac{1}{4}(1+\xi)(1+\eta)(\xi+\eta-1)$$
$$N_6 = \frac{1}{2}(1-\xi^2)(1+\eta)$$
$$N_7 = -\frac{1}{4}(1-\xi)(1+\eta)(\xi-\eta+1)$$
$$N_8 = \frac{1}{2}(1-\eta^2)(1-\xi)$$

$$x = \sum_{i=1}^{N_{nodes}} N_i x_i \qquad y = \sum_{i=1}^{N_{nodes}} N_i y_i$$

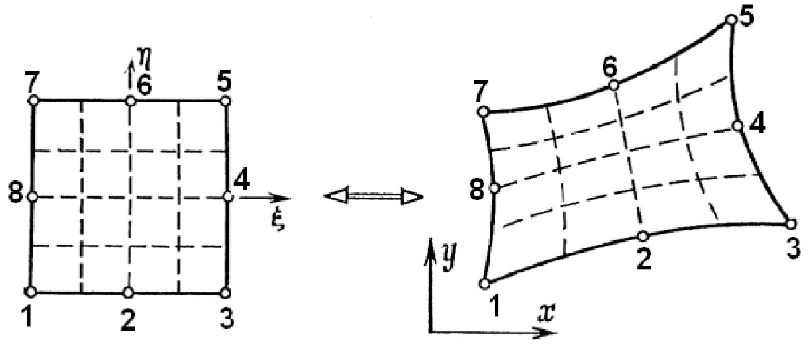

Use in FE grid meshing

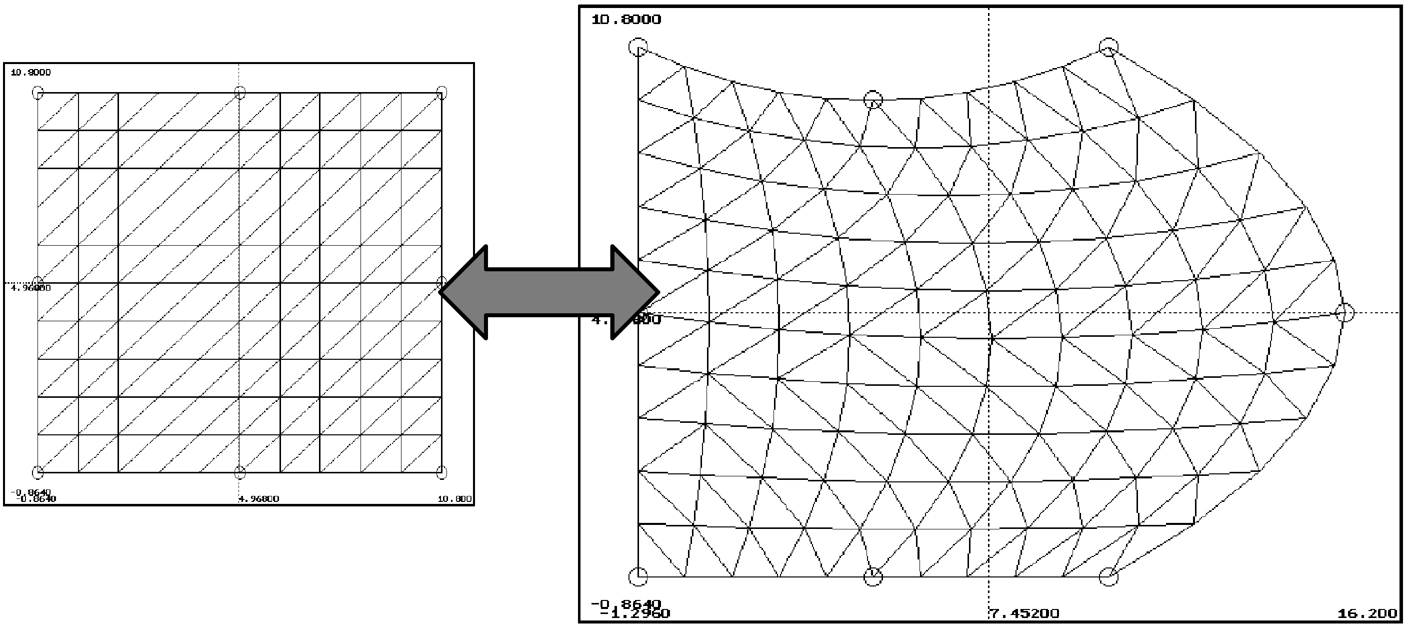

The computer simulation of the hot metal forming processes
Milenin Andrzej, AGH University of Science and Technology, 2012
AKADEMIA GÓRNICZO-HUTNICZA IM. STANISŁAWA STASZICA W KRAKOWIE
AGH

Triangle element

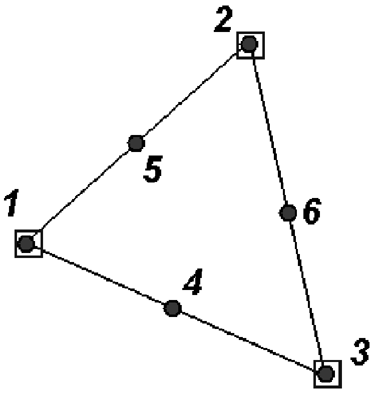

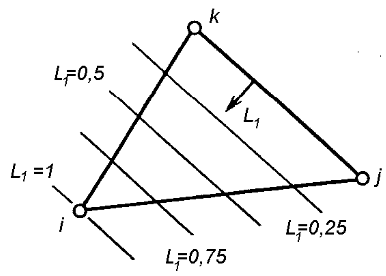

$$L_1 + L_2 + L_3 = 1$$

$$L_3 = 1 - L_1 - L_2$$

$$N_1 = L_1(2L_1 - 1)$$

$$N_2 = L_2(2L_2 - 1)$$

$$N_3 = L_3(2L_3 - 1)$$

$$N_4 = 4L_1L_3$$

$$N_5 = 4L_1L_2$$

$$N_6 = 4L_2L_3$$

$$\frac{\partial N_i}{\partial L_1} = \frac{\partial N_i}{\partial x}\frac{\partial x}{\partial L_1} + \frac{\partial N_i}{\partial y}\frac{\partial y}{\partial L_1}$$

$$\frac{\partial N_i}{\partial L_2} = \frac{\partial N_i}{\partial x}\frac{\partial x}{\partial L_2} + \frac{\partial N_i}{\partial y}\frac{\partial y}{\partial L_2}$$

$$\begin{Bmatrix} \dfrac{\partial N_i}{\partial L_1} \\ \dfrac{\partial N_i}{\partial L_2} \end{Bmatrix} = J \begin{Bmatrix} \dfrac{\partial N_i}{\partial x} \\ \dfrac{\partial N_i}{\partial y} \end{Bmatrix}$$

$$J = \begin{bmatrix} \dfrac{\partial x}{\partial L_1} & \dfrac{\partial y}{\partial L_1} \\ \dfrac{\partial x}{\partial L_2} & \dfrac{\partial y}{\partial L_2} \end{bmatrix}$$

$$\begin{Bmatrix} \dfrac{\partial N_i}{\partial x} \\ \dfrac{\partial N_i}{\partial y} \end{Bmatrix} = J^{-1} \begin{Bmatrix} \dfrac{\partial N_i}{\partial L_1} \\ \dfrac{\partial N_i}{\partial L_2} \end{Bmatrix} \qquad J^{-1} = \frac{1}{\det J} \begin{bmatrix} \dfrac{\partial y}{\partial L_2} & -\dfrac{\partial y}{\partial L_1} \\ -\dfrac{\partial x}{\partial L_2} & \dfrac{\partial x}{\partial L_1} \end{bmatrix}$$

$$N_1 = L_1(2L_1 - 1)$$
$$N_2 = L_2(2L_2 - 1)$$
$$N_3 = L_3(2L_3 - 1) \qquad L_3 = 1 - L_1 - L_2$$
$$N_4 = 4L_1L_3$$
$$N_5 = 4L_1L_2$$
$$N_6 = 4L_2L_3$$

Shape functions for Lagrangian elements

Lagrangian element

$$N_1 = \frac{1}{4}(1-\xi)(1-\eta)\xi\eta$$

$$N_2 = -\frac{1}{4}(1+\xi)(1-\eta)\xi\eta$$

$$N_3 = \frac{1}{4}(1+\xi)(1+\eta)\xi\eta$$

$$N_4 = -\frac{1}{4}(1-\xi)(1+\eta)\xi\eta$$

$$N_5 = -\frac{1}{2}(1-\xi^2)(1-\eta)\eta$$

$$N_6 = \frac{1}{2}(1+\xi)(1-\eta^2)\xi$$

$$N_7 = \frac{1}{2}(1-\xi^2)(1+\eta)\eta$$

$$N_8 = -\frac{1}{2}(1-\xi)(1-\eta^2)\xi$$

$$N_9 = (1-\xi^2)(1-\eta^2)$$

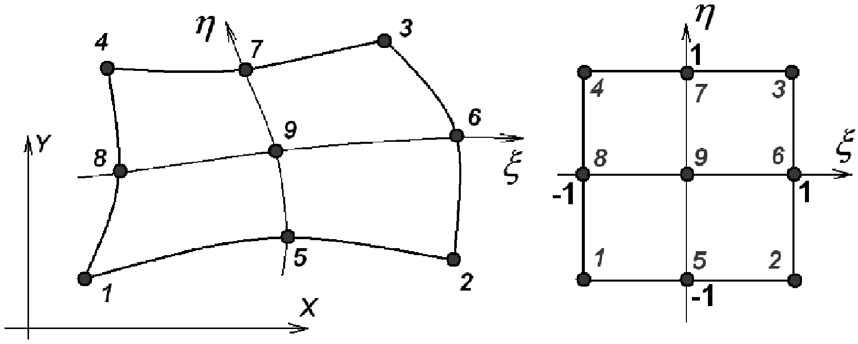

The computer simulation of the hot metal forming processes
Milenin Andrzej, AGH University of Science and Technology, 2012
AKADEMIA GÓRNICZO-HUTNICZA IM. STANISŁAWA STASZICA W KRAKOWIE
AGH

Lagrangian interpolation

$$L_i(x) = \frac{(x-x_0)(x-x_1)\ldots(x-x_{i-1})(x-x_{i+1})\ldots(x-x_n)}{(x_i-x_0)(x_i-x_1)\ldots(x_i-x_{i-1})(x_i-x_{i+1})\ldots(x_i-x_n)} = \prod_{\substack{j=0 \\ j\neq i}}^{n} \frac{x-x_j}{x_i-x_j}$$

$$L_i(x_j) = \delta_{ij} = \begin{cases} 1, for: i = j \\ 0, for: i \neq j \end{cases}$$

$$L_n(x) = \sum_{i=0}^{n} f(x_i) \prod_{\substack{j=0 \\ j\neq i}}^{n} \frac{x-x_j}{x_i-x_j} = \sum_{i=0}^{n} f(x_i) L_i(x) = \sum_{i=0}^{n} \varphi_i N_i$$

Example

x = -1; 0; 2; 3
y(x)= -1; 2; -4; -1

$$L_i(x) = \frac{(x-x_0)(x-x_1)\ldots(x-x_{i-1})(x-x_{i+1})\ldots(x-x_n)}{(x_i-x_0)(x_i-x_1)\ldots(x_i-x_{i-1})(x_i-x_{i+1})\ldots(x_i-x_n)}$$

$$y(x) = \sum_{i=0}^{4} y(x_i)L_i(x) = (-1)\frac{x(x-2)(x-3)}{(-1)(-3)(-4)} + 2\frac{(x+1)(x-2)(x-3)}{1(-2)(-3)} +$$

$$-4\frac{(x+1)x(x-3)}{3\cdot 2\cdot(-1)} - 1\frac{(x+1)x(x-2)}{4\cdot 3\cdot 1} = x^3 - 3x^2 - x + 2$$

$$y = x^3 - 3x^2 - x + 2$$

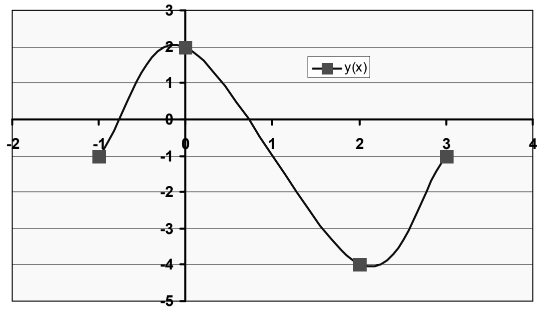

The computer simulation of the hot metal forming processes
Milenin Andrzej, AGH University of Science and Technology, 2012

2-dimensional shape functions

$$L_j(y) = \frac{(y-y_0)(y-y_1)\ldots(y-y_{j-1})(y-y_{j+1})\ldots(y-y_m)}{(y_j-y_0)(y_j-y_1)\ldots(y_j-y_{j-1})(y_j-y_{j+1})\ldots(y_j-y_m)}$$

$$L_i(x) = \frac{(x-x_0)(x-x_1)\ldots(x-x_{i-1})(x-x_{i+1})\ldots(x-x_n)}{(x_i-x_0)(x_i-x_1)\ldots(x_i-x_{i-1})(x_i-x_{i+1})\ldots(x_i-x_n)}$$

$$N_k = L_{ij}(x,y) = L_i(x)L_j(y)$$

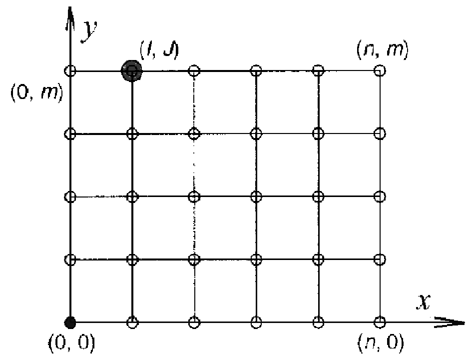

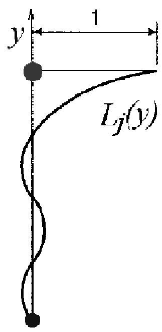

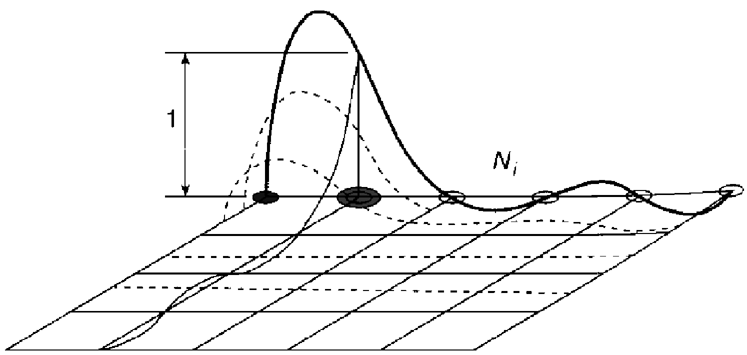

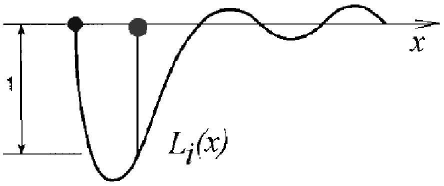

Numerical integration in FEM

$$\int_{-1}^{1} f(\xi)d\xi \approx W_0 f(\xi_0) + W_1 f(\xi_1) + \ldots + W_n f(\xi_n)$$

$$\int_{-1}^{1}\int_{-1}^{1} f(\xi,\eta)d\xi d\eta \approx W_0 f(\xi_0,\eta_0) + W_1 f(\xi_1,\eta_1) + \ldots + W_n f(\xi_n,\eta_n)$$

Gauss integration

$$\boxed{p+1 = 2(n+1)}$$

The computer simulation of the hot metal forming processes
Milenin Andrzej, AGH University of Science and Technology, 2012
AKADEMIA GÓRNICZO-HUTNICZA IM. STANISŁAWA STASZICA W KRAKOWIE

Gauss integration

$$p+1 = 2(n+1)$$

Number of points for integration, n+1	Rang of exactly integrated polinomial function, p
1	1
2	3
3	5
4	7

n=1

$$\xi_1 = -\xi_0 = \frac{1}{\sqrt{3}} \approx 0{,}577350269$$

$$W_0 = W_1 = 1{,}0$$

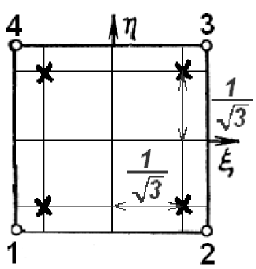

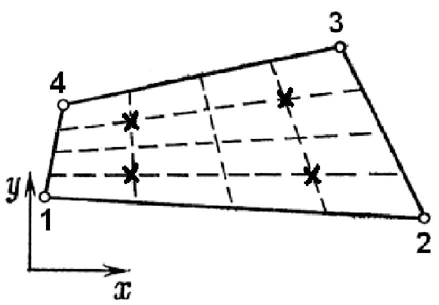

n=2

$$\xi_2 = -\xi_0 = \sqrt{\frac{3}{5}} \approx 0{,}774596669$$

$$\xi_1 = 0{,}0$$

$$W_0 = W_2 = \frac{5}{9} \approx 0{,}5555555556$$

$$W_1 = \frac{8}{9} \approx 0{,}8888888889.$$

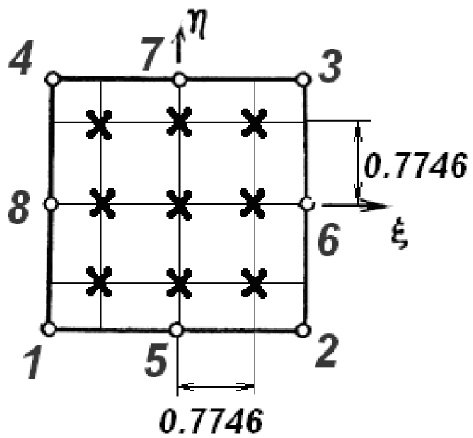

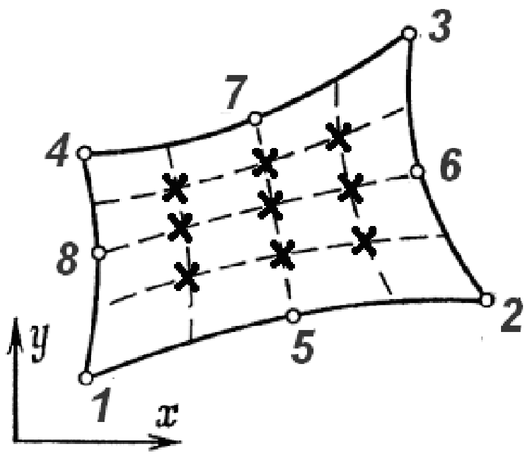

The computer simulation of the hot metal forming processes
Milenin Andrzej, AGH University of Science and Technology, 2012
AKADEMIA GÓRNICZO-HUTNICZA IM. STANISŁAWA STASZICA W KRAKOWIE AGH

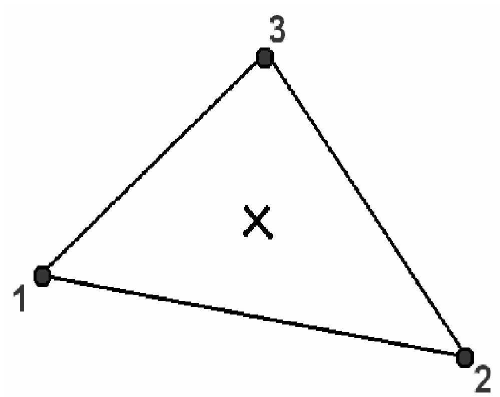

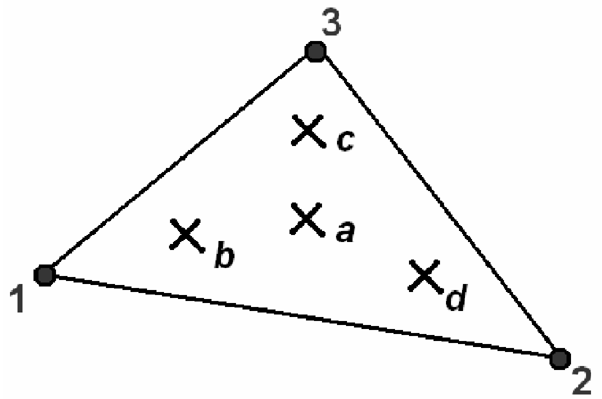

n=0
L_1 =1/3;
L_2=1/3;
L_3=1/3;
W=1/2.

a) L_1 =1/3; L_2=1/3; L_3=1/3; W= -27/96
b) L_1 =11/15; L_2=2/15; L_3=2/15; W= 25/96
c) L_1 =2/15; L_2=2/15; L_3=11/15; W= 25/96
d) L_1 =2/15; L_2=11/15; L_3=2/15; W=25/96

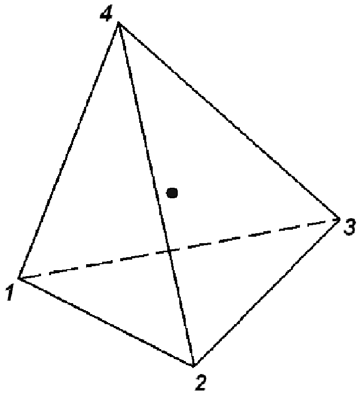

For n=0 :

$L_1 = 1/4$; $L_2 = 1/4$; $L_3 = 1/4$; $L_4 = 1/4$; $W = 1$;

For n=1 :

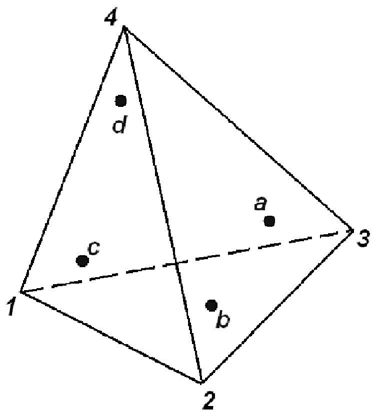

$\alpha = 0.58541020$; $\beta = 0.13819660$;

a) $L_1 = \alpha$; $L_2 = \beta$; $L_3 = \beta$; $L_4 = \beta$; $W = 1/4$;

b) $L_1 = \beta$; $L_2 = \alpha$; $L_3 = \beta$; $L_4 = \beta$; $W = 1/4$;

c) $L_1 = \beta$; $L_2 = \beta$; $L_3 = \alpha$; $L_4 = \beta$; $W = 1/4$;

d) $L_1 = \beta$; $L_2 = \beta$; $L_3 = \beta$; $L_4 = \alpha$; $W = 1/4$;

The computer simulation of the hot metal forming processes
Milenin Andrzej, AGH University of Science and Technology, 2012
AKADEMIA GÓRNICZO-HUTNICZA IM. STANISŁAWA STASZICA W KRAKOWIE AGH

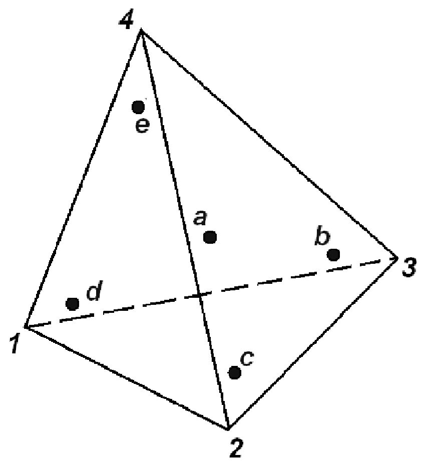

a) $L_1 = 1/4$; $L_2 = 1/4$; $L_3 = 1/4$; $L_4 = 1/4$; $W = -16/20$;

b) $L_1 = 1/3$; $L_2 = 1/6$; $L_3 = 1/6$; $L_4 = 1/6$; $W = 9/20$;

c) $L_1 = 1/6$; $L_2 = 1/3$; $L_3 = 1/6$; $L_4 = 1/6$; $W = 9/20$;

d) $L_1 = 1/6$; $L_2 = 1/6$; $L_3 = 1/3$; $L_4 = 1/6$; $W = 9/20$;

e) $L_1 = 1/6$; $L_2 = 1/6$; $L_3 = 1/6$; $L_4 = 1/3$; $W = 9/20$;

```
DO P=1, N_p
CALL Jacob_2d(J_, J_inv, P, N_p, NBN, N1, N2, X, Y, DetJ);
        DO i=1, NBN
                Ndx(i)= N1(i,p)*J_inv(1,1) + N2(i,p)*J_inv(1,2)
                Ndy(i)= N1(i,p)*J_inv(2,1) + N2(i,p)*J_inv(2,2)
        END DO;
        detJ = detJ* W(p);
        DO N=1, NBN
                DO I=1, NBN
                Hin = mK*(Ndx(n)*Ndx(i) + Ndy(n)*Ndy(i))*DetJ;
                est(n,i) = est(n,i) + Hin;
                END DO
        END DO
END DO

! *******************************************************************
! Milenin Andre, AGH, 2008, milenin@agh.edu.pl
! *******************************************************************
SUBROUTINE Jacob_2d(J_, J_inv, P, N_p, NBN, N1, N2, X, Y, DetJ);
IMPLICIT NONE;
REAL*8, DIMENSION(2,2) ::               J_, J_inv;
INTEGER*4                               P, N_p, NBN;
REAL*8, DIMENSION(NBN, N_p) ::          N1, N2;
REAL*8, DIMENSION(NBN)    ::            X,Y;
REAL*8                                  DetJ;
integer*4                               i;
J_=0.0;
J_inv=0.0;
DO I=1, NBN
        J_(1,1) = J_(1,1)+N1(i,p)*X(i);
        J_(1,2) = J_(1,2)+N1(i,p)*Y(i);
        J_(2,1) = J_(2,1)+N2(i,p)*X(i);
        J_(2,2) = J_(2,2)+N2(i,p)*Y(i);
END DO;
detJ = J_(1,1)*J_(2,2)-J_(1,2)*J_(2,1);
I=2;
CALL Inv_MAT(i, J_, J_inv);
END SUBROUTINE Jacob_2d;
```

$$\begin{Bmatrix} \dfrac{\partial N_i}{\partial x} \\ \dfrac{\partial N_i}{\partial y} \end{Bmatrix} = J^{-1} \begin{Bmatrix} \dfrac{\partial N_i}{\partial \xi} \\ \dfrac{\partial N_i}{\partial \eta} \end{Bmatrix}$$

$$J = \begin{bmatrix} \dfrac{\partial x}{\partial \xi} & \dfrac{\partial y}{\partial \xi} \\ \dfrac{\partial x}{\partial \eta} & \dfrac{\partial y}{\partial \eta} \end{bmatrix}$$

$$J^{-1} = \frac{1}{\det J} \begin{bmatrix} \dfrac{\partial y}{\partial \eta} & -\dfrac{\partial y}{\partial \xi} \\ -\dfrac{\partial x}{\partial \eta} & \dfrac{\partial x}{\partial \xi} \end{bmatrix}$$

Lection 3

Finite elements method in the theory of plastic flow of the incompressible materials. Finite elements method in the tasks of the calculated distribution of the temperature in the material during deformation.

Variation formulation in matrix form:

$$\{\sigma\} = \sigma_0 [I]^T + \{s\} = \sigma_0 [I]^T + [D]\{\xi\} \qquad [I] = [1 \quad 1 \quad 0] \qquad [I]^T = \begin{bmatrix} 1 \\ 1 \\ 0 \end{bmatrix}$$

$$\{\xi\} = \begin{Bmatrix} \xi_{xx} \\ \xi_{yy} \\ 2\xi_{xy} \end{Bmatrix} \qquad \xi_0 = [I]\{\xi\} = [1 \quad 1 \quad 0] \begin{Bmatrix} \xi_{xx} \\ \xi_{yy} \\ 2\xi_{xy} \end{Bmatrix} \qquad \sigma_0 = [I]\{\sigma\} = [1 \quad 1 \quad 0] \begin{Bmatrix} \sigma_{xx} \\ \sigma_{yy} \\ 2\sigma_{xy} \end{Bmatrix}$$

$$W = \int_V \frac{1}{2} \{\xi\}^T \{s\} dV + \int_V \sigma_0 [I]\{\xi\} dV \qquad \mathrm{J}(\mathrm{v_i}, \sigma_0) = \frac{1}{2} \int_V \mu \bar{\xi}^2 \mathrm{d}V + \int_V \xi_0 \sigma_0 \mathrm{d}V - \int_S \sigma_i \nu_\mathrm{i} \,\mathrm{d}S$$

$$W_p = \int_S \{v\}^T \{p\} dS$$

$$J = \int_V \frac{1}{2} \{\xi\}^T \{s\} dV + \int_V \sigma_0 [I]\{\xi\} dV - \int_S \{v\}^T \{p\} dS \qquad \{p\} = \begin{Bmatrix} p_x \\ p_y \end{Bmatrix}$$

The computer simulation of the hot metal forming processes
Milenin Andrzej, AGH University of Science and Technology, 2012

AKADEMIA GÓRNICZO-HUTNICZA IM. STANISŁAWA STASZICA W KRAKOWIE
AGH

$$J = \int_V \frac{1}{2} \{\xi\}^T \{s\} dV + \int_V \sigma_0 [I]\{\xi\} dV - \int_S \{v\}^T \{p\} dS$$

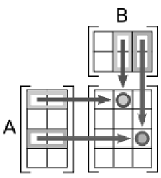

$$\{s\} = [D]\{\xi\} = \begin{Bmatrix} 2\mu\xi_{xx} \\ 2\mu\xi_{yy} \\ \mu 2\xi_{xy} \end{Bmatrix} \qquad \{\xi\} = \begin{Bmatrix} \xi_{xx} \\ \xi_{yy} \\ 2\xi_{xy} \end{Bmatrix}$$

$$\sigma_x = \sigma_0 + 2\mu\xi_x$$

$$\sigma_y = \sigma_0 + 2\mu\xi_y$$

$$\sigma_{xy} = \mu 2\xi_{xy}$$

$$[D] = \begin{bmatrix} 2\mu & 0 & 0 \\ 0 & 2\mu & 0 \\ 0 & 0 & \mu \end{bmatrix} \qquad \{s\} = \begin{Bmatrix} 2\mu\xi_{xx} \\ 2\mu\xi_{yy} \\ \mu 2\xi_{xy} \end{Bmatrix}$$

$$J = \int_V \frac{1}{2} \{\xi\}^T [D]\{\xi\} dV + \int_V \sigma_0 [I]\{\xi\} dV - \int_S \{v\}^T \{p\} dS \qquad \mu = \frac{\overline{\sigma}}{\overline{\xi}}$$

$$\{\xi\}=\begin{Bmatrix}\xi_x\\ \xi_y\\ 2\xi_{xy}\end{Bmatrix}=\begin{bmatrix}\dfrac{\partial}{\partial x} & 0\\ 0 & \dfrac{\partial}{\partial y}\\ \dfrac{\partial}{\partial y} & \dfrac{\partial}{\partial x}\end{bmatrix}\begin{Bmatrix}v_x\\ v_y\end{Bmatrix}=\begin{bmatrix}\dfrac{\partial}{\partial x} & 0\\ 0 & \dfrac{\partial}{\partial y}\\ \dfrac{\partial}{\partial y} & \dfrac{\partial}{\partial x}\end{bmatrix}\begin{Bmatrix}[N]\{\mathrm{v_x}\}\\ [N]\{\mathrm{v_y}\}\end{Bmatrix}=\begin{bmatrix}\dfrac{\partial[N]}{\partial x} & 0\\ 0 & \dfrac{\partial[N]}{\partial y}\\ \dfrac{\partial[N]}{\partial y} & \dfrac{\partial[N]}{\partial x}\end{bmatrix}\begin{Bmatrix}\{\mathrm{v_x}\}\\ \{\mathrm{v_y}\}\end{Bmatrix}=[B]\{\mathrm{v}\}$$

$$v_x=[N]\{\mathrm{v_x}\}$$
$$v_y=[N]\{\mathrm{v_y}\}$$

$$\{\xi\}=[B]\{\mathrm{v}\}$$

$$[B]=\begin{bmatrix}\dfrac{\partial[N]}{\partial x} & 0\\ 0 & \dfrac{\partial[N]}{\partial y}\\ \dfrac{\partial[N]}{\partial y} & \dfrac{\partial[N]}{\partial x}\end{bmatrix}$$

The computer simulation of the hot metal forming processes
Milenin Andrzej, AGH University of Science and Technology, 2012
AKADEMIA GÓRNICZO-HUTNICZA IM. STANISŁAWA STASZICA W KRAKOWIE
AGH

$$\{v\}=\begin{Bmatrix}v_x\\ v_y\end{Bmatrix}=\begin{bmatrix}[N] & 0\\ 0 & [N]\end{bmatrix}\begin{Bmatrix}\{\mathrm{v}_x\}\\ \{\mathrm{v}_y\}\end{Bmatrix}=[\overline{N}]\{\mathrm{v}\}$$

$$[\overline{N}]=\begin{bmatrix}N_1 & N_2\ldots & N_p & 0 & 0\ldots & 0\\ 0 & 0\ldots & 0 & N_1 & N_2\ldots & N_p\end{bmatrix}=\begin{bmatrix}[N] & 0\\ 0 & [N]\end{bmatrix}$$

Approximation of mean stress: $\sigma_0=[N]\{\sigma_0\}$ $\sigma_0=[H]\{\sigma_0\}$

$$\xi_0=[I]\{\xi\}=[1\quad 1\quad 0]\begin{Bmatrix}\xi_{xx}\\ \xi_{yy}\\ 2\xi_{xy}\end{Bmatrix}=[I][B]\{\mathrm{v}\}=[E]\{\mathrm{v}\}$$

$$[E]=[I][B]=\begin{bmatrix}\dfrac{\partial[N]}{\partial x} & \dfrac{\partial[N]}{\partial y}\end{bmatrix}$$

$$\{s\}=[D][B]\{\mathrm{v}\}$$

$$J=\int_V \frac{1}{2}\{v\}^T[B]^T[D][B]\{v\}dV+\int_V \sigma_0[E]\{v\}dV-\int_S \{v\}^T\left[\overline{N}\right]^T\{p\}dS=0$$

$$J=\int_V \frac{1}{2}\{v\}^T[B]^T[D][B]\{v\}dV+\int_V [H]\{\sigma_0\}[E]\{v\}dV-\int_S \{v\}^T\left[\overline{N}\right]^T\{p\}dS=0$$

$$\frac{\partial J}{\partial\{v\}}=\left(\int_V [B]^T[D][B]dV\right)\{v\}+\left(\int_V [E]^T[H]dV\right)\{\sigma_0\}-\int_S \left[\overline{N}\right]^T\{p\}dS=0$$

$$\frac{\partial J}{\partial\{\sigma_0\}}=\left(\int_V [H]^T[E]dV\right)\{v\}=0$$

$$[K]\{v,\sigma_0\}+\{F\}=0$$

The computer simulation of the hot metal forming processes
Milenin Andrzej, AGH University of Science and Technology, 2012
AKADEMIA GÓRNICZO-HUTNICZA IM. STANISŁAWA STASZICA W KRAKOWIE
AGH

Stiffness matrix [K]:

$$[B]^T[D][B]=\begin{bmatrix}\frac{\partial[N]^T}{\partial x} & 0 & \frac{\partial[N]^T}{\partial y}\\ 0 & \frac{\partial[N]^T}{\partial y} & \frac{\partial[N]^T}{\partial x}\end{bmatrix}\begin{bmatrix}2\mu & 0 & 0\\ 0 & 2\mu & 0\\ 0 & 0 & \mu\end{bmatrix}\begin{bmatrix}\frac{\partial[N]}{\partial x} & 0\\ 0 & \frac{\partial[N]}{\partial y}\\ \frac{\partial[N]}{\partial y} & \frac{\partial[N]}{\partial x}\end{bmatrix}$$

$$[B]^T[D]=\begin{bmatrix}2\mu\frac{\partial[N]^T}{\partial x} & 0 & \mu\frac{\partial[N]^T}{\partial y}\\ 0 & 2\mu\frac{\partial[N]^T}{\partial y} & \mu\frac{\partial[N]^T}{\partial x}\end{bmatrix}$$

$$[B]^T[D][B]=\begin{bmatrix}2\mu\frac{\partial[N]^T}{\partial x}\frac{\partial[N]}{\partial x}+\mu\frac{\partial[N]^T}{\partial y}\frac{\partial[N]}{\partial y} & \mu\frac{\partial[N]^T}{\partial x}\frac{\partial[N]}{\partial y}\\ \mu\frac{\partial[N]^T}{\partial x}\frac{\partial[N]}{\partial y} & 2\mu\frac{\partial[N]^T}{\partial y}\frac{\partial[N]}{\partial y}+\mu\frac{\partial[N]^T}{\partial x}\frac{\partial[N]}{\partial x}\end{bmatrix}$$

Stiffness matrix [K]:

$$\frac{\partial J}{\partial\{\mathrm{v}\}}=\left(\int\limits_{\mathrm{V}}[B]^T[D][B]dV\right)\{\mathrm{v}\}+\left(\int\limits_{\mathrm{V}}[E]^T[H]dV\right)\{\sigma_0\}-\int\limits_{\mathrm{S}}[\overline{N}]^T\{p\}dS=0$$

$$\frac{\partial J}{\partial\{\sigma_0\}}=\left(\int\limits_{\mathrm{V}}[H]^T[E]dV\right)\{\mathrm{v}\}=0$$

$$[K]=\int\limits_V\left[\begin{array}{c|c|c} 2\mu\frac{\partial[N]^T}{\partial x}\frac{\partial[N]}{\partial x}+ \mu\frac{\partial[N]^T}{\partial y}\frac{\partial[N]}{\partial y} & \mu\frac{\partial[N]^T}{\partial y}\frac{\partial[N]}{\partial x} & \frac{\partial[N]^T}{\partial x}[H] \\ \hline \mu\frac{\partial[N]^T}{\partial x}\frac{\partial[N]}{\partial y} & 2\mu\frac{\partial[N]^T}{\partial y}\frac{\partial[N]}{\partial y}+\mu\frac{\partial[N]^T}{\partial y}\frac{\partial[N]}{\partial y} & \frac{\partial[N]^T}{\partial y}[H] \\ \hline [H]^T\frac{\partial[N]}{\partial x} & [H]^T\frac{\partial[N]}{\partial y} & 0 \end{array}\right]dV.$$

Load vector:

$$\{F\}=\int\limits_S\left\{\begin{array}{c}[N]^T p_x\\ [N]^T p_y\\ 0\end{array}\right\}dS$$

The computer simulation of the hot metal forming processes
Milenin Andrzej, AGH University of Science and Technology, 2012
AKADEMIA GÓRNICZO-HUTNICZA IM. STANISŁAWA STASZICA W KRAKOWIE
AGH

Example of FORTRAN code

```
        DO P=1, ELSlv%N_p
                DO N=1,NBN
                        Row1 = N;
                        Row2 = NBN + N;
                        Row3 = 2*NBN + N;
                        DO I=1,NBN
                                C1 = I;
                                C2 = NBN + I;
                                C3 = 2*NBN + I;
feSM(Row1,C1)=feSM(Row1,C1) + m*(2*Ndx(N)*Ndx(i)+Ndy(N)*Ndy(i))*DetJ;
feSM(Row1,C2)=feSM(Row1,C2) + m*Ndx(i)*Ndy(N)*DetJ;

if (i<=NBNp) feSM(Row1,C3)=feSM(Row1,C3) + Ndx(N)*detJ*Hk(i,p);

feSM(Row2,C1)=feSM(Row2,C1) + m*Ndx(N)*Ndy(i)*DetJ;
feSM(Row2,C2)=feSM(Row2,C2) + m*(2*Ndy(N)*Ndy(i)+Ndx(N)*Ndx(i))*DetJ

if (i<=NBNp) feSM(Row2,C3) = feSM(Row2,C3) + Ndy(N)*detJ*Hk(i,p);

                if (N<=NBNp) then
feSM(Row3,C1) = feSM(Row3,C1) + Ndx(i)*detJ*Hk(n,p);
feSM(Row3,C2) = feSM(Row3,C2) + Ndy(i)*detJ*Hk(n,p);
                 end if
                        END DO
                END DO
        END DO
```

Graphic interpretation of local stiffness matrix [K]:

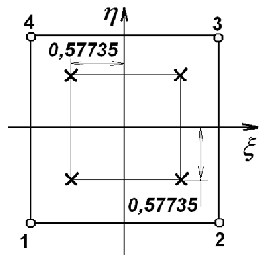

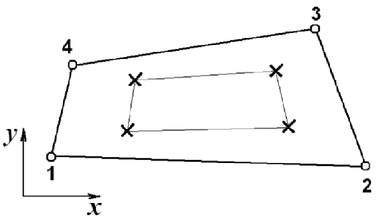

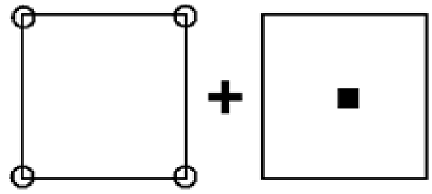

$$[K]=\int_V \left[\begin{array}{c|c|c} 2\mu\frac{\partial[N]^T}{\partial x}\frac{\partial[N]}{\partial x}+ + \mu\frac{\partial[N]^T}{\partial y}\frac{\partial[N]}{\partial y} & \mu\frac{\partial[N]^T}{\partial y}\frac{\partial[N]}{\partial x} & \frac{\partial[N]^T}{\partial x}[H] \\ \hline \mu\frac{\partial[N]^T}{\partial x}\frac{\partial[N]}{\partial y} & 2\mu\frac{\partial[N]^T}{\partial y}\frac{\partial[N]}{\partial y}+ + \mu\frac{\partial[N]^T}{\partial x}\frac{\partial[N]}{\partial x} & \frac{\partial[N]^T}{\partial y}[H] \\ \hline [H]^T\frac{\partial[N]}{\partial x} & [H]^T\frac{\partial[N]}{\partial y} & 0 \end{array}\right] dV.$$

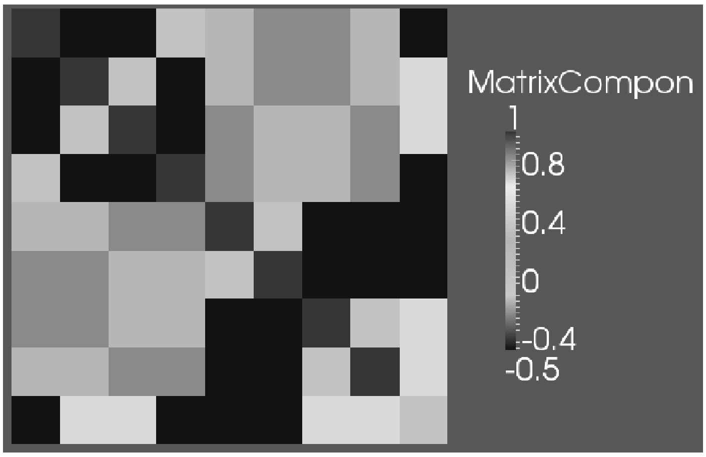

The computer simulation of the hot metal forming processes
Milenin Andrzej, AGH University of Science and Technology, 2012
AKADEMIA GÓRNICZO-HUTNICZA IM. STANISŁAWA STASZICA W KRAKOWIE
AGH

Graphic interpretation of global stiffness matrix [K]:

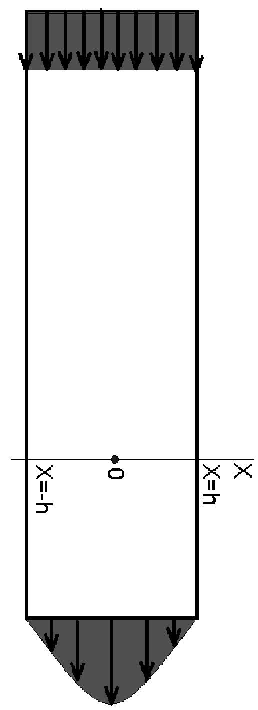

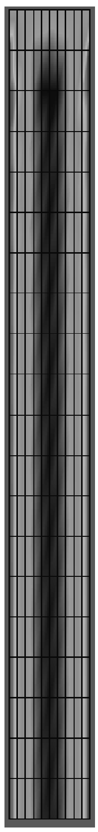

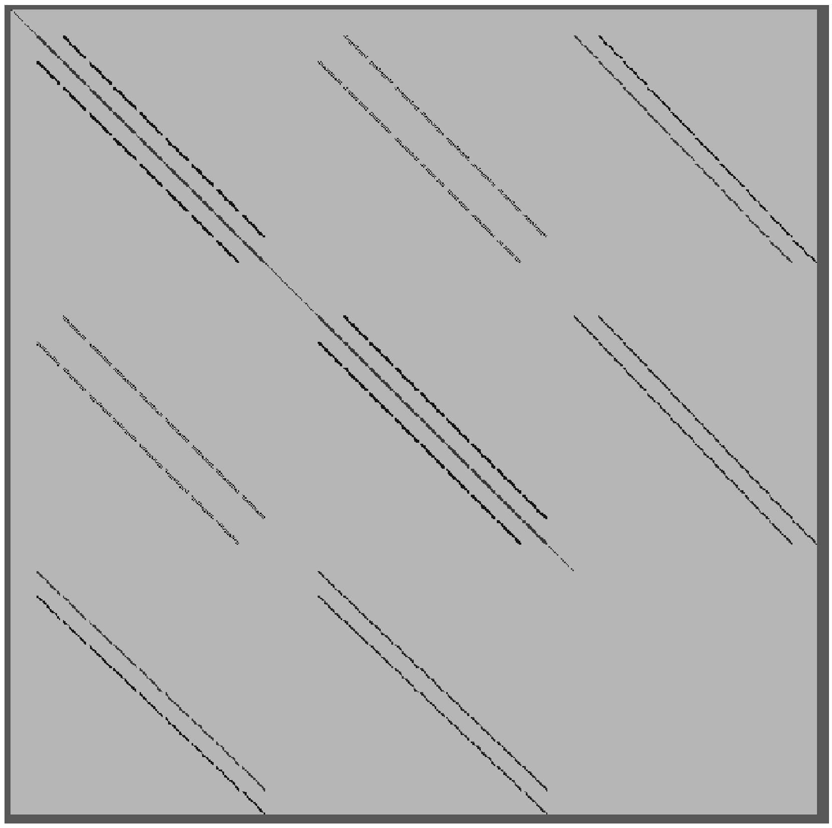

Stabile interpolations N (❍) and H (■)

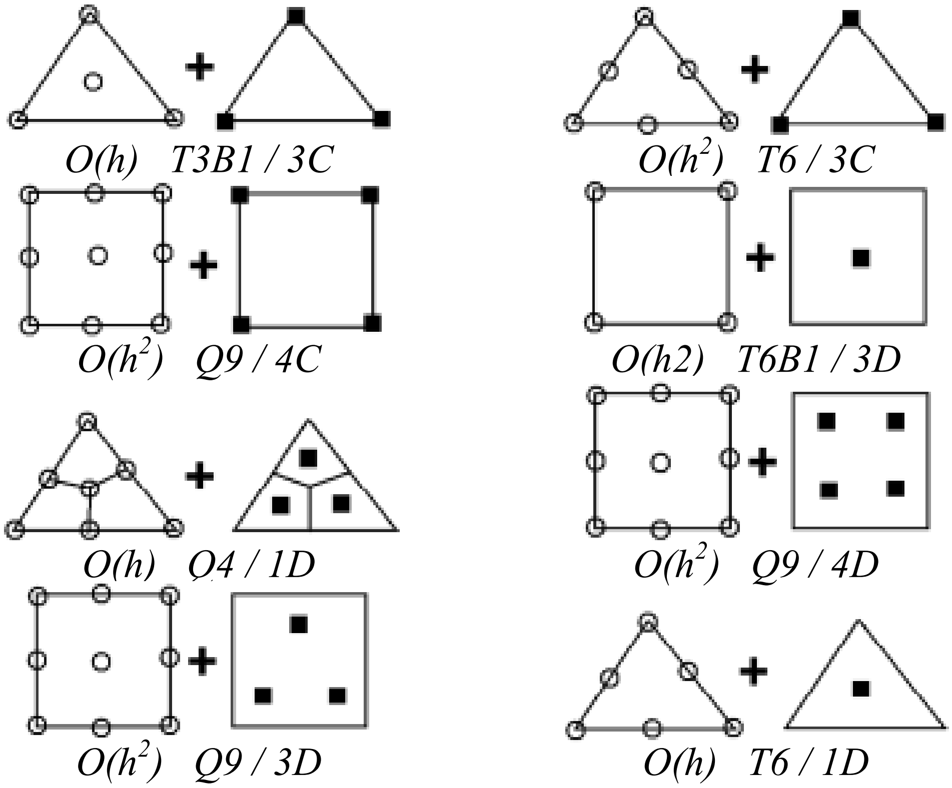

Boundary condition in stiffness matrix.

	v_{x1}	v_{x2}	v_{x3}	v_{y1}	v_{y2}	v_{y3}	σ_1	σ_2	σ_3
v_{x1}	k_{11}	k_{12}	k_{13}	k_{14}	k_{15}	k_{16}	k_{17}	k_{18}	k_{19}
v_{x2}	k_{21}	k_{22}	k_{23}	k_{24}	k_{25}	k_{26}	k_{27}	k_{28}	k_{29}
v_{x3}	k_{31}	k_{32}	k_{33}	k_{34}	k_{35}	k_{36}	k_{37}	k_{38}	k_{39}
v_{y1}	k_{41}	k_{42}	k_{43}	k_{44}	k_{45}	k_{46}	k_{47}	k_{48}	k_{49}
v_{y2}	k_{51}	k_{52}	k_{53}	k_{54}	k_{55}	k_{56}	k_{57}	k_{58}	k_{59}
v_{y3}	k_{61}	k_{62}	k_{63}	k_{64}	k_{65}	k_{66}	k_{67}	k_{68}	k_{69}
σ_1	k_{71}	k_{72}	k_{73}	k_{74}	k_{75}	k_{76}	k_{77}	k_{78}	k_{79}
σ_2	k_{81}	k_{82}	k_{83}	k_{84}	k_{85}	k_{86}	k_{87}	k_{88}	k_{89}
σ_3	k_{91}	k_{92}	k_{93}	k_{94}	k_{95}	k_{96}	k_{97}	k_{98}	k_{99}

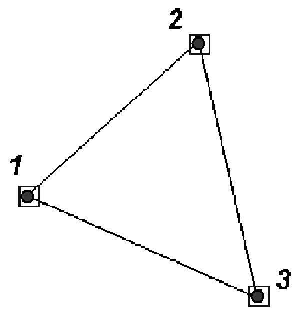

$$[N]=[H]$$

$$[k]=\int_V \begin{bmatrix} \mu\left(2\frac{\partial[N]^T}{\partial x}\frac{\partial[N]}{\partial x}+\frac{\partial[N]^T}{\partial y}\frac{\partial[N]}{\partial y}\right) & \mu\frac{\partial[N]^T}{\partial x}\frac{\partial[N]}{\partial y} & \frac{\partial[N]^T}{\partial x}[H] \\ \mu\frac{\partial[N]^T}{\partial x}\frac{\partial[N]}{\partial y} & \mu\left(2\frac{\partial[N]^T}{\partial y}\frac{\partial[N]}{\partial y}+\frac{\partial[N]^T}{\partial y}\frac{\partial[N]}{\partial y}\right) & \frac{\partial[N]^T}{\partial y}[H] \\ [H]^T\frac{\partial[N]}{\partial x} & [H]^T\frac{\partial[N]}{\partial y} & 0 \end{bmatrix} dV$$

Stiffness matrix. Code fragment.

```
                    DO n=1,NBN (I)
                          Row1 = n;
                          Row2 = NBN + n;
                          Row3 = 2*NBN + n;
                          DO i=1,NBN   (J)
                                C1 = i;
                                C2 = NBN + i;
                                C3 = 2*NBN + i;
feSM(Row1,C1)=feSM(Row1,C1) + m*(2*Ndx(n)*Ndx(i)+Ndy(n)*Ndy(i))*DetJ;
feSM(Row1,C2)=feSM(Row1,C2) + m*Ndx(i)*Ndy(n)*DetJ;
feSM(Row1,C3)=feSM(Row1,C3) + Ndx(n)*detJ*Hk(i,p);
feSM(Row2,C1)=feSM(Row2,C1) + m*Ndx(n)*Ndy(i)*DetJ;
feSM(Row2,C2)=feSM(Row2,C2) + m*(2*Ndy(n)*Ndy(i)+Ndx(n)*Ndx(i))*DetJ
feSM(Row2,C3) = feSM(Row2,C3) + Ndy(n)*detJ*Hk(i,p);
feSM(Row3,C1) = feSM(Row3,C1) + Ndx(i)*detJ*Hk(n,p);
feSM(Row3,C2) = feSM(Row3,C2) + Ndy(i)*detJ*Hk(n,p);
                          END DO
                    END DO
```


Boundary condition in stiffness matrix. Code fragment.

	v_{x1}	v_{x2}	v_{x3}	v_{y1}	v_{y2}	v_{y3}	σ_1	σ_2	σ_3	
v_{x1}	k_{11}	k_{12}	k_{13}	k_{14}	k_{15}	k_{16}	k_{17}	k_{18}	k_{19}	f_1
v_{x2}	k_{21}	k_{22}	k_{23}	k_{24}	k_{25}	k_{26}	k_{27}	k_{28}	k_{29}	f_2
v_{x3}	k_{31}	k_{32}	k_{33}	k_{34}	k_{35}	k_{36}	k_{37}	k_{38}	k_{39}	f_3
v_{y1}	k_{41}	k_{42}	k_{43}	k_{44}	k_{45}	k_{46}	k_{47}	k_{48}	k_{49}	f_4
v_{y2}	k_{51}	k_{52}	k_{53}	k_{54}	k_{55}	k_{56}	k_{57}	k_{58}	k_{59}	f_5
v_{y3}	k_{61}	k_{62}	k_{63}	k_{64}	k_{65}	k_{66}	k_{67}	k_{68}	k_{69}	f_6
σ_1	k_{71}	k_{72}	k_{73}	k_{74}	k_{75}	k_{76}	k_{77}	k_{78}	k_{79}	f_7
σ_2	k_{81}	k_{82}	k_{83}	k_{84}	k_{85}	k_{86}	k_{87}	k_{88}	k_{89}	f_8
σ_3	k_{91}	k_{92}	k_{93}	k_{94}	k_{95}	k_{96}	k_{97}	k_{98}	k_{99}	f_9

$$v_{x2} = v_{tool}$$

	v_{x1}	v_{x2}	v_{x3}	v_{y1}	v_{y2}	v_{y3}	σ_1	σ_2	σ_3	
v_{x1}	k_{11}	k_{12}	k_{13}	k_{14}	k_{15}	k_{16}	k_{17}	k_{18}	k_{19}	f_1
v_{x2}	0	k_{22}	0	0	0	0	0	0	0	$k_{22}v_{tool}$
v_{x3}	k_{31}	k_{32}	k_{33}	k_{34}	k_{35}	k_{36}	k_{37}	k_{38}	k_{39}	f_3
v_{y1}	k_{41}	k_{42}	k_{43}	k_{44}	k_{45}	k_{46}	k_{47}	k_{48}	k_{49}	f_4
v_{y2}	k_{51}	k_{52}	k_{53}	k_{54}	k_{55}	k_{56}	k_{57}	k_{58}	k_{59}	f_5
v_{y3}	k_{61}	k_{62}	k_{63}	k_{64}	k_{65}	k_{66}	k_{67}	k_{68}	k_{69}	f_6
σ_1	k_{71}	k_{72}	k_{73}	k_{74}	k_{75}	k_{76}	k_{77}	k_{78}	k_{79}	f_7
σ_2	k_{81}	k_{82}	k_{83}	k_{84}	k_{85}	k_{86}	k_{87}	k_{88}	k_{89}	f_8
σ_3	k_{91}	k_{92}	k_{93}	k_{94}	k_{95}	k_{96}	k_{97}	k_{98}	k_{99}	f_9

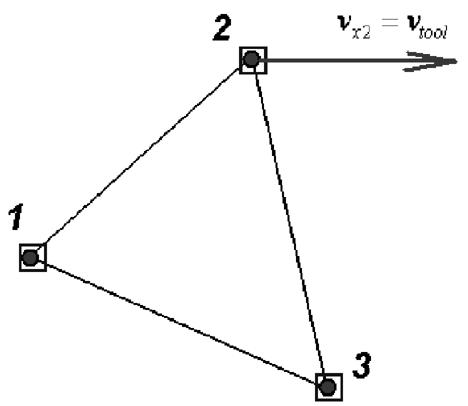

	v_{x1}	v_{x2}	v_{x3}	v_{y1}	v_{y2}	v_{y3}	σ_1	σ_2	σ_3	
v_{x1}	k_{11}	0	k_{13}	k_{14}	k_{15}	k_{16}	k_{17}	k_{18}	k_{19}	$f_1 - k_{12}v_{tool}$
v_{x2}	0	k_{22}	0	0	0	0	0	0	0	$k_{22}v_{tool}$
v_{x3}	k_{31}	0	k_{33}	k_{34}	k_{35}	k_{36}	k_{37}	k_{38}	k_{39}	$f_3 - k_{32}v_{tool}$
v_{y1}	k_{41}	0	k_{43}	k_{44}	k_{45}	k_{46}	k_{47}	k_{48}	k_{49}	$f_4 - k_{32}v_{tool}$
v_{y2}	k_{51}	0	k_{53}	k_{54}	k_{55}	k_{56}	k_{57}	k_{58}	k_{59}	$f_5 - k_{32}v_{tool}$
v_{y3}	k_{61}	0	k_{63}	k_{64}	k_{65}	k_{66}	k_{67}	k_{68}	k_{69}	$f_6 - k_{32}v_{tool}$
σ_1	k_{71}	0	k_{73}	k_{74}	k_{75}	k_{76}	k_{77}	k_{78}	k_{79}	$f_7 - k_{32}v_{tool}$
σ_2	k_{81}	0	k_{83}	k_{84}	k_{85}	k_{86}	k_{87}	k_{88}	k_{89}	$f_8 - k_{32}v_{tool}$
σ_3	k_{91}	0	k_{93}	k_{94}	k_{95}	k_{96}	k_{97}	k_{98}	k_{99}	$f_9 - k_{32}v_{tool}$

	v_{x1}	v_{x2}	v_{x3}	v_{y1}	v_{y2}	v_{y3}	σ_1	σ_2	σ_3
v_{x1}	k_{11}	0	k_{13}	k_{14}	k_{15}	k_{16}	k_{17}	k_{18}	k_{19}
v_{x2}	0	k_{22}	0	0	0	0	0	0	0
v_{x3}	k_{31}	0	k_{33}	k_{34}	k_{35}	k_{36}	k_{37}	k_{38}	k_{39}
v_{y1}	k_{41}	0	k_{43}	k_{44}	k_{45}	k_{46}	k_{47}	k_{48}	k_{49}
v_{y2}	k_{51}	0	k_{53}	k_{54}	k_{55}	k_{56}	k_{57}	k_{58}	k_{59}
v_{y3}	k_{61}	0	k_{63}	k_{64}	k_{65}	k_{66}	k_{67}	k_{68}	k_{69}
σ_1	k_{71}	0	k_{73}	k_{74}	k_{75}	k_{76}	0	0	0
σ_2	k_{81}	0	k_{83}	k_{84}	k_{85}	k_{86}	0	0	0
σ_3	k_{91}	0	k_{93}	k_{94}	k_{95}	k_{96}	0	0	0

$$\begin{Bmatrix} f_1 - k_{12}v_{tool} \\ k_{22}v_{tool} \\ f_3 - k_{32}v_{tool} \\ f_4 - k_{32}v_{tool} \\ f_5 - k_{32}v_{tool} \\ f_6 - k_{32}v_{tool} \\ 0 - k_{32}v_{tool} \\ 0 - k_{32}v_{tool} \\ 0 - k_{32}v_{tool} \end{Bmatrix}$$

$$[K]=\int_V \begin{bmatrix} 2\mu\frac{\partial[N]^T}{\partial x}\frac{\partial[N]}{\partial x}+ +\mu\frac{\partial[N]^T}{\partial y}\frac{\partial[N]}{\partial y} & \mu\frac{\partial[N]^T}{\partial x}\frac{\partial[N]}{\partial y} & \frac{\partial[N]^T}{\partial x}[H] \\ \mu\frac{\partial[N]^T}{\partial x}\frac{\partial[N]}{\partial y} & 2\mu\frac{\partial[N]^T}{\partial y}\frac{\partial[N]}{\partial y}+ +\mu\frac{\partial[N]^T}{\partial y}\frac{\partial[N]}{\partial y} & \frac{\partial[N]^T}{\partial y}[H] \\ [H]^T\frac{\partial[N]}{\partial x} & [H]^T\frac{\partial[N]}{\partial y} & 0 \end{bmatrix} dV$$

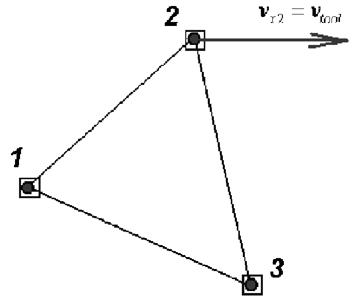

Boundary conditions in stiffness matrix. Code fragment.

```
do i=1,nbn
j  = abs(feVrtxMapSlv(I,nElem));
                Status=vrtxStatusSlv(j);
                SELECT CASE(Status)
                case(5,69,11,75 )
                Nzad=1;
                NUM_zad(1)=i;       VAL_zad(1)=0.0;
                case(10,74 )
                Nzad=2;
                NUM_zad(1)=i;          VAL_zad(1)=vrtxVelSlv(1,j);
                NUM_zad(2)=i+nbn;   VAL_zad(2)=vrtxVelSlv(2,j);
                case(8,72 )
                Nzad=2;
                NUM_zad(1)=i;       VAL_zad(1)=vrtxVelSlv(1,j);
                NUM_zad(2)=i+nbn;   VAL_zad(2)=vrtxVelSlv(2,j);
                END SELECT;

                do ii=1,Nzad
call mat_corr(Num_zad(ii),VAL_zad(ii),feUknCount,feSM,feRhs);
                end do;
end do;
```

```
subroutine mat_corr(Num, VAL_, ncn, est, r);
integer*4 ncn;
integer*4 Num;
real*8 VAL_;
real(8), dimension(ncn,ncn) :: est;
real(8), dimension(ncn)     :: r;
integer i, j;
          do j=1,ncn
             if (j.NE.Num) est(Num,j)=0;
          end do;
          r(Num) = est(Num,Num)*VAL_;
          do i=1,ncn
             if
(i.NE.Num) then
                         r(i)=r(i)-est(i,Num)*Val_;
                         est(i,Num)=0;
             end if;
          end do;
end subroutine mat_corr;
```

Problems

1. Classical mixed formulation: Many variables.

$$J(v_i,\sigma_0)=\frac{1}{2}\int_V \mu\bar{\xi}^2 dV+\int_V \sigma_0\xi_0 dV-\int_S p_i v_i dS$$

2. Limitations. Conditions of tool surface impenetrate

$$J(v_i,\sigma_0)=\frac{1}{2}\int_V \mu\bar{\xi}^2 dV+\int_V \sigma_0\xi_0 dV-\int_S p_i v_i dS+K_w\int_S (w_n-v_n)^2 dS$$

3. Incompressibility.

$$J(v_i)=\frac{1}{2}\int_V \mu\bar{\xi}^2 dV+K_{pen}\int_V (\xi_0)^2 dV-\int_S p_i v_i dS$$

4. Modeling of friction:

$$J(v_i,\sigma_0)=\frac{1}{2}\int_V \mu\bar{\xi}^2 dV+\int_V \sigma_0\xi_0 dV-K_\tau^{(p)}\int_S (v_\tau)^2 dS \qquad K_\tau^{(p)}=\left|\frac{\sigma_\tau^{(p-1)}}{v_\tau^{(p-1)}}\right|$$

2. Conditions of tool surface impenetrate

$$J(v_i,\sigma_0)=\frac{1}{2}\int_V \mu\bar{\xi}^2 dV+\int_V \sigma_0\xi_0 dV-\int_S p_i v_i dS+K_w\int_S (w_n-v_n)^2 dS$$

$$v_n(x,t)\le w_n(x,t)$$

```
DetJ_dop = DetJ_dop +
POVSlv(N_POV_GL)%DetJ(p)*SfSlv(N_pov_LOK)%W(p);

DO N=1,NBN
Id  = abs(feVrtxMapSlv(N,nElem));
Row1 = N;
Row2 = NBN + N;
Pen_dop = DetJ_dop*G(N)*NdsSlv(idPov)%penalty*10000; !*VtoolSlv;

feSM(Row1,Row1)=feSM(Row1,Row1) + Pen_dop*( AxT(n)*AxT(n) );
feSM(Row1,Row2)=feSM(Row1,Row2) + Pen_dop*( AxT(n)*AyT(n) );
feSM(Row2,Row1)=feSM(Row2,Row1) + Pen_dop*( AyT(n)*AxT(n) );
feSM(Row2,Row2)=feSM(Row2,Row2) + Pen_dop*( AyT(n)*AyT(n) );
feRhs(Row1) = feRhs(Row1) + Pen_dop*AxT(n)*Wnt(n);
feRhs(Row2) = feRhs(Row2) + Pen_dop*AyT(n)*Wnt(n);
END DO;
```

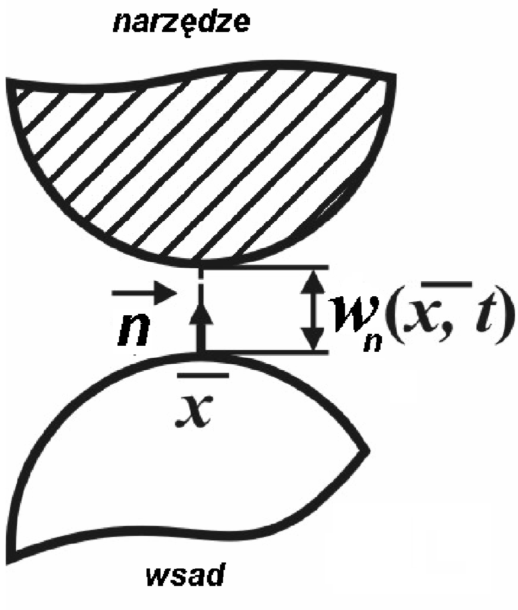

3. Incompressibility.

$$J(v_i,\sigma_0)=\frac{1}{2}\int_V \mu\bar{\xi}^2 dV + K_{pen}\int_V (\xi_0)^2 dV - \int_S p_i v_i dS$$

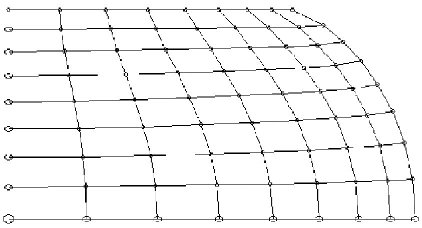

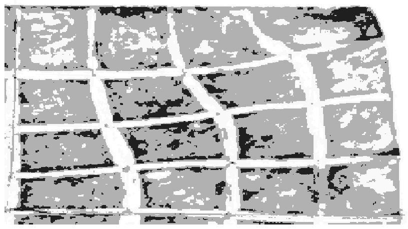

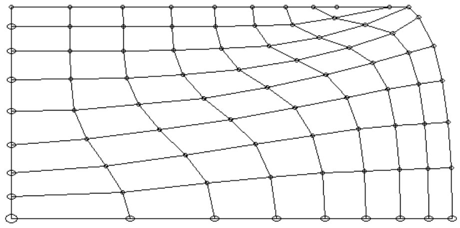

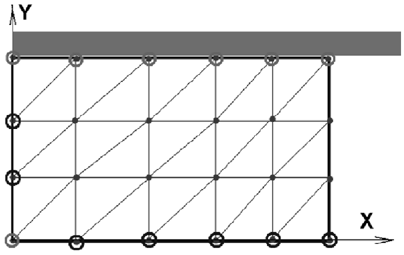

DOF = 2*10+7=27

Ncond = ne = 30

DOF<Ncond

$n_{dof} \geq n_\sigma$ Condition of Babuska-Brezzi $K_{lock}=\frac{n_\sigma}{n_{dof}}$

The computer simulation of the hot metal forming processes
Milenin Andrzej, AGH University of Science and Technology, 2012
AKADEMIA GÓRNICZO-HUTNICZA IM. STANISŁAWA STASZICA W KRAKOWIE
AGH

3. Incompressibility.

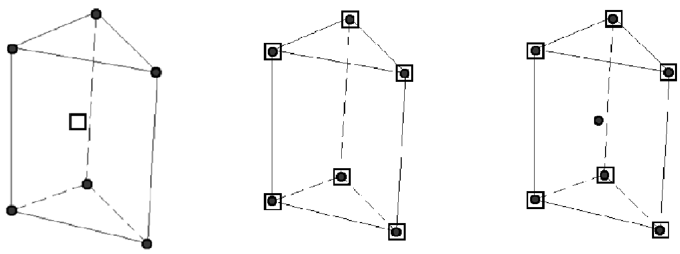

1) 2) 3)

Test example (Poiseuille test):

$$v_z=\frac{3}{2}\frac{B}{h^3}\left(h^2-x^2\right)$$

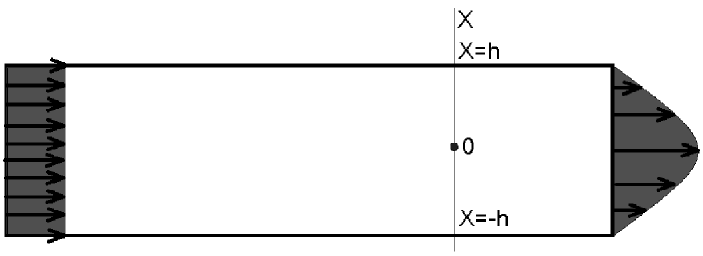

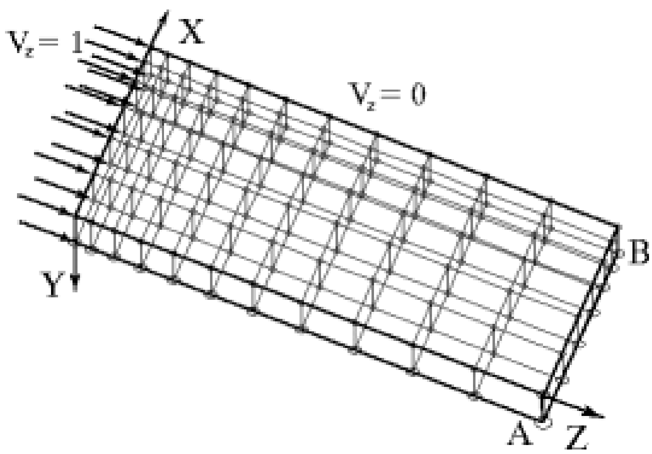

Test example 1 (penalty method)

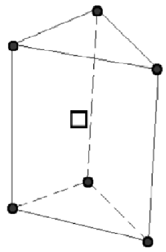

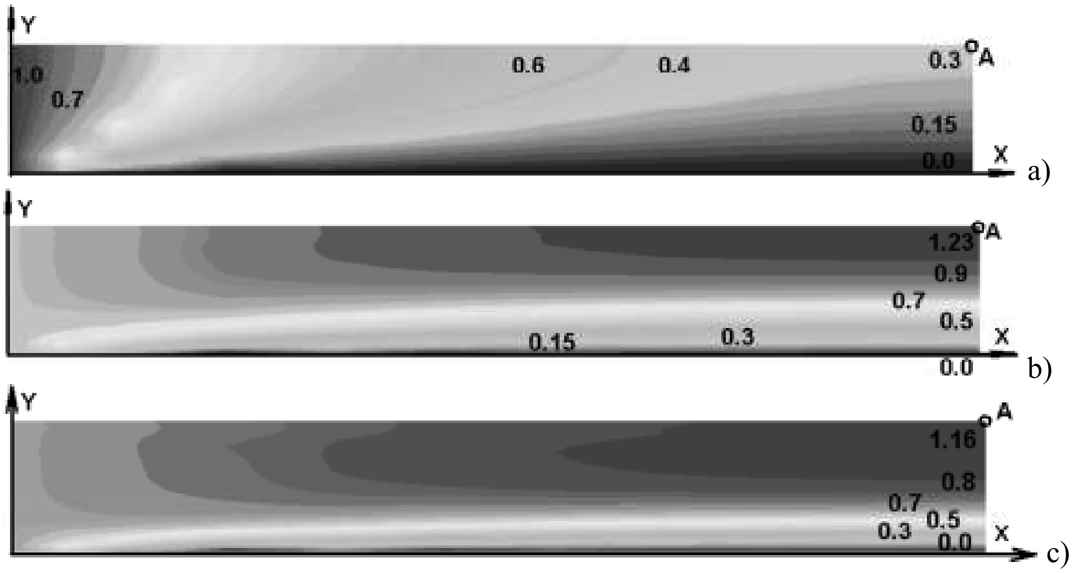

Puazeil test, a – K_p=500μ; b – K_p =25000μ; c – K_p =100000μ.

The computer simulation of the hot metal forming processes
Milenin Andrzej, AGH University of Science and Technology, 2012

Test example 2

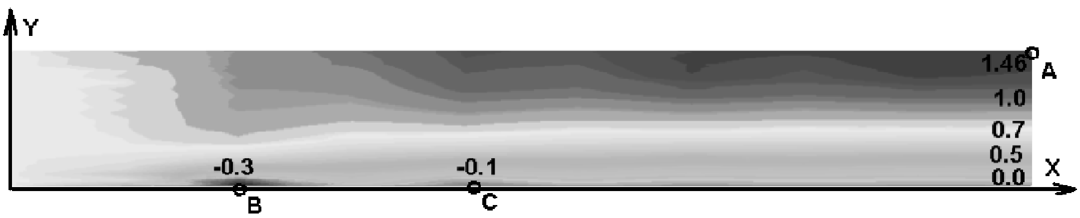

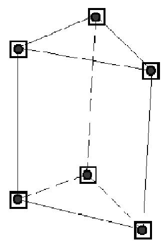

Test example 3

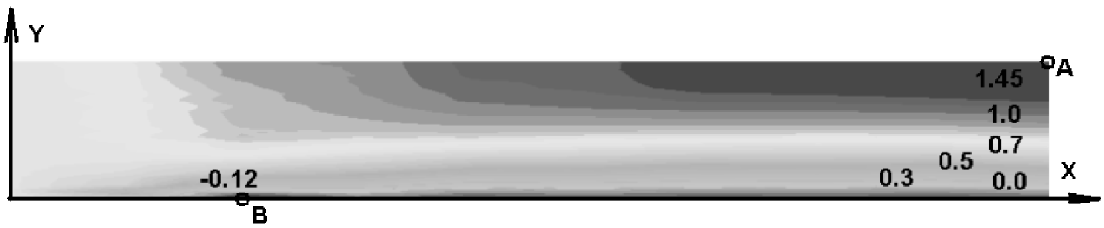

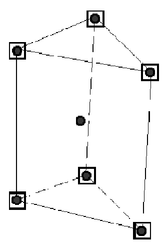

4. Modeling friction with help of penalty function :

$$\mathrm{J}(v_i,\sigma_0)=\frac{1}{2}\int_V \mu\bar{\xi}^2 \mathrm{d}V+\int_V \sigma_0\xi_0 dV - K_\tau^{(p)}\int_S (\nu_\tau)^2 dS \qquad K_\tau^{(p)}=\left|\frac{\sigma_\tau^{(p-1)}}{\nu_\tau^{(p-1)}}\right|$$

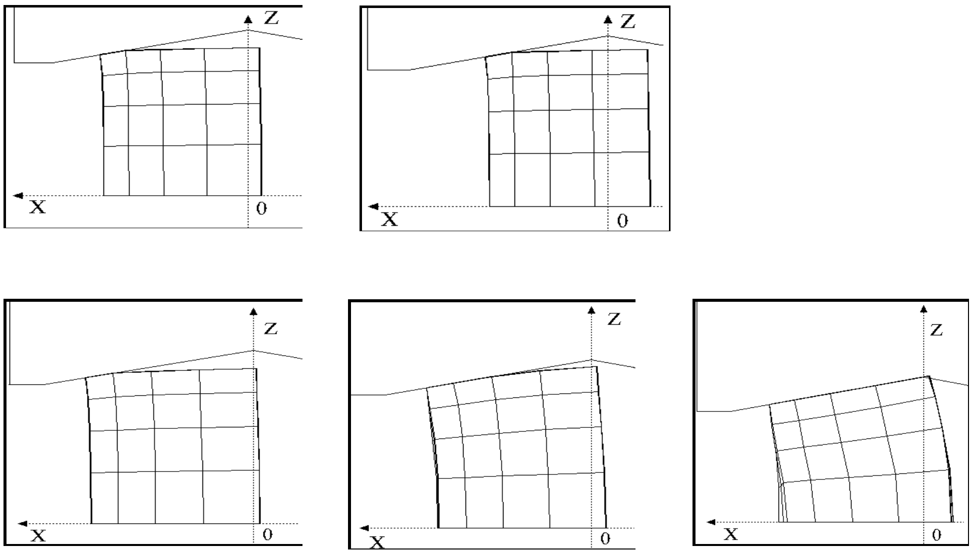

Modeling friction with help of penalty function: code example.

```
DO N=1,NBN
        Row1 = N;
        Row2 = NBN + N;
        Wes=8.0/9.0;
        if (N<=3) Wes=5.0/9.0;

        Vmax = dV(n);
        SigmaFr = m(n)*Ti(n)*(1-dexp(-0.722*Sx(n)/Ti(n)));
        Pen_dop =  Wes*DetJ_dop*X(n)*SigmaFr /Vmax;

        feSM(Row1,Row1)=feSM(Row1,Row1) + Pen_dop !* Ax1(n)*Ax1(n);
        feSM(Row1,Row2)=feSM(Row1,Row2) + Pen_dop !* Ax1(n)*Ay1(n);
        feSM(Row2,Row1)=feSM(Row2,Row1) + Pen_dop !* Ay1(n)*Ax1(n);
        feSM(Row2,Row2)=feSM(Row2,Row2) + Pen_dop !* Ay1(n)*Ay1(n);
        feRhs(Row1) = feRhs(Row1) + Pen_dop * ( Ax1(n) * W1(n) );
        feRhs(Row2) = feRhs(Row2) + Pen_dop * ( Ay1(n) * W1(n) );
                                end if;
END DO;
```

Example of implementation:

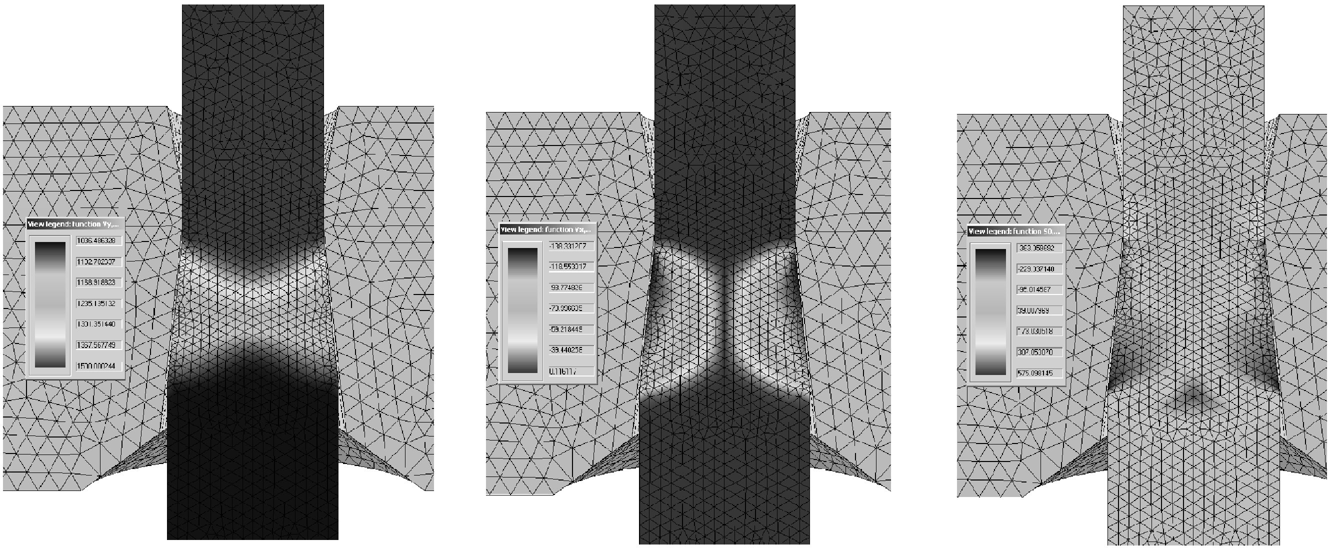

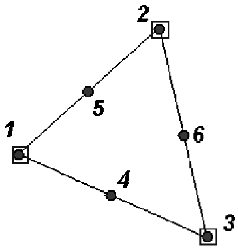

$$N_1 = L_1(2L_1 - 1) \qquad N_4 = 4L_1L_3$$

$$N_2 = L_2(2L_2 - 1) \qquad N_5 = 4L_1L_2$$

$$N_3 = L_3(2L_3 - 1) \qquad N_6 = 4L_2L_3$$

Temperature distribution

$$\frac{\partial}{\partial x}\left(k_x(t)\frac{\partial t}{\partial x}\right)+\frac{\partial}{\partial y}\left(k_y(t)\frac{\partial t}{\partial y}\right)+\frac{\partial}{\partial z}\left(k_z(t)\frac{\partial t}{\partial z}\right)+Q=c_{eff}\,\rho\,\frac{\partial t}{\partial \tau}$$

$$k(t)\left(\frac{\partial t}{\partial x}a_x+\frac{\partial t}{\partial y}a_y+\frac{\partial t}{\partial z}a_z\right)=\alpha_{konw}\left(t-t_\infty\right)$$

α_{konw} (W/m^2 K);

$$k(t)\left(\frac{\partial t}{\partial x}a_x+\frac{\partial t}{\partial y}a_y+\frac{\partial t}{\partial z}a_z\right)=\sigma_{rad}\left(t^4-t_\infty^4\right)$$

σ_{rad} (W/m^{2}K^4).

$$\boxed{J=\int_V\left[\frac{k(t)}{2}\left(\left(\frac{\partial t}{\partial x}\right)^2+\left(\frac{\partial t}{\partial y}\right)^2+\left(\frac{\partial t}{\partial z}\right)^2\right)-Qt\right]dV+\int_S\frac{\alpha}{2}\left(t-t_\infty\right)^2dS+\int_S qt\,dS}$$

Dyscretisation

$$t = \sum_{i=1}^{n} N_i t_i = \{N\}^T \{t\} = [N]\{t\}$$

$$\frac{\partial t}{\partial x} = \frac{\partial}{\partial x}\left(\{N\}^T \{t\}\right) = \left\{\frac{\partial \{N\}}{\partial x}\right\}^T \{t\}$$

$$J = \int_V \left[\frac{k(t)}{2} \left(\left(\left\{\frac{\partial \{N\}}{\partial x}\right\}^T \{t\} \right)^2 + \left(\left\{\frac{\partial \{N\}}{\partial y}\right\}^T \{t\} \right)^2 + \left(\left\{\frac{\partial \{N\}}{\partial z}\right\}^T \{t\} \right)^2 \right) - Q\{N\}^T\{t\} \right] dV +$$

$$+ \int_S \frac{\alpha}{2} \left(\{N\}^T \{t\} - t_\infty\right)^2 dS + \int_S q\{N\}^T \{t\} dS.$$

The computer simulation of the hot metal forming processes
Milenin Andrzej, AGH University of Science and Technology, 2012
AKADEMIA GÓRNICZO-HUTNICZA IM. STANISŁAWA STASZICA W KRAKOWIE
AGH

Minimization of functional

$$\frac{\partial J}{\partial \{t\}} = \int_V \left[k(t) \left(\left\{\frac{\partial \{N\}}{\partial x}\right\}\left\{\frac{\partial \{N\}}{\partial x}\right\}^T + \left\{\frac{\partial \{N\}}{\partial y}\right\}\left\{\frac{\partial \{N\}}{\partial y}\right\}^T + \left\{\frac{\partial \{N\}}{\partial z}\right\}\left\{\frac{\partial \{N\}}{\partial z}\right\}^T \right)\{t\} - Q\{N\} \right] dV +$$

$$\int_S \alpha\left(\{N\}^T \{t\} - t_\infty\right)\{N\} dS + \int_S q\{N\} dS = 0$$

$$[H]\{t\} + \{P\} = 0$$

$$[H] = \int_V k(t) \left(\left\{\frac{\partial \{N\}}{\partial x}\right\}\left\{\frac{\partial \{N\}}{\partial x}\right\}^T + \left\{\frac{\partial \{N\}}{\partial y}\right\}\left\{\frac{\partial \{N\}}{\partial y}\right\}^T + \left\{\frac{\partial \{N\}}{\partial z}\right\}\left\{\frac{\partial \{N\}}{\partial z}\right\}^T \right) dV + \int_S \alpha \{N\}\{N\}^T dS,$$

$$\{P\} = -\int_S \alpha\{N\} t_\infty dS - \int_V Q\{N\} dV + \int_S q\{N\} dS$$

Example:

$$
\boxed{\begin{aligned}
\left[H\right] &= \int_V k\left\{\frac{\partial\{N\}}{\partial x}\right\}\left\{\frac{\partial\{N\}}{\partial x}\right\}^T dV + \int_S \alpha\{N\}\{N\}^T dS \\
\{P\} &= -\int_S \alpha\{N\} t_\infty dS + \int_S q\{N\} dS
\end{aligned}}
$$

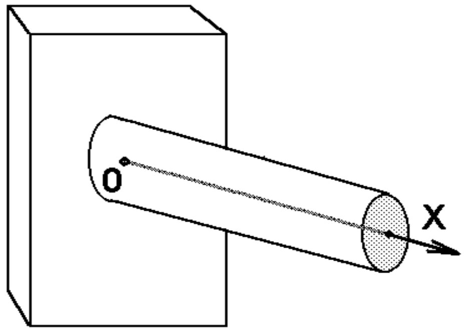

$$
\{N\} = \begin{Bmatrix} N_i \\ N_j \end{Bmatrix} = \begin{Bmatrix} \dfrac{x_j - x}{L} \\ \dfrac{x - x_i}{L} \end{Bmatrix}
$$

$$
\{N\}^T = \{N_i \quad N_j\} = \left\{\frac{x_j - x}{L}; \quad \frac{x - x_i}{L}\right\}
$$

$$
\left\{\frac{\partial\{N\}}{\partial x}\right\} = \begin{Bmatrix} -\dfrac{1}{L} \\ \dfrac{1}{L} \end{Bmatrix}
$$

$$
\left\{\frac{\partial\{N\}}{\partial x}\right\}^T = \left\{-\frac{1}{L} \quad \frac{1}{L}\right\}
$$

$$
[H] = k\begin{Bmatrix} -\dfrac{1}{L} \\ \dfrac{1}{L} \end{Bmatrix}\left\{-\frac{1}{L} \quad \frac{1}{L}\right\} SL + \alpha\begin{Bmatrix} N_i \\ N_j \end{Bmatrix}\{N_i \quad N_j\} S
$$

$$
\boxed{[H] = \int_V k\begin{Bmatrix} -\dfrac{1}{L} \\ \dfrac{1}{L} \end{Bmatrix}\left\{-\frac{1}{L} \quad \frac{1}{L}\right\} dV + \int_S \alpha\begin{Bmatrix} \dfrac{x_j - x}{L} \\ \dfrac{x - x_i}{L} \end{Bmatrix}\left\{\frac{x_j - x}{L}; \quad \frac{x - x_i}{L}\right\} dS}
$$

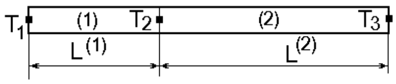

$$
[H] = k\begin{Bmatrix} -\dfrac{1}{L} \\ \dfrac{1}{L} \end{Bmatrix}\left\{-\frac{1}{L} \quad \frac{1}{L}\right\} SL + \alpha\begin{Bmatrix} N_i \\ N_j \end{Bmatrix}\{N_i \quad N_j\} S
$$

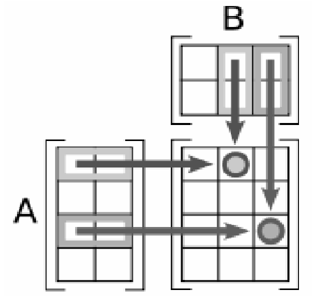

$$
[H]^{(1)} = k\begin{bmatrix} \dfrac{1}{L^{(1)2}} & -\dfrac{1}{L^{(1)2}} \\ -\dfrac{1}{L^{(1)2}} & \dfrac{1}{L^{(1)2}} \end{bmatrix} SL^{(1)} = \begin{bmatrix} \dfrac{Sk}{L^{(1)}} & -\dfrac{Sk}{L^{(1)}} \\ -\dfrac{Sk}{L^{(1)}} & \dfrac{Sk}{L^{(1)}} \end{bmatrix}
$$

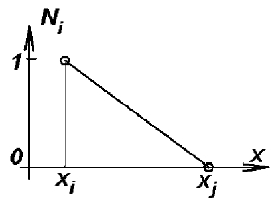

$$
[H]^{(2)} = k\begin{bmatrix} \dfrac{1}{L^{(2)2}} & -\dfrac{1}{L^{(2)2}} \\ -\dfrac{1}{L^{(2)2}} & \dfrac{1}{L^{(2)2}} \end{bmatrix} SL^{(2)} + \alpha\begin{Bmatrix} N_iN_i & N_iN_j \\ N_iN_j & N_jN_j \end{Bmatrix} S
$$

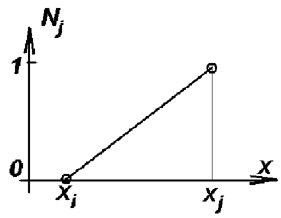

$$
[H]^{(2)} = \begin{bmatrix} \dfrac{Sk}{L^{(2)}} & -\dfrac{Sk}{L^{(2)}} \\ -\dfrac{Sk}{L^{(2)}} & \dfrac{Sk}{L^{(2)}} \end{bmatrix} + \begin{Bmatrix} 0 & 0 \\ 0 & \alpha S \end{Bmatrix} = \begin{bmatrix} \dfrac{Sk}{L^{(2)}} & -\dfrac{Sk}{L^{(2)}} \\ -\dfrac{Sk}{L^{(2)}} & \dfrac{Sk}{L^{(2)}} + \alpha S \end{bmatrix}
$$

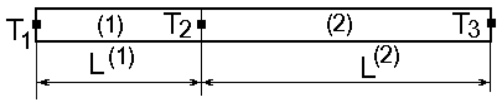

$$\{P\} = -\int_S \alpha \{N\} t_\infty dS + \int_S q \{N\} dS$$

$$\boxed{\{P\} = -\int_S \alpha \begin{Bmatrix} N_i \\ N_j \end{Bmatrix} t_\infty dS + \int_S q \begin{Bmatrix} N_i \\ N_j \end{Bmatrix} dS}$$

$$\{N\} = \begin{Bmatrix} N_i \\ N_j \end{Bmatrix} = \begin{Bmatrix} \dfrac{x_j - x}{L} \\ \dfrac{x - x_i}{L} \end{Bmatrix} \qquad \{N\}^T = \{N_i \quad N_j\} = \left\{ \frac{x_j - x}{L}; \quad \frac{x - x_i}{L} \right\}$$

$$\{P\}^{(1)} = q \begin{Bmatrix} N_i \\ N_j \end{Bmatrix} S = q \begin{Bmatrix} 1 \\ 0 \end{Bmatrix} S = \begin{Bmatrix} qS \\ 0 \end{Bmatrix}$$

$$\{P\}^{(2)} = -\alpha t_\infty S \begin{Bmatrix} N_i \\ N_j \end{Bmatrix} = -\alpha t_\infty S \begin{Bmatrix} 0 \\ 1 \end{Bmatrix} = \begin{Bmatrix} 0 \\ -\alpha t_\infty S \end{Bmatrix}$$

Global stiffness matrix

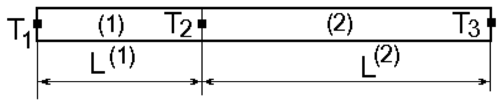

$$[H] = \sum_{e=1}^{n_e} [H]^{(e)}$$

Positions of stiffness matrix for FE number 2

	1	2
1	2, 2	2, 3
2	3, 2	3, 3

$$[H]=[H]^{(1)}+[H]^{(2)}=\begin{bmatrix}\frac{Sk}{L^{(1)}} & -\frac{Sk}{L^{(1)}} & 0\\ -\frac{Sk}{L^{(1)}} & \frac{Sk}{L^{(1)}} & 0\\ 0 & 0 & 0\end{bmatrix}+\begin{bmatrix}0 & 0 & 0\\ 0 & \frac{Sk}{L^{(2)}} & -\frac{Sk}{L^{(2)}}\\ 0 & -\frac{Sk}{L^{(2)}} & \frac{Sk}{L^{(2)}}+\alpha S\end{bmatrix}=$$

$$=\begin{bmatrix}\frac{Sk}{L^{(1)}} & -\frac{Sk}{L^{(1)}} & 0\\ -\frac{Sk}{L^{(1)}} & Sk\left(\frac{1}{L^{(1)}}+\frac{1}{L^{(2)}}\right) & -\frac{Sk}{L^{(2)}}\\ 0 & -\frac{Sk}{L^{(2)}} & \frac{Sk}{L^{(2)}}+\alpha S\end{bmatrix}$$

$$\{P\}=\{P\}^{(1)}+\{P\}^{(2)}=\begin{Bmatrix}qS\\0\\0\end{Bmatrix}+\begin{Bmatrix}0\\0\\-\alpha t_\infty S\end{Bmatrix}=\begin{Bmatrix}qS\\0\\-\alpha t_\infty S\end{Bmatrix}$$

Non- stationary problem

$$\frac{\partial}{\partial x}\left(k_x(t)\frac{\partial t}{\partial x}\right)+\frac{\partial}{\partial y}\left(k_y(t)\frac{\partial t}{\partial y}\right)+\frac{\partial}{\partial z}\left(k_z(t)\frac{\partial t}{\partial z}\right)+\boxed{\left(Q-c_{eff}\rho\frac{\partial t}{\partial \tau}\right)}=0$$

Q'

$$t=\{N\}^T\{t\}$$

$$Q'=Q-c_{eff}\rho\frac{\partial t}{\partial \tau}=Q-c_{eff}\rho\frac{\partial}{\partial \tau}\{t\}\{N\}^T$$

Stiffness matrix :

$$[H]=\int_V k(t)\left(\left\{\frac{\partial\{N\}}{\partial x}\right\}\left\{\frac{\partial\{N\}}{\partial x}\right\}^T+\left\{\frac{\partial\{N\}}{\partial y}\right\}\left\{\frac{\partial\{N\}}{\partial y}\right\}^T+\left\{\frac{\partial\{N\}}{\partial z}\right\}\left\{\frac{\partial\{N\}}{\partial z}\right\}^T\right)dV+\int_S \alpha\{N\}\{N\}^T dS,$$

$$\{P\}=-\int_S \alpha\{N\}t_\infty dS-\int_V Q\{N\}dV+\int_S q\{N\}dS$$

$$\boxed{Q'=Q-c_{eff}\rho\frac{\partial t}{\partial\tau}=Q-c_{eff}\rho\frac{\partial}{\partial\tau}\{t\}\{N\}^T}$$

$$[H]\{t\}+\{P\}=0 \quad \Rightarrow \quad \boxed{\begin{gathered}[H]\{t\}+[C]\frac{\partial}{\partial\tau}\{t\}+\{P\}=0\\ [C]=\int_V\{N\}\rho c_{eff}\{N\}^T dV\end{gathered}}$$

Derivatives in time

$$\{t\}=\{N_0,N_1\}\begin{Bmatrix}\{t_0\}\\ \{t_1\}\end{Bmatrix}$$

$$N_0=\frac{\Delta\tau-\tau}{\Delta\tau}$$

$$N_1=\frac{\tau}{\Delta\tau}$$

$$\Rightarrow \quad \frac{\partial\{t\}}{\partial\tau}=\left\{\frac{\partial N_0}{\partial\tau},\frac{\partial N_1}{\partial\tau}\right\}\begin{Bmatrix}\{t_0\}\\ \{t_1\}\end{Bmatrix}=\frac{1}{\Delta\tau}\{-1,1\}\begin{Bmatrix}\{t_0\}\\ \{t_1\}\end{Bmatrix}$$

$$\boxed{[H]\{t\}+[C]\frac{\partial}{\partial\tau}\{t\}+\{P\}=0 \qquad (1)}$$

$$\boxed{\frac{\partial\{t\}}{\partial\tau}=\left\{\frac{\partial N_0}{\partial\tau},\frac{\partial N_1}{\partial\tau}\right\}\begin{Bmatrix}\{t_0\}\\\{t_1\}\end{Bmatrix}=\frac{1}{\Delta\tau}\{-1,1\}\begin{Bmatrix}\{t_0\}\\\{t_1\}\end{Bmatrix}=\frac{\{t_1\}-\{t_0\}}{\Delta\tau}. \qquad (2)}$$

1. $\{t\}=\{t_0\}$,

$$[H]\{t_0\}+[C]\frac{\{t_1\}-\{t_0\}}{\Delta\tau}+\{P\}=0$$

$$\boxed{\{t_1\}=\{t_0\}-\frac{\Delta\tau}{[C]}\left([H]\{t_0\}+\{P\}\right)}$$

$$\boxed{[H]\{t\}+[C]\frac{\partial}{\partial\tau}\{t\}+\{P\}=0 \qquad (1)}$$

$$\boxed{\frac{\partial\{t\}}{\partial\tau}=\left\{\frac{\partial N_0}{\partial\tau},\frac{\partial N_1}{\partial\tau}\right\}\begin{Bmatrix}\{t_0\}\\\{t_1\}\end{Bmatrix}=\frac{1}{\Delta\tau}\{-1,1\}\begin{Bmatrix}\{t_0\}\\\{t_1\}\end{Bmatrix}=\frac{\{t_1\}-\{t_0\}}{\Delta\tau}. \qquad (2)}$$

2. $\{t\}=\{t_1\}$:

$$[H]\{t_1\}+[C]\frac{\{t_1\}-\{t_0\}}{\Delta\tau}+\{P\}=0$$

$$\boxed{\left([H]+\frac{[C]}{\Delta\tau}\right)\{t_1\}-\left(\frac{[C]}{\Delta\tau}\right)\{t_0\}+\{P\}=0}$$

$$\boxed{[H]\{t\}+[C]\frac{\partial}{\partial\tau}\{t\}+\{P\}=0 \qquad (1)}$$

$$\boxed{\frac{\partial\{t\}}{\partial\tau}=\left\{\frac{\partial N_0}{\partial\tau},\frac{\partial N_1}{\partial\tau}\right\}\begin{Bmatrix}\{t_0\}\\ \{t_1\}\end{Bmatrix}=\frac{1}{\Delta\tau}\{-1,1\}\begin{Bmatrix}\{t_0\}\\ \{t_1\}\end{Bmatrix}=\frac{\{t_1\}-\{t_0\}}{\Delta\tau}. \qquad (2)}$$

3. $$\{t\}=\frac{1}{2}\left(\{t_1\}+\{t_0\}\right)$$

$$\{P\}^*=\frac{1}{2}\left(\{P_1\}+\{P_0\}\right)$$

$$[H]\frac{1}{2}\left(\{t_1\}+\{t_0\}\right)+[C]\frac{\{t_1\}-\{t_0\}}{\Delta\tau}+\{P\}^*=0$$

$$\left(\frac{[H]}{2}+\frac{[C]}{\Delta\tau}\right)\{t_1\}+\left(\frac{[H]}{2}-\frac{[C]}{\Delta\tau}\right)\{t_0\}+\{P\}^*=0$$

$$\boxed{\left([H]+\frac{2[C]}{\Delta\tau}\right)\{t_1\}+\left([H]-\frac{2[C]}{\Delta\tau}\right)\{t_0\}+2\{P\}^*=0}$$

$$\boxed{[H]\{t\}+[C]\frac{\partial}{\partial\tau}\{t\}+\{P\}=0 \qquad (1)}$$

$$\boxed{\frac{\partial\{t\}}{\partial\tau}=\left\{\frac{\partial N_0}{\partial\tau},\frac{\partial N_1}{\partial\tau}\right\}\begin{Bmatrix}\{t_0\}\\ \{t_1\}\end{Bmatrix}=\frac{1}{\Delta\tau}\{-1,1\}\begin{Bmatrix}\{t_0\}\\ \{t_1\}\end{Bmatrix}=\frac{\{t_1\}-\{t_0\}}{\Delta\tau}. \qquad (2)}$$

4. $$N_0=\frac{\Delta\tau-\tau}{\Delta\tau} \qquad N_1=\frac{\tau}{\Delta\tau}$$

$$\int_0^{\Delta\tau}N_1\left[[H]\{N_0,N_1\}\begin{Bmatrix}\{t_0\}\\ \{t_1\}\end{Bmatrix}+C\left\{\frac{\partial N_0}{\partial\tau},\frac{\partial N_1}{\partial\tau}\right\}\begin{Bmatrix}\{t_0\}\\ \{t_1\}\end{Bmatrix}+\{P\}\right]d\tau=0$$

$$\int_0^{\Delta\tau}\frac{\tau}{\Delta\tau}\left[[H]\{N_0,N_1\}\begin{Bmatrix}\{t_0\}\\ \{t_1\}\end{Bmatrix}+C\left\{\frac{\partial N_0}{\partial\tau},\frac{\partial N_1}{\partial\tau}\right\}\begin{Bmatrix}\{t_0\}\\ \{t_1\}\end{Bmatrix}+\{P\}\right]d\tau=0$$

$$\int_0^{\Delta\tau}\frac{\tau}{\Delta\tau}\left[[H]\left(\frac{\Delta\tau-\tau}{\Delta\tau}\{t_0\}+\frac{\tau}{\Delta\tau}\{t_1\}\right)+\frac{C}{\Delta\tau}\left(-\{t_0\}+\{t_1\}\right)+\{P\}\right]d\tau=0$$

$$\boxed{\left(2[H]+\frac{3}{\Delta\tau}[C]\right)\{t_1\}+\left([H]-\frac{3}{\Delta\tau}[C]\right)\{t_0\}+3\{P\}=0}$$

Lection 4

Application of the finite elements method to the solution of the problems of hot metal forming. Calculation of the mechanical properties of the workable metal in the algorithm, based on FEM.

EXAMPLE OF FEM SOFTWARE

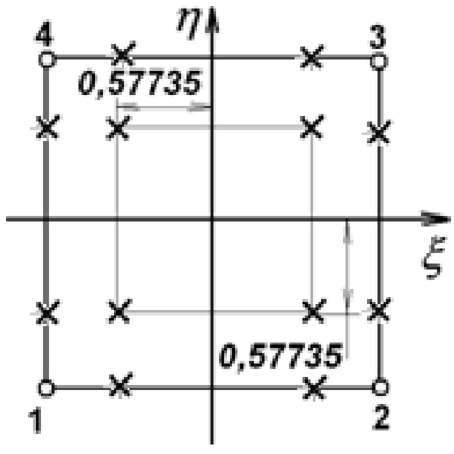

FORMULATION OF THERMAL PROBLEM

$$\left([H]+\frac{[C]}{\Delta\tau}\right)\{t_1\}-\left(\frac{[C]}{\Delta\tau}\right)\{t_0\}+\{P\}=0,$$

where

$$[H]=\int_V k\left(\left\{\frac{\partial\{N\}}{\partial x}\right\}\left\{\frac{\partial\{N\}}{\partial x}\right\}^T+\left\{\frac{\partial\{N\}}{\partial y}\right\}\left\{\frac{\partial\{N\}}{\partial y}\right\}^T\right)dV+\int_S \alpha\{N\}\{N\}^T dS,$$

$$\{P\}=-\int_S \alpha\{N\}t_\infty dS,$$

$$[C]=\int_V c\rho\{N\}\{N\}^T dV.$$

DATA FOR SIMULATION

100	mTbegin	Initial temperature, C
1000	mTime	Time of process, s
1	mdTime	Time step, s
1200	mT_otoczenia	Temperature of invironpment C
300	mAlfa	W/Cm2
100	mH0	h, mm
100	mB0	b, mm
25	mNhH	nh
25	mNhH	nb
700	mC	c, J/Ckg
25	mK	k
7800	mR	ro kg/m3

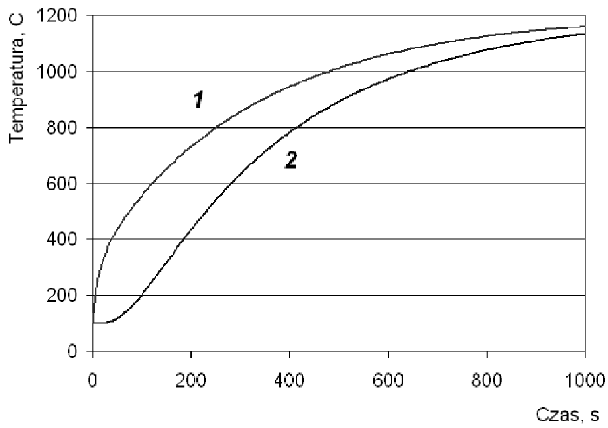

The computer simulation of the hot metal forming processes
Milenin Andrzej, AGH University of Science and Technology, 2012
AKADEMIA GÓRNICZO-HUTNICZA IM. STANISŁAWA STASZICA W KRAKOWIE
AGH

Mechanical properties of the workable metal

Shape of samples after tests

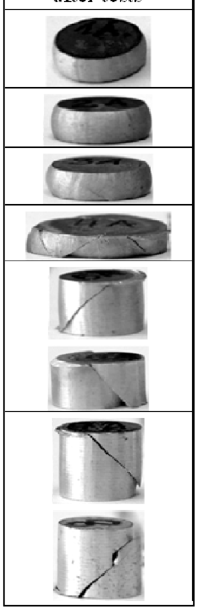

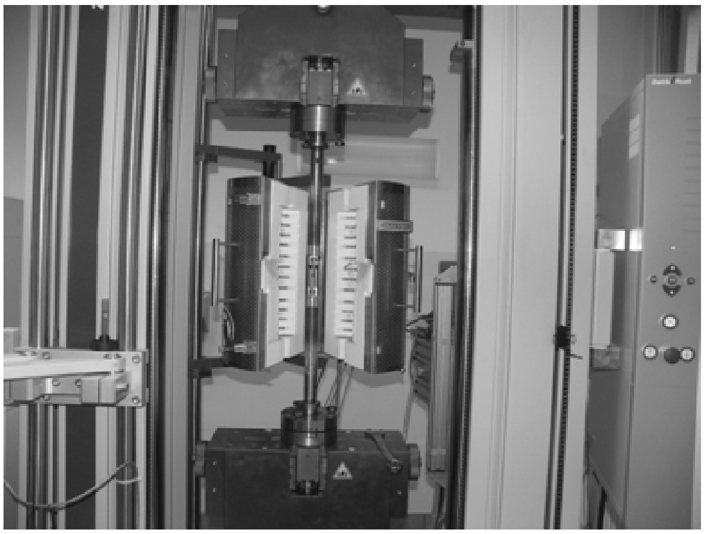

Problems:

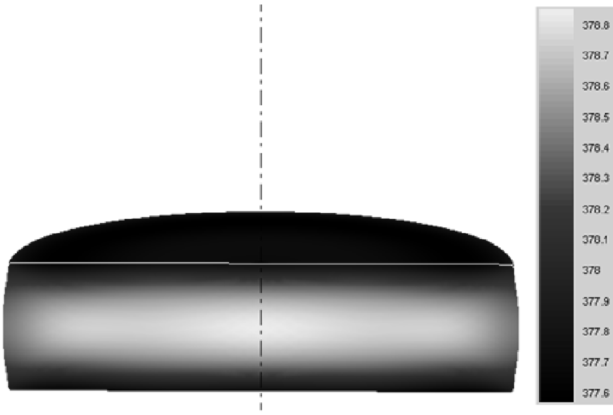

a)

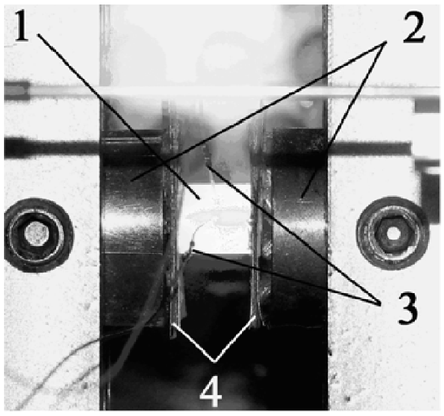

b)

Inverse method

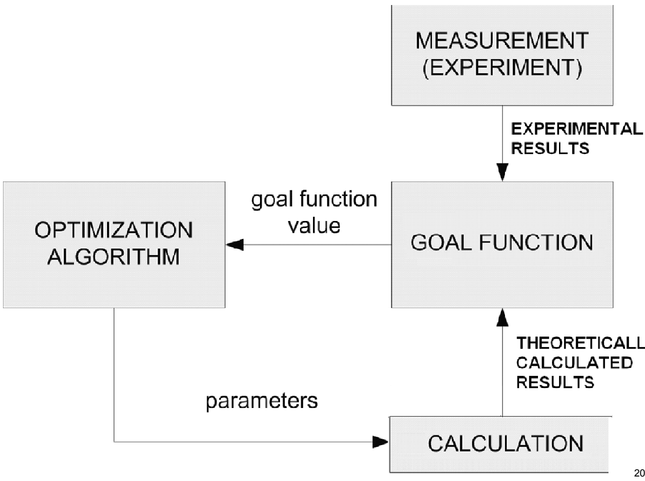

$$grad(t) \approx 0 \qquad c\rho \frac{dt}{d\tau} = 0{,}9\xi_i \sigma_s$$

$$c\rho \frac{t_1 - t_0}{\Delta\tau} = 0{,}9\xi_i \sigma_s \qquad t_1 = t_0 + \frac{\Delta\tau 0{,}9\xi_i \sigma_s}{c\rho}$$

$$P^{calc} = \sigma_s(\varepsilon_i, \xi_i, t)\left(1 + \frac{fd(h)}{3h}\right)S(h)$$

$$\delta = \sum_{m}^{m_{test}} \sum_{n=1}^{n_{pnt}} \left(P_{mn}^{calc} - P_{mn}^{exp}\right)^2$$

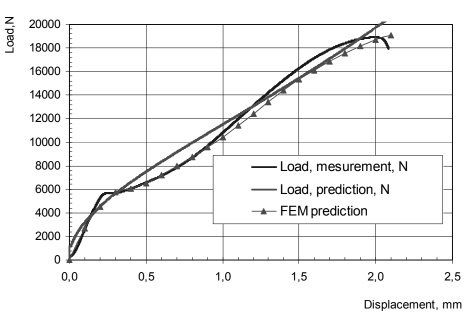

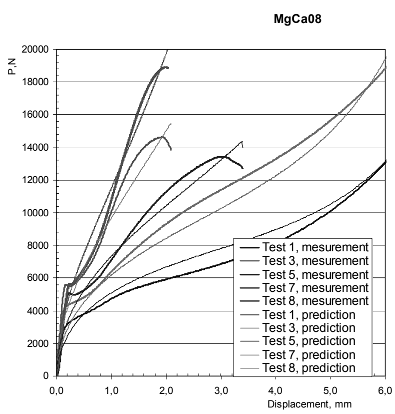

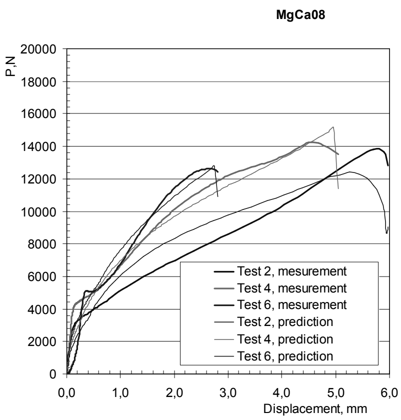

Results of inverse method

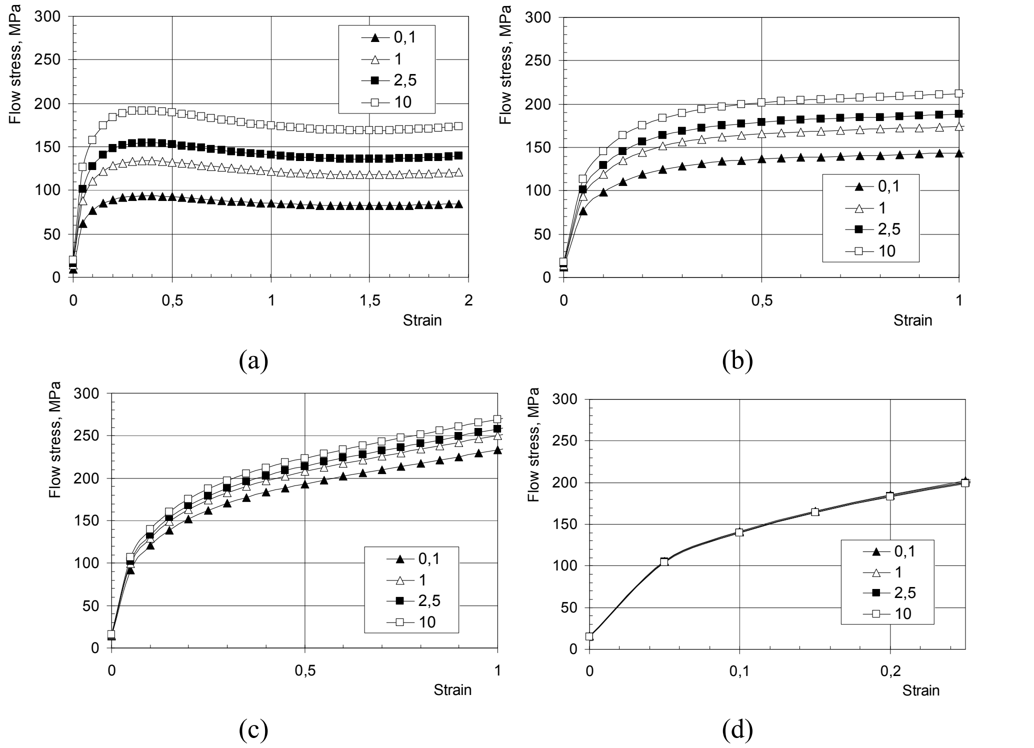

Stress strain curves of MgCa0.8 magnesium alloy for temperatures (a) – 300 °C, (b) – 250 °C, (c) – 200 °C, (d) – 150 °C and strain rates 0.1, 1.0, 2.5 and 10 s^{-1}.

Lection 5.

Special features of FEM simulation of the extrusion.
Special features of FEM simulation of the forging and stamping.
Special features of FEM simulation of the hot rolling.

Special features of FEM simulation of the extrusion.

The material is considered as incompressible rigid-viscous-plastic continua and elastic deformation are neglected. The system of governing equation includes:

- Equilibrium equations:

$$\sigma_{ij,i} = 0, \qquad (1)$$

- compatibility condition:

$$\xi_{ij} = \frac{1}{2}\left(v_{i,j} + v_{j,i}\right), \qquad (2)$$

- constitutive equations:

$$s_{ij} = \frac{2\bar{\sigma}}{3\bar{\xi}}\xi_{ij}, \qquad (3)$$

- incompressibility equation:

$$v_{i,j} = 0, \qquad (4)$$

- energy balance equation for steady-state boundary problem:

$$k\left(t_{,i}\right)_{,i} + \beta\bar{\sigma}\bar{\xi} = 0 \qquad (5)$$

- and expression for flow stress:

$$\bar{\sigma} = \bar{\sigma}\left(\varepsilon, \bar{\xi}, t\right), \qquad (6)$$

where σ_{ij} – stress tensor, ξ_{ij} – strain rate tensor and v_i – velocity component respectively, $\sigma_{ij}^{`}$ – deviator of stress tensor, $\bar{\sigma}, \bar{\varepsilon}, \bar{\xi}$ – effective stress, effective strain and effective strain-rate, respectively, t – temperature, β – heat generation efficiency which is usually assumed as β=0.9-9.95, k – thermal conductivity.

Overview of the software Extrusion3d capability

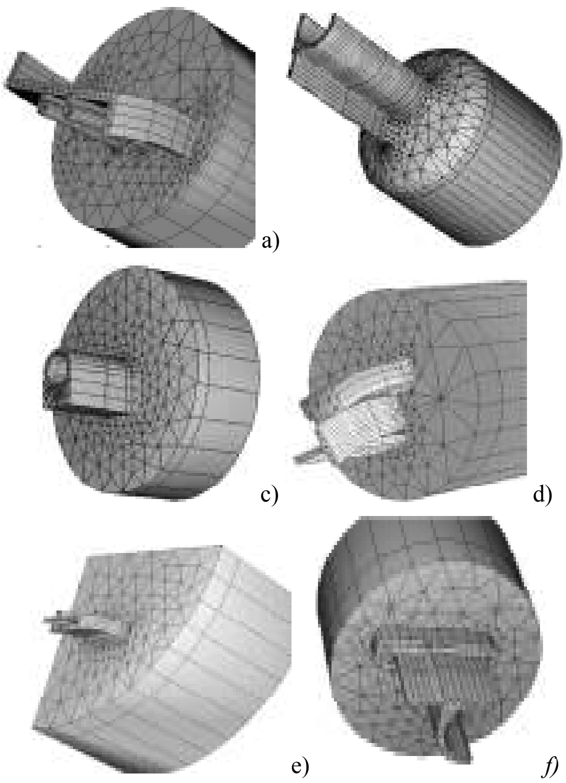

Types of extrusion processes which can be simulated with Extrusion3 program.

CAD &geometry capture

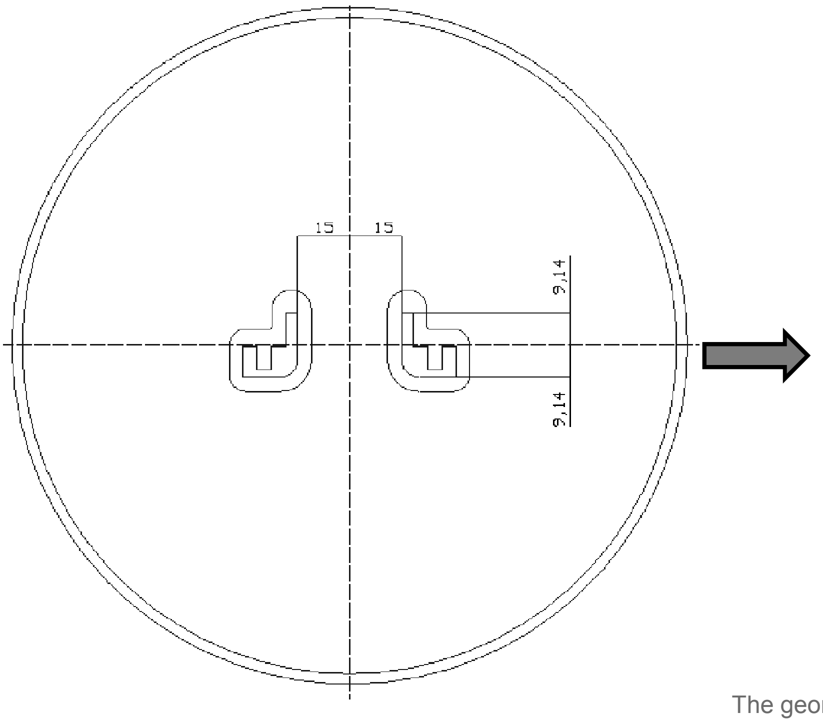

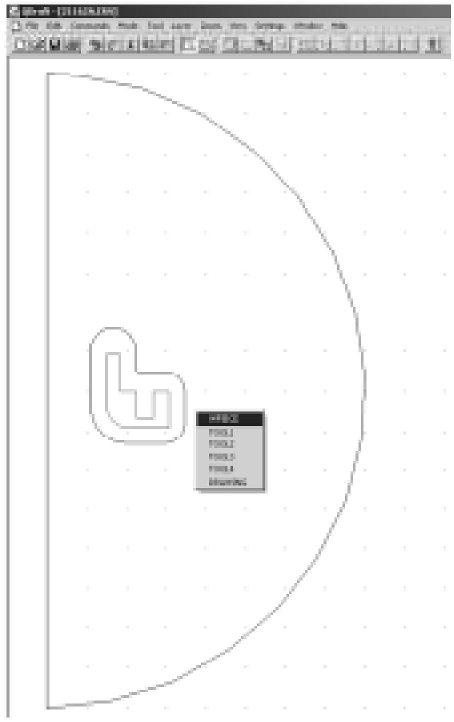

The geometrical source data in Qdraft program (Quantor Form).

The computer simulation of the hot metal forming processes
Milenin Andrzej, AGH University of Science and Technology, 2012
AKADEMIA GÓRNICZO-HUTNICZA IM. STANISŁAWA STASZICA W KRAKOWIE AGH

FEM formulation

For velocity and pressure approximation the standard FEM approach is used:

$$v_x = [N]\{\mathrm{v_x}\}, \tag{7}$$

$$v_y = [N]\{\mathrm{v_y}\}, \tag{8}$$

$$v_z = [N]\{\mathrm{v_z}\}, \tag{9}$$

$$\sigma_0 = [H]\{\sigma_0\}, \tag{10}$$

Where [N] and [H] are finite elements shape functions.
The virtual work-rate principle was describe in matrix form:

$$J = \int_{\mathrm{V}} \frac{1}{2}\{\mathrm{v}\}^T [B]^T [D][B]\{\mathrm{v}\} dV + \int_{\mathrm{V}} [H]\{\sigma_0\}[E]\{\mathrm{v}\} dV - \int_{\mathrm{S}} \{\mathrm{v}\}^T \left[\overline{N}\right]^T \{p\} dS = 0 \tag{11}$$

$$[B] = \begin{bmatrix} \frac{\partial[N]}{\partial x} & 0 & 0 \\ 0 & \frac{\partial[N]}{\partial y} & 0 \\ 0 & 0 & \frac{\partial[N]}{\partial z} \\ \frac{\partial[N]}{\partial y} & \frac{\partial[N]}{\partial x} & 0 \\ 0 & \frac{\partial[N]}{\partial z} & \frac{\partial[N]}{\partial y} \\ \frac{\partial[N]}{\partial z} & 0 & \frac{\partial[N]}{\partial x} \end{bmatrix} \quad [D] = \begin{bmatrix} 2\mu & 0 & 0 & 0 \\ 0 & 2\mu & 0 & 0 \\ 0 & 0 & 2\mu & 0 \\ 0 & 0 & 0 & \mu \end{bmatrix} \quad [E] = \begin{bmatrix} \frac{\partial[N]}{\partial x} & \frac{\partial[N]}{\partial y} & \frac{\partial[N]}{\partial z} \end{bmatrix}$$

The stress deviator components were calculated by follow equation:

$$\{s\} = [D][B]\{\mathrm{v}\}. \qquad (15)$$

For variable $\{\mathrm{v}\}$ and $\{\sigma_0\}$ determinate the follow principle was use:

$$\frac{\partial J}{\partial\{\mathrm{v}\}} = \left(\int_V [B]^T [D][B] dV\right)\{\mathrm{v}\} + \left(\int_V [E]^T [H] dV\right)\{\sigma_0\} - \int_S \left[\overline{N}\right]^T \{p\} dS = 0, \qquad (16)$$

$$\frac{\partial J}{\partial\{\sigma_0\}} = \left(\int_V [H]^T [E] dV\right)\{\mathrm{v}\} = 0. \qquad (17)$$

The result of equation (16) and (17) was present in matrix form:

$$[K]\{\mathrm{v},\sigma_0\} + \{F\} = 0 \qquad (18)$$

where:

$$[K] = \sum_{e=1}^{n_e} [K_e] \qquad (19)$$

$$\{F\} = \sum_{e=1}^{n_e} \{F_e\} \qquad (20)$$

$$[K] = \int_V \left[\begin{array}{c|c|c|c}
2\mu \frac{\partial[N]^T}{\partial x}\frac{\partial[N]}{\partial x} + \mu \frac{\partial[N]^T}{\partial y}\frac{\partial[N]}{\partial y} + \mu \frac{\partial[N]^T}{\partial z}\frac{\partial[N]}{\partial z} & \mu \frac{\partial[N]^T}{\partial x}\frac{\partial[N]}{\partial y} & \mu \frac{\partial[N]^T}{\partial x}\frac{\partial[N]}{\partial z} & \frac{\partial[N]^T}{\partial x}[H] \\ \hline
\mu \frac{\partial[N]^T}{\partial y}\frac{\partial[N]}{\partial x} & 2\mu \frac{\partial[N]^T}{\partial y}\frac{\partial[N]}{\partial y} + \mu \frac{\partial[N]^T}{\partial x}\frac{\partial[N]}{\partial x} + \mu \frac{\partial[N]^T}{\partial z}\frac{\partial[N]}{\partial z} & \mu \frac{\partial[N]^T}{\partial y}\frac{\partial[N]}{\partial z} & \frac{\partial[N]^T}{\partial y}[H] \\ \hline
\mu \frac{\partial[N]^T}{\partial z}\frac{\partial[N]}{\partial x} & \mu \frac{\partial[N]^T}{\partial z}\frac{\partial[N]}{\partial y} & 2\mu \frac{\partial[N]^T}{\partial z}\frac{\partial[N]}{\partial z} + \mu \frac{\partial[N]^T}{\partial x}\frac{\partial[N]}{\partial x} + \mu \frac{\partial[N]^T}{\partial y}\frac{\partial[N]}{\partial y} & \frac{\partial[N]^T}{\partial z}[H] \\ \hline
[H]^T \frac{\partial[N]}{\partial x} & [H]^T \frac{\partial[N]}{\partial y} & [H]^T \frac{\partial[N]}{\partial z} & 0
\end{array}\right] dV$$

$$\{F\} = \int_S \begin{Bmatrix} [N]^T p_x \\ [N]^T p_y \\ [N]^T p_z \\ 0 \end{Bmatrix} dS$$

Type of elements

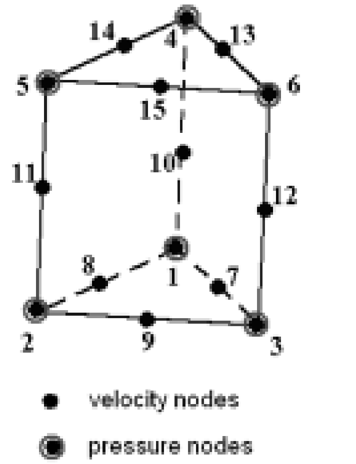

The 15-nodes prismatic finite element.

$$N_1 = \frac{1}{2}L_1(2L_1-1)(1-\xi) - \frac{1}{2}L_1(1-\xi^2)$$
$$N_2 = \frac{1}{2}L_2(2L_2-1)(1-\xi) - \frac{1}{2}L_2(1-\xi^2)$$
$$N_3 = \frac{1}{2}L_3(2L_3-1)(1-\xi) - \frac{1}{2}L_3(1-\xi^2)$$
$$N_4 = \frac{1}{2}L_1(2L_1-1)(1+\xi) - \frac{1}{2}L_1(1-\xi^2)$$
$$N_5 = \frac{1}{2}L_2(2L_2-1)(1+\xi) - \frac{1}{2}L_2(1-\xi^2)$$
$$N_6 = \frac{1}{2}L_3(2L_3-1)(1+\xi) - \frac{1}{2}L_3(1-\xi^2)$$
$$N_7 = 2L_3L_1(1-\xi)$$
$$N_8 = 2L_2L_1(1-\xi)$$
$$N_9 = 2L_3L_2(1-\xi)$$
$$N_{10} = L_1(1-\xi^2)$$
$$N_{11} = L_2(1-\xi^2)$$
$$N_{12} = L_3(1-\xi^2)$$
$$N_{13} = 2L_3L_1(1+\xi)$$
$$N_{14} = 2L_2L_1(1+\xi)$$
$$N_{15} = 2L_3L_2(1+\xi)$$

$$H_1 = \frac{1}{2}L_1(1-\xi)$$
$$H_2 = \frac{1}{2}L_2(1-\xi)$$
$$H_3 = \frac{1}{2}L_3(1-\xi)$$
$$H_4 = \frac{1}{2}L_1(1+\xi)$$
$$H_5 = \frac{1}{2}L_2(1+\xi)$$
$$H_6 = \frac{1}{2}L_3(1+\xi).$$

Meshing

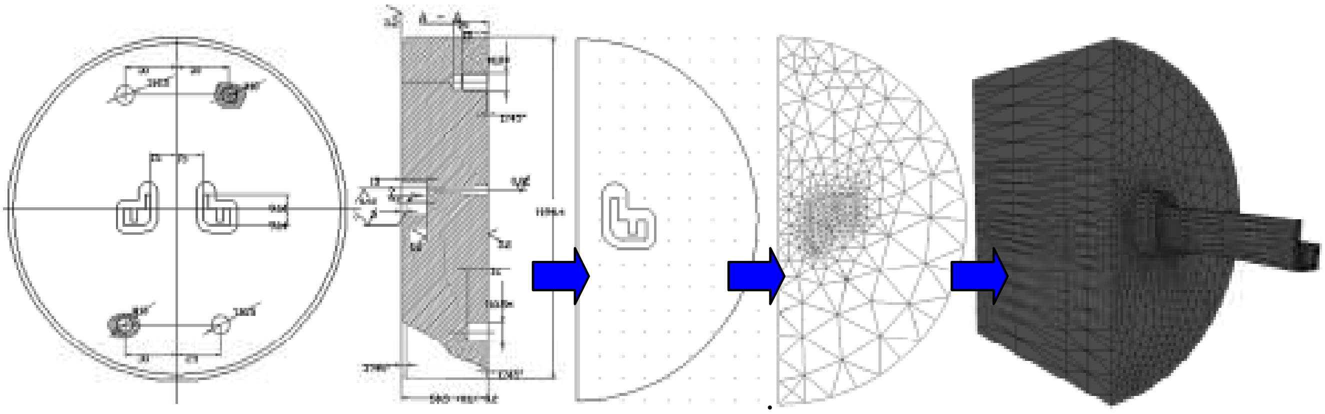

Example of automatic 3d mesh generation

The automatic generator of a three-dimensional grid is based on an "extrusion" from two-dimensional triangular grids. At generation of two-dimensional grids the algorithm of grid generation in a closed loop is used.

Lishnij, AI; Biba, NV; Milenin, AA Two levels approach to the problem of steady state extrusion process optimisation // SIMULATION OF MATERIALS PROCESSING: THEORY, METHODS AND APPLICATIONS p627-631 1998

Visualization

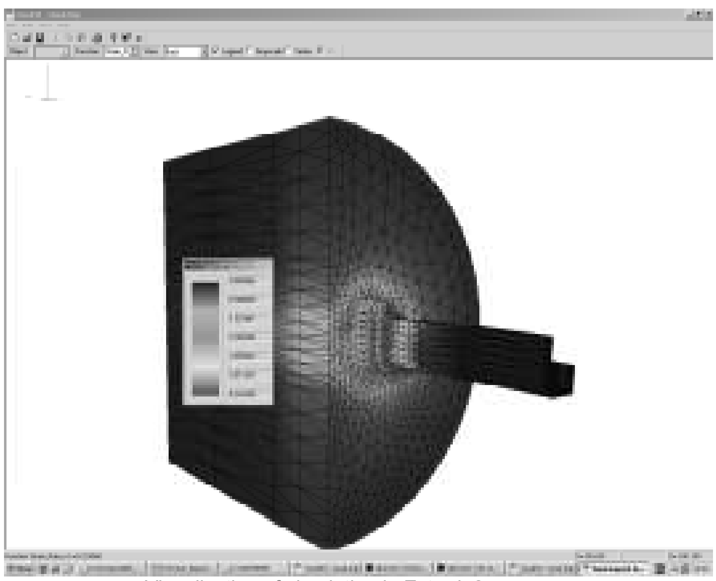

Visualization of simulation in Extrude3 program.

The visualisation procedure in Extrusion3 program is based on DirectX library. The window with visualisation of results is shown on fig. The integral results of simulation such as extrusion load, profile band, etc are presented in the tabular form.

Defect prediction

The results of simulation (case 1) of extrusion are presented in figs. The following input data were used:

- The ram speed of 4.5 mm/s was assumed.
- Friction factor was 0.3;
- Temperature of billet was 460 ^{O}C;
- Temperature of die was 430 ^{O}C.

The extrusion process was performing with out working bend. The profile band (defect) was 165 mm/m. The profile twisting also was very big and was 77 degree/m.

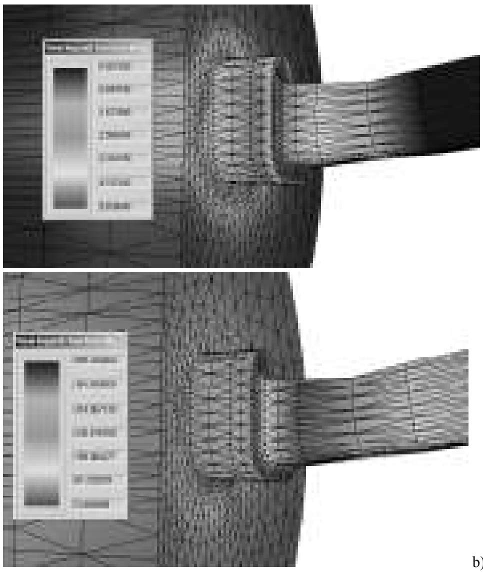

a)

b)

Distribution of strain rate (a) and mean stress (b) in deformation zone during extrusion with out working bend.

Bend of the profile and longitudinal velocity component distribution in deformation zone during extrusion with out working bend.

Correction of extrusion technology was based on working bend use during extrusion (variant 2). The length of bend was 5 mm.

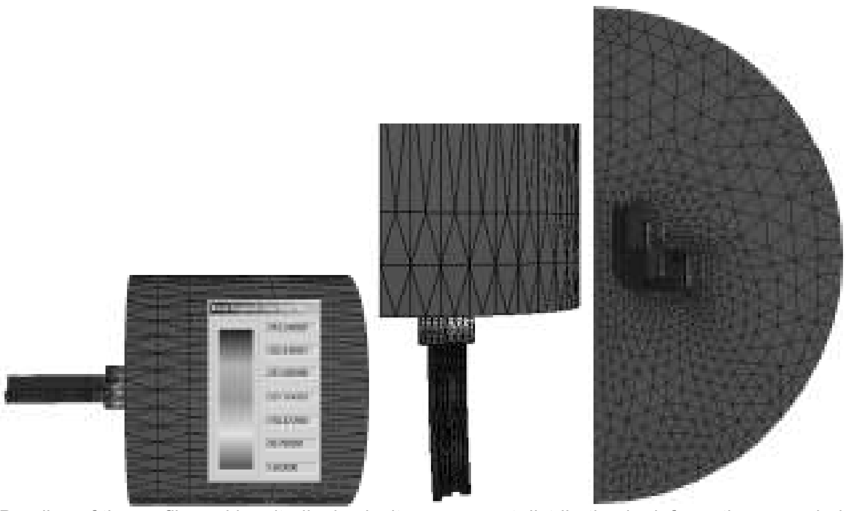

Bending of the profile and longitudinal velocity component distribution in deformation zone during extrusion with working bend (b= 5 mm).

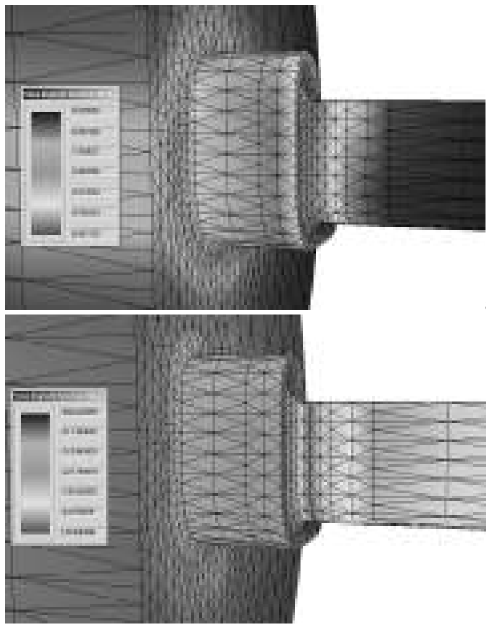

a)

b)

Distribution of strain rate (a) and mean stress (b) in deformation zone during extrusion with working bend (b= 5 mm).

The profile bending (defect) was 28,2 mm/m. The profile twisting is also very big, it was predicted to be 11,3 degree/m.

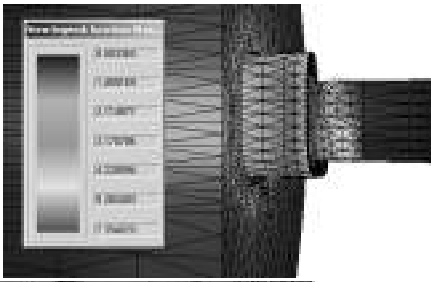

a)

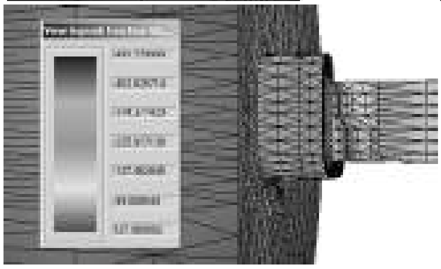

b)

Distribution of strain rate (a) and mean stress (b) in deformation zone during extrusion with working bend (b is variable according fig.).

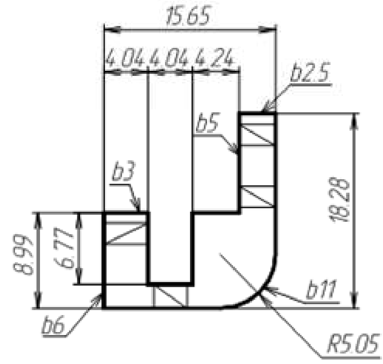

Workings bend distribution on profile channel perimeter.

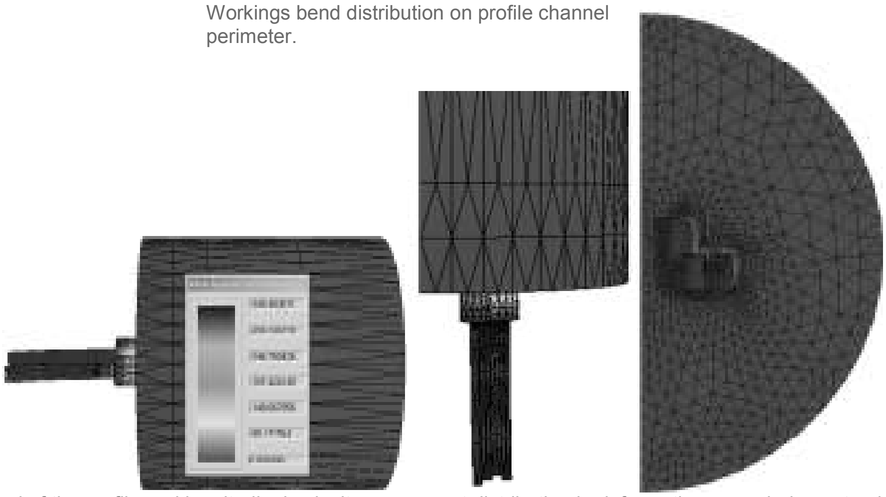

Bend of the profile and longitudinal velocity component distribution in deformation zone during extrusion with working bend (b is variable according fig.).

The computer simulation of the hot metal forming processes
Milenin Andrzej, AGH University of Science and Technology, 2012

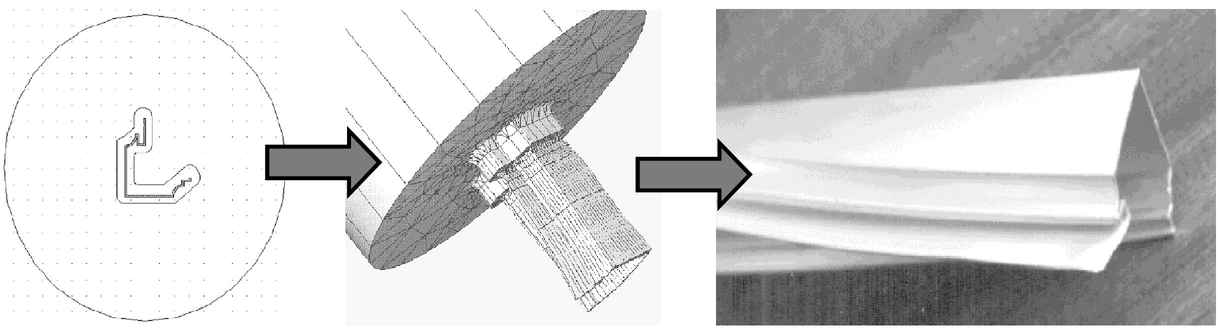

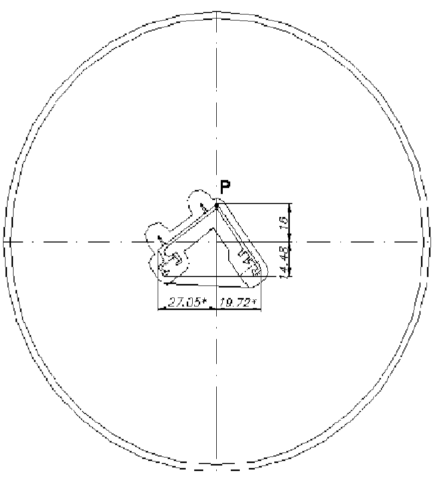

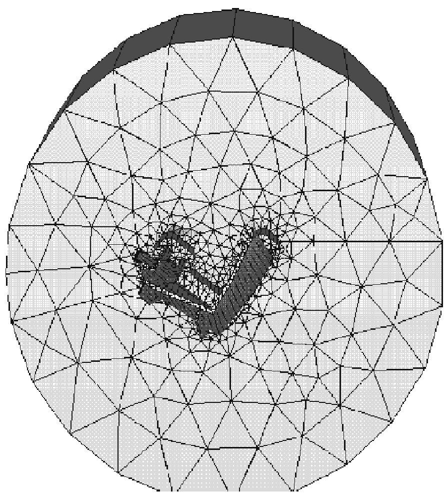

Milenin, AA; Golovko, AN; Mamuzic, I The application of three-dimensional computer simulation when developing dies for extrusion of aluminium shapes // METALURGIJA 41 (1):p53-55 2002

Special features of FEM simulation of the forging and stamping

Problem description
Solving technological problems:
- Die filling analysis
- Saving the material
- Prediction of material flow defects
- Positioning and gravity

Type of elements

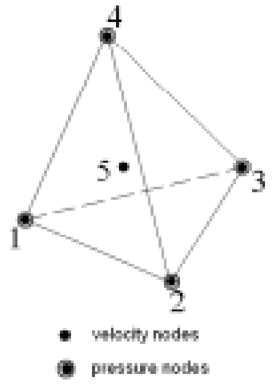

The 4-nodes finite element.

$$v_{i,j} = 0$$

$$\sigma_{ij,i} = 0$$

$$\xi_{ij} = \frac{1}{2}\left(v_{i,j} + v_{j,i}\right)$$

$$\sigma'_{ij} = \frac{2\overline{\sigma}}{3\overline{\xi}}\xi_{ij}$$

$$k\left(t_{,i}\right)_{,i} + \beta\overline{\sigma}\overline{\xi} = 0$$

$$\overline{\sigma} = \overline{\sigma}\left(\overline{\varepsilon}, \overline{\xi}, t\right)$$

Prediction of material flow defects

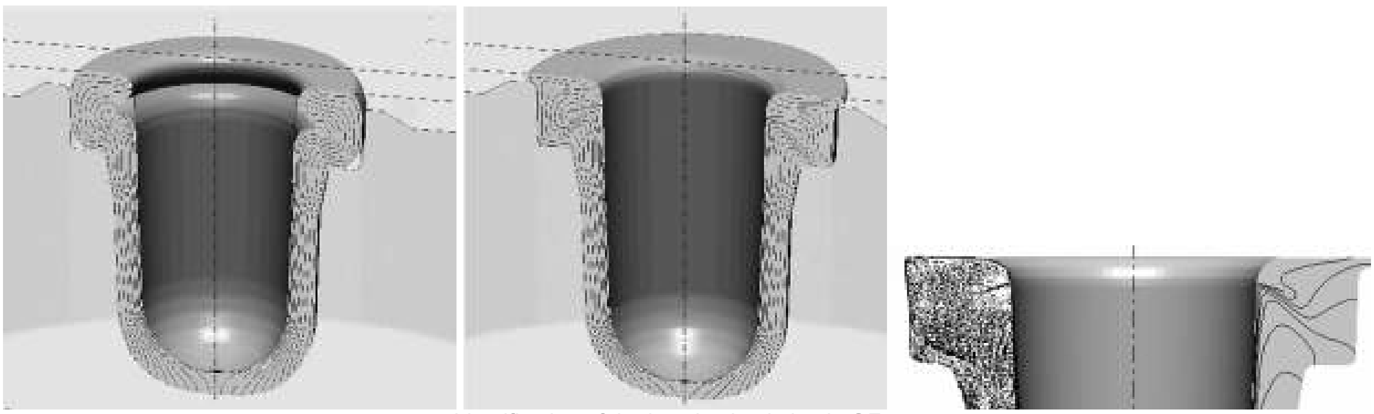

Identification of the laps in simulation in QForm

[1] N. Biba, A. Lishny, S. Stebunov, A. Vlasov Optimal design of assembled and pre-stressed dies by means of numerical simulation The 8th International Conference on Metal Forming 2000, Krakow, Poland, September 3-7, 2000, pp. 127-131
[2] N. Biba, S. Stebunov, A. Lishny, A. Vlasov New approach to 3D finite-element simulation of material flow and its application to bulk metal forming7th International Conference on Technology of Plasticity, 27 Oktober – 1 November, 2002, Yokohama, pp.829-834

QFORM3D
The most easy-to-use forging simulation software
QUANTOR FORM

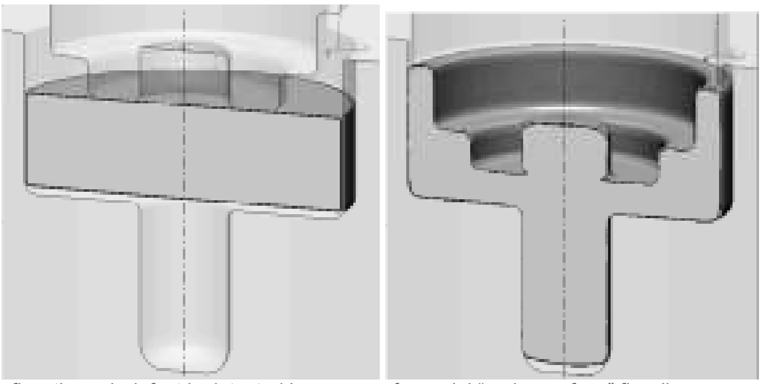

The flow-through defect is detected by means of special "under-surface" flow lines

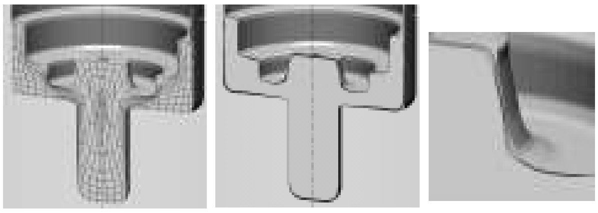

The forged part without flow-through defect

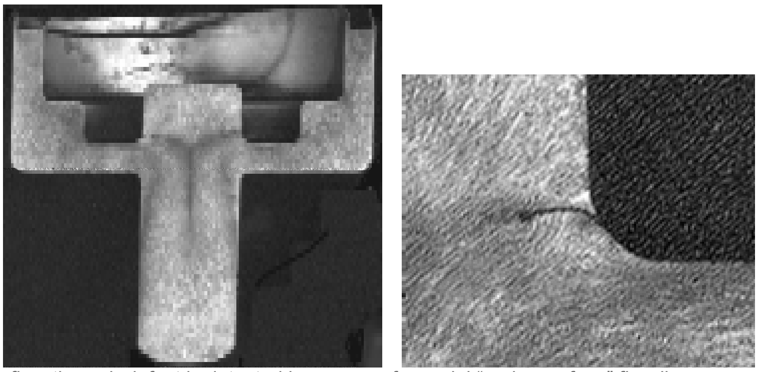

The flow-through defect is detected by means of special "under-surface" flow lines (experiments)

Material saving

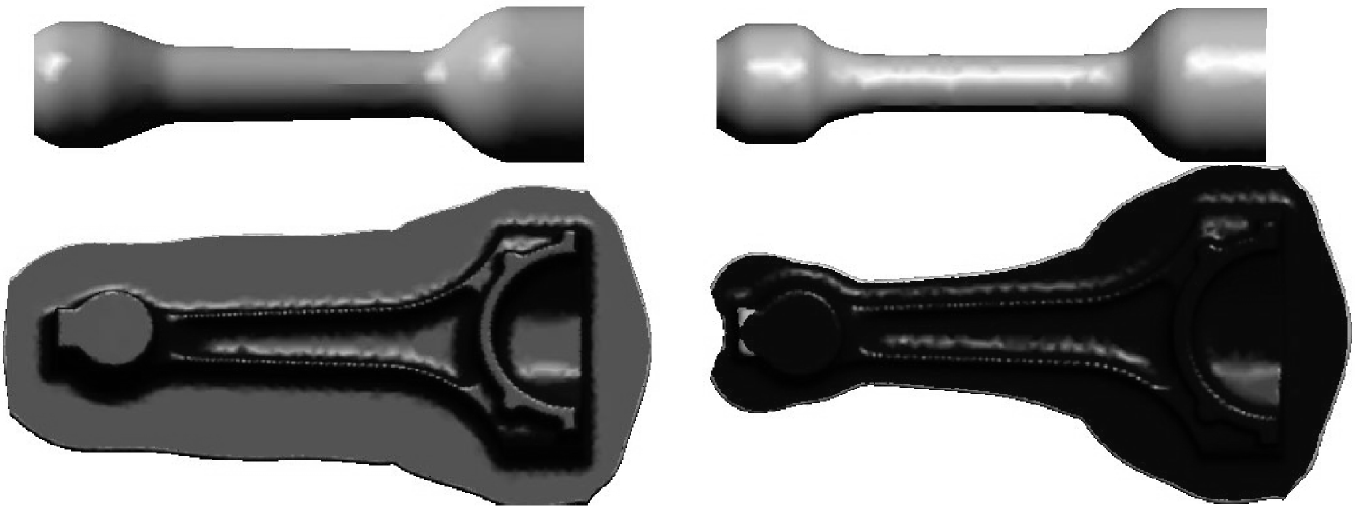

Special features of FEM simulation of the hot rolling.

To obtain the solution, the theory of the non-isothermal plastic flow of incompressible non-linear viscous medium need to be applied.

The main idea of the method involves the using of penalty function to reckon the conditions of metal-tools interaction in complex configuration of tools and billet. Solution should be obtain from the stationary condition of the modified Markov functional:

$$J=\frac{1}{2}\int_V \mu\,\dot{\varepsilon}_i^{\,2}\,dV+\int_V \sigma_0\dot{\varepsilon}_0\,dV+K_\tau\int_F (v_\tau)^2\,dF+K_n\int_F (v_n-w_n)^2\,dF$$

$$K_\tau^{(p)}=\frac{\tau^{(p-1)}}{v_\tau^{(p-1)}}$$

$$\mu^{(p)}=\frac{2\sigma_s^{(p-1)}}{\sqrt{3}\dot{\varepsilon}_i^{(p-1)}}$$

where: p – iteration number;
v_τ – slip metal velocity over the tool,
v_n – metal velocity normal to the tool surface,
w_n – velocity of tool surface point normal to the tool surface, τ – friction stress, σs – yield stress,

σ – mean stress,
ε_I – *effective strain rate,*
ε_0 – *volumetric strain rate,*
$K\tau$ – the penalty coefficient accounting the metal slip velocity over the tool,
Kn – the penalty coefficient on the metal penetration into the tool,
μ – effective metal viscosity computed from by the method of hydrodynamic approaches,
V – volume,
F – contact surface.

2. MATHEMATICAL MODEL OF METAL DEFORMATION DURING ROLLING

If the penalty coefficient K_τ increases, the metal slip over the contact surface is hampered.

$K_\tau = 0$ is related to frictionless case of deformation.

In the discrete formulation some integral terms in Markov functional should be change as following:

$$K_n\int_F (v_n-w_n)^2\,dF=K_n\sum_{i=1}^{N_{pov}}(v_{ni}-w_{ni})^2F_i$$

$$K_\tau\int_F (v_\tau)^2\,dF=K_\tau\sum_{i=1}^{N_{pov}}v_\tau^2F_i$$

where:
N_{pov} – number of grid nodes in contact with the tool,
F_i – metal–tool contact surface area attached to i-th node.

Milenin, AA Mathematical modeling of the spread of metals with different rheological properties on rolling RUSSIAN METALLURGY (4): p64-68 1998

3. MATHEMATICAL MODEL OF HEAT TRANSFEAR PROCESSES DURING ROLLING

Algorithm of 3D solution of heat transfer during rolling
is build upon the sequent solutions of the plane tasks which is corresponding to the movement of the cross-section of billet with the rolling speed through deformation zone and air cooling zone.

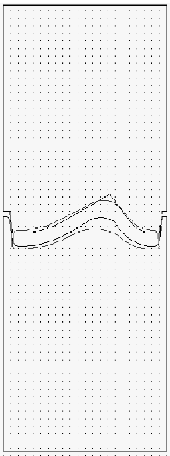

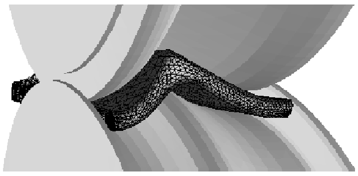

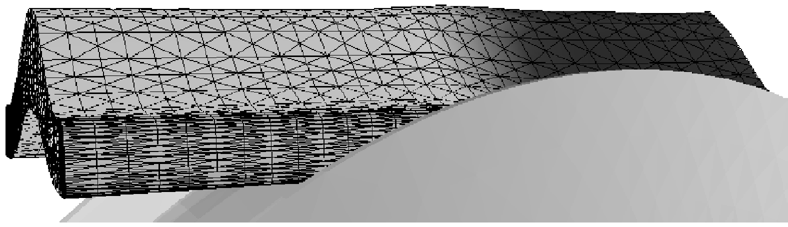

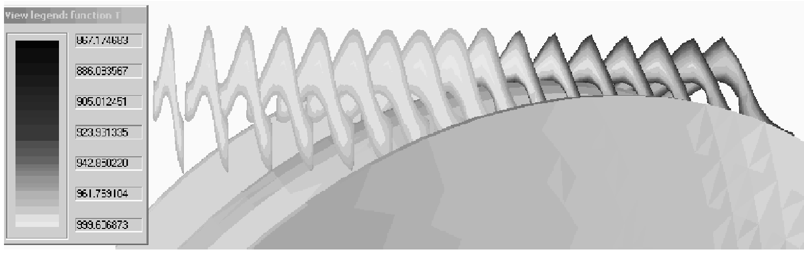

The computer simulation of the hot metal forming processes
Milenin Andrzej, AGH University of Science and Technology, 2012
AKADEMIA GÓRNICZO-HUTNICZA IM. STANISŁAWA STASZICA W KRAKOWIE
AGH

3. MATHEMATICAL MODEL OF HEAT TRANSFEAR PROCESSES DURING ROLLING

Algorithm of 3D solution of heat transfer during rolling based on the following equation.

$$c_{eff}\,\rho \frac{dt}{d\tau} = k\left(\frac{\partial^2 t}{\partial x^2} + \frac{\partial^2 t}{\partial y^2}\right)$$

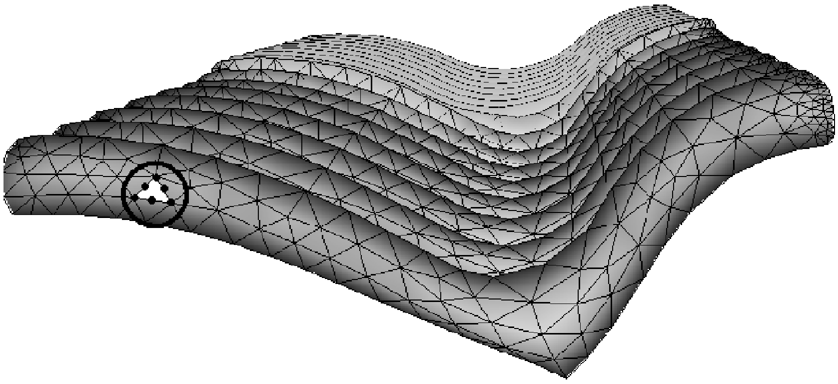

Where:
ρ – metal density,
t – temperature,
τ – time,
c_{eff} – effective specific heat

TYPE OF FINITE ELEMENTS

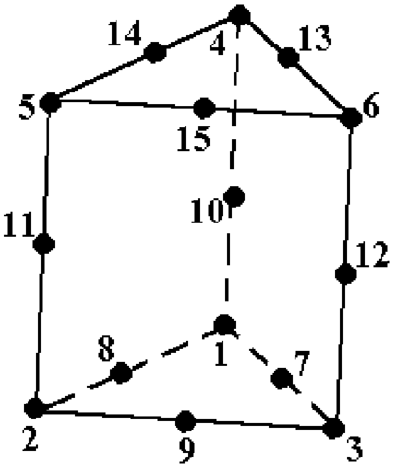

For velocity approximation

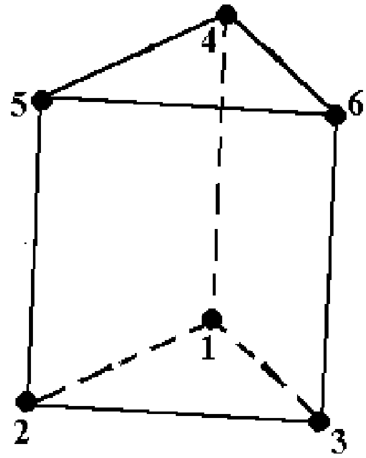

For average stress approximation

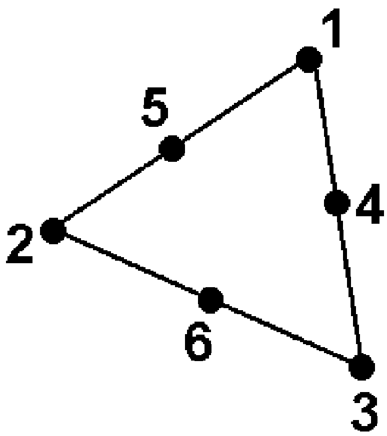

For temperature approximation

Plastometric investigation of a steels

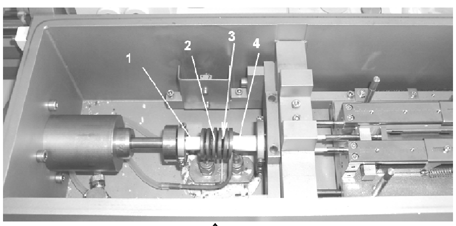

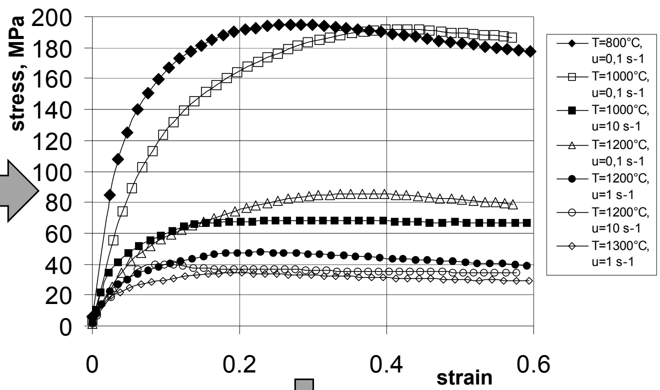

$$\sigma_s = \alpha_1 \varepsilon^{\alpha_2} u^{\alpha_3} \exp\left(-\alpha_4 t\right)$$

Сталь	α_1	α_2	α_3	α_4
ШХ15СГ	23956	0.132382	0.144023	0.005021
Сталь 45	11072	0.172602	0.187701	0.004454
Сталь 20	12624	0.206601	0.187003	0.004465
Сталь 40Н	8028	0.206851	0.156801	0.003912
Сталь 75РМЛ	5244	0.197703	0.141104	0.003748

Determination of a yield stress with help of a dislocation theory

$$\sigma_s = \alpha G b \sqrt{\rho}$$

$$\frac{d\rho}{d\tau} = \frac{\varepsilon}{bl} - k_2 \rho(\tau) - \frac{A_3}{D} \rho(\tau) r \left[\rho(\tau) - \rho_{cr}\right]$$

$$\sigma_S = X_9 + X_{10} \sqrt{\rho}$$

$$\frac{d\rho}{d\tau} = X_1 \dot{\varepsilon}^{X_2} \exp\left(\frac{X_3}{\bar{t}}\right) - X_4 \rho \exp\left(X_5 \bar{t}\right) - X_6 \rho^{X_7} \exp\left(X_8 \bar{t}\right)$$

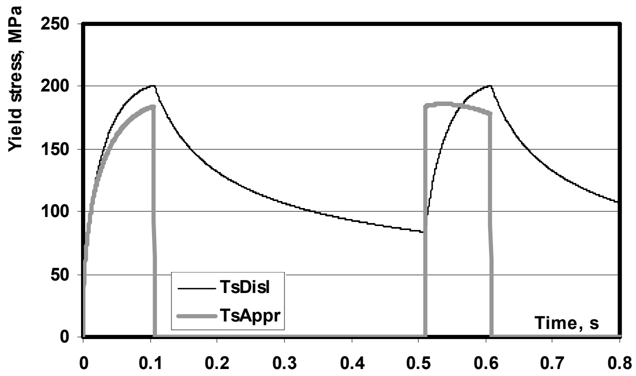

The computer simulation of the hot metal forming processes
Milenin Andrzej, AGH University of Science and Technology, 2012
AKADEMIA GÓRNICZO-HUTNICZA IM. STANISŁAWA STASZICA W KRAKOWIE
AGH

SIMULATION OF THE ROLLING of ANGLE

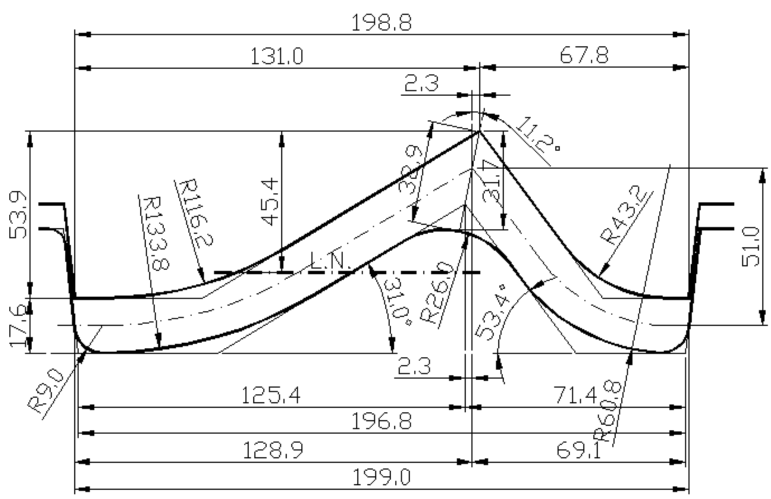

Blueprint of grooves used for angle billet in pass #4.

Milenin, AA; Dyja, H; Mroz, S Simulation of metal forming during multi-pass rolling of shape bars// JOURNAL OF MATERIALS PROCESSING TECHNOLOGY 153 p108-114 Part 1 2004

SIMULATION OF THE ROLLING OF ANGLE

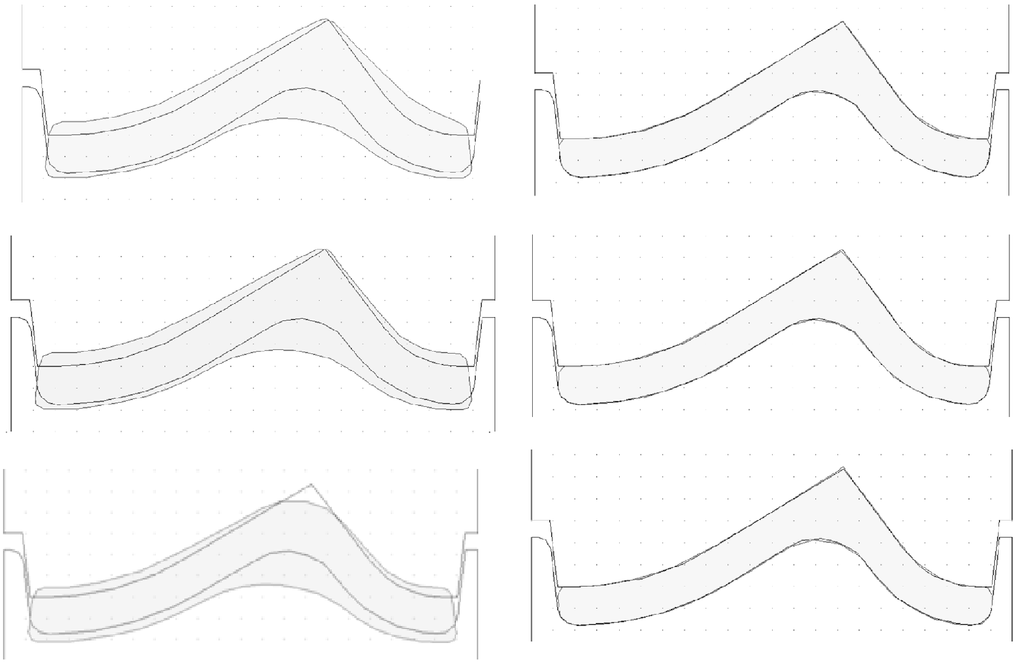

Variant 1

Variant 2

Variant 3

SIMULATION OF THE ROLLING of ANGLE

The vertical speed distributions for the variant 1 and 3 are shown on the Figures. One can see the vertical speed differences arise when we go from variant 1 to variant 3.

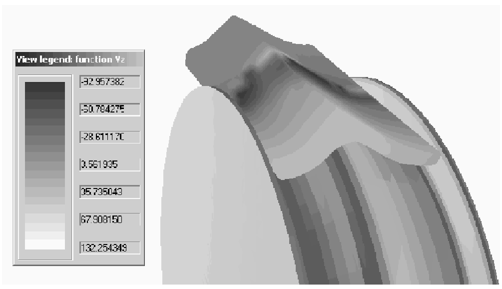

Variant 1

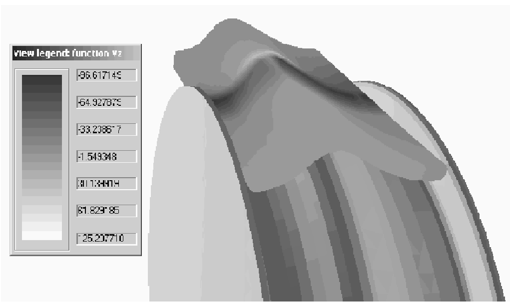

Variant 3

The calculations showed that the least torsion and bending are observed in the variant 3.

Thus the differences of metal speed perpendicular to rolling direction for thee variants are 22.7 mm/s, 17.3 mm/s and 11.4 mm/s.

While average speed in rolling direction is 620 mm/s.

Therefore the variant 3 was taken as a basis for development of angle rolling schedule in six passes.

Modeling and optimization of a angle profile rolling processes

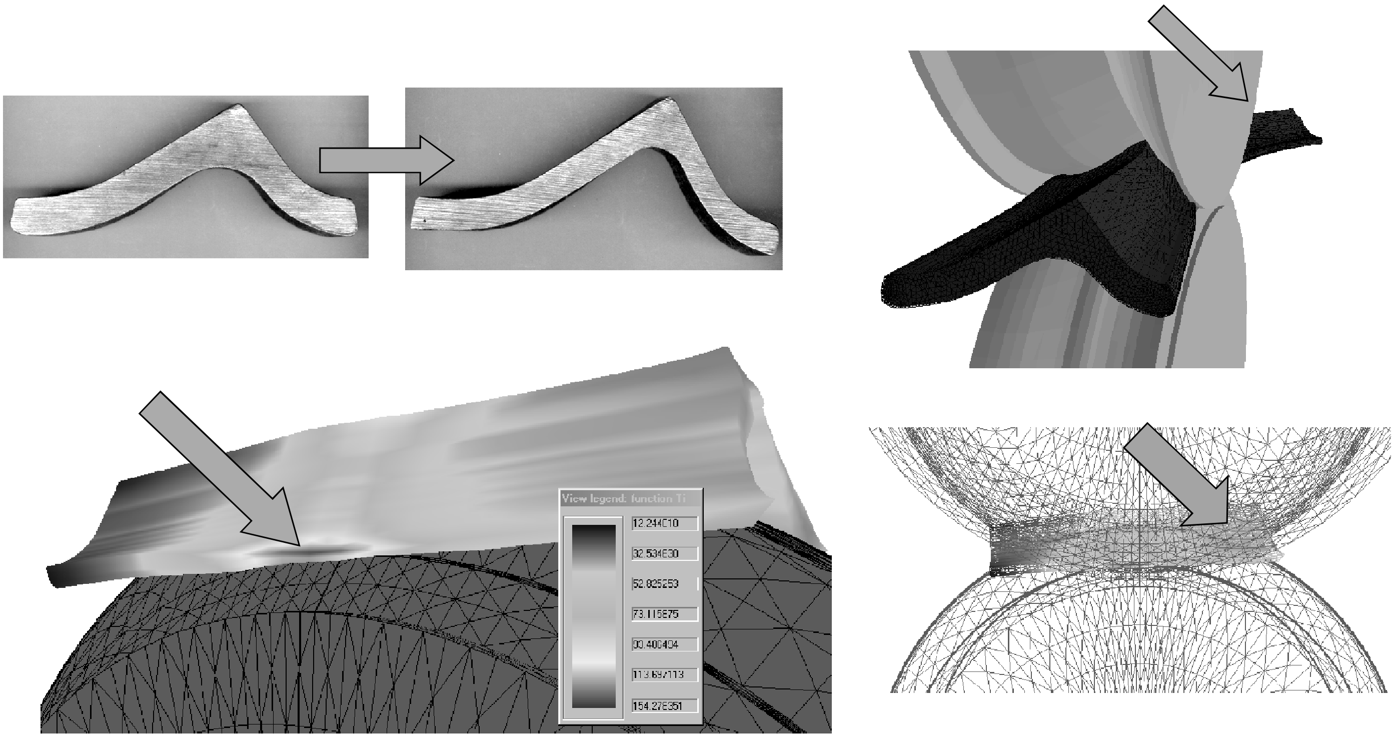

Modeling and optimization of a angle profile rolling processes

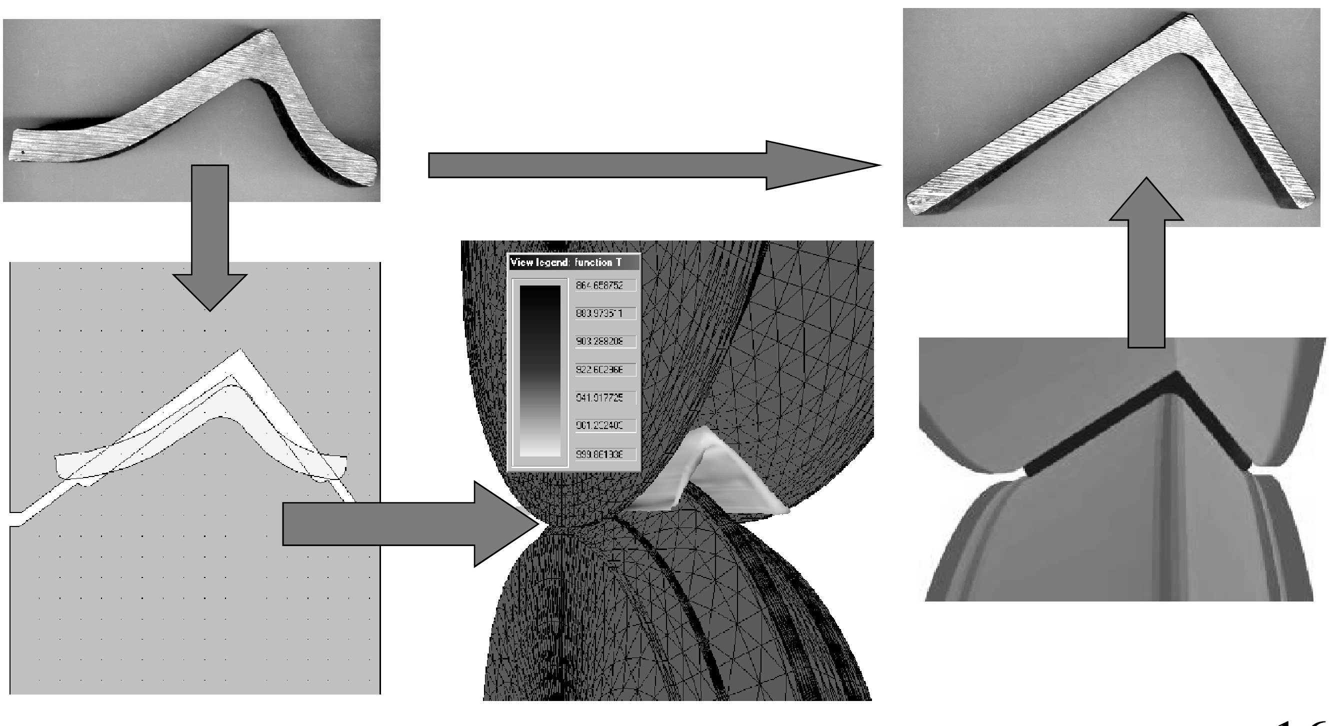

Processing technology

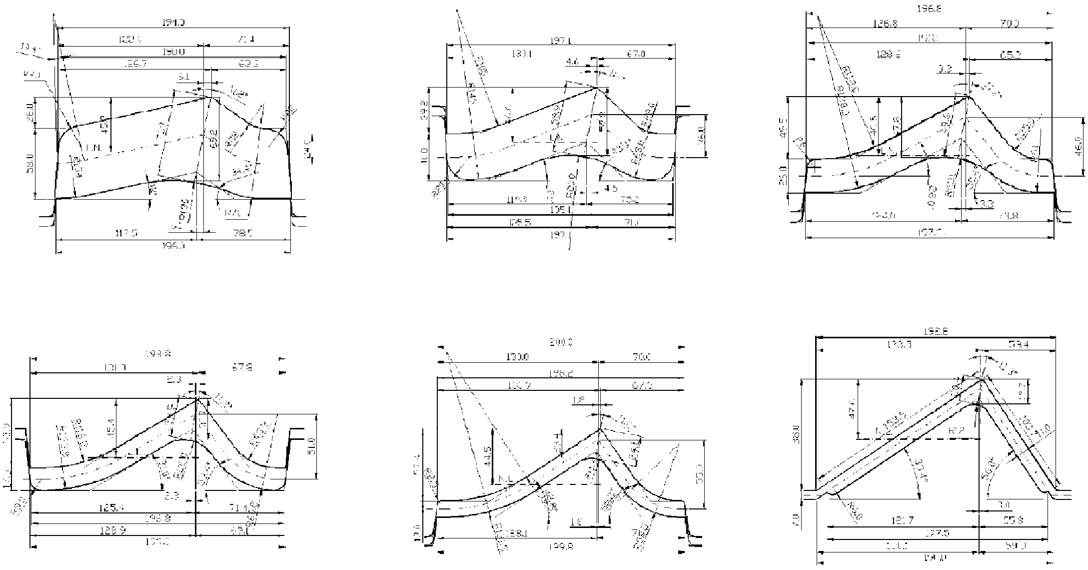

Shape and dimensions of passes applied in the rolling of 150x100x10 mm angle bar.

Processing technology

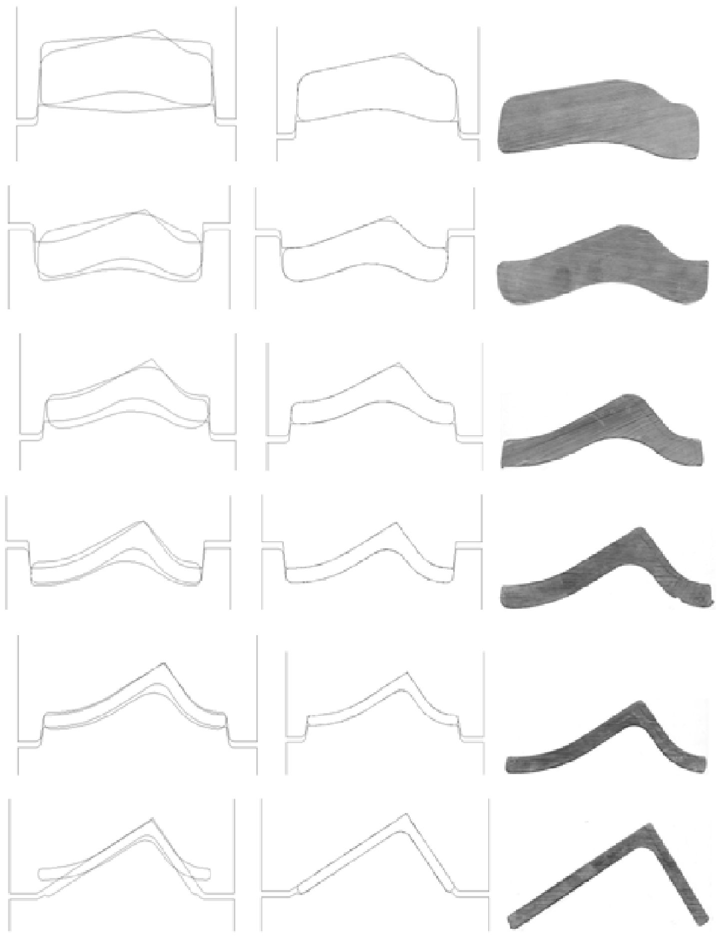

Initial positioning of rolls and the stock (a); the results of numerical computations (b) and tests (c) of the process of rolling 150x100x10 mm angle bar.

Modeling of a shape rolling processes (bimetal Cu-Al)
Grid generation for bimetal rods

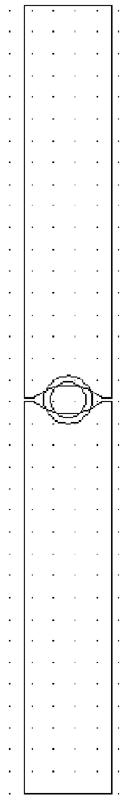

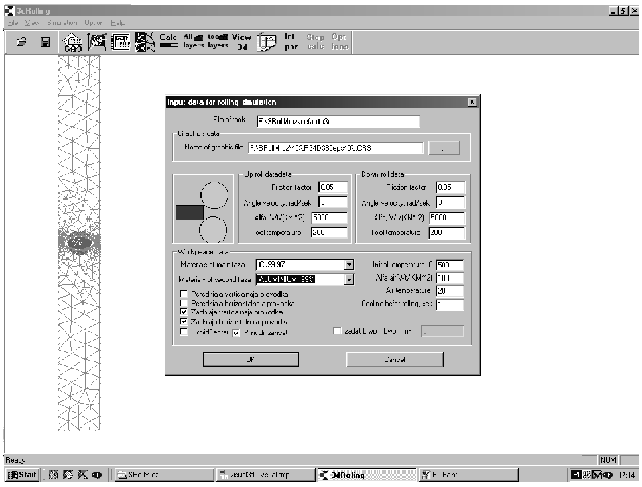

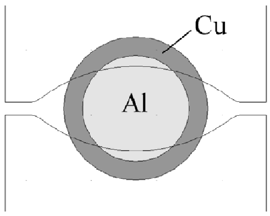

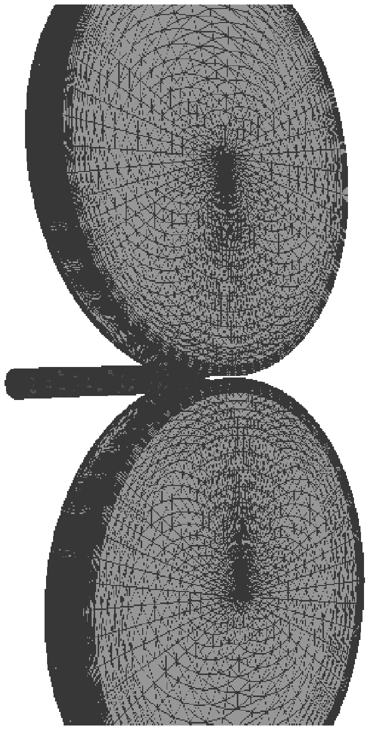

The computer simulation of the hot metal forming processes
Milenin Andrzej, AGH University of Science and Technology, 2012

AKADEMIA GÓRNICZO-HUTNICZA
IM. STANISŁAWA STASZICA W KRAKOWIE
AGH

Modeling of a shape rolling processes (bimetal Cu-Al)

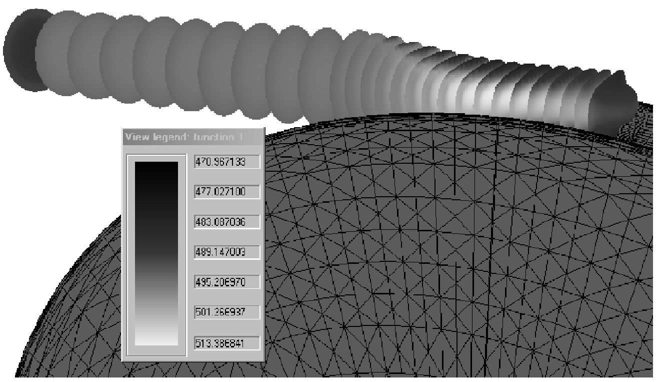

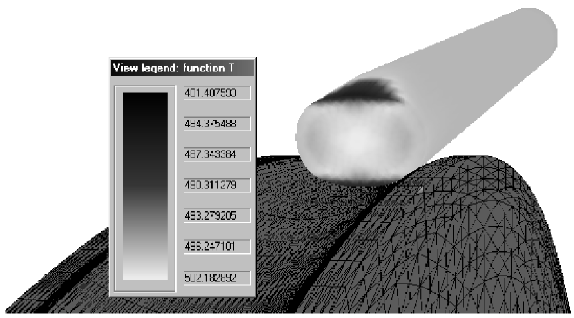

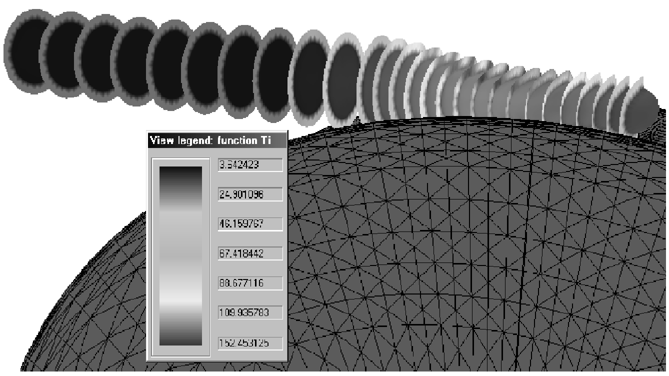

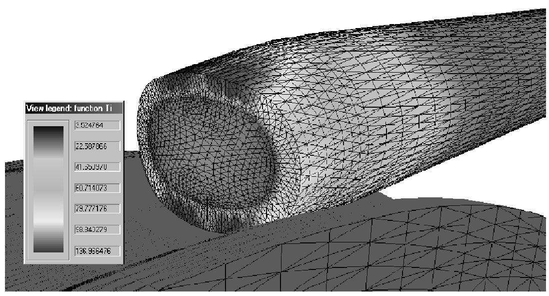

Modeling and optimization of a shape rolling processes (bimetal Cu-Steel55)

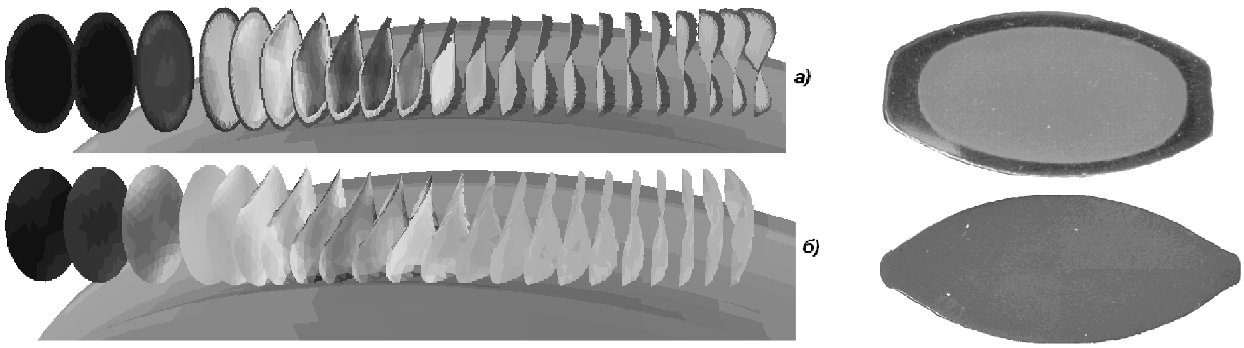

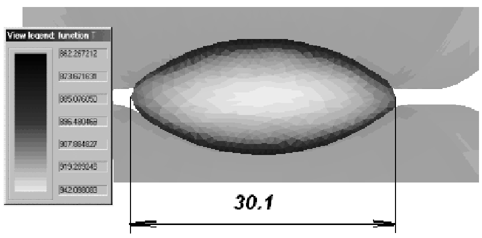

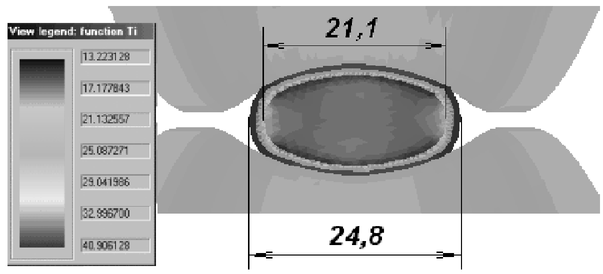

The computer simulation of the hot metal forming processes
Milenin Andrzej, AGH University of Science and Technology, 2012
AKADEMIA GÓRNICZO-HUTNICZA IM. STANISŁAWA STASZICA W KRAKOWIE
AGH

Processing technology

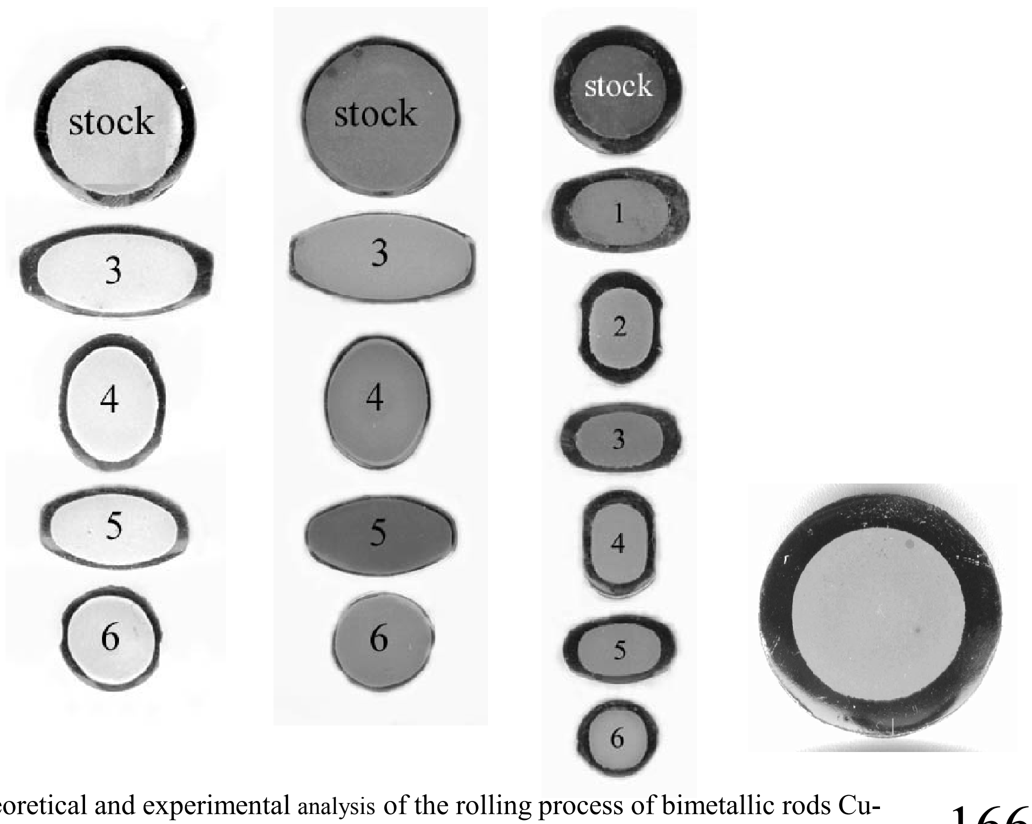

Dyja, H; Mroz, S; Milenin, A Theoretical and experimental analysis of the rolling process of bimetallic rods Cu-steel and Cu-Al. // JOURNAL OF MATERIALS PROCESSING TECHNOLOGY 153 p100-107 Part 1 2004

Lection 6.

Example of commercial FEM programs for the simulation of the processes of hot deformation of metals. Programs Qform and Forge3. Example of development its own FEM codes and solution of the untypical problems of theory of metal forming.

The computer simulation of the hot metal forming processes
Milenin Andrzej, AGH University of Science and Technology, 2012
AKADEMIA GÓRNICZO-HUTNICZA IM. STANISŁAWA STASZICA W KRAKOWIE
AGH

Example of commercial FEM programs for the simulation of the processes of hot deformation of metals. Programs Qform and Forge3.

QForm window ready for new problem

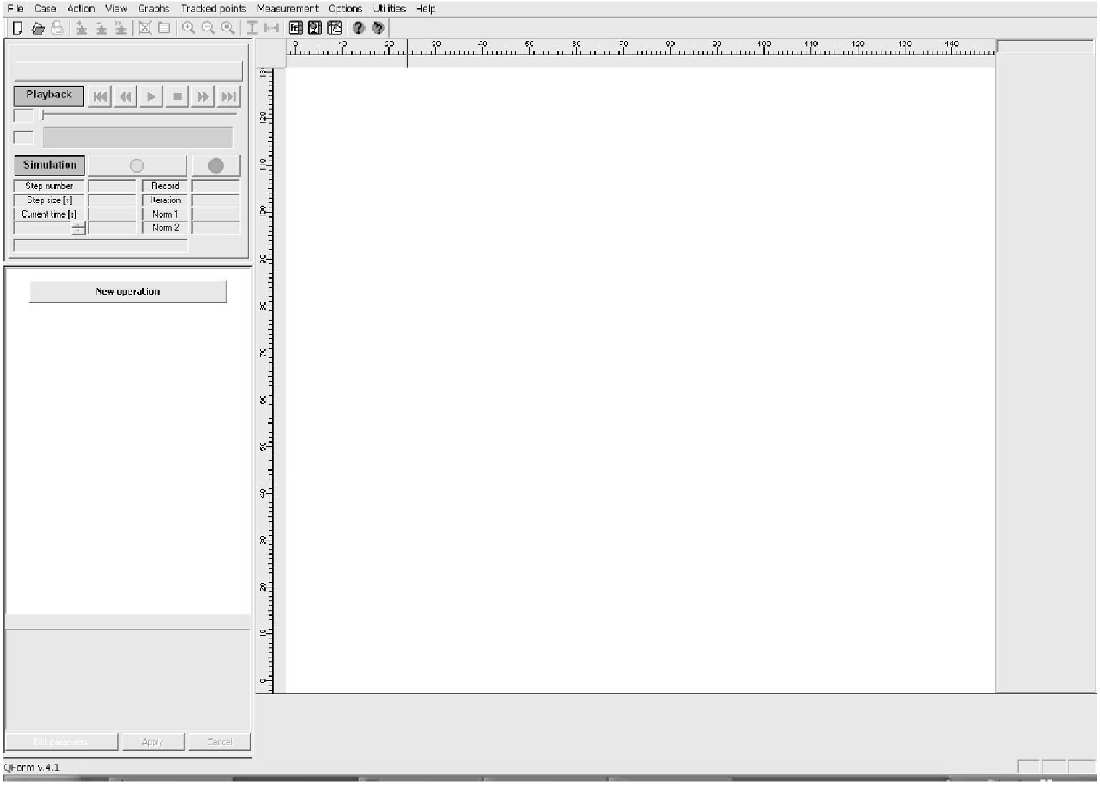

Data preparation Wizard

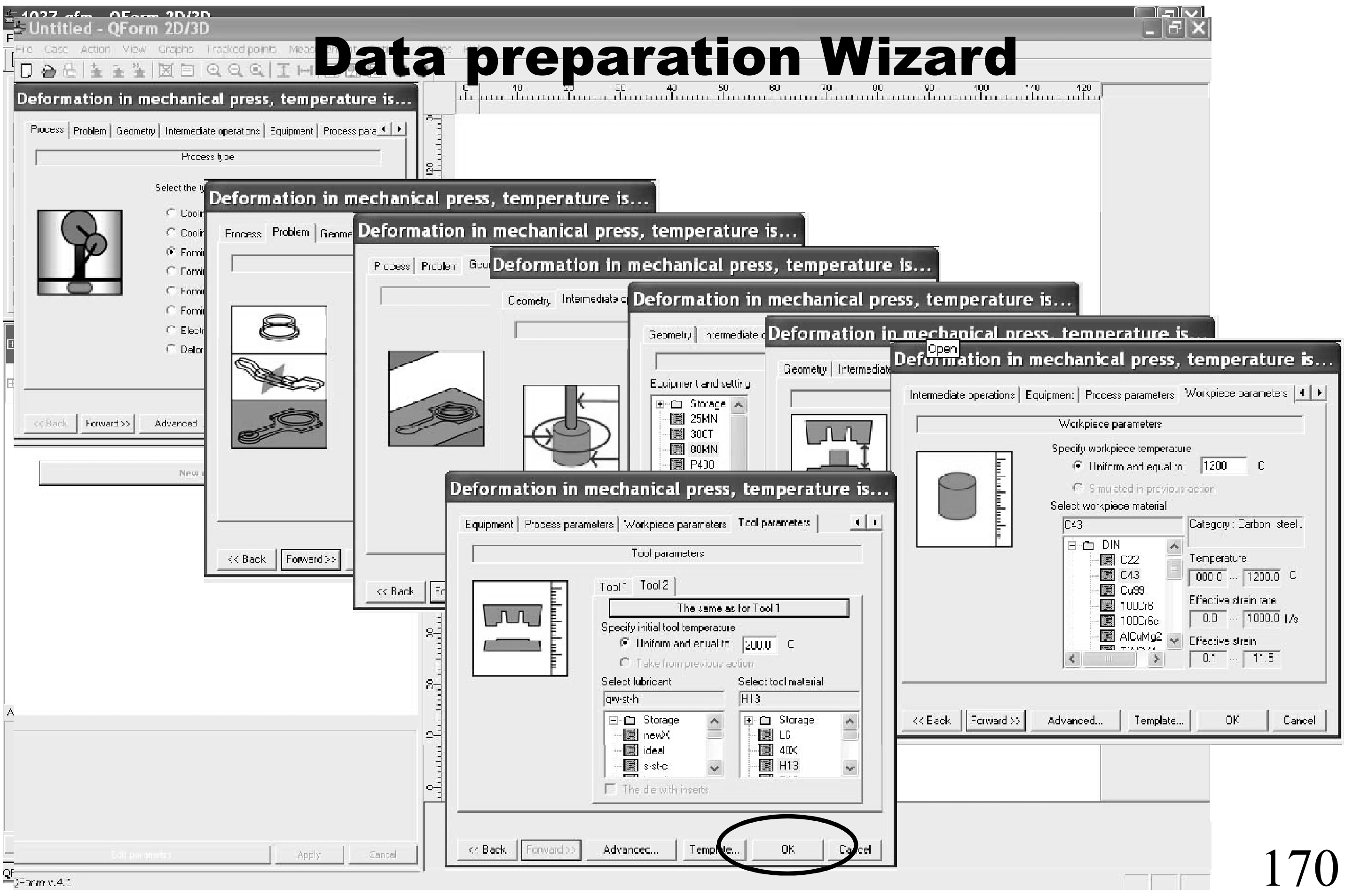

Simulation: Action 2 – Finish

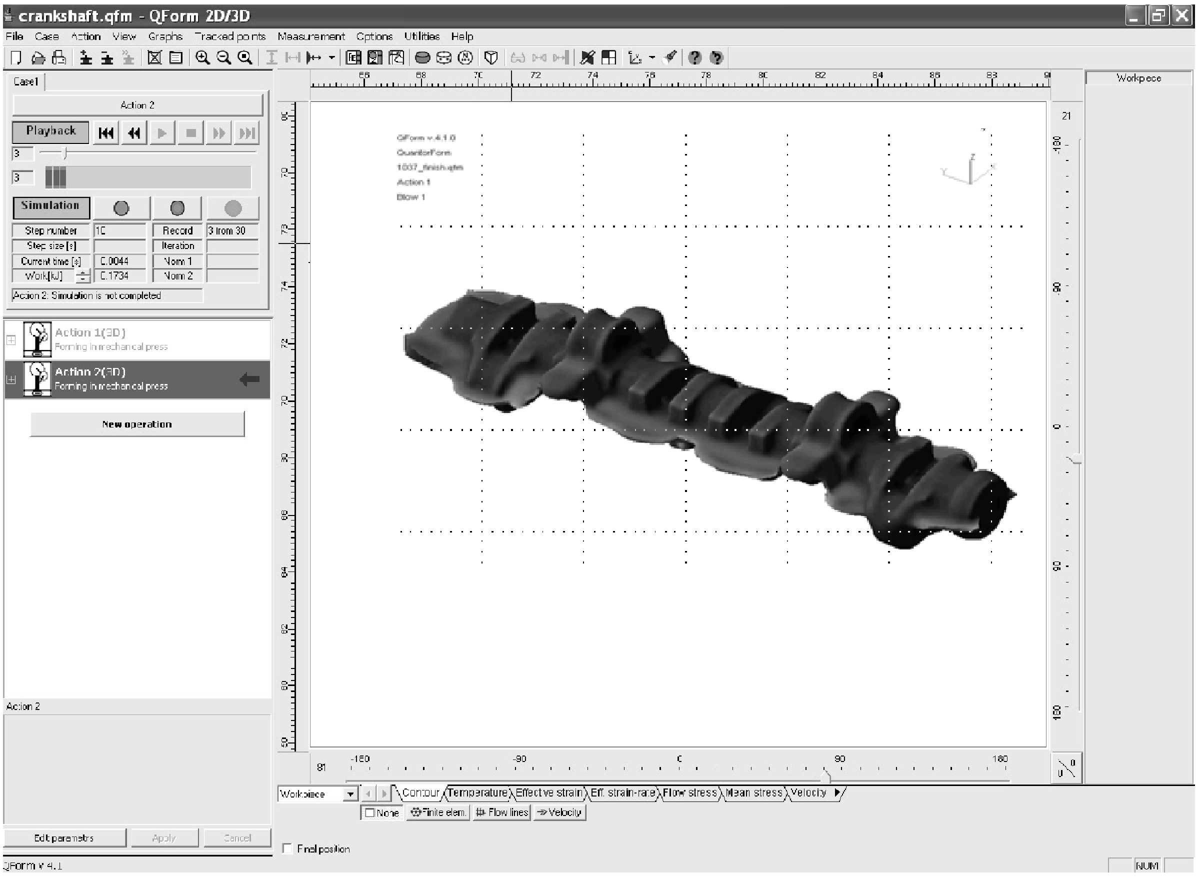

The computer simulation of the hot metal forming processes
Milenin Andrzej, AGH University of Science and Technology, 2012
AKADEMIA GÓRNICZO-HUTNICZA IM. STANISŁAWA STASZICA W KRAKOWIE
AGH

Accurately Predicted Final Flash Thickness and Flash Widths

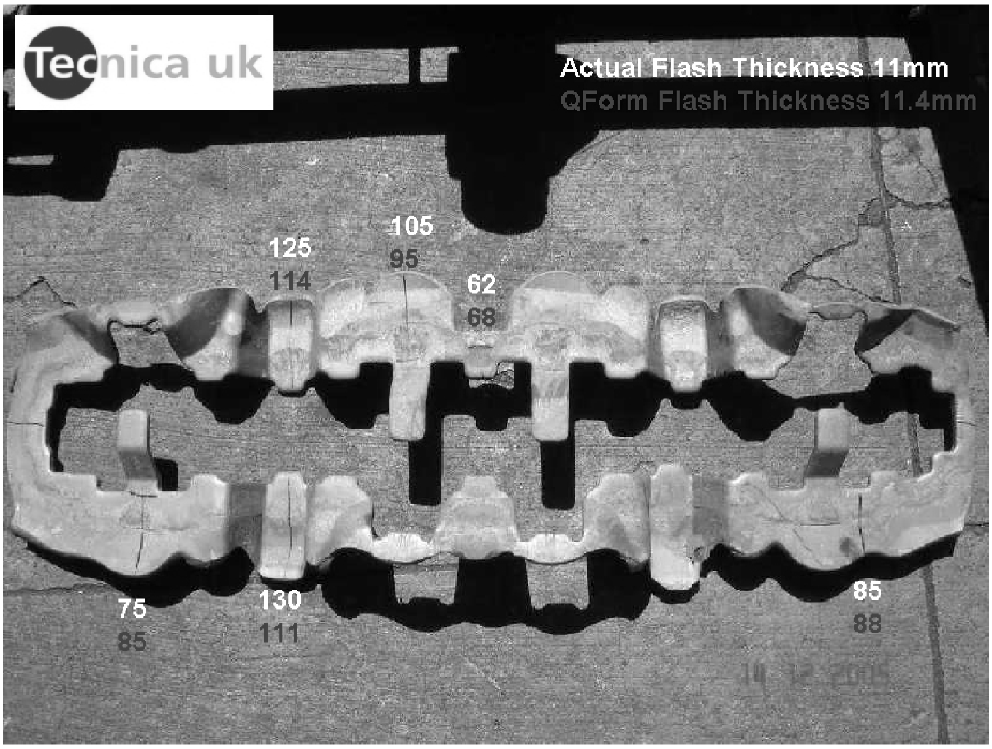

Analyze the grain flow layer by layer

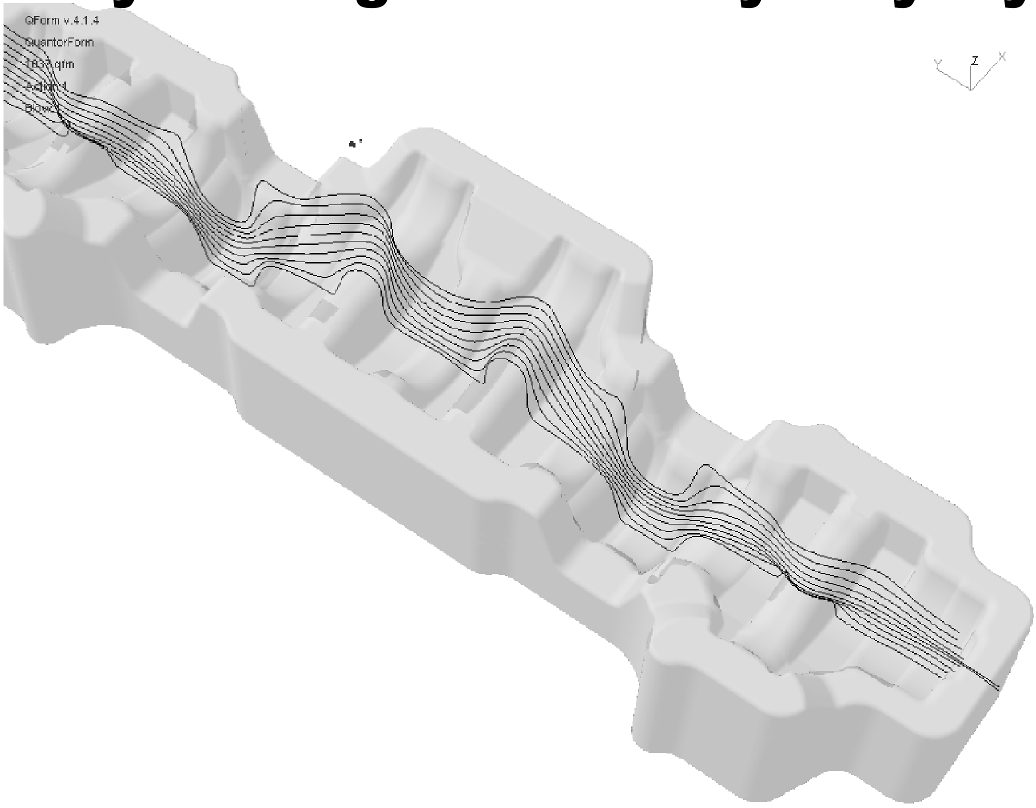

The computer simulation of the hot metal forming processes
Milenin Andrzej, AGH University of Science and Technology, 2012
AKADEMIA GÓRNICZO-HUTNICZA IM. STANISŁAWA STASZICA W KRAKOWIE
AGH

What is required for the simulation

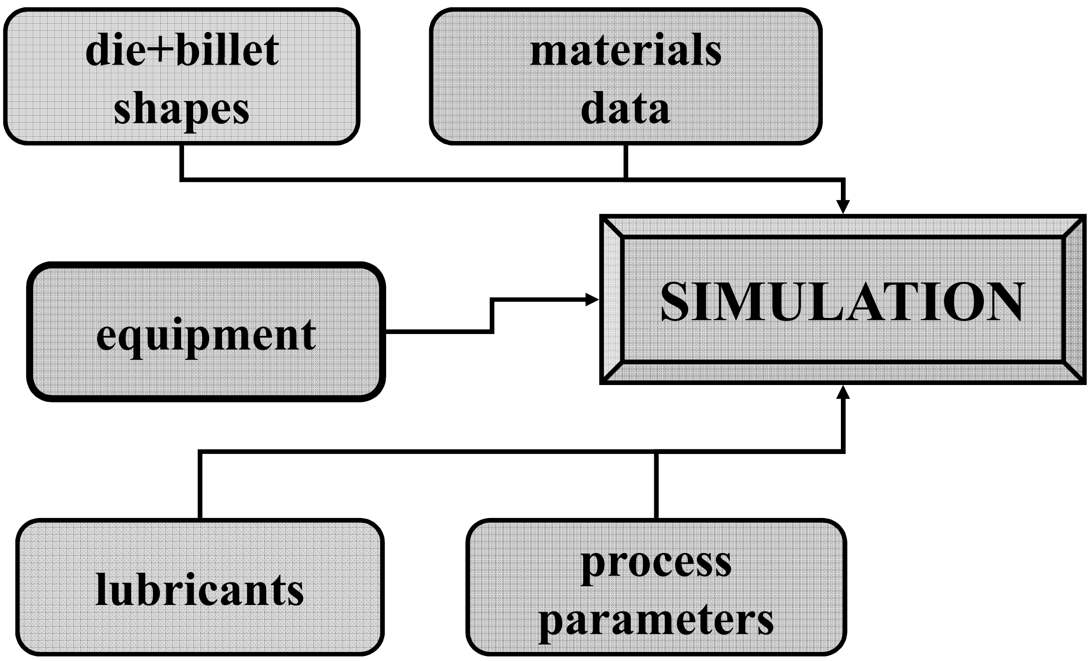

Simulation can be performed for any type of equipment

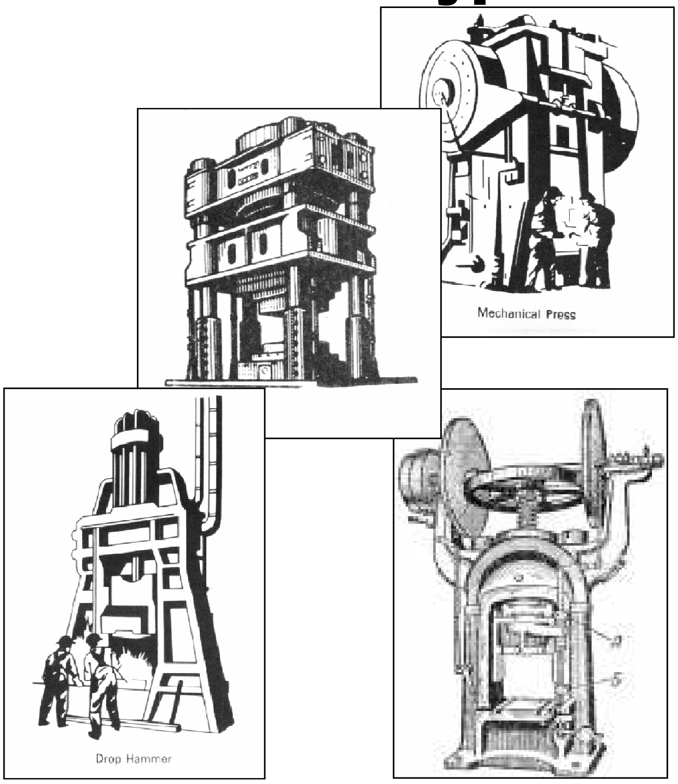

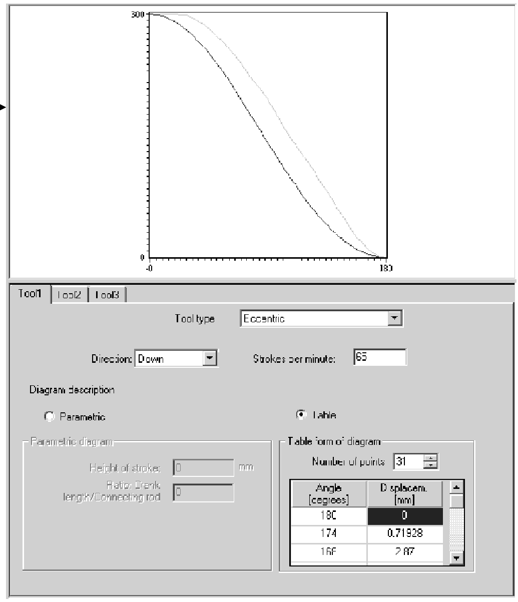

Example: Kinematics of the mechanical press with a holder

The computer simulation of the hot metal forming processes
Milenin Andrzej, AGH University of Science and Technology, 2012
AGH Akademia Górniczo-Hutnicza im. Stanisława Staszica w Krakowie

The project, the cases, the actions

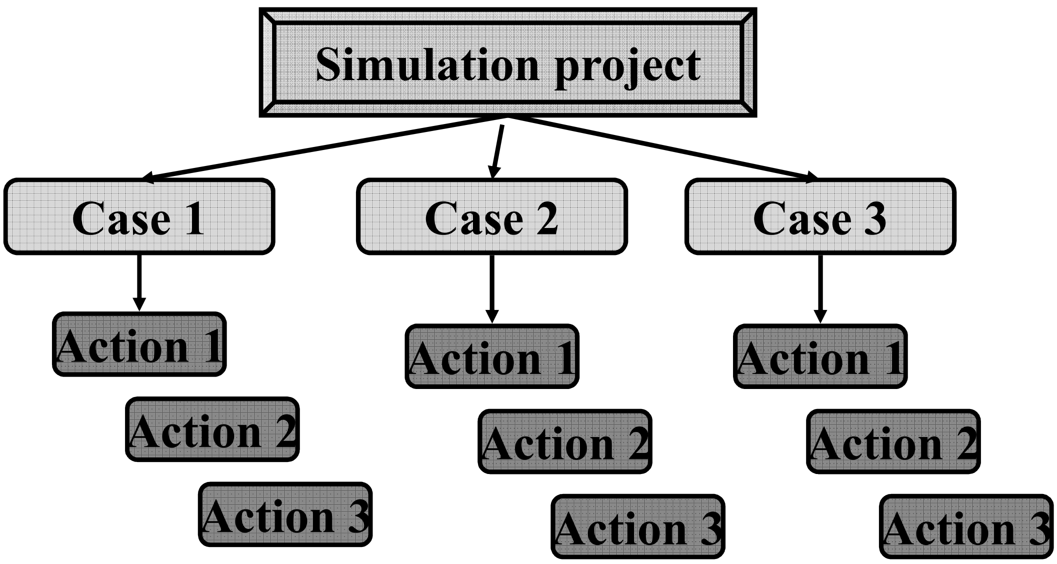

Simulation of electric upsetting

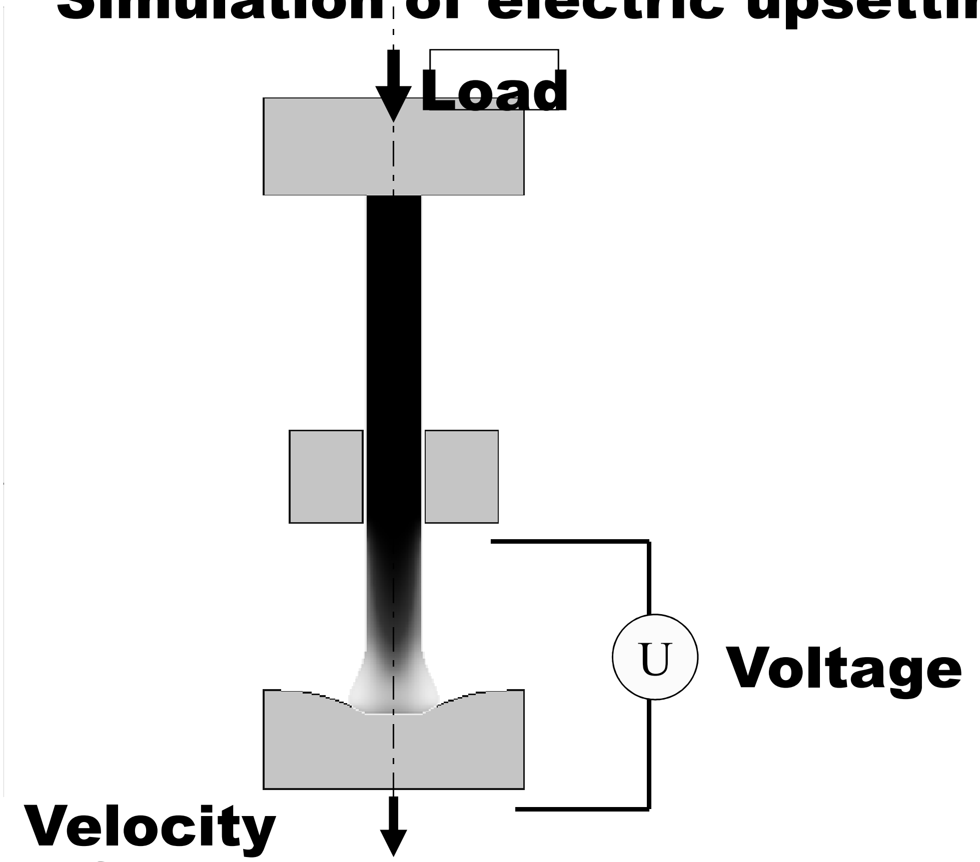

Scheme of electric upsetting process

The computer simulation of the hot metal forming processes
Milenin Andrzej, AGH University of Science and Technology, 2012
AKADEMIA GÓRNICZO-HUTNICZA IM. STANISŁAWA STASZICA W KRAKOWIE
AGH

Die stress in solid die block

- Maximum Stress Shown Where Dies Were Cracking

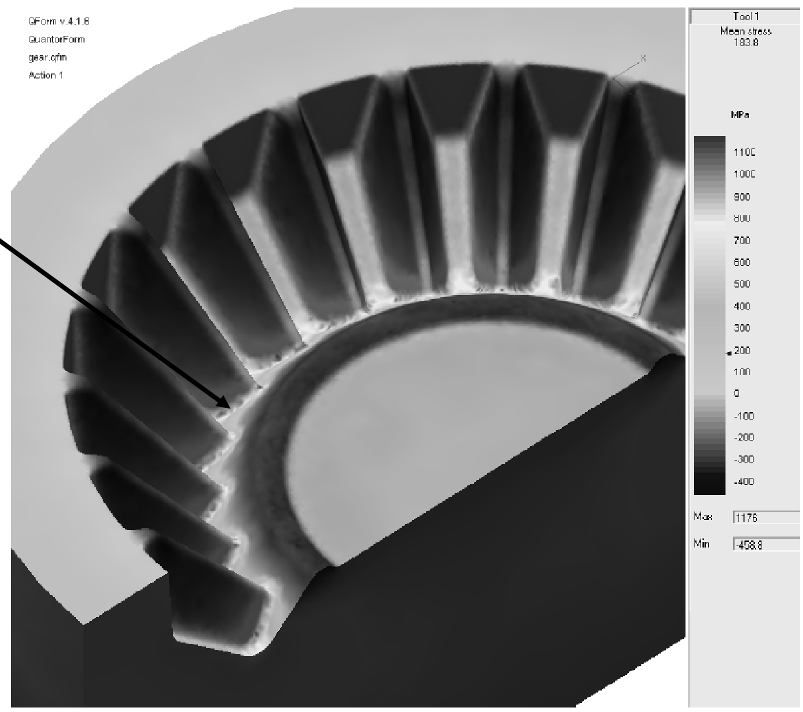

Effective stress distribution in assembled die

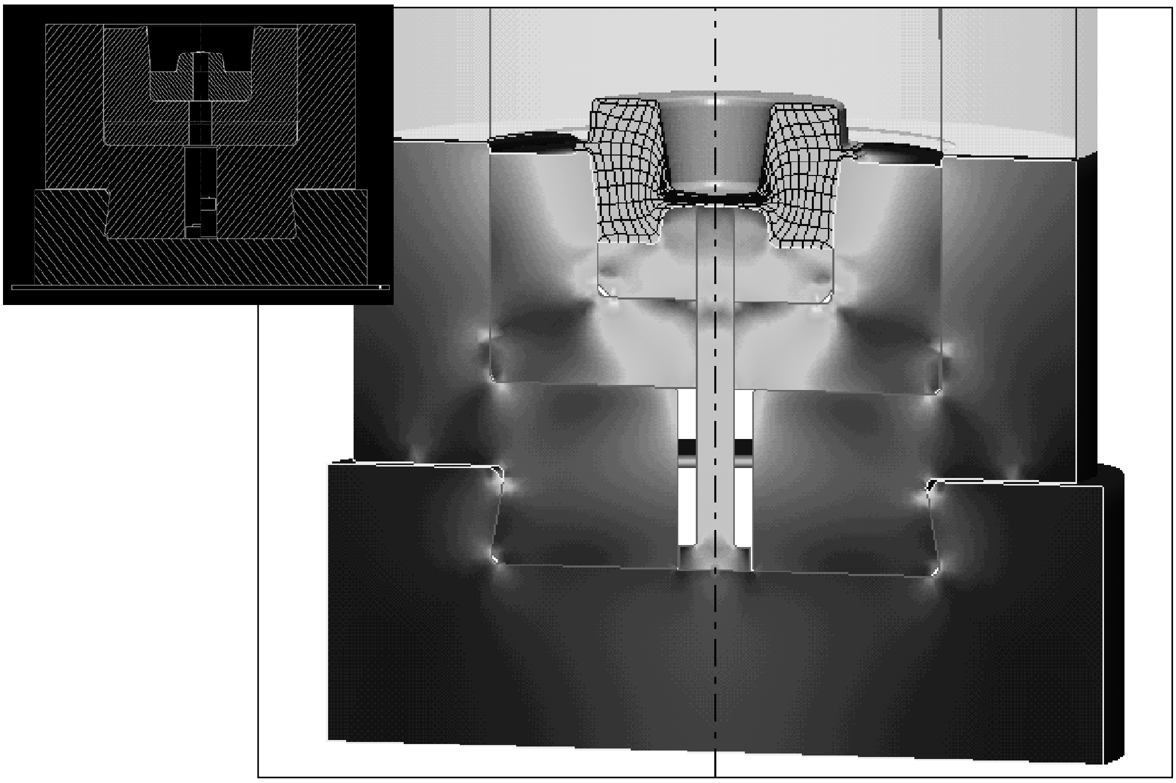

Quantor Form

QFORM2D/3D

Coupled mechanical simulation of the tools and the forged part

Sample of upsetting in "soft" dies

Workpiece – steel
Upper tool – $E^{*}=2150$ MPa $(E_{real}/100)$
Lower tool – $E^{*}=430$ MPa $(E_{real}/500)$

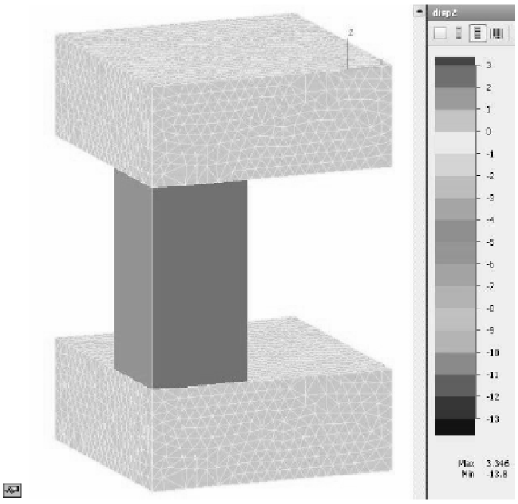

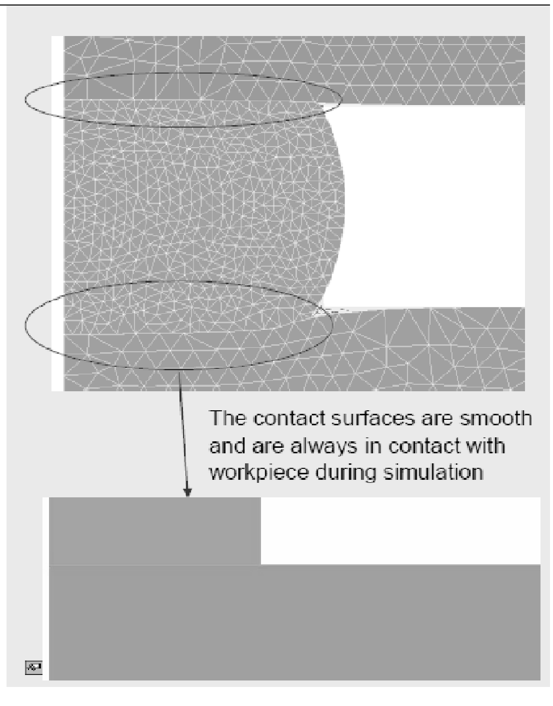

Finite element mesh for coupled deformation and thermal problem

Design scheme of hydraulic press 10 MN

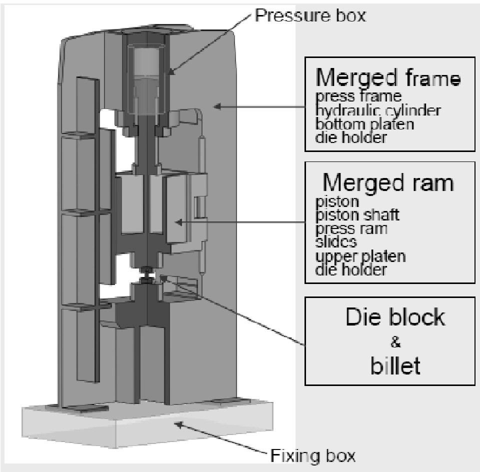

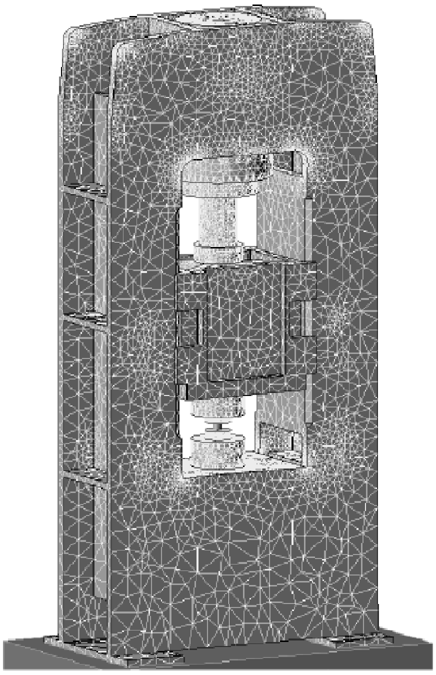

Vertical displacements in the die block

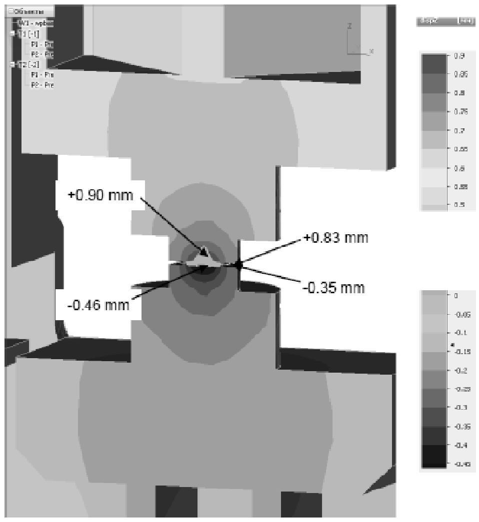

Total deformation in gutter area is about 1.2 mm, additional deformation of die cavity is ~0.1 mm

QForm3D-Extrusion

A specialized program for simulation and development of extrusion technology

The material flow starting from the domain position

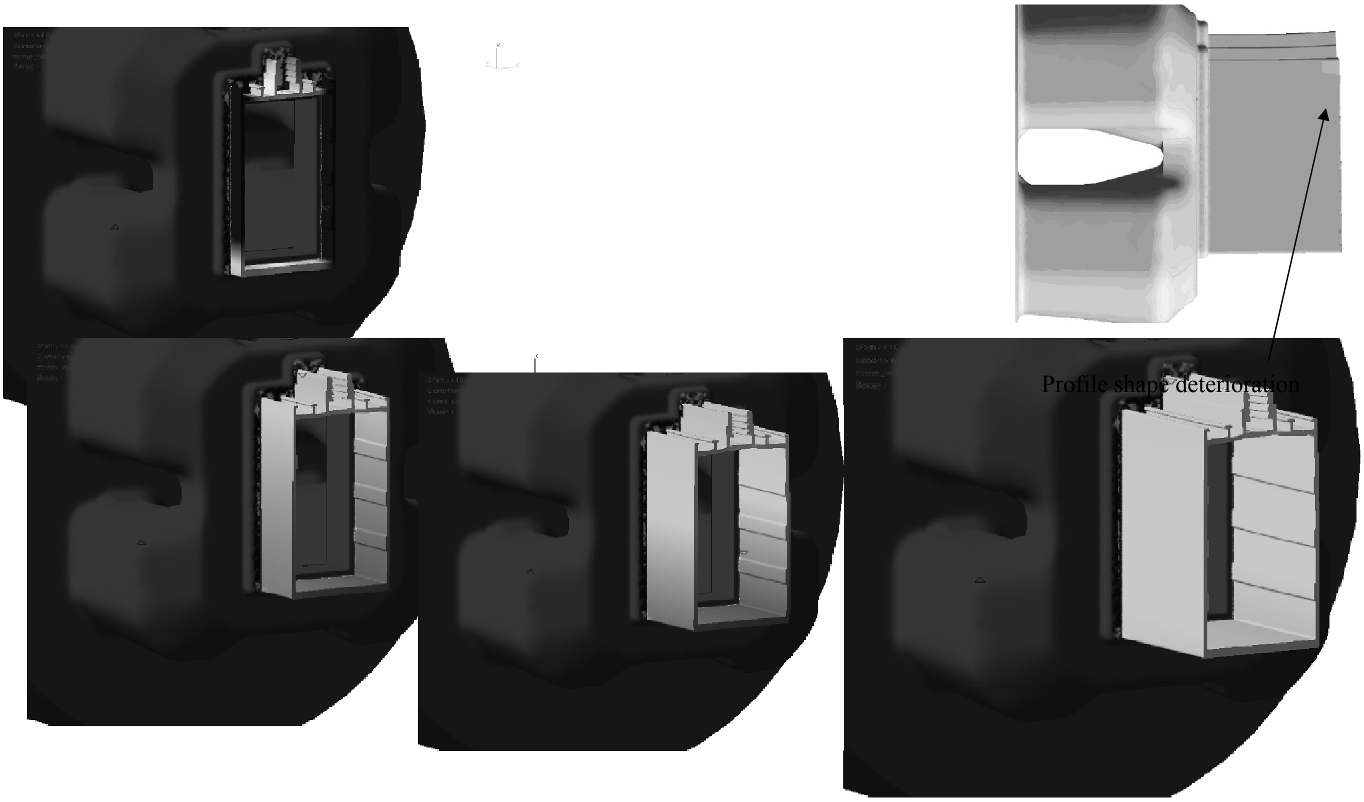

Experimental verification of the profile tip shape (Compes, Italy)

Real tip

Simulation by QForm-extrusion

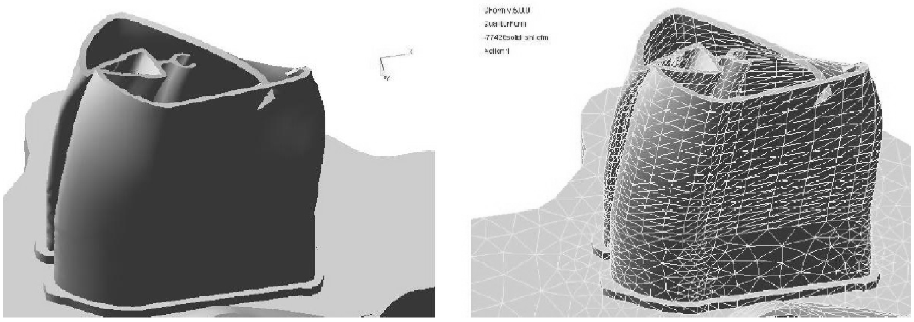

Experimental verification of the profile tip shape (profile 79468, Compes, Italy)

Real tip.

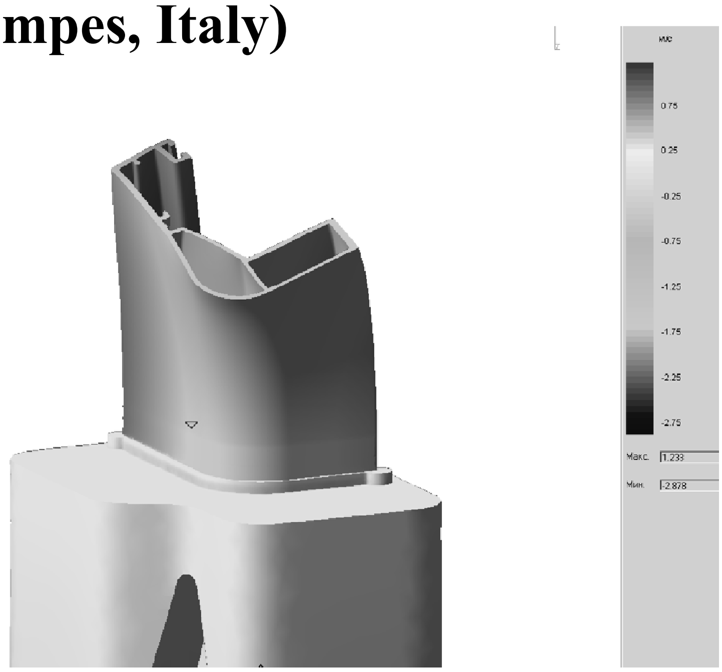

Simulation by QForm-extrusion

The influence of the bearing design on the material flow

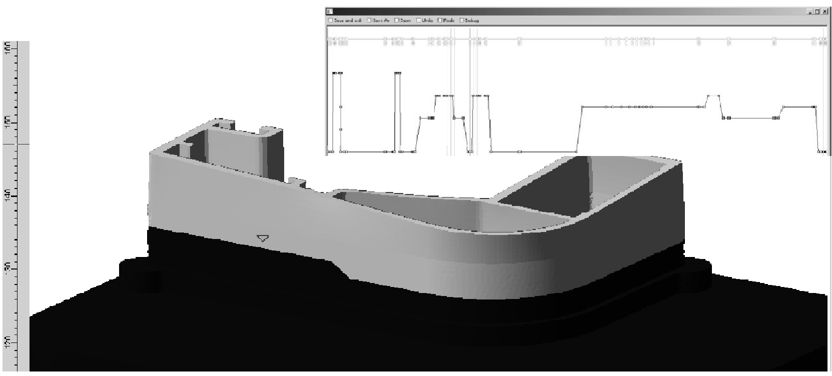

Original bearing design

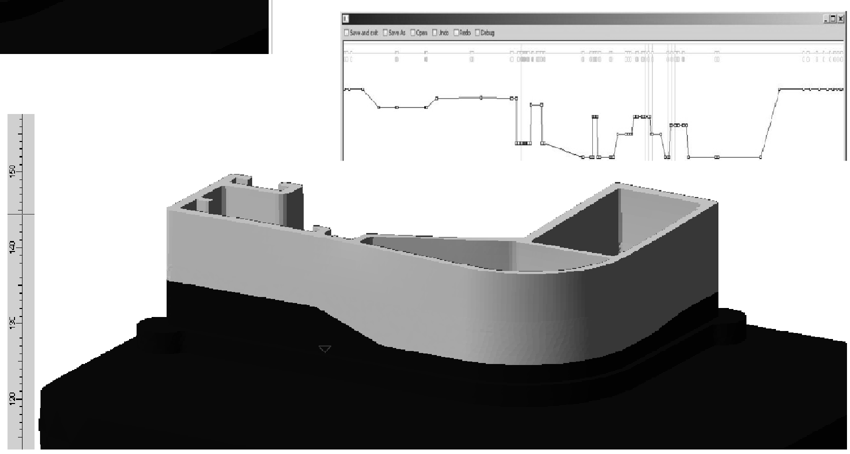

Modified bearing design

Equalizing the velocity by variation of bearing design

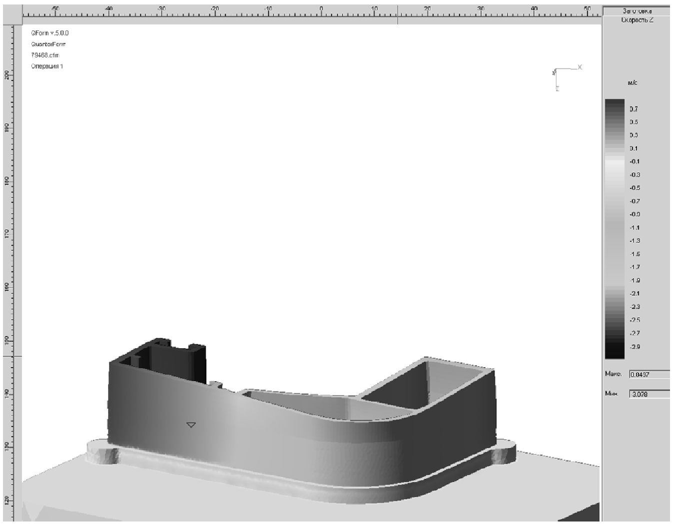

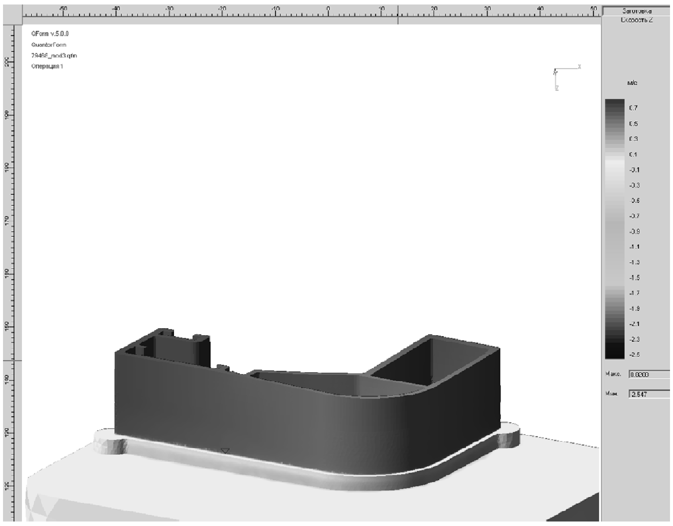

Original bearing design – uneven material flow

Modified bearing design – flow velocity is equalised

The computer simulation of the hot metal forming processes
Milenin Andrzej, AGH University of Science and Technology, 2012

QForm-Extrusion provides complete and reliable

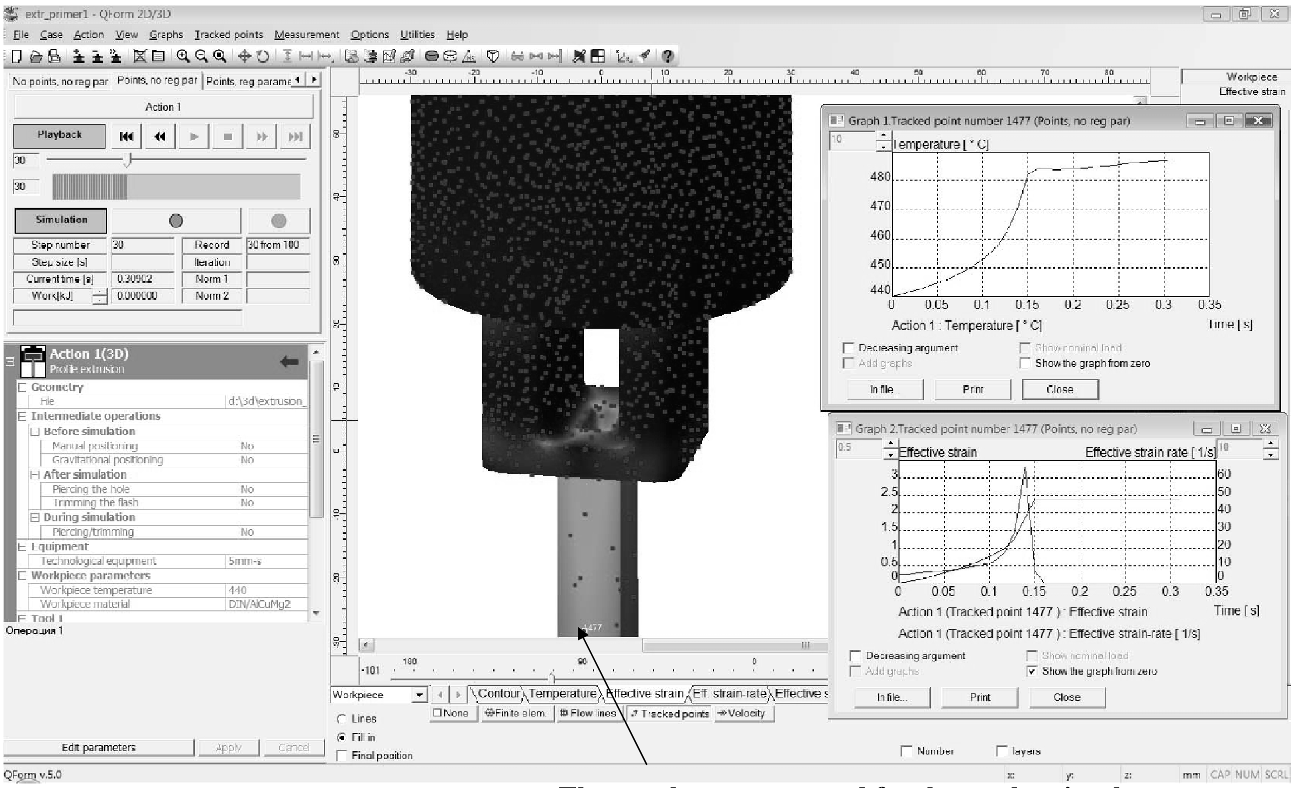

The graphs are presented for the track point that has passed the deformation zone

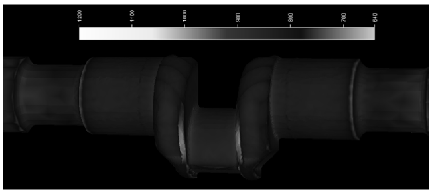

Program Forge 3 in computer aided design of the TR forging technology for crank shafts

1. W. Walczyk, A. Milenin, M. Pietrzyk: Computer aided design of new forging technology for crank shafts, steel research international // Steel Research Int., 82 (2011), 187-194.
2. A. Milenin, W. Walczyk, M. Pietrzyk: Numerical modelling of microstructure evolution during forging of crank shafts // Steel Research Int., (in press)
3. M. Sztangret, A. Milenin, W. Walczyk, M. Pietrzyk: // Computer aided design of the TR forging technology for crank shafts – sensitivity to model and process parameters Steel Research Int., (in press)

The technology of forging of crank shafts developed at the Metal Forming Institute in Poznan, Poland (TR method – following the name of the inventor) is the subject of this presentation.

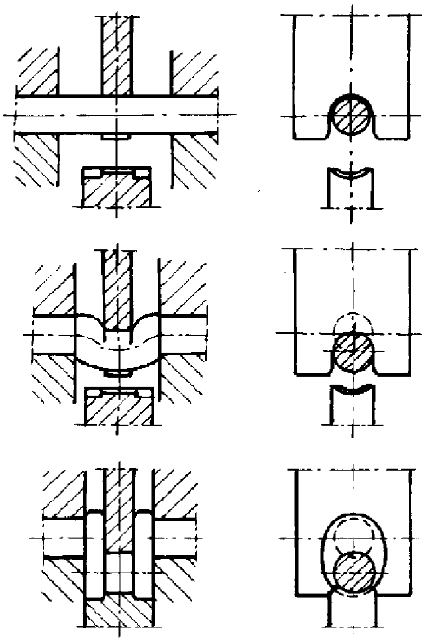

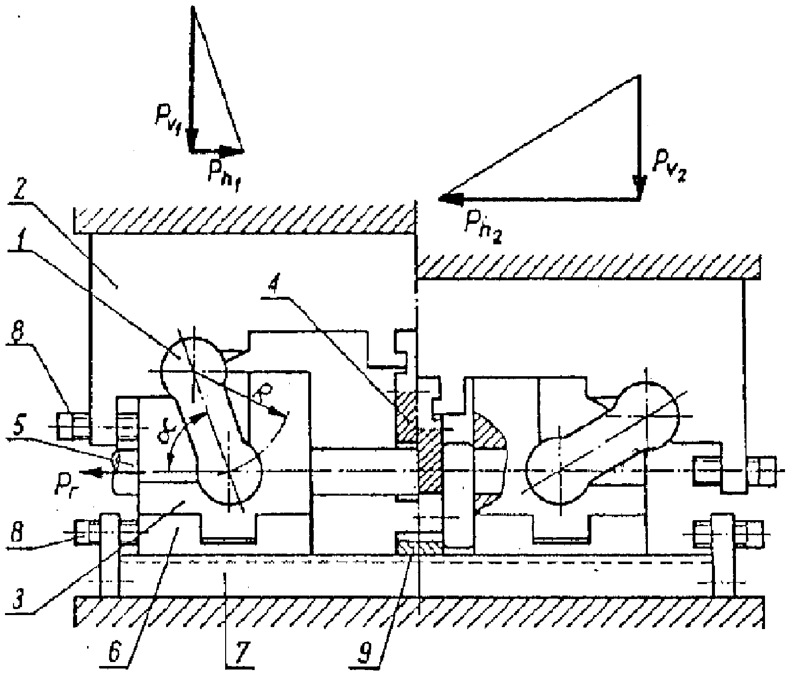

T. Rut, W. Walczyk: Obróbka plastyczna Metali, 11 (2000), 5-8 (in Polish).
T. Rut, W. Walczyk: Part I. Archiwum Technologii Maszyn i Automatyzacji, 22 (2002), 177-186; Part II. Archiwum Technologii Maszyn i Automatyzacji, 22 (2002), 187-196 (in Polish).

License

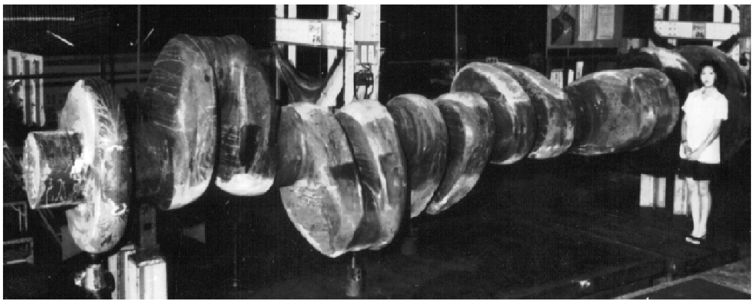

License:
Forjas y Aceros de Reinosa S.A. Spain;
"Huta Ostrowiec" Sp. z o.o.– Ostrowiec Świętokrzyski; Poland;
Huta Stalowa Wola S.A. Poland;
Endo Co. – Osaka, Japan;
Kakegawa Endo Iron Works Co. Ltd. – Kakegawa, Japan;
Krupp AG, Germany;
Japan Steel Works – Muroran Plant; Japan;
Wuhan Forging Works, China;
CSR Ziyang Locomotive Works, China;
Hyundai – Ulsan; S. Korea;
Alfing Kessler GmbH – Wasseralfingen, Germany;
Schmiedewerke Gröditz GmbH, Germany
ELLWOOD GROUP, INC., USA.

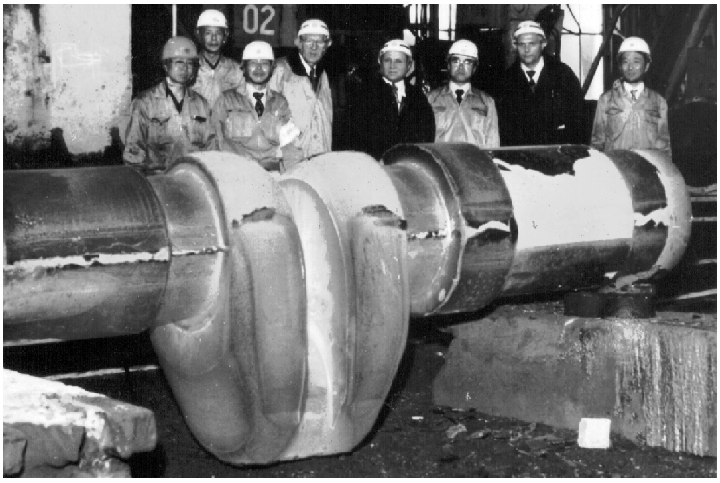

RLA56 Japan Steel Works

The computer simulation of the hot metal forming processes
Milenin Andrzej, AGH University of Science and Technology, 2012

AKADEMIA GÓRNICZO-HUTNICZA IM. STANISŁAWA STASZICA W KRAKOWIE
AGH

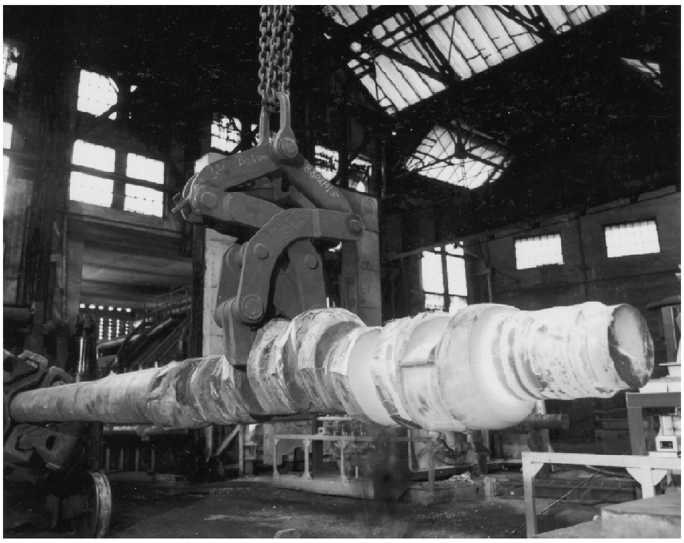

Thyssen – Krupp (Germany)

Alfing Kessler (Germany)

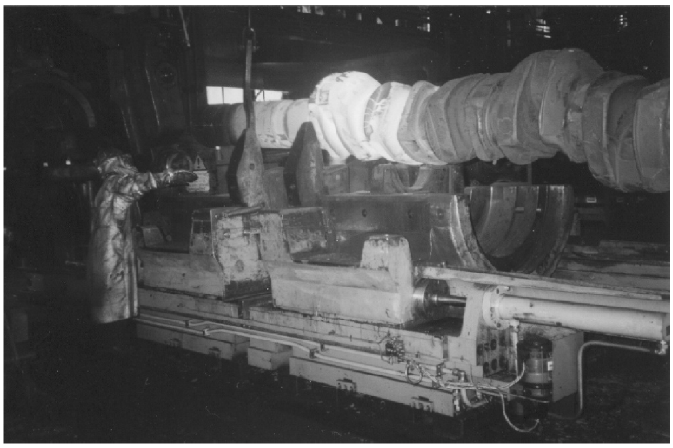

Motivation

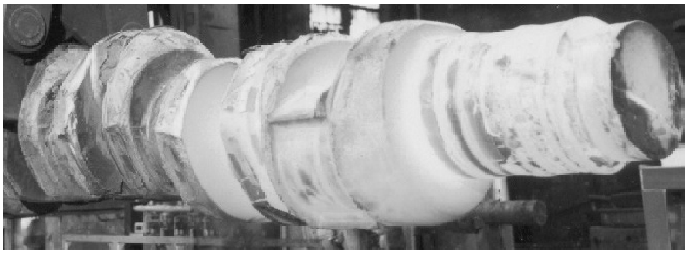

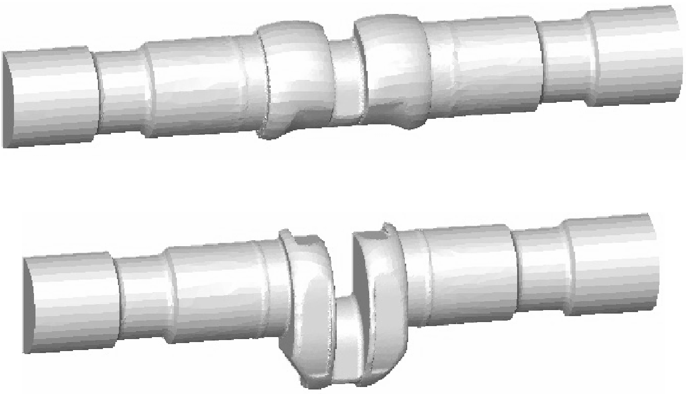

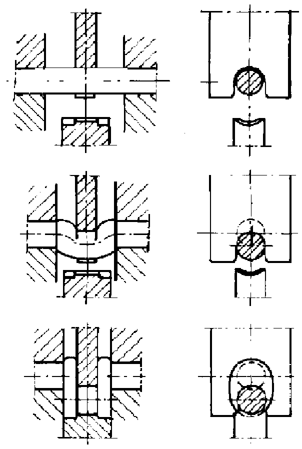

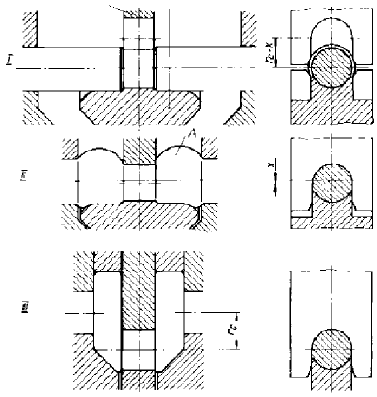

Agenda

- Modification of TR process
- Physical simulation
- Numerical simulation
  - Analyze of different variants of process TR
  - Comparison of load
  - Modeling of microstructure
- Optimization
- Conclusion

Modification of TR process

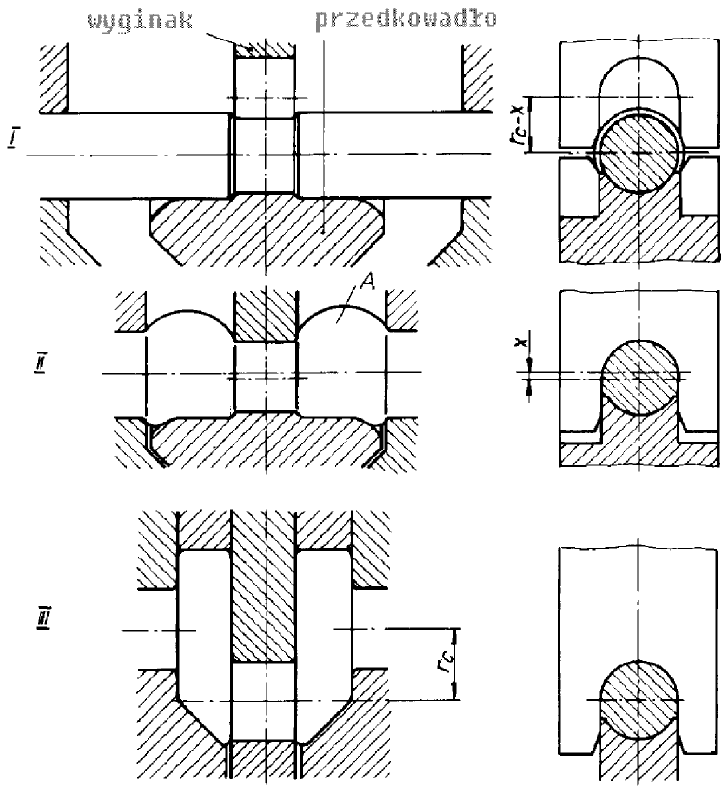

Modification of TR process

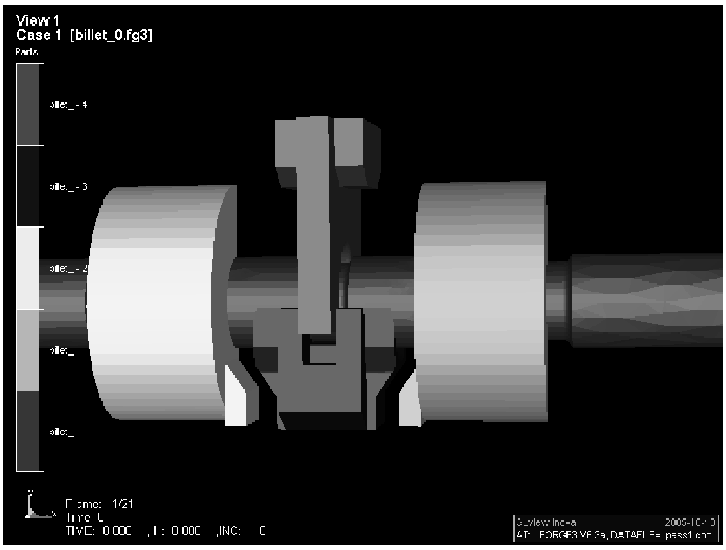

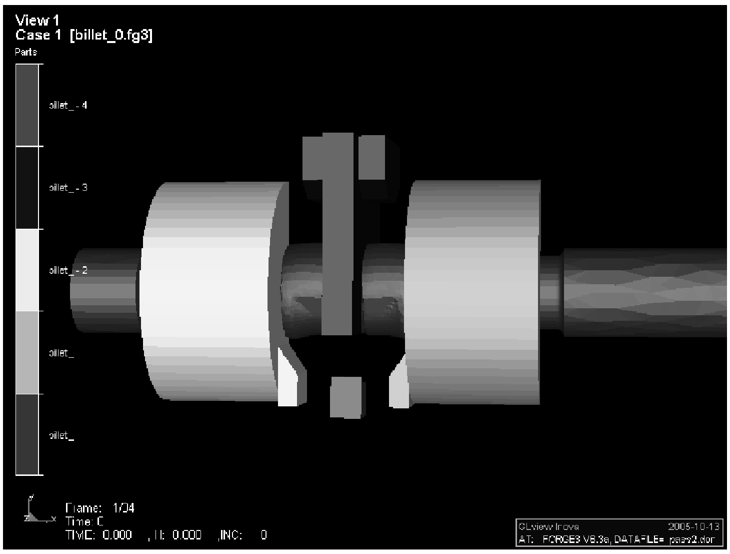

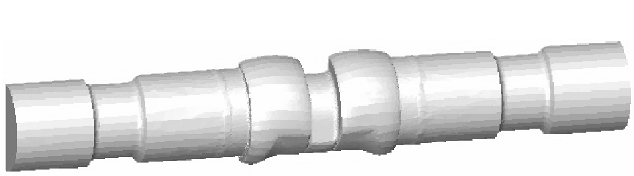

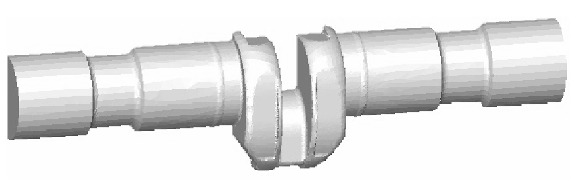

Objective

Development of a finite element model of forging of crankshafts and the application of this model to simulate various technological variants

Numerical analysis of various technological variants of the TR forging and optimization

To include microstructure evolution model in the simulation and predict grain size distribution in the final product.

Schematic illustration of forging

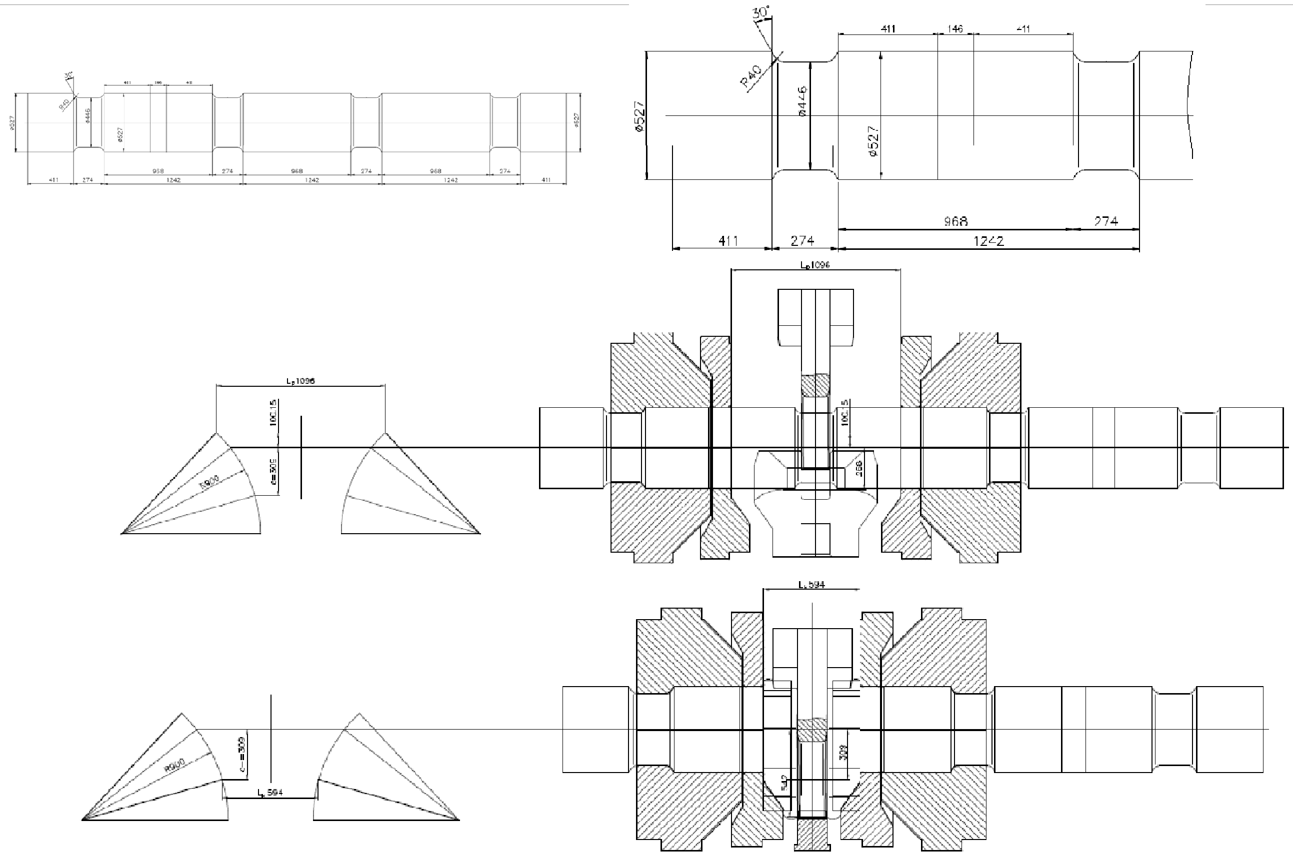

Physical simulation

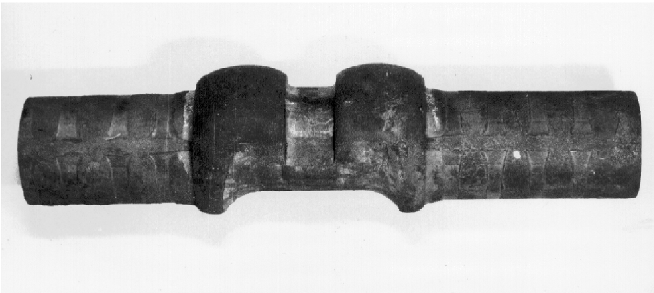

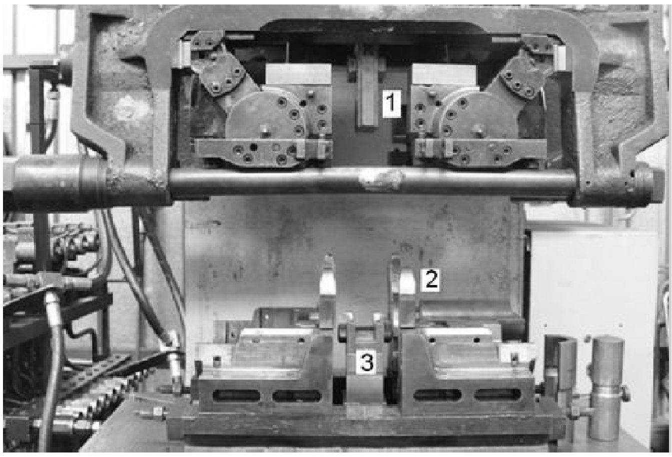

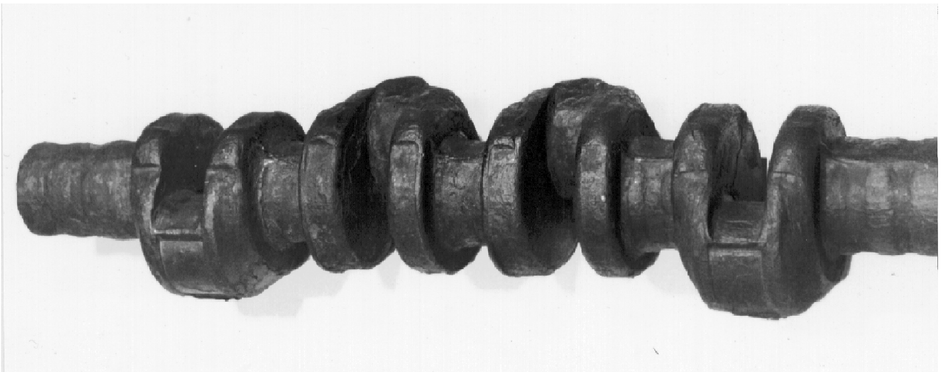

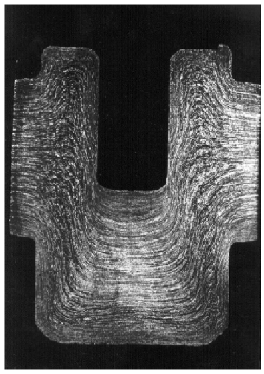

Rheological model

Experiment:

Gleeble 3800 IMŻ Gliwice (**30CrMo12** i 34CrNiMo6).

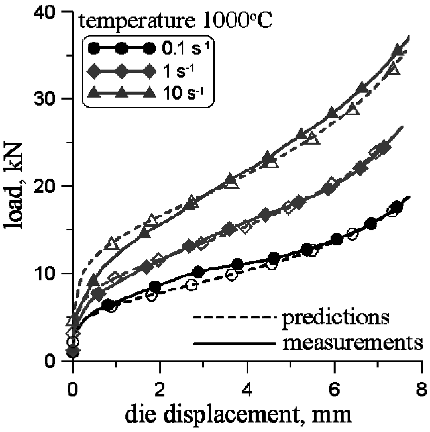

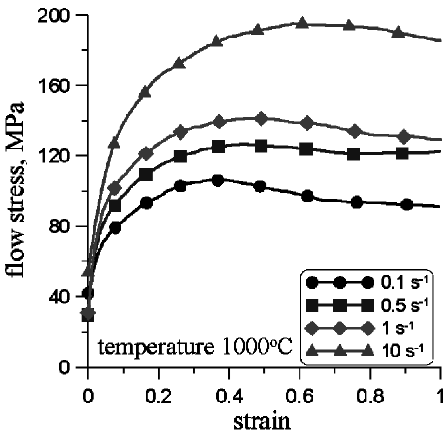

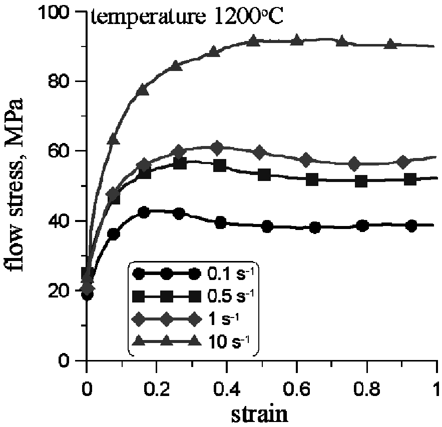

$$\Phi = \sqrt{\frac{1}{Npt}\sum_{i=1}^{Npt}\left[\frac{1}{Nps}\sum_{j=1}^{Nps}\left(\frac{F_{cji}(\mathbf{x},\mathbf{p}_i)-F_{mji}}{F_{mji}}\right)^2\right]} \qquad \sigma = A\varepsilon^n \exp(-B\varepsilon)\dot{\varepsilon}^m \exp(-CT)$$

stal	A	n	B	m	C	Φ
30CrMo12	13525	0.28	0.59686	0.16204	4.089×10^{-3}	0.060434
34CrNiMo6	7136.6	0.172	0.3693	0.1718	3.7455×10^{-3}	0.05276

Models in Forge environment

1. Material model
2. Templet for simulation of forging by TR method
3. Model of tools movement
4. Model of microstructure evaluation

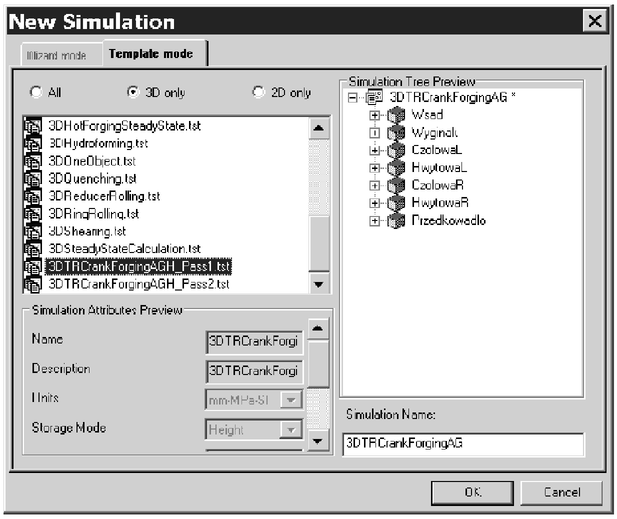

Variants of simulation

I – Basic variant (fig).
II – Without the anvil (5).
III - Without the juts (3a) at both sides at the top of the bending tool (3). These juts form the shape of the top part of the crank webs in variants I and II.
IV – Without the anvil (5) and without the juts at both sides at the top of the bending tool (3).

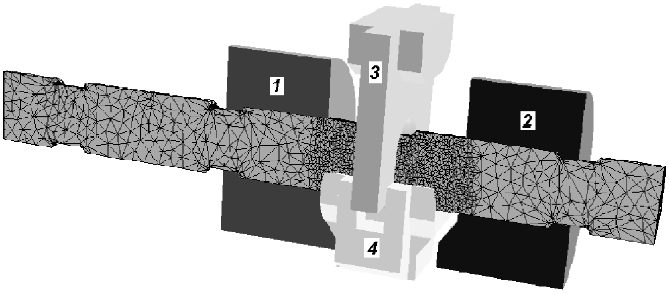

a)

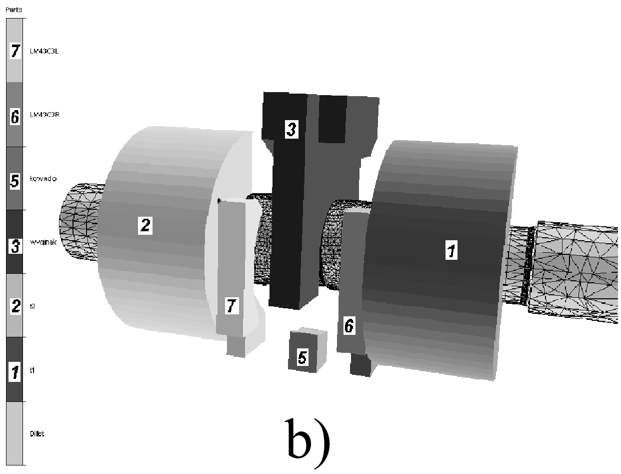

b)

Pre upsetting

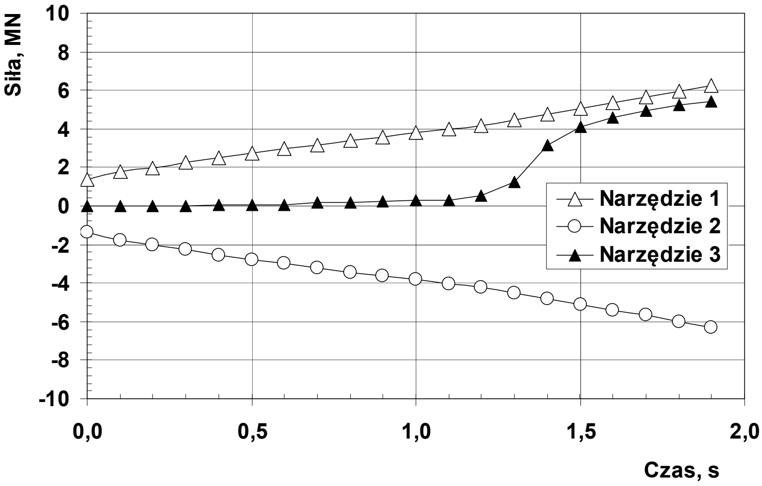

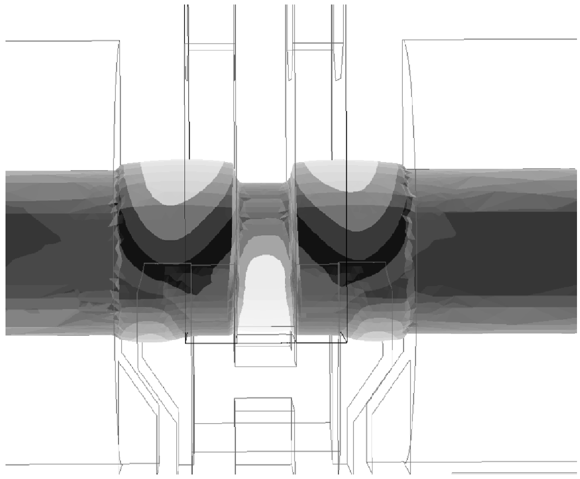

Distribution of the displacements Uz at the final stage of the unsymmetrical pre upsetting.

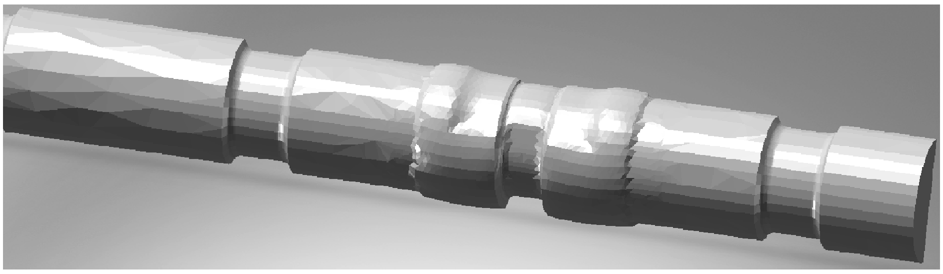

Variant 1

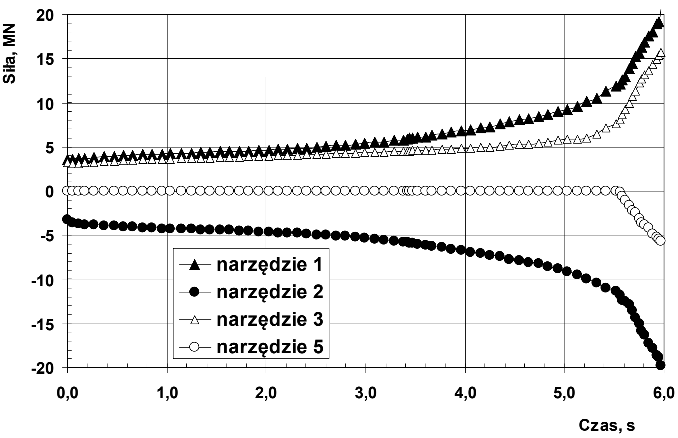

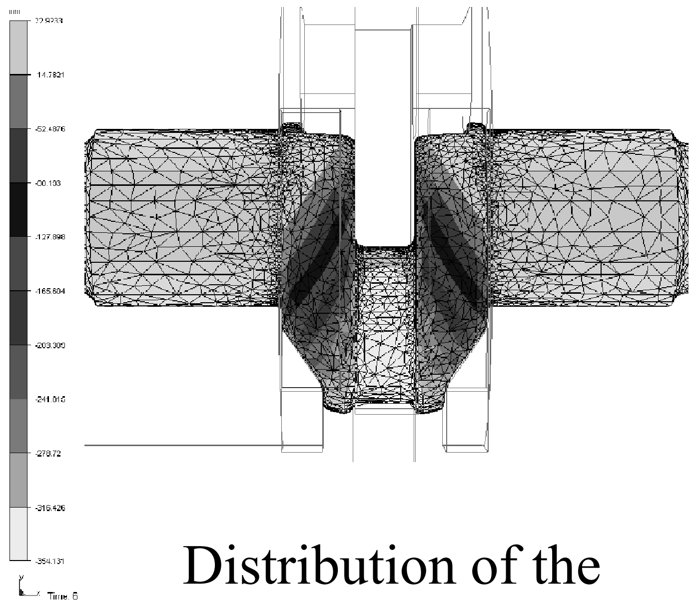

Distribution of the displacements Uz at the final stage of the forging

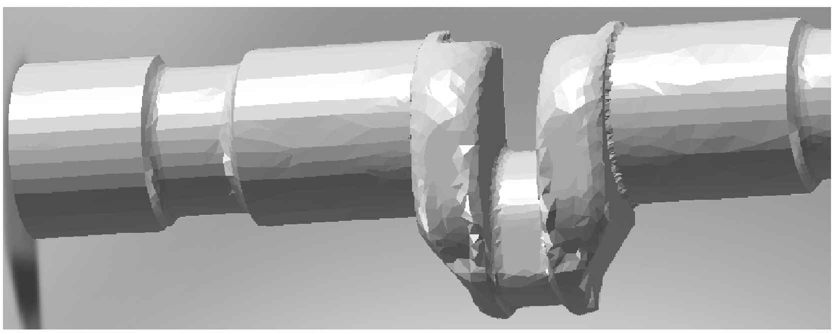

Variant 2

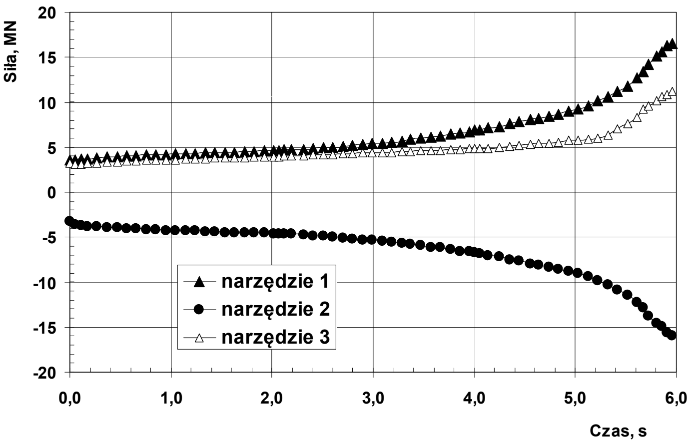

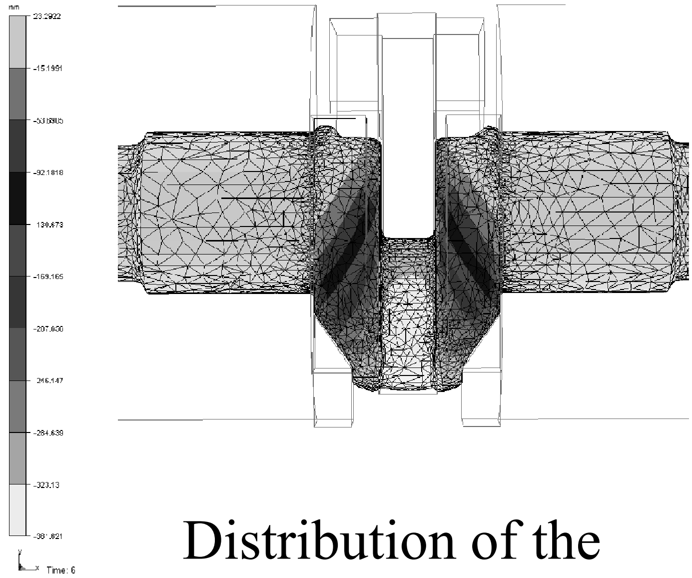

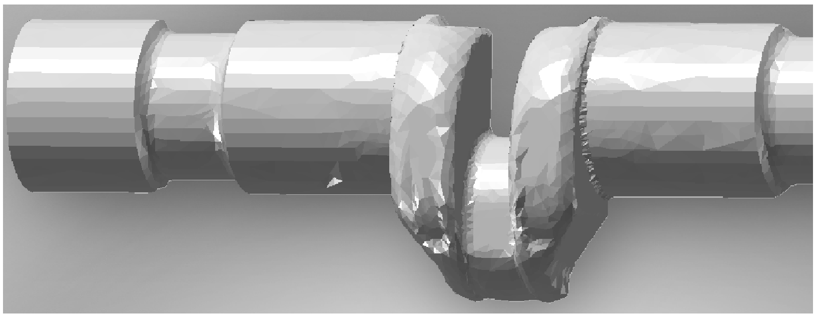

Distribution of the displacements Uz at the final stage of the forging

The computer simulation of the hot metal forming processes
Milenin Andrzej, AGH University of Science and Technology, 2012
AKADEMIA GÓRNICZO-HUTNICZA IM. STANISŁAWA STASZICA W KRAKOWIE
AGH

Variant 3

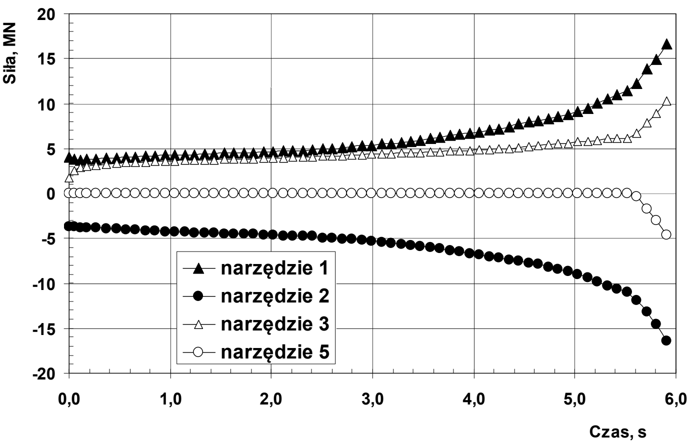

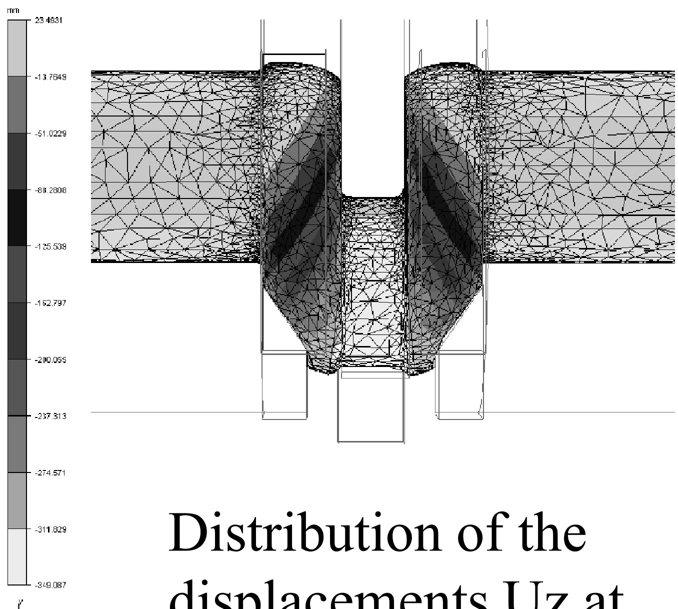

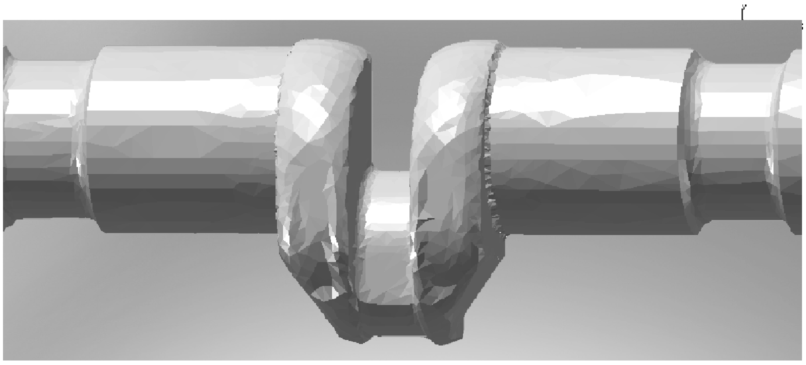

Distribution of the displacements Uz at the final stage of the forging

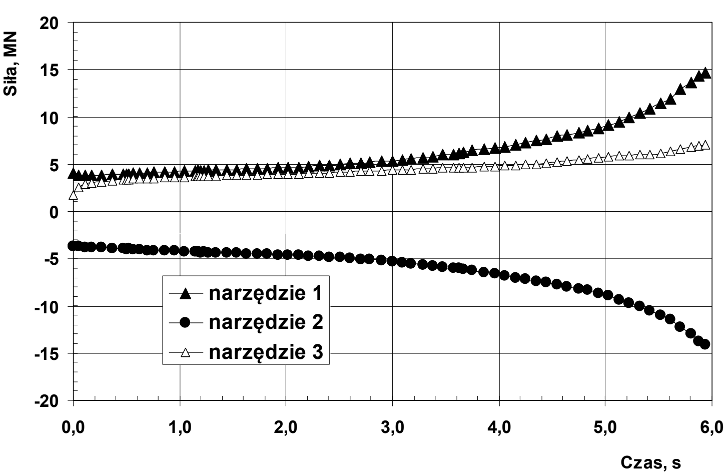

Variant 4

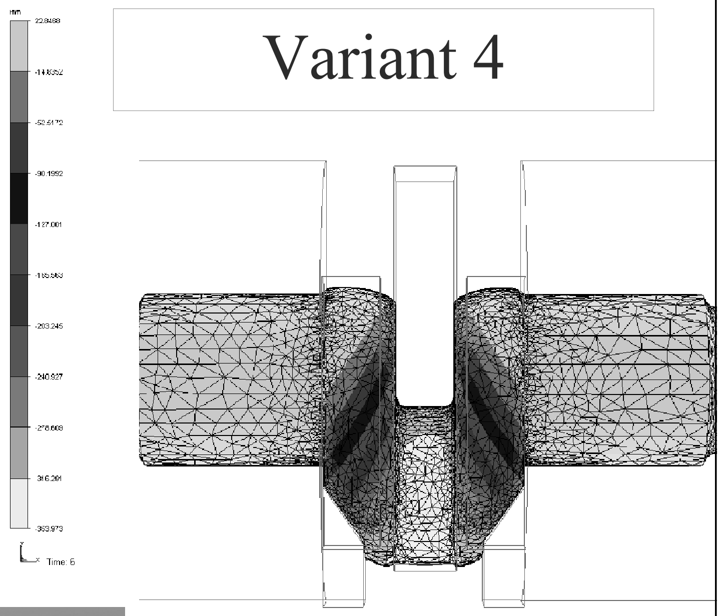

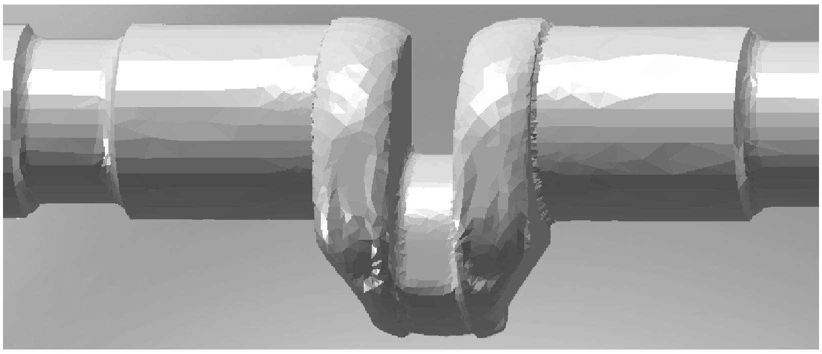

Distribution of the displacements Uz at the final stage of the forging

Microstructure evolution model

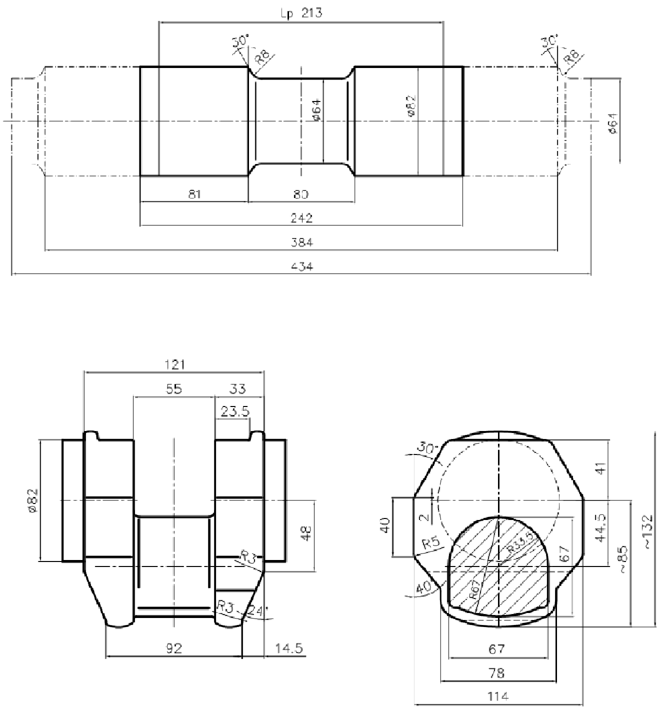

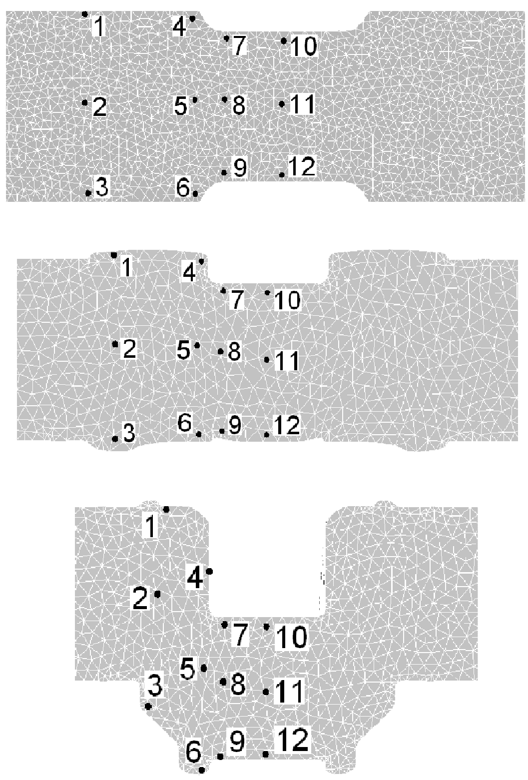

Microstructure evolution model

The majority of works in this field uses modifications of equations proposed first by Sellars to describe processes of recrystallization and grain growth. Since the steel investigated in the present work contains 0.026% Nb, the equations proposed for niobium steel in [*] were used:

$$X = 1 - \exp\left[\ln(0.5)\left(\frac{t}{t_{0.5}}\right)^{1.5}\right]$$

$$t_{0.5} = \left(-5.24 + 550[\mathrm{Nb}]\right)\times 10^{-18}\varepsilon^{(-4+77[\mathrm{Nb}])}D_0^{\,2}\exp\left(\frac{330\,000}{RT}\right)$$

$$D_{rx} = D^{0.67}\varepsilon^{0.67}$$

$$D(t)^q = D_{rx}^q + 4.1\times 10^{23}\, t\exp\left(-\frac{435000}{RT}\right)$$

$$\varepsilon_{ret} = \varepsilon(1-X)$$

where: X – recrystallized volume fraction, $t_{0.5}$ – time to 50% recrystallization, t – time, D_0 – grain size priori to deformation, [Nb] – niobium content in steel, D_{rx} – recrystallized grain size, $D(t)$ – grain size during growth, ε_{ret} – retained strain.

1. [*] P.D. Hodgson: Mat. Forum, 17 (1993), 403-410.

Temperature distribution

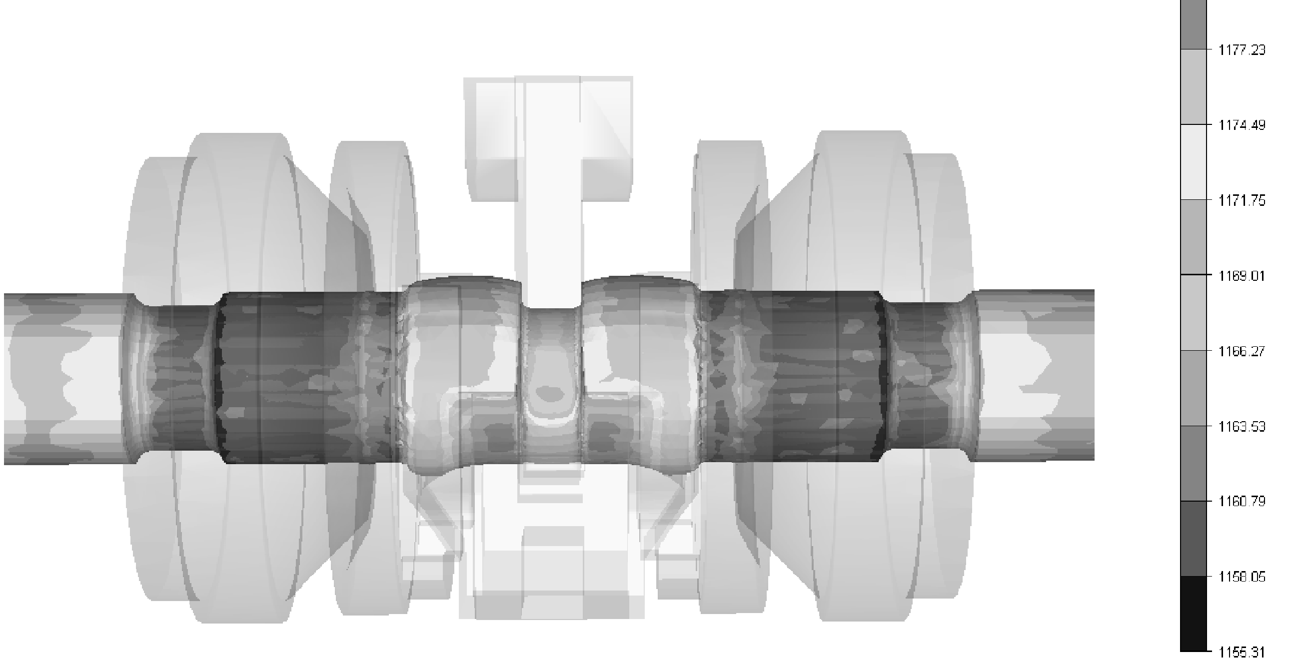

Temperature distribution

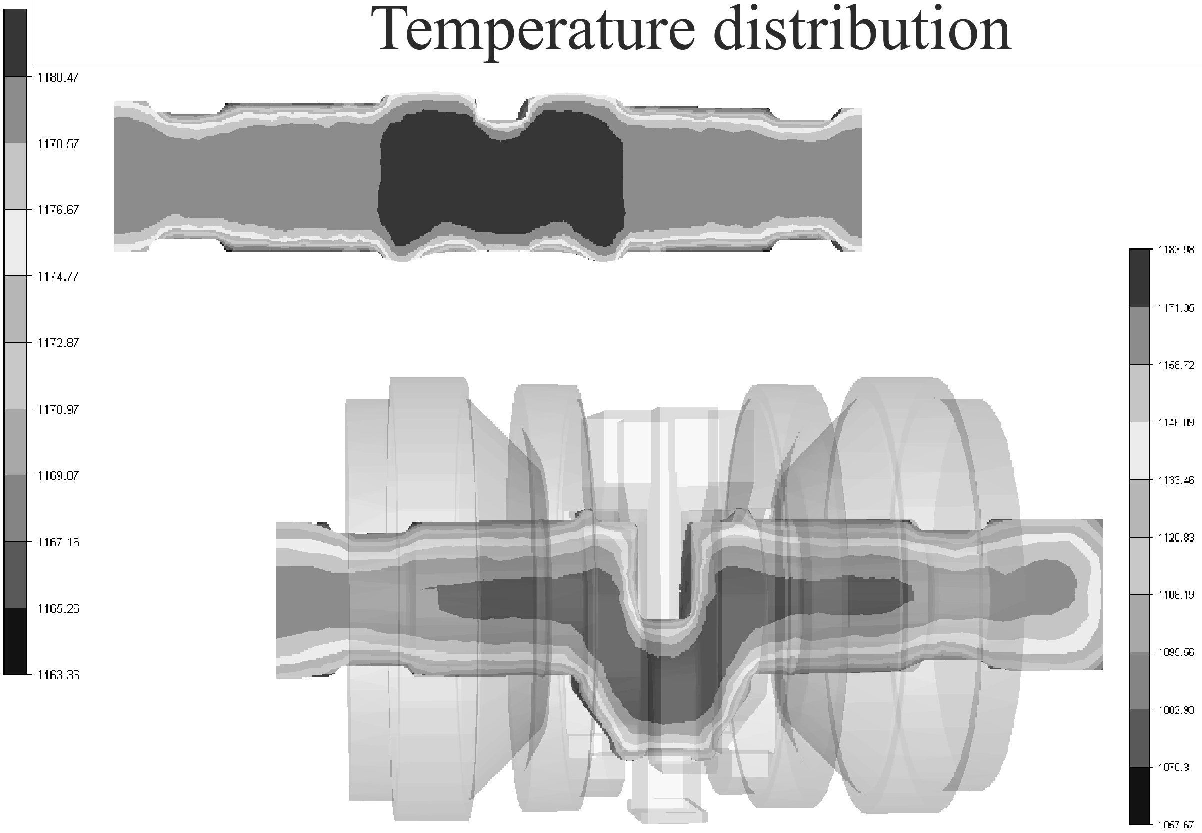

Changes of the temperature, strain accounting for recrystallization, recrystallized volume fraction and austenite grain size

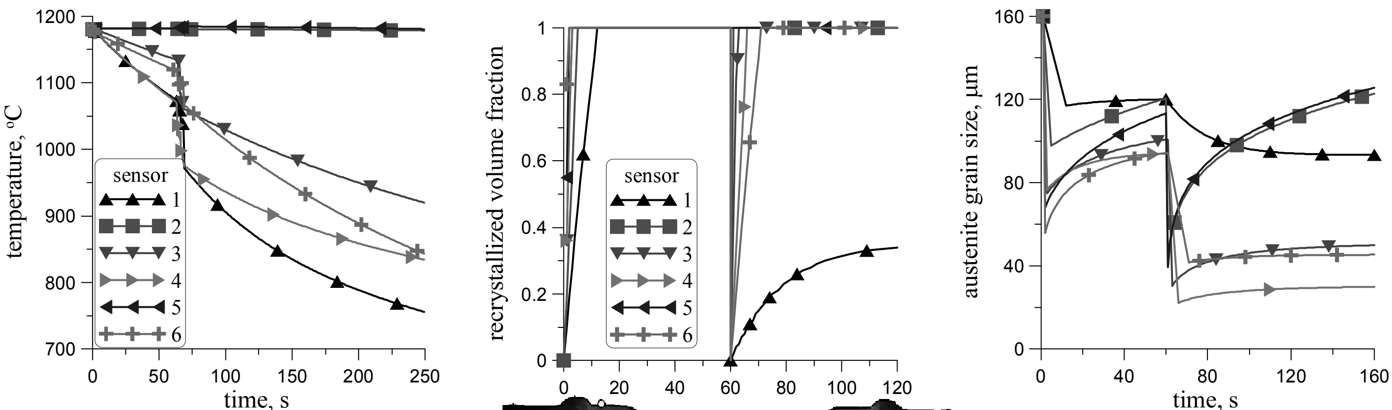

Grain size calculated at the locations of sensors on background of the effective strain distribution in the pass 2

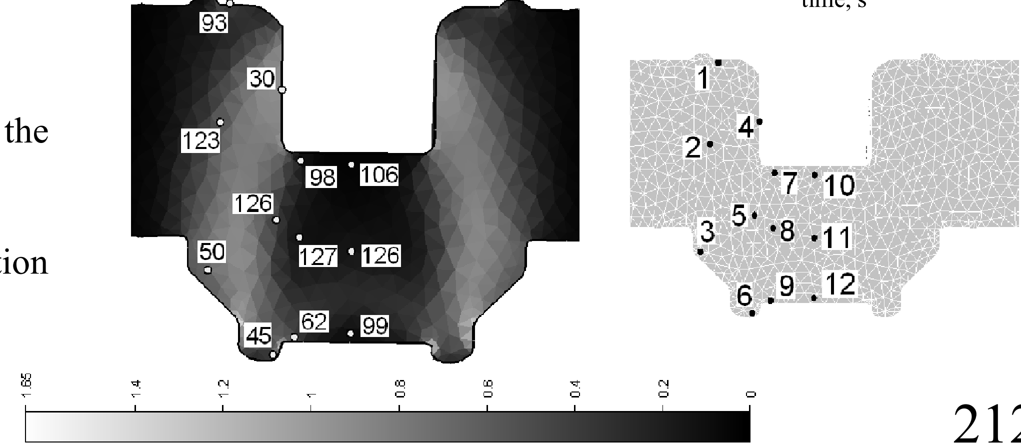

Optimization

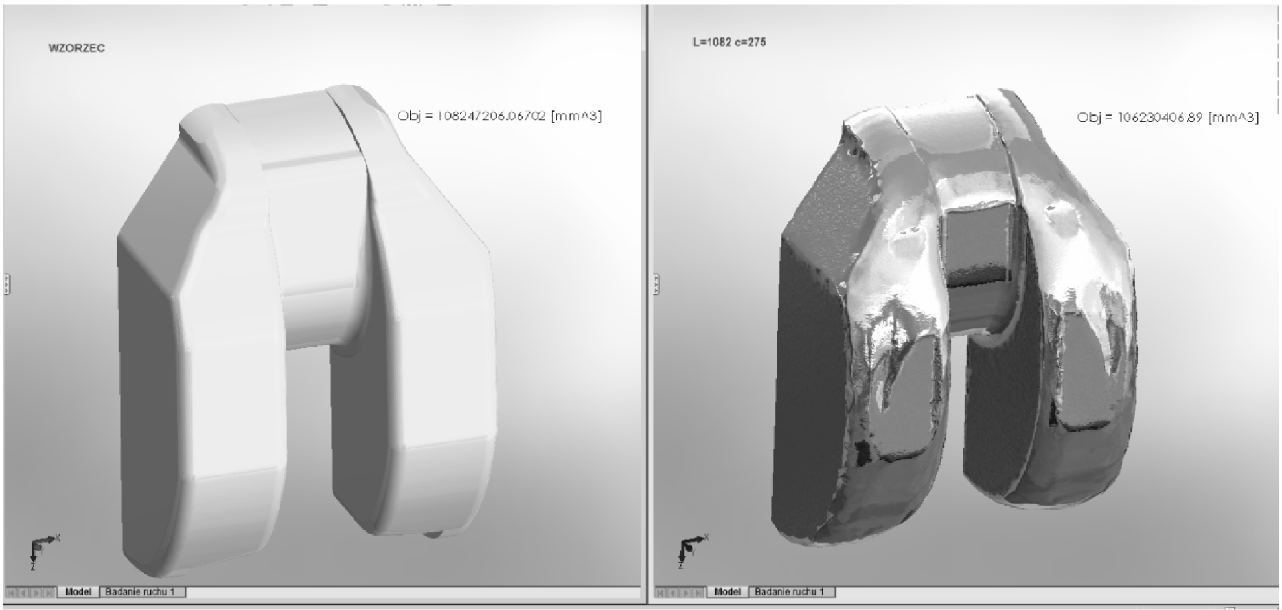

$$F = V_{fog} - V_{calc} \xrightarrow[\min]{}$$

$$F \geq 0$$

Optimization

Lp.	$V_{wzorcowe}$ [mm^3]	Proces	Kształt odkuwki	V [mm^3]	ΔV [mm^3]	ΔV [%]
1	292 725 595,64	V_M43V_L1354_c275	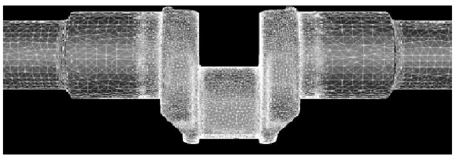	289 599 405,04	-3 126 190,60	**-1,07%**
2		V_M43V_L1354_c285	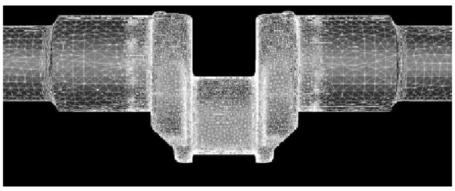	289 826 152,94	-2 899 442,70	**-0,99%**
3		V_M43V_L1354_c295	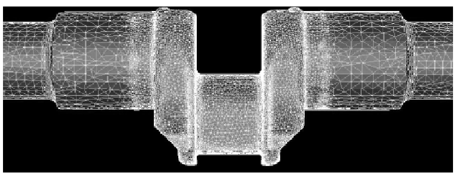	289 870 332,26	-2 855 263,38	**-0,98%**
4		V_M43V_L1368_c275	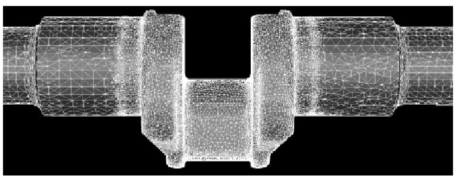	292 935 968,80	210 373,16	0,07%

5		V_M43V_L1368_c285	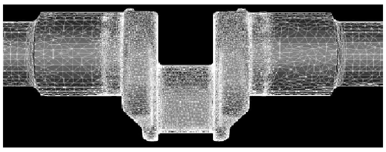	293 133 738,82	408 143,18	0,14%
6		V_M43V_L1368_c295	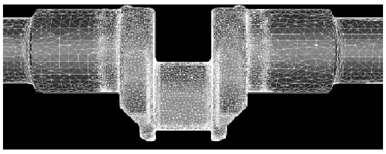	293 497 734,20	772 138,56	0,26%
7		V_M43V_L1382_c275	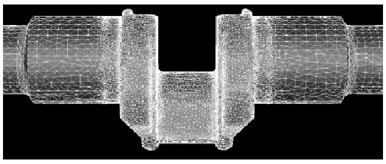	295 452 544,26	2 726 946,62	0,93%
8		V_M43V_L1382_c285	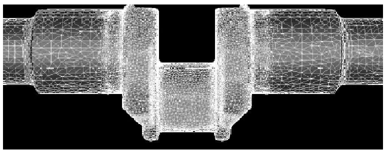	295 803 338,56	3 077 742,92	1,05%
9		V_M43V_L1382_c295	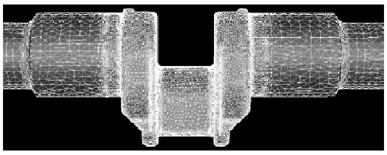	296 288 416,16	3 562 820,52	1,22%

The computer simulation of the hot metal forming processes
Milenin Andrzej, AGH University of Science and Technology, 2012
AKADEMIA GÓRNICZO-HUTNICZA IM. STANISŁAWA STASZICA W KRAKOWIE
AGH

Optimization

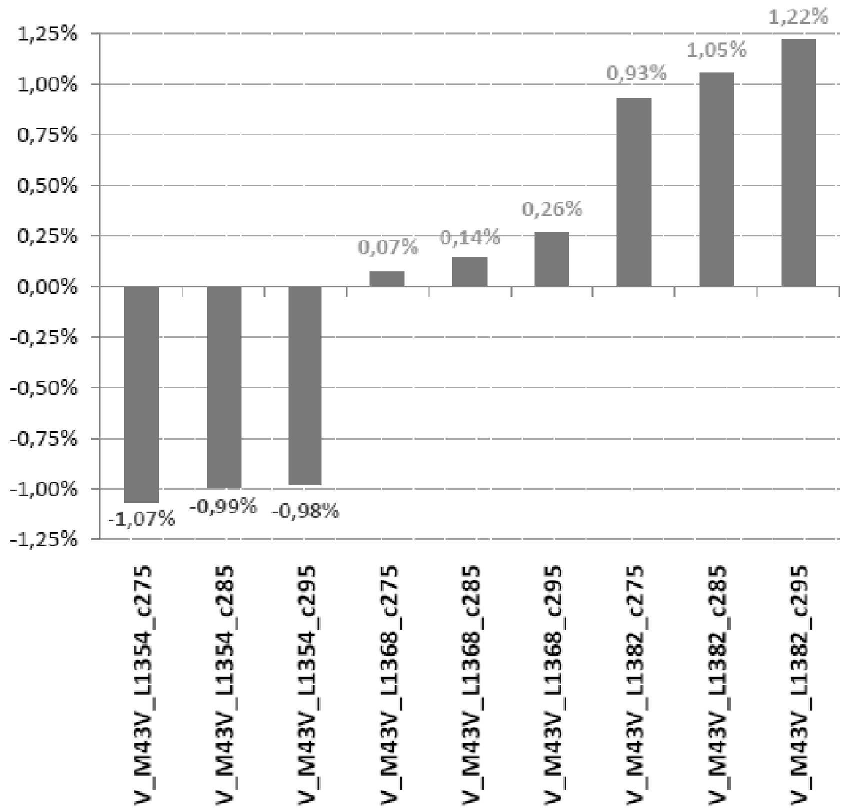

Extrusion example

One of a problem in extrusion of aluminium is increase temperature in profile during extrusion process. The value of temperature increment may be more 100 C. The conclusion of this fact is inhomogeneous property and microstructure along product. The isothermal extrusion will be a method of solved of this problem. One of case of isothermal extrusion technology is introduction of temperature gradient in billet, which compensate a longitudinal gradient of temperature in profile.

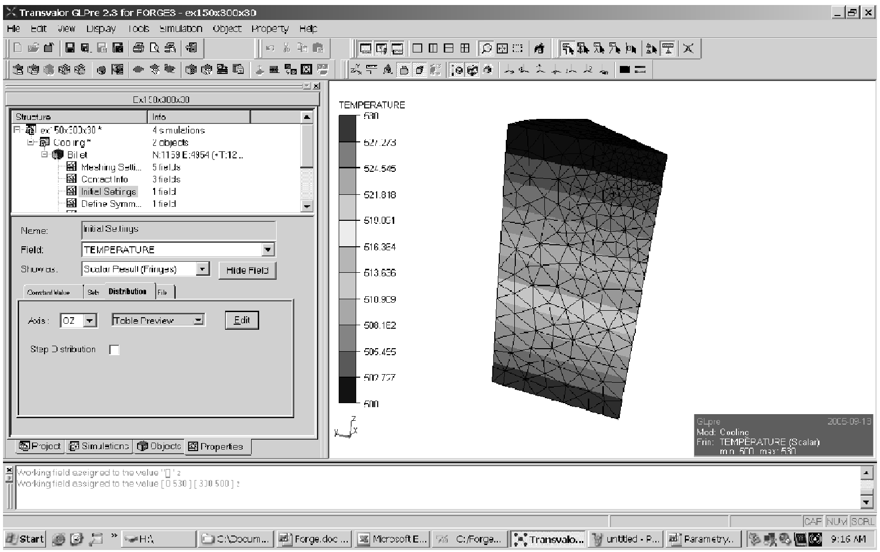

Extrusion example

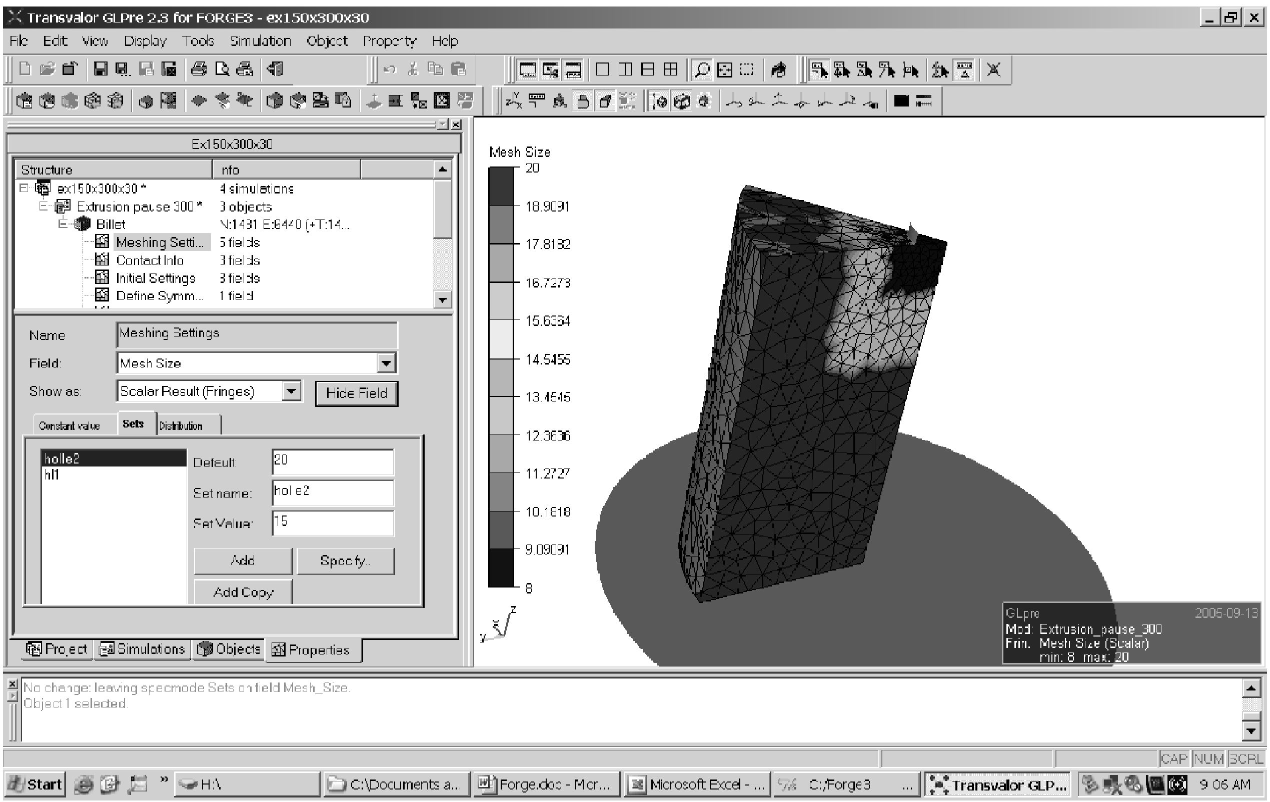

Isotermal extrusion

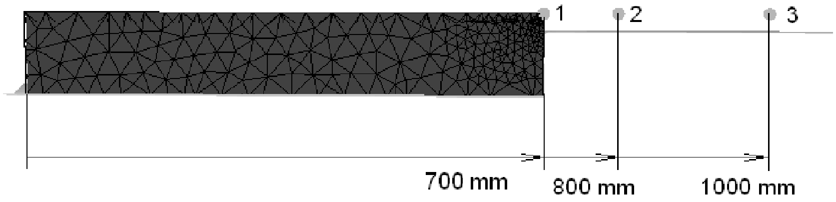

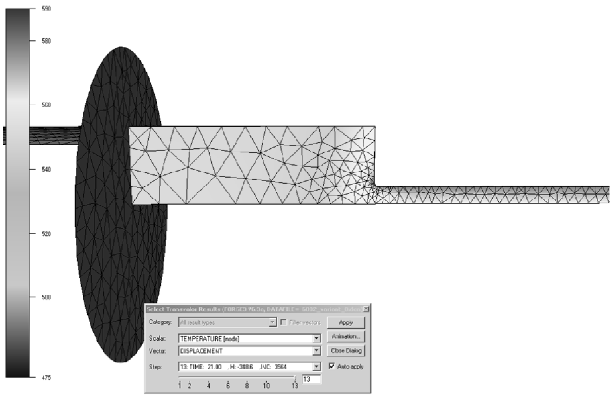

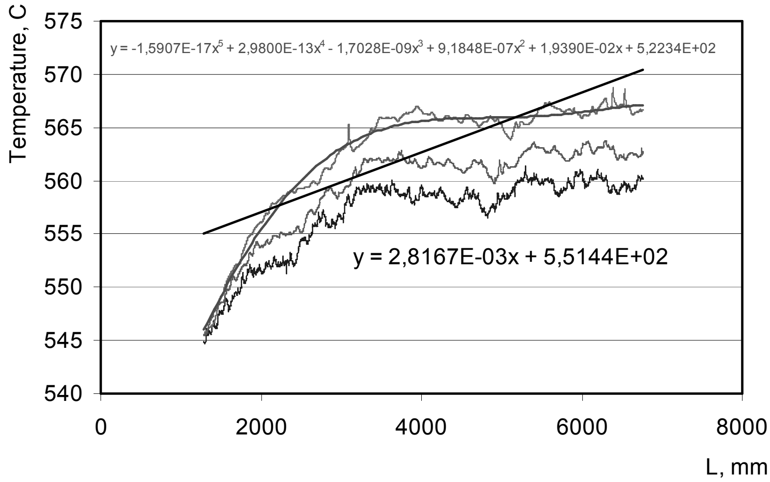

The computer simulation of the hot metal forming processes
Milenin Andrzej, AGH University of Science and Technology, 2012
AGH Akademia Górniczo-Hutnicza im. Stanisława Staszica w Krakowie

Isotermal extrusion

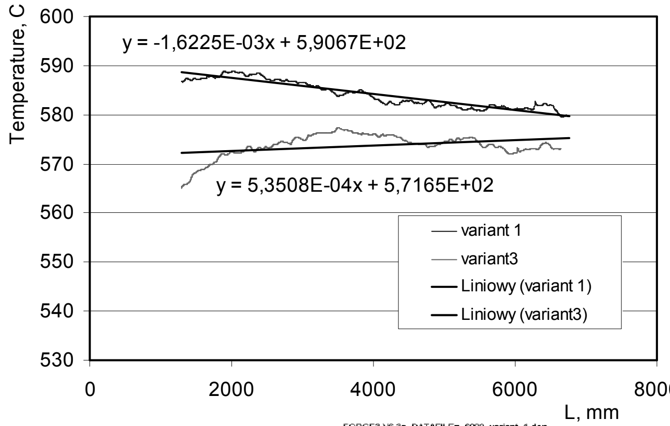

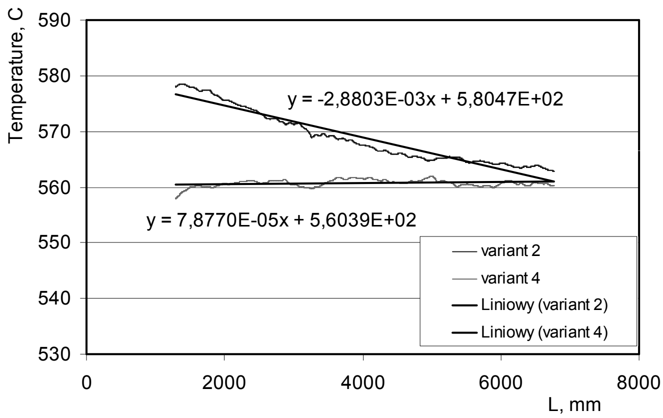

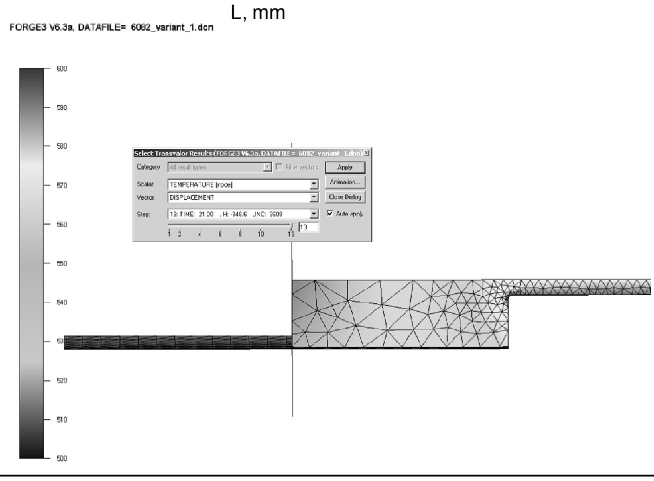

Example of development of own FEM codes and solution of the unconventional problems in the theory of metal forming.

The computer simulation of the hot metal forming processes
Milenin Andrzej, AGH University of Science and Technology, 2012
AGH Akademia Górniczo-Hutnicza im. Stanisława Staszica w Krakowie

Development and Validation of a Numerical Model of Rolling with Cyclic Horizontal Movement of Rolls

$$\boxed{J = \tfrac{1}{2}\int_V \mu\,\dot{\varepsilon}_i^{\,2}\,dV + \int_V \sigma\dot{\varepsilon}_0\,dV + K_\tau \int_F (v_\tau)^2\,dF + K_n \int_F (v_n - w_n)^2\,dF,}$$

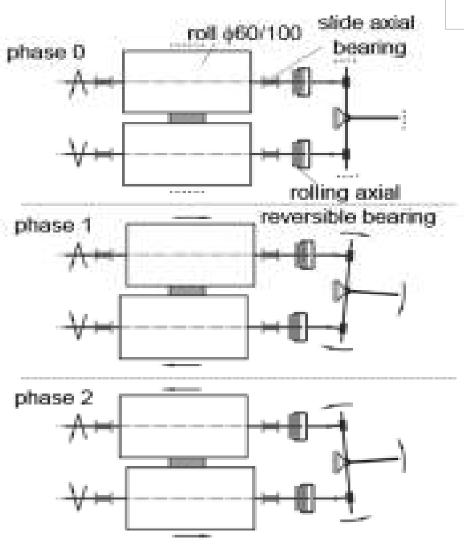

Kinematical scheme of rolling mill with additional cyclic horizontal movement of rolls.

$$\mu^{(p)} = \frac{\sigma_s^{(p-1)}}{\dot{\varepsilon}_i^{(p-1)}}$$

$$\boxed{K_\tau^{(p)} = \frac{\tau^{(p-1)}}{v_\tau^{(p-1)}}}$$

$$\boxed{v_\tau^2 = v_1^2 + v_2^2}$$

$$\int_F \left(K_{\tau 1} v_1^2 + K_{\tau 2} v_2^2\right) dF$$

$$\boxed{K_{\tau 1}^{(p)} = \frac{m_1 \sigma_s}{v_\tau}} \qquad \boxed{K_{\tau 2}^{(p)} = \frac{m_2 \sigma_s}{v_\tau}}$$

$$\sigma_n \geq 0 \qquad v_2 = \frac{\pi U_{wy}}{\tau_{wy}} \sin\left(2\pi \frac{\tau}{\tau_{wy}}\right)$$

A. Milenin, F. Grosman, L. Madej,J. Pawlicki Development and Validation of a Numerical Model of Rolling with Ciclic Horizontal Movement of Rolls //STEEL RESEARCH INTERNATIONAL 81 (3):p204-209 2010

Laboratory rolling mill capable to impose strain path change on the material

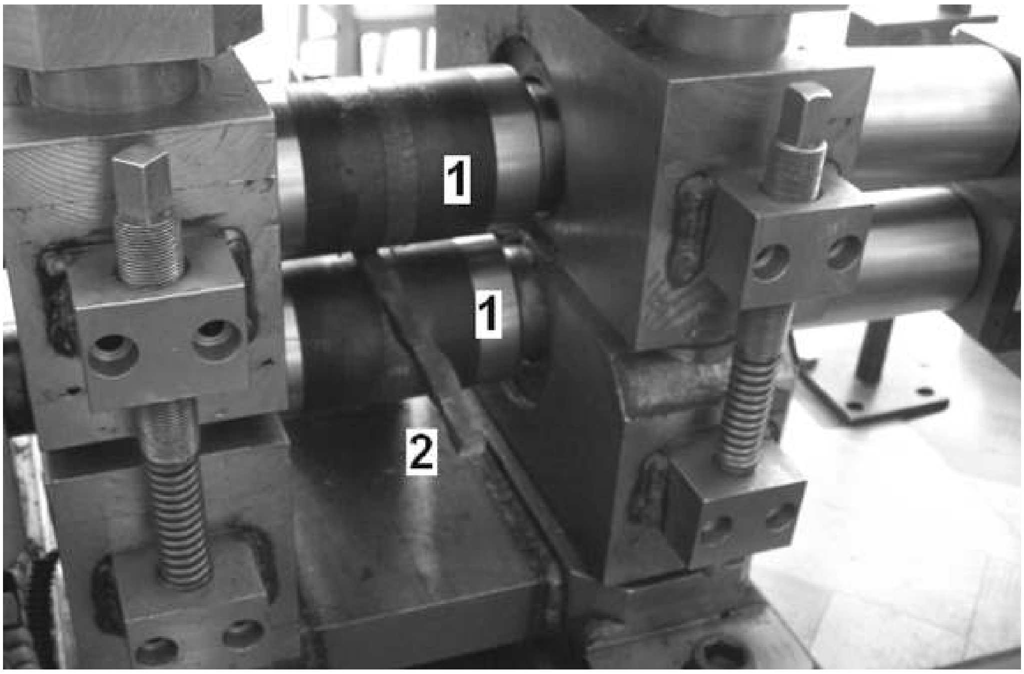

Picture of the laboratory rolling mill capable to impose strain path change on the material, 1 – top and bottom rolls, 2 sample.

Equivalent strain along the vertical line of symmetry at the exit of the roll gap during the MEFASS process

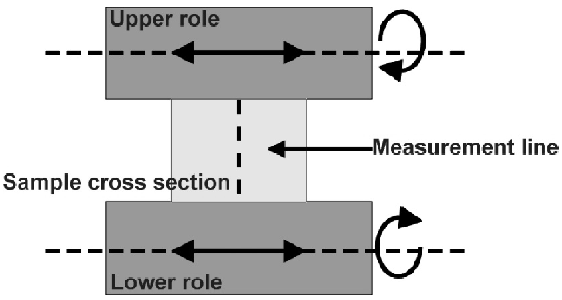

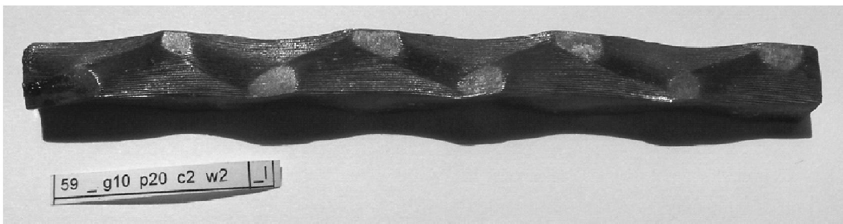

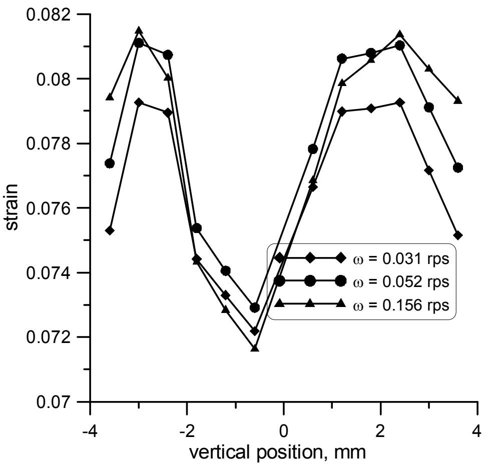

Equivalent strain along the vertical line of symmetry at the exit of the roll gap during conventional rolling process

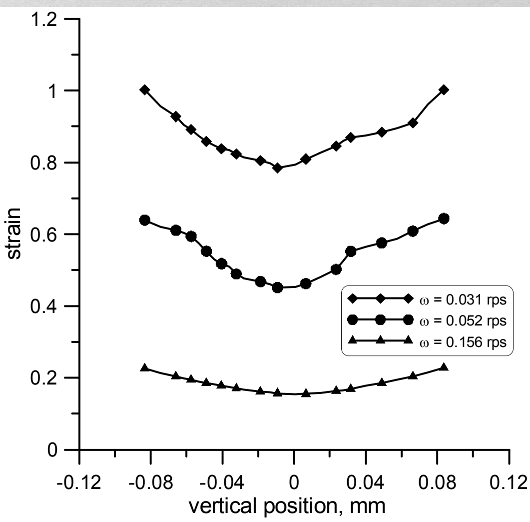

Equivalent strain along the vertical line of symmetry at the exit of the roll gap during the MEFASS process

FEM simulation of rolling process with cyclic horizontal movement of rolls, (rolling speed w=0.031 rps)

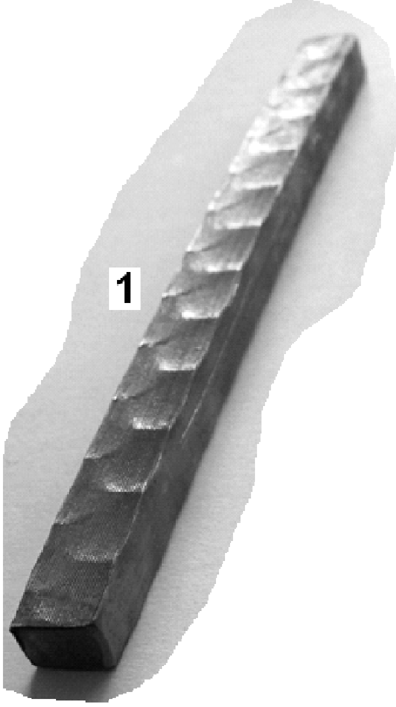

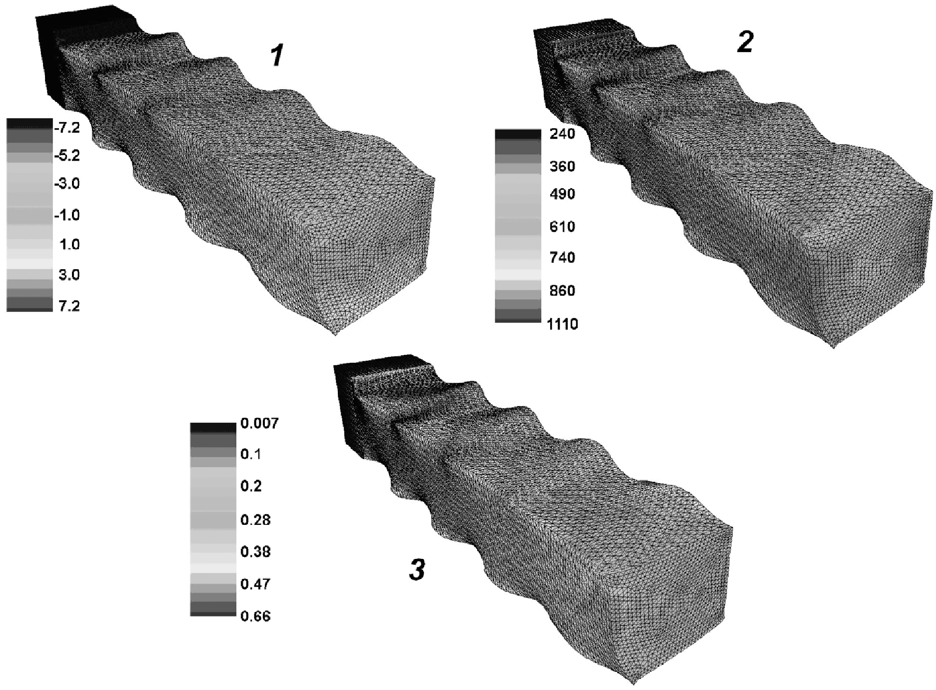

The computer simulation of the hot metal forming processes
Milenin Andrzej, AGH University of Science and Technology, 2012
AKADEMIA GÓRNICZO-HUTNICZA IM. STANISŁAWA STASZICA W KRAKOWIE
AGH

FEM simulation of rolling process with cyclic horizontal movement of rolls (rolling speed w=0.052 rps)

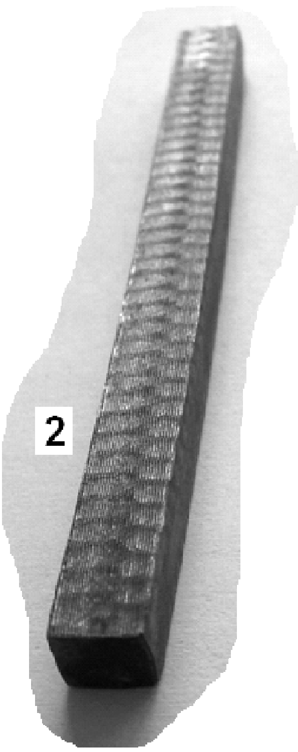

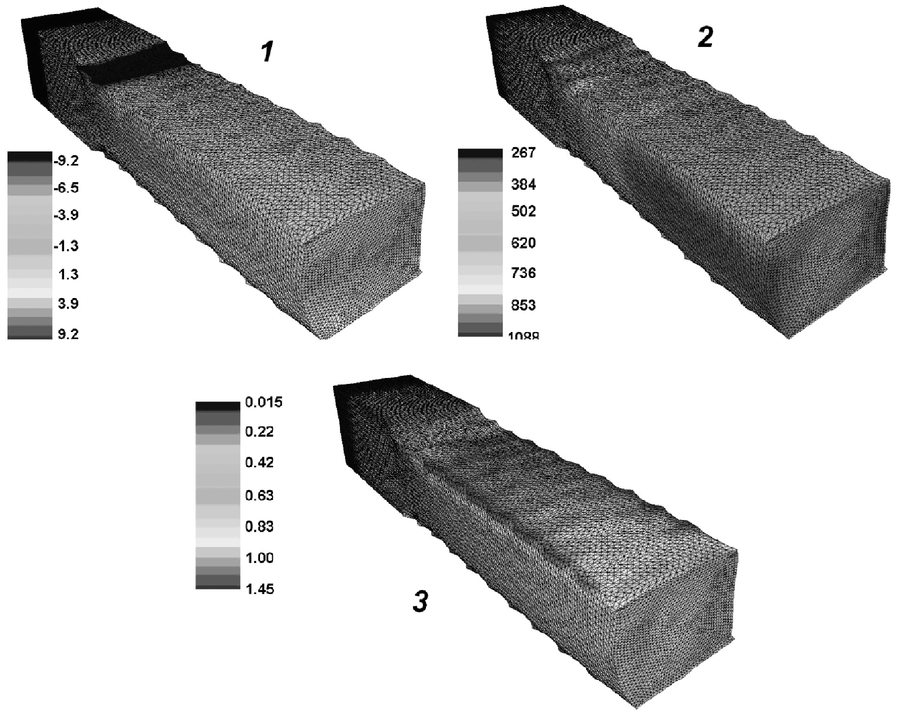

FEM simulation of rolling process with cyclic horizontal movement of rolls (rolling speed w=0.156 rps)

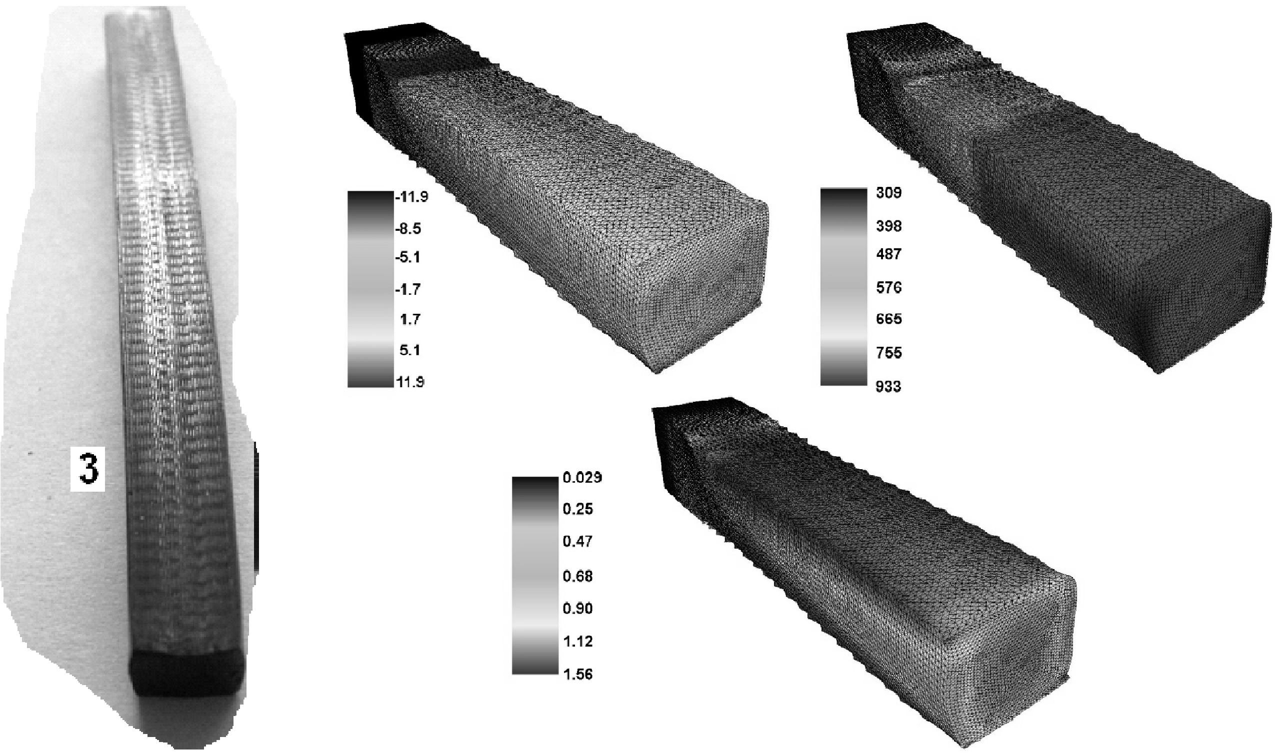

The computer simulation of the hot metal forming processes
Milenin Andrzej, AGH University of Science and Technology, 2012
Akademia Górniczo-Hutnicza im. Stanisława Staszica w Krakowie
AGH

Development and Validation of a Mathematical Model of Warm Drawing Process of Magnesium Alloys in Heated Dies

A. Milenin, P.Kustra*
*Faculty of Metal Engineering and Industrial Computer Science, AGH University of Science and Technology, Al. Mickiewicza 30, 30-059, Krakow, Poland, milenin@agh.edu.pl

Abstract
Due to high compatibility and solubility in human organism, special magnesium alloys are applied in bioengineering. Production of surgical threads to integration of tissue can be application of these types of alloys. This sort of application calls for fine wires with diameters from 0.1 to 0.9 mm. The warm drawing process in heated dies is proposed to increase the workability of the Mg alloys. The purpose of this paper is development and experimental validation of a mathematical model of a warm drawing process of wires made of MgCa0.8 and Ax30 alloys and determination of optimal parameters with the objective function defined as maximum of workability. The first part of investigation is focused on development of a numerical model, which is based on FE solution. The second part of paper is focused on experimental upsetting and tensile tests. Basing on these tests the flow stress and ductility models were obtained. The materials models are implemented into the Authors' FE code, which is dedicated to modelling of drawing processes. Experimental validation of model is based on thermo visual measurement of wire temperature during drawing.

[1] A. Milenin, D.J. Byrska, O. Gryfin The multi-scale physical and numerical modeling of fracture phenomena in the MgCa0.8 alloy// Computers and Structures 89 (2011) 1038–1049 (Proc. 6th MIT Conferense, 06.2011)
[2] A. MILENIN, P. KUSTRA Mathematical model of warm drawing process of magnesium alloys in heated dies// STEEL RESEARCH INTERNATIONAL vol. 81 no. 9 spec. ed. s. 1251–1254 2010
[3] Milenin, A., Seitz, J.-M., Bach, Fr.-W., Bormann, D., Kustra, P., 2010a. Production of thin wires of magnesium alloys for surgical applications. Proc. Conf. Wire Expo 2010 Milwaukee, USA, pp. 61-70.

Introduction. Technology.

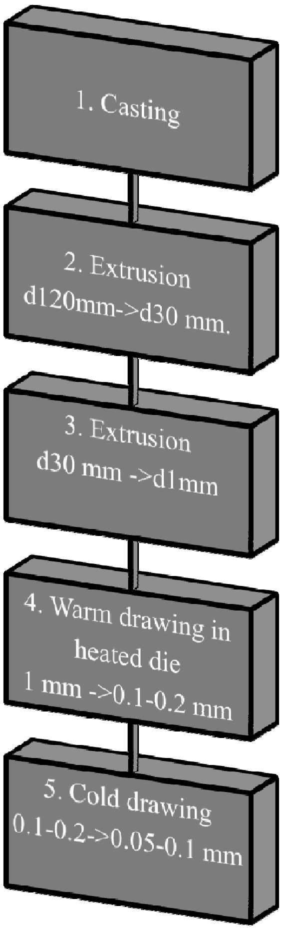

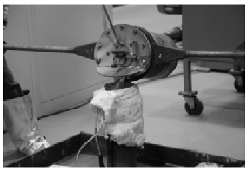

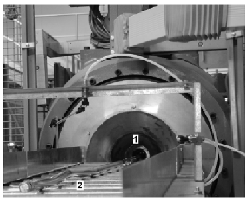

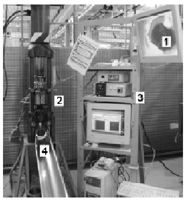

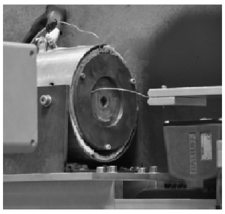

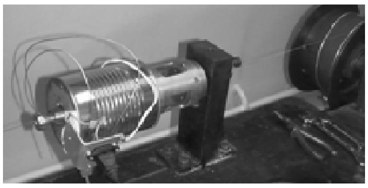

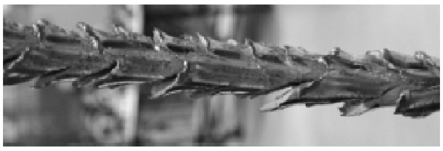

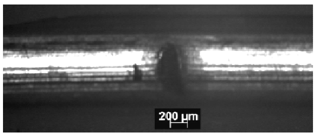

A. Milenin, P. Kustra, J.-M. Seitz, Fr.-W. Bach, D. Bormann Development and Validation of a Mathematical Model of Warm Drawing Process of Magnesium Alloys in Heated Dies // Proc. Conf. InterWire 2011, Atlanta, Georgia, USA, May 2011, Wire Ass. Int. Inc

The computer simulation of the hot metal forming processes
Milenin Andrzej, AGH University of Science and Technology, 2012
AKADEMIA GÓRNICZO-HUTNICZA IM. STANISŁAWA STASZICA W KRAKOWIE
AGH

FEM Model of Wire Drawing. Model of Metal Deformation.

The FE code Drawing2d developed by Milenin (2005, 2008) is used in the present work. The FE model solves a boundary problem considering such phenomena as metal deformation, heat transfer in a die and in a wire, metal heating due to deformation and friction. Solution of the boundary problem is obtained by using variation principle of rigid-plastic theory:

$$J = \int_V \int_0^{\xi_i} \sigma_s(\varepsilon_i, \xi_i, t) d\xi_i dV + \int_V \sigma_0 \xi_0 dV - \int_S \sigma_\tau v_\tau dS ,$$

where: ξ_i – strain rate, σ_s – yield stress, ε_i – effective strain, t – temperature, V – volume, σ_0 – mean stress, ξ_0 – volumetric strain rate; S – contact area between alloy and die, σ_τ – friction stress, v_τ – alloy slip velocity along area of die.

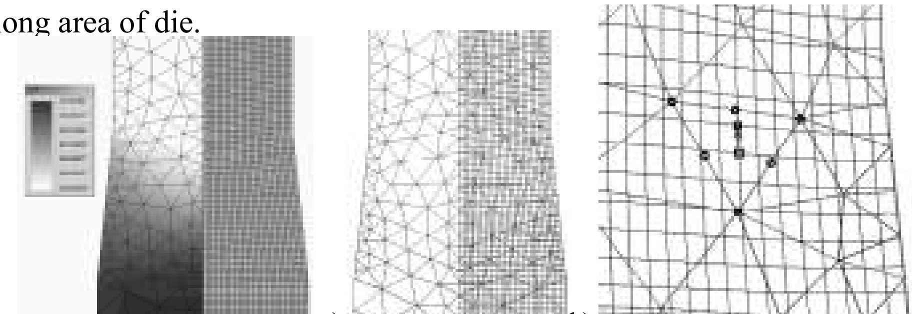

a) b) c)

The scheme to the determination flow lines point location; a – velocity field in drawing direction and flow lines mesh; b – the flow line mesh placed on FEM mesh; c – the scheme to the determination the next point of current flow lines.

Milenin A., Kustra P.: The multiscale FEM simulation of wire fracture phenomena during drawing of Mg alloy, Steel Research International, ISSN 1611-3683. - 79(2008) spec. ed. s. 717–722.
Milenin A.: Program komputerowy Drawing2d – narzędzie do analizy procesów technologicznych ciągnienia wielostopniowego, Hutnik, No 2, 2005. - s. 100-104 (In Polish).

The algorithm of FEM model of metal deformation

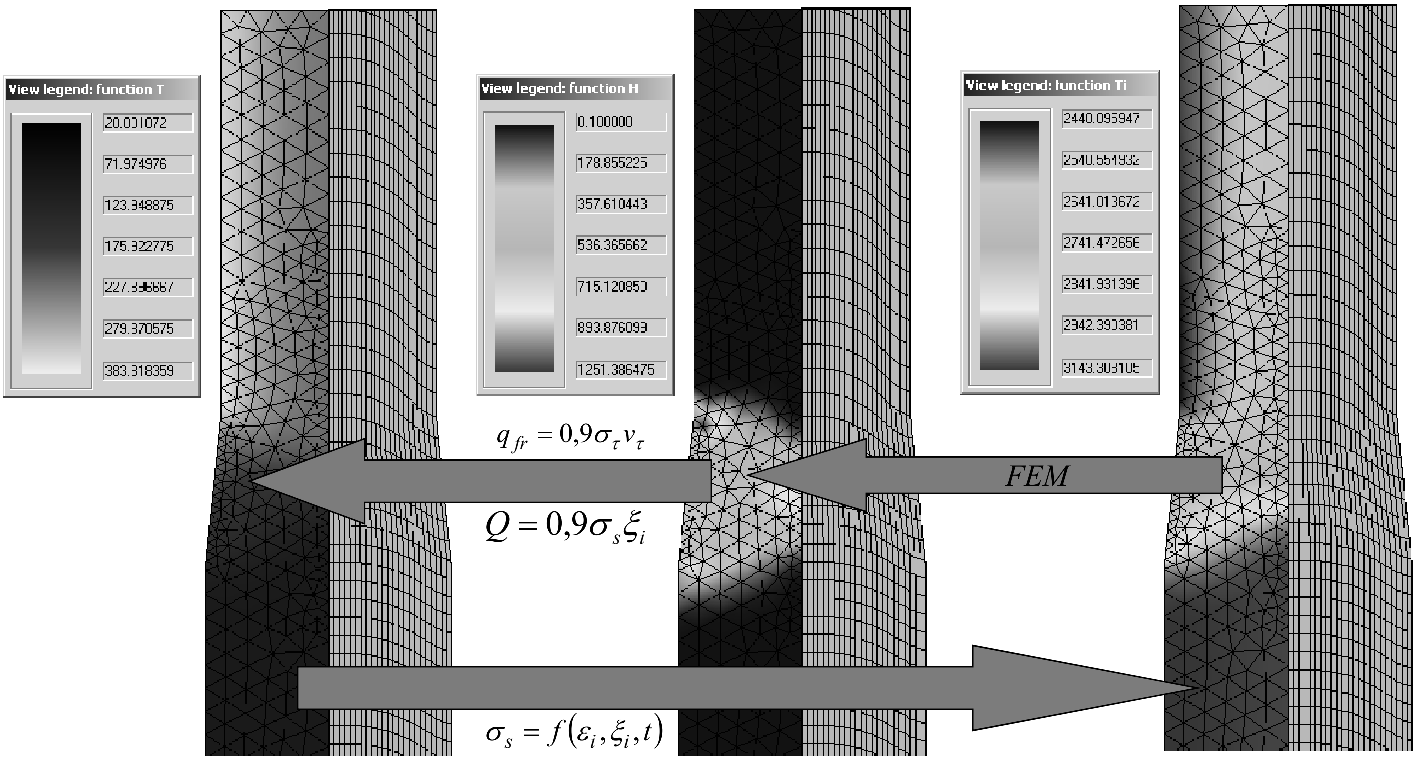

FEM Solution of Thermal Problem in Die

Heating

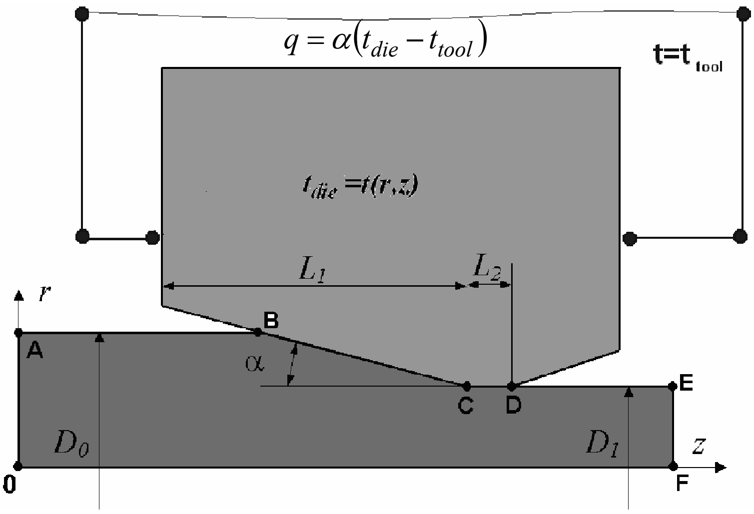

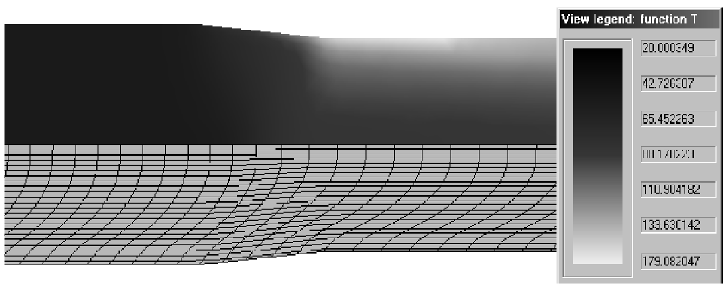

FEM grids

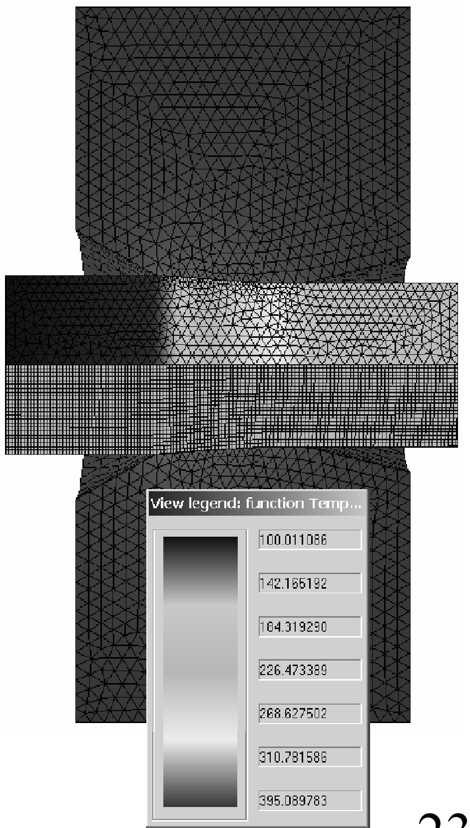

FEM Couple Solution of Thermal Problem in Metal and Die

THE FEM SOLUTION OF THE THERMAL PROBLEM IN METAL

Thermal problem is solved by applying the following method. The passage of the section through the zone of deformation is simulated. For this section at each time step the non-stationary temperature problem is examined:

$$\lambda\left(\frac{\partial^2 t}{\partial r^2}+\frac{1}{r}\frac{\partial t}{\partial r}\right)+Q_d=c\rho\frac{dt}{d\tau}$$

where: $Q_d = 0.9\sigma_s\xi_i$ – deformation power, c – specific heat; ρ – alloy density, τ – time, λ – thermal conductivity coefficient (the following values are used for MgCa0.8 alloy: c = 624 J /kgK, ρ = 1738 kg /m^3, λ = 126 J /mK). Heat exchange between the alloy and the die is defined as:

$$q_{conv}=\alpha\left(t-t_{die}\right)$$

where: t_{die} – die temperature, α – heat exchange coefficient.

The generation of heat from friction is calculated according to the formula:

$$q_{fr}=0.9\sigma_\tau v_\tau\ .$$

FEM SOLUTION OF THERMAL PROBLEM IN THE DIE

The model of temperature distribution in the die is based on the solution of Fourier equation in the cylindrical coordinate system:

$$\lambda\left(\frac{\partial^2 t}{\partial r^2}+\frac{1}{r}\frac{\partial t}{\partial r}+\frac{\partial^2 t}{\partial y^2}\right)+Q_h=0$$

where: Q_h – power of the heating element, r, y cylindrical coordinates.
The heat Q_h is generated in the finite elements, which correspond to the position of heating device. For the areas, which are in contact with the metal, the temperature of the alloy is obtained from the solution of the thermal problem for the metal.

Preliminary Simulations for Determination of Materials Tests Conditions

Strain rate, 1/s

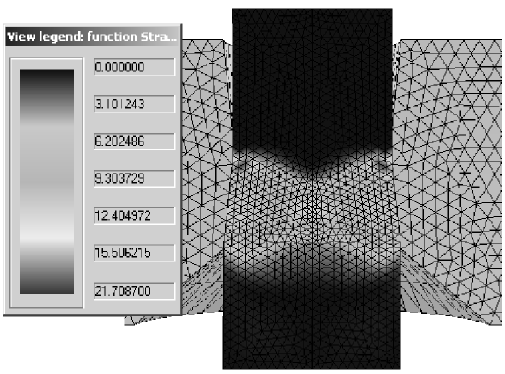

Triaxility factor

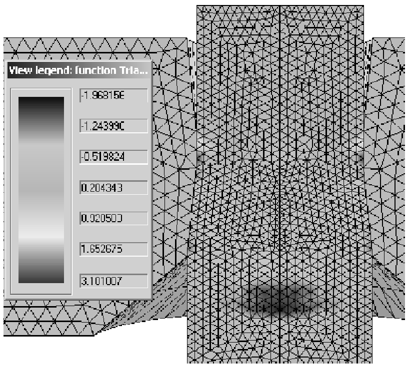

Strain intensity

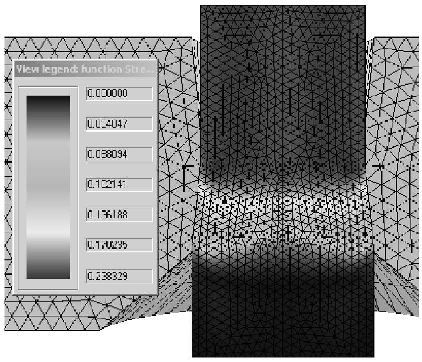

Temperature, v=0.05 m/s

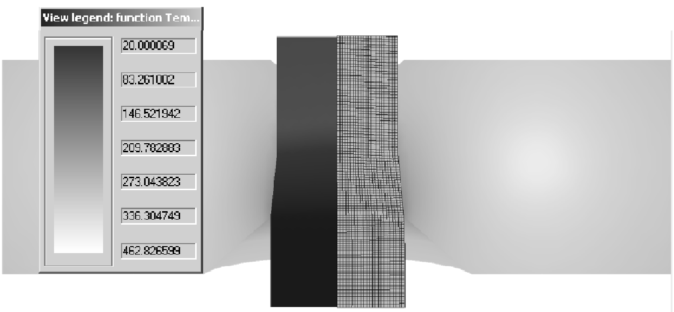

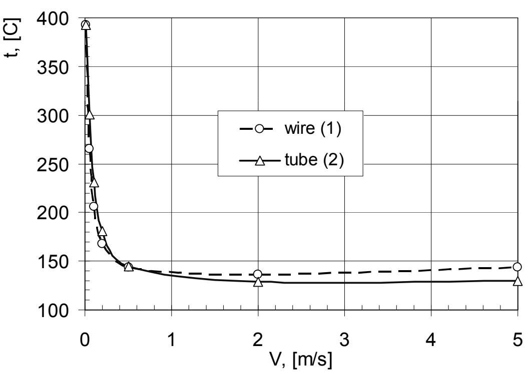

Yield Stress and Ductility Models

Yield Stress Model. For obtaining the model of flow stress the load-displacement curves from upsetting tests were used. Model of yield stress was proposed as a modified Henzel-Spittel equation:

$$\boxed{\sigma_s = Ae^{-m_1 t}\varepsilon_i^{m_2}\xi_i^{m_3\left(\frac{t-20}{280}\right)^{m_6}} e^{\frac{m_4}{\varepsilon_i}}\left(1+\varepsilon_i\right)^{m_5 t} e^{m_7\varepsilon_i}\xi_i^{m_8 t} t^{m_9}}$$

where: A, m_1 - m_9 – empirical coefficients.

Ductility Model. The key parameter, which presents fracture is called **ductility function**. This parameter is defined by the following formula:

$$\psi = \frac{\varepsilon_i}{\varepsilon_p\left(k,t,\xi_i\right)} < 1$$

where: k – triaxility factor, $k = \sigma_0 / \sigma_s$.

Critical deformation function $\varepsilon_p\left(k,t,\xi_i\right)$ is obtained on the basis of experimental results for the upsetting and the tension tests.

$$\psi = \int_0^\tau \frac{\xi_i}{\varepsilon_p\left(k,t,\xi_i\right)} d\tau \approx \sum_{m=1}^{m=m_\tau} \frac{\xi_i^{(m)}}{\varepsilon_p\left(k,t,\xi_i\right)} \Delta\tau^{(m)}$$

where: τ – time of deformation, $\Delta\tau^{(m)}$ – time increment, $\xi_i^{(m)}$ – the values of the strain rate in the current time, m – a index number of time step during numerical integration along the flow line.

The following function of critical deformation is proposed:

$$\boxed{\varepsilon_p = d_1 \exp\left(-d_2 k\right)\exp\left(d_3 t\right)\xi_i^{d_4}}$$

Materials tests and data processing

Upsetting and tensile tests were performed on the Zwick Z250 machine at the AGH University of Science and Technology.

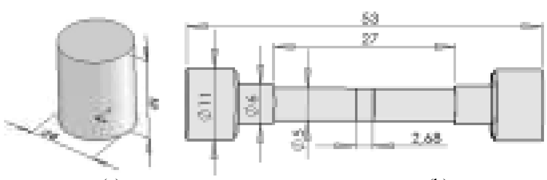

(a) (b)

Shape and dimension of samples for upsetting test (a) and tensile test (b).

Sample	Initial temperature, °C	Tool velocity, mm/min	The deformation, which corresponds to destruction of sample, mm (MgCa0.8 /Ax 30)	Samples (MgCa0.8 /Ax 30)
1u	300	60	6.08* / 6.8*	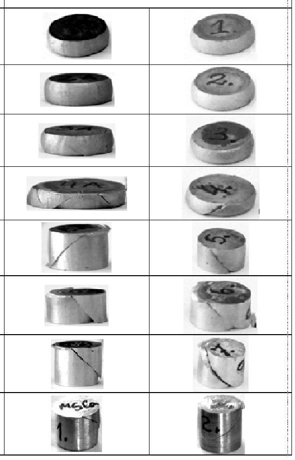
2u	300	600	5.79* / 6.5*	
3u	250	60	6.70 / 6.9	
4u	250	600	5.0 / 6.7	
5u	200	60	3.40 / 3.8	
6u	200	600	2.80 / 2.85	
7u	100	60	2.2 / 1.8	
8u	20	10	1.9 / 1.5	

Sample	Initial temperature, °C	Tool velocity, mm/min	The deformation, which corresponds to destruction of sample, mm (MgCa0.8 / Ax30)	Samples (MgCa0.8 /Ax 30)
1t	300	60	22.5 / 12.8	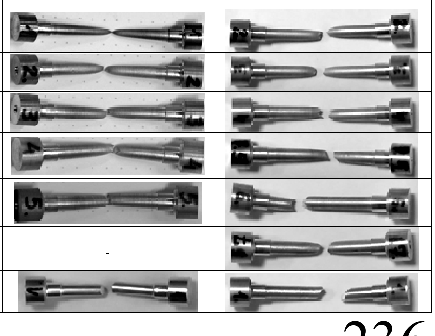
2t	300	600	16.0 / 12.8	
3t	250	60	14.0 / 10.5	
4t	250	600	8.50 / 9.4	
5t	200	60	6.4 / 7.2	
6t	200	600	- / 6.15	-
8t	20	10	2.66 / 4.15	

Determination of wire drawing schedule

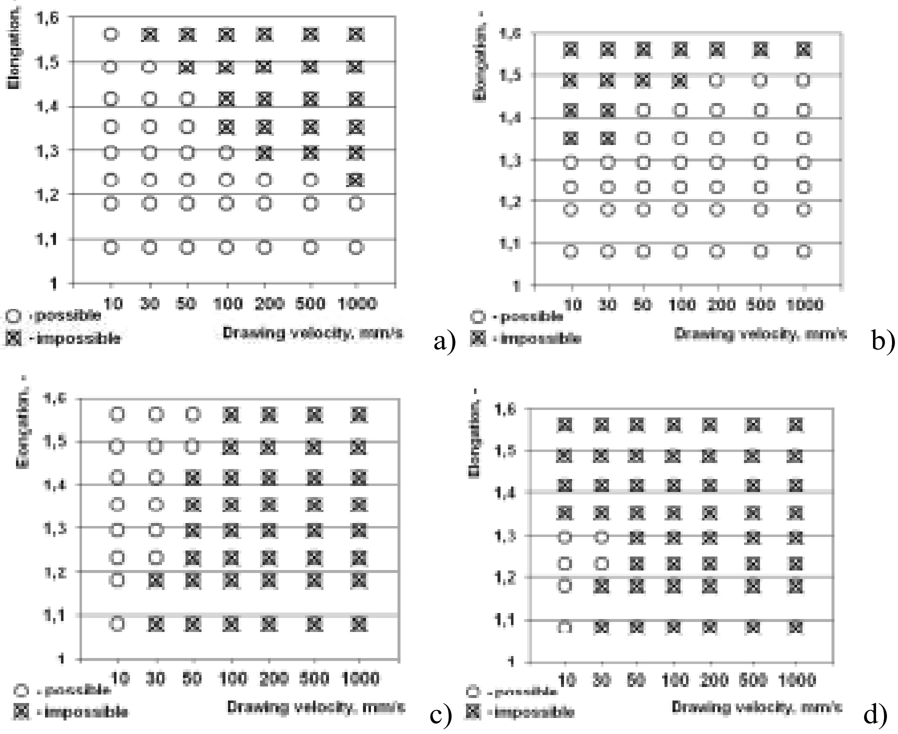

Maps of possible elongations per pass: (a) – because the fracture criteria (13); (b) – because the relationship σ_y/σ_s criteria (wire breaking); (c) – because temperature conditions; (d) – summary map

Production of thin wire

Equipment for drawing (construction of AGH, Krakow)

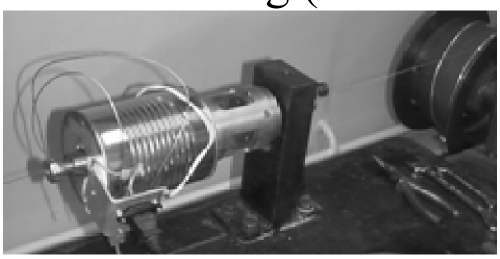

Wire after drawing

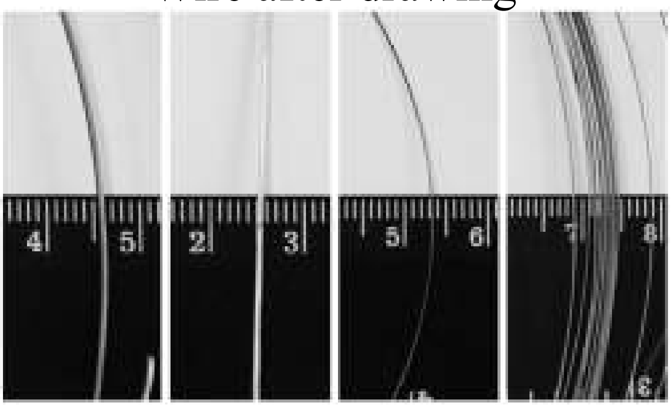

(a) (b) (c) (d)

Diameters if wire from Ax30 alloy after drawing: (a) 0,761 – pass 3 , (b) 0,694 – pass 4, (c) 0,306 – pass 13, (d) 0,233 – pass 16.

Ropes for surgical application (produced in Department of Biomedical Engineering and Lightweight Constructions, Institute of Materials Science, Hannover

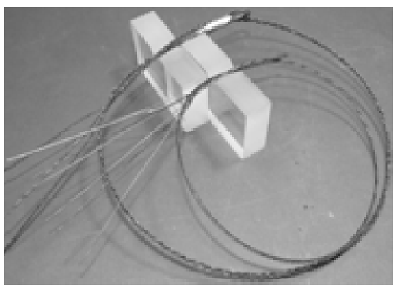

Production of thin wire

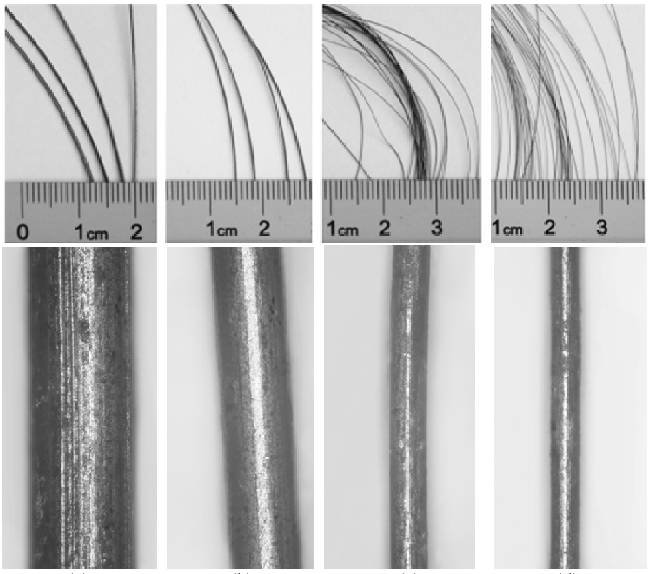

(a) (b) (c) (d)

Wire after drawing process of MgCa0.8 in heated die: (a) ø0.634 mm, (b) ø0.402 mm, (c) ø0.162 mm, (d) ø0.100 mm.

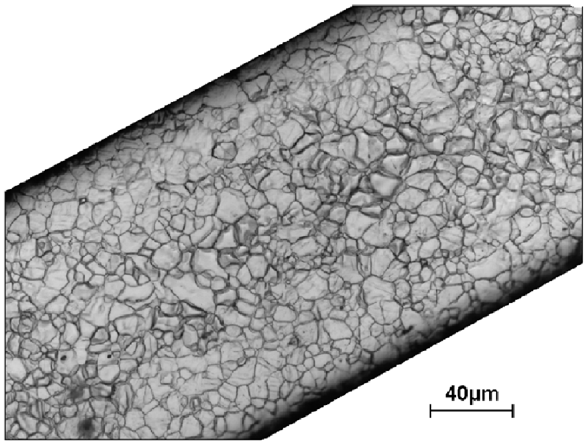

Microphotographs of the microstructure of Ax30 thin wire after 25th pass.

Conclusions

1. Flow formulation
2. Different approximation for velocity and pressure
3. Special methods for modeling of boundary conditions
4. Selection between use a commercial FEM software and development of FEM code.
5. Control of error in both cases

Thank You for attention